

Université de Montréal

Interactions du système nerveux autonome
avec les effets des antiarythmiques (I et III)
sur le créneau d'excitabilité du flutter auriculaire
chez l'homme et chez le chien.

par

Élise Jalil

Département de Pharmacologie

Faculté de Médecine

Thèse présentée à la Faculté des études supérieures

en vue de l'obtention du grade de

Philosophiæ Doctor (Ph.D.)

en pharmacologie

Décembre, 2001

©Élise Jalil, 2001



W
4
US8
2002
v. 014

Université de Montréal

Faculté des études supérieures

Cette thèse intitulée:

Interactions du système nerveux autonome
avec les effets des antiarythmiques (I et III)
sur le créneau d'excitabilité du flutter auriculaire
chez l'homme et chez le chien.

présenté par:

Élise Jalil

a été évalué par un jury composé des personnes suivantes:

Dr Louis Dumont (président du jury)

Dre Teresa Kus (directrice de recherche)

Dr Alain Vinet (codirecteur)

Dr Réginald Nadeau (membre du jury)

Dr Paul Dorian (examineur externe du jury)

Dr Jacques Bélair (représentant du doyen)

Thèse acceptée le: 19 Décembre, 2001

SOMMAIRE

Le flutter auriculaire demeure un défi majeur à la thérapie pharmacologique car sa prévention et son traitement avec les médicaments antiarythmiques est fréquemment inefficace. Il consiste en un front d'ondes circulant autour d'un circuit bien défini, qui est caractérisé par la présence d'un créneau d'excitabilité où le tissu peut avoir retrouvé partiellement ou complètement son excitabilité ainsi permettant de la réentrée. La durée et la composition de ce créneau sont déterminées non seulement par la longueur du circuit et ses caractéristiques électrophysiologiques mais aussi par des influences externes dont le système nerveux autonome. Dans un modèle de flutter auriculaire chez le chien, nous avons étudié les propriétés du circuit, en absence et suivant une infusion de la propafénone, afin de déterminer les mécanismes par lequel le médicament agit. La propafénone est un antiarythmique de la classe IC qui déprime la phase 0 de dépolarisation et prolonge aussi la phase 3 de repolarisation. Nous avons également étudié chez le chien les effets de la noradrénaline (sympathique) et de l'acétylcholine (parasymphatique) en présence de la propafénone. Enfin, chez l'humain nous avons abordé l'étude du créneau d'excitabilité et l'influence d'une activation sympathique en présence des antiarythmiques de la classe I (propafénone) et III (sotalol et amiodarone). Chez le chien, le flutter auriculaire était induit par stimulation électrique rapide en présence d'une lésion en forme de Y sur l'oreillette droite. La circulation du flutter autour de la valve tricuspide a été enregistré par une série d'électrodes bipolaires. Le créneau d'excitabilité du circuit de réentrée a été caractérisé par la méthode du "reset-response" utilisant un stimulus prématuré introduit durant le flutter auriculaire. Nos études ont démontré que le phénomène de "reset" n'était pas uniquement dû à l'effet de la prématurité (où le front de réentrée antérograde stimulé circule dans la queue du potentiel d'action du flutter) mais aussi à l'effet de collision. Ce dernier résulte de la propagation du front de réentrée antérograde stimulé à travers du tissu qui a été laissé partiellement réfractaire par la collision entre le front de réentrée rétrograde et le front du flutter original. L'analyse des temps de conduction entre les électrodes dans les différentes régions du circuit a révélé, en fait, un ralentissement de la conduction due à la prématurité, à l'effet de collision, ou à l'hétérogénéité spatiale. Nous avons aussi évalué

la variation des temps de conduction en fonction de la prématurité de la stimulation dans chaque section du circuit. La gamme de prématurité effective était large dans la première ou les deux premières sections adjacentes au site de stimulation dans la direction de la propagation. Les sections au-delà de ces portions avaient une gamme de prématurité de 10 ms ou moins et démontraient des changements minimes des temps de conduction. Donc, nos études ont démontré que la courbe "reset-response" obtenue en stimulant à seulement un site prédit très probablement le créneau d'excitabilité dans la région de la stimulation prématurée ou la section adjacente. Par contre, il ne peut pas prédire les caractéristiques globales du créneau d'excitabilité pour tout le circuit de réentrée, ce qui est présentement suggéré dans la plupart des études.

En présence de la propafénone, les courbes "reset-response" ont démontré une prolongation significative du cycle du flutter et de la période réfractaire effective, mais un effet variable sur le créneau d'excitabilité et sur la portion complètement excitable en avant du front de réentrée. En analysant les caractéristiques spatiales des effets de la propafénone, nous avons observé que la prolongation du cycle est en grande partie due à l'augmentation des temps de conduction localisés principalement dans une ou deux sections du circuit de réentrée démontrant que l'effet tonique de la propafénone est inhomogène dans l'espace. L'administration de la noradrénaline dans l'artère coronaire droite en présence de la propafénone a légèrement diminué le cycle du flutter et la période réfractaire effective mais avait un effet variable sur la durée totale du créneau d'excitabilité de même que la portion complètement excitable. Par contre, l'acétylcholine en présence de la propafénone n'a pas affecté le cycle du flutter, ni la période réfractaire effective, ni le créneau d'excitabilité et a peu augmenté la région complètement excitable devant le front de réentrée. Ceci confirme un effet bêta-bloqueur léger de la propafénone mais démontre aussi un effet anticholinergique significatif.

Dans le flutter auriculaire commun chez l'humain, des courbes "reset-response" ont été déterminées en utilisant la même technique de stimulation prématurée chez des patients se présentant au laboratoire d'électrophysiologie pour conversion en rythme sinusal par entraînement électrique rapide de l'oreillette. Nous avons démontré que les récurrences du flutter auriculaire chez les patients prenant du sotalol, de l'amiodarone ou de la

propafénone sont associées avec la persistance du créneau d'excitabilité de même que la présence de tissu complètement excitable en avant du front de réentrée. Des études faites en position couchée et debout (70°), ce qui produit une activation du système sympathique et un retrait vagal ont démontré que malgré une réduction du cycle du flutter auriculaire, une augmentation de la durée du créneau d'excitabilité et du tissu complètement excitable peut se produire. Ceci explique la viabilité persistante du circuit du flutter malgré une thérapie antiarythmique chez ces patients.

MOTS CLÉS: Flutter auriculaire, Propafénone, Système nerveux autonome, Reset-Response, Créneau d'excitabilité

TABLE DES MATIÈRES

| | |
|--|----------|
| SOMMAIRE | iii |
| TABLE DES MATIÈRES | vi |
| LISTE DES TABLEAUX | xiv |
| LISTE DES FIGURES | xvi |
| LISTE DES ABRÉVIATIONS | xxi |
| REMERCIEMENTS | xxvi |
| | |
| CHAPITRE I: INTRODUCTION | 1 |
| 1- Le potentiel d'action et les courants ioniques | 2 |
| 2- Le système nerveux autonome | 6 |
| 2.1- Le système parasympathique | 7A |
| 2.2- Le système sympathique | 8 |
| 2.3- Interactions entre les systèmes sympathique et parasympathique | 9 |
| 2.4- Le système nerveux intrinsèque..... | 10 |
| 2.5- Le système nerveux autonome et les courants..... | 13 |
| 2.5.1- Interaction avec une stimulation bêta-adrénergique | 13 |
| 2.5.2- Interaction avec l'acétylcholine | 15 |
| 2.6- Le système nerveux autonome et les arythmies..... | 16 |
| 3- Électrophysiologie du cœur..... | 17 |
| 4- Les arythmies | 18 |

| | |
|--|----|
| 4.1- Les mécanismes des arythmies | 20 |
| 5- Le flutter auriculaire | 21 |
| 5.1- Le mécanisme du flutter auriculaire - la réentrée | 22 |
| 5.1.1- Réentrée autour d'un obstacle anatomique | 26 |
| 5.1.2- Réentrée autour d'un obstacle fonctionnel | 26 |
| 6- Le créneau d'excitabilité d'une réentrée et la méthode du "reset-response" | 28 |
| 7- Des études antérieures du flutter auriculaire chez les animaux | 33 |
| 8- Les antiarythmiques | 35 |
| 8.1- La classe I | 37 |
| 7.1.1- Les sous-groupes de la classe I | 37 |
| 8.2- La classe II | 39 |
| 8.3- La classe III | 39 |
| 8.4- La classe IV | 40 |
| 8.5- La propafénone | 41 |
| 8.5.1- Effets électrophysiologiques | 41 |
| 8.5.1a- Bloqueur sodique | 41 |
| 8.5.1b- Bêta-bloqueur | 42 |
| 8.5.1c- Bloqueur calcique | 43 |
| 8.5.1d- Bloqueur potassique | 43 |
| 8.5.2- Métabolisme | 44 |
| 8.5.3- Les arythmies | 45 |
| 8.6- Le sotalol | 46 |

| | |
|---|-----|
| 8.7- L'amiodarone..... | 47 |
| 8.8- Effets des antiarythmiques sur le créneau d'excitabilité | 49 |
| 8.9- Interaction du système nerveux autonome et les antiarythmiques ... | 50 |
| 9- Le traitement pharmacologique du flutter auriculaire | 51 |
| 9.1- Le traitement aigu | 51 |
| 9.2- Le traitement à long terme | 53 |
| 9.2.1- L'ablation par cathéter..... | 53 |
| 9.2.2- Les antiarythmiques..... | 54 |
| 10- Hypothèse | 55 |
| 10.1- Études expérimentale..... | 56 |
| 10.2- Étude clinique | 58A |

CHAPITRE II: INFLUENCE OF PROPAFENONE ON RESETTING

| | |
|---|-----------|
| AND TERMINATION OF CANINE ATRIAL FLUTTER..... | 59 |
| Abstract | 60 |
| Introduction..... | 60 |
| Method | 61 |
| -Surgical Technique | 61 |
| -Measurement of Electrophysiological Parameters | 61 |
| -Pacing Protocol During AF | 61 |
| -Data Analysis..... | 62 |
| -Statistical Analysis..... | 62 |
| -Numerical Simulations | 63 |

| | |
|--|----|
| Results | 63 |
| -Hints From a Simple Model | 63 |
| -Construction of the RRC | 65 |
| -Effects of PPF on the EG and the CRRC | 66 |
| -Mechanism of Resetting | 69 |
| -Single Stimulus | 69 |
| -Multiple Stimuli | 72 |
| -Termination of AF | 76 |
| Discussion | 77 |
| Limitation of the studies | 78 |
| Conclusion | 78 |
| Acknowledgement | 78 |
| References | 79 |

**CHAPITRE III: EFFECTS OF PROPAFENONE ON THE SPATIO-
TEMPORAL ELECTROPHYSIOLOGICAL CHARACTERISTICS OF
THE REENTRY CIRCUIT IN A CANINE MODEL OF ATRIAL**

| | |
|---|-----------|
| FLUTTER | 80 |
| Abstract | 82 |
| Introduction | 84 |
| Methods | 85 |
| -Surgical technique | 85 |
| -Measurement of electrophysiological parameters | 86 |

| | |
|---|-----|
| -Data analysis | 93 |
| -Statistical analysis | 93 |
| Results | 94 |
| -Drug plasma levels | 94 |
| -Global effects of propafenone on the excitable gap characteristics and reset-response curve | 95 |
| -Spatial characteristics of the effects of propafenone..... | 101 |
| -Prematurity effect..... | 107 |
| Discussion..... | 107 |
| Acknowledgements | 113 |
| References | 114 |
| Figure Legends | 119 |

CHAPITRE IV : INTERACTIONS OF THE AUTONOMIC NERVOUS SYSTEM WITH PROPAFENONE ON THE EXCITABLE GAP

| | |
|---|-----|
| COMPOSITION IN A CANINE MODEL OF ATRIAL FLUTTER..... | 125 |
| Abstract..... | 127 |
| Introduction..... | 129 |
| Methods..... | 131 |
| -Surgical technique | 131 |
| -Measurement of electrophysiological parameters | 132 |
| -Data analysis..... | 139 |
| -Statistical analysis..... | 139 |

| | |
|---|-----|
| Results..... | 140 |
| -Drug plasma levels | 140 |
| -Global effects of propafenone and the autonomic neurohormones on excitable gap composition and reset-response | 142 |
| -Global Effect of PPF..... | 142 |
| -Global Effect of NE..... | 142 |
| -Global Effect of ACh..... | 146 |
| -Spatial characteristics on the effects of norepinephrine and acetylcholine . | 147 |
| -Prematurity effect | 150 |
| Discussion..... | 153 |
| -Prematurity effect | 157 |
| -Clinical implications..... | 157 |
| Limitations of the study | 158 |
| Acknowledgements..... | 159 |
| References..... | 160 |
| Figure Legends..... | 170 |

| | |
|---|------------|
| CHAPITRE V: EXCITABLE GAP COMPOSITION IN THE PRESENCE OF ANTIARRHYTHMIC DRUGS IN COMMON HUMAN ATRIAL FLUTTER | 174 |
| Summary | 176 |
| Abstract..... | 177 |
| Introduction..... | 178 |

| | |
|---|---------|
| Methods..... | 179 |
| -Population | 179 |
| -Measurement of Electrophysiological Parameters | 182 |
| -Data analysis..... | 185 |
| -Statistical analysis..... | 186 |
| Results..... | 186 |
| -Global effects of drug on the excitable gap characteristics and reset-response curve..... | 186 |
| -Effects of tilt on the excitable gap characteristics and reset-response curve..... | 190 |
| Discussion | 190 |
| -Effect of tilt..... | 193 |
| Limitations of the study | 194 |
| References..... | 195 |
| Figure legends | 202 |
| CHAPITRE VI : DISCUSSION ET CONCLUSION | 204 |
| Propriétés électrophysiologiques du circuit de flutter avec la méthode du "reset-response" | 205 |
| Effets de la propafénone | 210 |
| Le système nerveux autonome..... | 215 |
| -Implications cliniques..... | 220 |
| Étude clinique | 222 |

| | |
|---------------------------------|-----|
| -L'activation sympathique | 224 |
| Les limites de l'étude | 226 |
| -Expérimentale | 226 |
| -Clinique..... | 227 |
| | |
| SOURCES DOCUMENTAIRES | 229 |

LISTE DES TABLEAUX

CHAPITRE II: INFLUENCE OF PROPAFENONE ON RESETTING AND TERMINATION OF CANINE ATRIAL FLUTTER

TABLE I: Effects of propafenone on atrial flutter using the corrected method 68

TABLE II: Effects of propafenone on atrial flutter using the standard method 68

CHAPITRE III: : EFFECTS OF PROPAFENONE ON THE SPATIO- TEMPORAL ELECTROPHYSIOLOGICAL CHARACTERISTICS OF THE REENTRY CIRCUIT IN A CANINE MODEL OF ATRIAL FLUTTER

TABLE I: Effects of propafenone on atrial flutter and excitable gap parameters 96

CHAPITRE IV : INTERACTIONS OF THE AUTONOMIC NERVOUS SYSTEM WITH PROPAFENONE ON THE EXCITABLE GAP COMPOSITION IN A CANINE MODEL OF ATRIAL FLUTTER

| | |
|---|-----|
| TABLE I : Effects of neurotransmitters on the mean plasma concentrations of propafenone | 141 |
| TABLE II : Effects of neurotransmitters and propafenone on atrial flutter and excitable gap parameters..... | 143 |
| TABLE III : Effects of neurotransmitters and propafenone on the fully excitable portion of the excitable gap..... | 145 |

CHAPITRE V: EXCITABLE GAP COMPOSITION IN THE PRESENCE OF ANTIARRHYTHMIC DRUGS IN COMMON HUMAN ATRIAL FLUTTER

| | |
|---|-----|
| TABLE I : Population characteristics | 180 |
| TABLE II : Effects of drug on atrial flutter and excitable gap characteristics | 187 |
| TABLE III : Effects of tilt on atrial flutter and excitable gap characteristics | 191 |

LISTE DES FIGURES

CHAPITRE I: INTRODUCTION

| | |
|--|----|
| Figure 1a- Représentation schématique d'un modèle de myocyte auriculaire canin..... | 4 |
| Figure 1b- Modèle d'un potentiel d'action auriculaire | 4 |
| Figure 2- Les plexus ganglionnaires auriculaires chez le chien..... | 12 |
| Figure 3- Les temps d'activation autour d'un cycle cardiaque normal..... | 19 |
| Figure 4- Modèle de la réentrée | 24 |
| Figure 5- Circuit de réentrée avec son créneau d'excitabilité | 25 |
| Figure 6- L'activation auriculaire dans le flutter auriculaire typique humain | 27 |
| Figure 7a- Réentrée autour d'un obstacle fixe avec possibilité de tissu excitable | 29 |
| Figure 7b- Réentrée autour d'un obstacle fonctionnel sans tissu excitable à l'intérieur du circuit..... | 29 |
| Figure 8- Représentation schématique des 3 courbes "reset-response" observées durant une tachycardie ventriculaire (TV) | 31 |

CHAPITRE II: INFLUENCE OF PROPAFENONE ON RESETTING AND TERMINATION OF CANINE ATRIAL FLUTTER

| | |
|---|----|
| Figure 1- Endocardial bipolar recording at site M during atrial flutter | 62 |
| Figure 2- Reentry on a ring model of 23 cm in length and cycle length of 325 ms | 64 |
| Figure 3- Comparison of the reset-response curves obtained with the standard and the corrected methods without propafenone | 65 |
| Figure 4- The reset-response curves and their corresponding corrected reset-response curve before and after drug infusion | 67 |
| Figure 5- Relative conduction time versus corrected coupling interval in the different regions of atrial flutter circuit..... | 70 |
| Figure 6- Relative conduction time versus corrected coupling interval in the different regions of atrial flutter circuit..... | 71 |
| Figure 7- Relative conduction time versus corrected coupling interval for one and three stimulations in the different regions of the atrial flutter circuit with propafenone, using 16 recording sites..... | 72 |
| Figure 8- The reset-response curves and their corresponding corrected reset-reponse curve for single and double stimuli, and single and triple stimuli with propafenone..... | 73 |
| Figure 9- Relative conduction time versus corrected coupling interval for one and five stimulations in the different regions of the atrial flutter circuit with propafenone, using 16 electrode sites | 74 |
| Figure 10- Relative conduction time versus the corrected coupling interval for the last | |

| | |
|---|----|
| Stimulus in pacing with 5 or 20 stimuli after drug infusion | 75 |
| Figure 11- The different types of atrial flutter termination..... | 76 |

CHAPITRE III: EFFECTS OF PROPAFENONE ON THE SPATIO-TEMPORAL ELECTROPHYSIOLOGICAL CHARACTERISTICS OF THE REENTRY CIRCUIT IN A CANINE MODEL OF ATRIAL FLUTTER

| | |
|---|-----|
| Figure 1- The right posterior view of the heart | 87 |
| Figure 2- Epicardial bipolar recording during atrial flutter | 89 |
| Figure 3- Method to approximate the measure of the coupling interval and the return cycle at the stimulation site | 90 |
| Figure 4- Two exemples of the effects of propafenone on the reset-response curve..... | 98 |
| Figure 5- Maximum resting corrected for the change in effective refractory period | 100 |
| Figure 6- Inhomogeneity of propafenone effect on conduction time around the atrial flutter circuit in free running flutter | 102 |
| Figure 7- Variability of the conduction time for each section | 104 |
| Figure 8- Effect of the variability of the conduction time on the effect of propafenone on conduction time..... | 105 |
| Figure 9- Cycle length fluctuations for each section | 106 |
| Figure 10- Effect of prematurity on the different sections of the reentry circuit..... | 108 |

CHAPITRE IV : INTERACTIONS OF THE AUTONOMIC NERVOUS SYSTEM WITH PROPAFENONE ON THE EXCITABLE GAP COMPOSITION IN A CANINE MODEL OF ATRIAL FLUTTER

| | |
|---|-----|
| Figure 1- The right posterior view of the heart..... | 133 |
| Figure 2- Epicardial bipolar recording during atrial flutter | 135 |
| Figure 3- Method to approximate the measure of the coupling interval and return cycle at the stimulation site | 136 |
| Figure 4- Effects of norepinephrine and acetylcholine on the reset-response curve during an infusion of propafenone | 144 |
| Figure 5- Inhomogeneity of propafenone effect on conduction time around the atrial flutter circuit in free running flutter | 148 |
| Figure 6- Effect of prematurity on the different sections of the reentry circuit..... | 152 |

CHAPITRE V: EXCITABLE GAP COMPOSITION IN THE PRESENCE OF ANTIARRHYTHMIC DRUGS IN COMMON HUMAN ATRIAL FLUTTER

| | |
|---|-----|
| Figure 1- Schematic representation of the atria in a left anterior oblique view, from the tricuspid (left) and mitral rings..... | 181 |
| Figure 2- Bipolar recording during atrial flutter | 183 |
| Figure 3- Method to approximate the measure of the coupling interval and return cycle | |

at the stimulation site 184

Figure 4- Effects of sotalol, propafenone and amiodarone on the reset-response curve 189

LISTE DES ABRÉVIATIONS

| | |
|----------------------------------|--|
| A | : Antegrade |
| AERP | : Atrial effective refractory period |
| AF | : Atrial flutter |
| AFI | : Atrial flutter |
| Amio | : Amiodarone |
| AMPC | : Adénosine monophosphate cyclique |
| AP | : Artère pulmonaire |
| A-V | : Auriculo-Ventriculaire |
| C | : Control |
| Ca ²⁺ | : Calcium |
| [Ca ²⁺] _i | : Concentration intracellulaire de calcium |
| CCI | : Corrected coupling interval |
| CE | : Collision effect |
| Cl ⁻ | : Chlore |
| [Cl ⁻] _i | : Concentration intracellulaire de chlore |
| CL | : Cycle Length |
| cm | : Centimètre |
| CR | : Cycle de retour |
| CRRC | : Corrected reset-response curve |
| CT | : Conduction time |
| Ctrl | : Control |
| dV/dt max | : Dérivée temporelle maximum du potentiel |

| | |
|-----------------------------|---|
| <i>et al.</i> | : et alias |
| et coll. | : et collaborateurs |
| Eg. | : Exemple |
| EG | : Excitable Gap |
| ERP | : Effective Refractory Period |
| F | : Preexisting wavefront |
| FEP | : Fully excitable portion |
| F _{SM} | : Temps de conduction entre l'électrode de stimulation et de détection |
| hrs | : heures |
| Hz | : Hertz |
| i.e. | : Id est |
| I _{b,Na} | : Courant calcique de fond |
| IC | : Intervalle de couplage |
| I _{CaL} | : Courant calcique de type L |
| I _{CaT} | : Courant calcique de type T |
| I _{Cl⁻} | : Courant chlore |
| I(f) | : Courant hyperpolarisant |
| I _{K,ACh} | : Courant potassique acétylcholine-dépendant |
| I _{KI} | : Courant potassique rectificateur interne |
| I _{Kr} | : Courant potassique rapide |
| I _{Kur} | : Courant potassique ultra-rapide |
| I _{Kur,d} | : Courant potassique ultra-rapide chez le chien |

| | |
|------------|--|
| I_{Ks} | : Courant potassique lent |
| I_{leak} | : Courant calcique de fuite du réticulum sarcoplasmique |
| I_{Na} | : Courant sodique |
| $I_{p,Ca}$ | : Courant de la pompe calcique sarcoplasmique |
| I_{rel} | : Courant calcique de libération du réticulum sarcoplasmique |
| I_{to} | : Courant transitoire sortant (Transient Outward Current) |
| I_{up} | : Courant entrant calcique dans le réticulum sarcoplasmique |
| i.v. | : Intraveineux |
| IV | : Intravenous |
| K^+ | : Potassium |
| $[K^+]_i$ | : Concentration intracellulaire de potassium |
| kg | : Kilogramme |
| M | : Recording electrode |
| mA/mAmp | : Milliampère |
| mg | : Milligramme |
| mg/kg | : Milligramme/Kilogramme |
| mg/kg/min | : Milligramme/Kilogramme/Minute |
| mg/kg/hr | : Milligramme/Kilogramme/Heure |
| mg/min | : Milligramme/Minute |
| min | : Minute |
| ml | : Millilitre |
| mm | : Millimètre |
| mm Hg | : Millimètre de Mercure |

| | |
|-----------------|---|
| MR | : Maximum resetting |
| ms | : Milliseconde |
| mV | : Millivolt |
| Na ⁺ | : Sodium |
| NCVL | : Nerf cardiaque ventro-latéral |
| NE | : Norépinéphrine |
| OG | : Oreillette gauche |
| OH | : Hydroxy |
| P | : Probabilité |
| pA/pF | : Picoampère/picofarad |
| PE | : Prematurity effect |
| PGOD | : Plexus ganglionnaire de l'oreillette droite |
| PG(OGI-VCI) | : Plexus ganglionnaire situé à la jonction de l'oreillette gauche inférieure et de la veine cave inférieure |
| PGOGd | : Plexus ganglionnaire de l'oreillette gauche dorsal |
| PGOGv | : Plexus ganglionnaire de l'oreillette gauche ventral |
| PKA | : Protéine kinase A |
| PPF | : Propafenone |
| R | : Retrograde |
| RC | : Return Cycle |
| ReC | : Rentry Circuit |
| RCT | : Relative conduction time |
| R _E | : Recording electrode |

| | |
|------------------|-------------------------------------|
| RRC | : Reset-Response Curve |
| RS | : Réticulum sarcoplasmique |
| S | : Stimulus ou Stimulating electrode |
| SA | : Nœud sinusal |
| SC | : Sinus Coronaire |
| SD | : Standard Deviation |
| S _E | : Stimulating electrode |
| Sot | : Sotalol |
| TV | : Tachycardie ventriculaire |
| μg/ml | : Microgramme/millilitre |
| μg/min | : Microgramme/minute |
| μm | : micromètre |
| μM | : Micromolaire |
| VCI | : Veine cave inférieure |
| VCS | : Veine cave supérieure |
| VD | : Ventricule droit |
| VG | : Ventricule gauche |
| VP | : Veines pulmonaires |
| V _{max} | : Vitesse Maximale |

REMERCIEMENTS

Je tiens à exprimer ma plus profonde gratitude à ma directrice de recherche, Dre Teresa Kus, qui par son support, son encouragement, et sa patience m'a permis de réaliser ce projet. Je tiens à remercier également mon codirecteur de recherche, Dr Alain Vinet, qui par sa disponibilité et son enthousiasme m'a permis de terminer ma thèse.

Je tiens aussi à remercier les Drs Guy Rousseau, James Nasmith, Franck Molin, Réginald Nadeau, René Cardinal et Chantal Pharand pour leurs contributions.

Ma gratitude va aussi à Caroline Bouchard, Pierre Fortier, Denis Guérette, Louis Chiocchio pour leur aide technique; et à Linda Fréchette, Diane Abastado et Suzan Sénéchal.

Je remercie également Philippe Comtois, Pierre Rocque, Gaéтан Tremblay, Bruno Dubé, Michel Vermeulen, Natalie Lemarec pour leur collaboration qui fut bien appréciée.

Enfin, je remercie Shirley, Betty, Megan, Sophie, Steph, Phil et ma famille pour leur support moral.

Ce projet a été soutenu par le Conseil de recherches médicales du Canada.

À Alain

mon conjoint, mon ami

qui m'a supporté inconditionnellement

CHAPITRE I
INTRODUCTION

INTRODUCTION

Les canaux ioniques sont des protéines qui résident dans la membrane cellulaire. En réponse à des stimuli externes, comme un changement dans le potentiel entre l'extérieur et l'intérieur de la membrane cellulaire, ces canaux peuvent former des pores qui permettent aux ions d'entrer et de sortir de la cellule. Le comportement intégré de milliers de canaux ioniques dans une cellule résulte en un courant ionique; et le comportement intégré de plusieurs courants provoque le potentiel d'action cardiaque. Les arythmies cardiaques peuvent résulter d'anomalies dans la structure, la fonction ou dans le nombre des canaux ioniques. Ces anomalies peuvent être primaires ou elles peuvent être causées par d'autres facteurs dans l'environnement de la cellule. L'ischémie aiguë, des changements dans les neurohormones circulantes, ou une surcharge de calcium intracellulaire peuvent tous modifier la fonction de ces canaux. L'approche pharmacologique traditionnelle pour contrôler les arythmies cardiaques utilise des médicaments qui modifient le milieu externe, ou des drogues qui directement activent ou bloquent un ou plusieurs courants ioniques (Roden et George, 1996).

1. Le potentiel d'action et les courants ioniques

Le potentiel d'action cardiaque est la manifestation de la variation du voltage transmembranaire de la cellule cardiaque en fonction du temps (Hille, 1992)(Figure 1a,b). Dans les cellules cardiaques excitables et non-automatiques des oreillettes et des ventricules, la dépolarisation du potentiel d'action (phase 0) est principalement générée

par une augmentation très large mais brève de la conductance au sodium membranaire (I_{Na}) (Weidmann 1955; Gettes et Reuter, 1974). Celle-ci est suivie par une phase de repolarisation précoce (phase 1). La repolarisation rapide résulte d'une inactivation voltage dépendante de I_{Na} accompagnée par l'activation d'un courant sortant transitoire (I_{to}) qui comporte au moins deux composantes. I_{to1} est un courant potassique voltage dépendant qui s'active, puis se désactive rapidement, pour recouvrer ensuite lentement. (Fermini et coll., 1992). I_{to2} est un courant de chlore dépendant du calcium qui est activé par le calcium traversant les canaux de type L ($I_{Ca,L}$) (Zygmunt et Gibbons, 1991). Durant une stimulation adrénergique, les ions Cl^- peuvent aussi contribuer à la repolarisation précoce via un courant rapide I_{Cl^-} (Harvey et coll., 1990).

La phase de plateau (phase 2) suit la repolarisation rapide. Les courants entrant pendant cette phase sont a) les courants calciques qui sont activés par la dépolarisation du potentiel d'action ($I_{Ca,T}$ et $I_{Ca,L}$); et b) l'échangeur de Na^+-Ca^{2+} ; et dans les cellules ventriculaires et de Purkinje c) un courant sodique qui s'inactive lentement (Patlak et Ortiz, 1985). Le courant potassique dominant au potentiel de repos (I_{K1}) contribue peu à la phase 2 à cause de sa rectification interne. Le courant potassique rectificateur externe (I_K) s'active lentement pendant cette phase et est le plus dominant des courants sortant. Trois types de courants potassiques existent dans l'oreillette: a) I_{Kur} qui s'active très rapidement; b) I_{Kr} qui s'active rapidement; et c) I_{Ks} qui s'active plus lentement (Sanguinetti et Jurkiewicz, 1990; Wang et coll., 1994). La repolarisation (phase 3) est contrôlée par des courants potassiques (I_K et I_{K1}) avec une petite contribution de la pompe Na^+-K^+ . Le début de la phase 3 est due au courant I_K , et au cours de cette phase

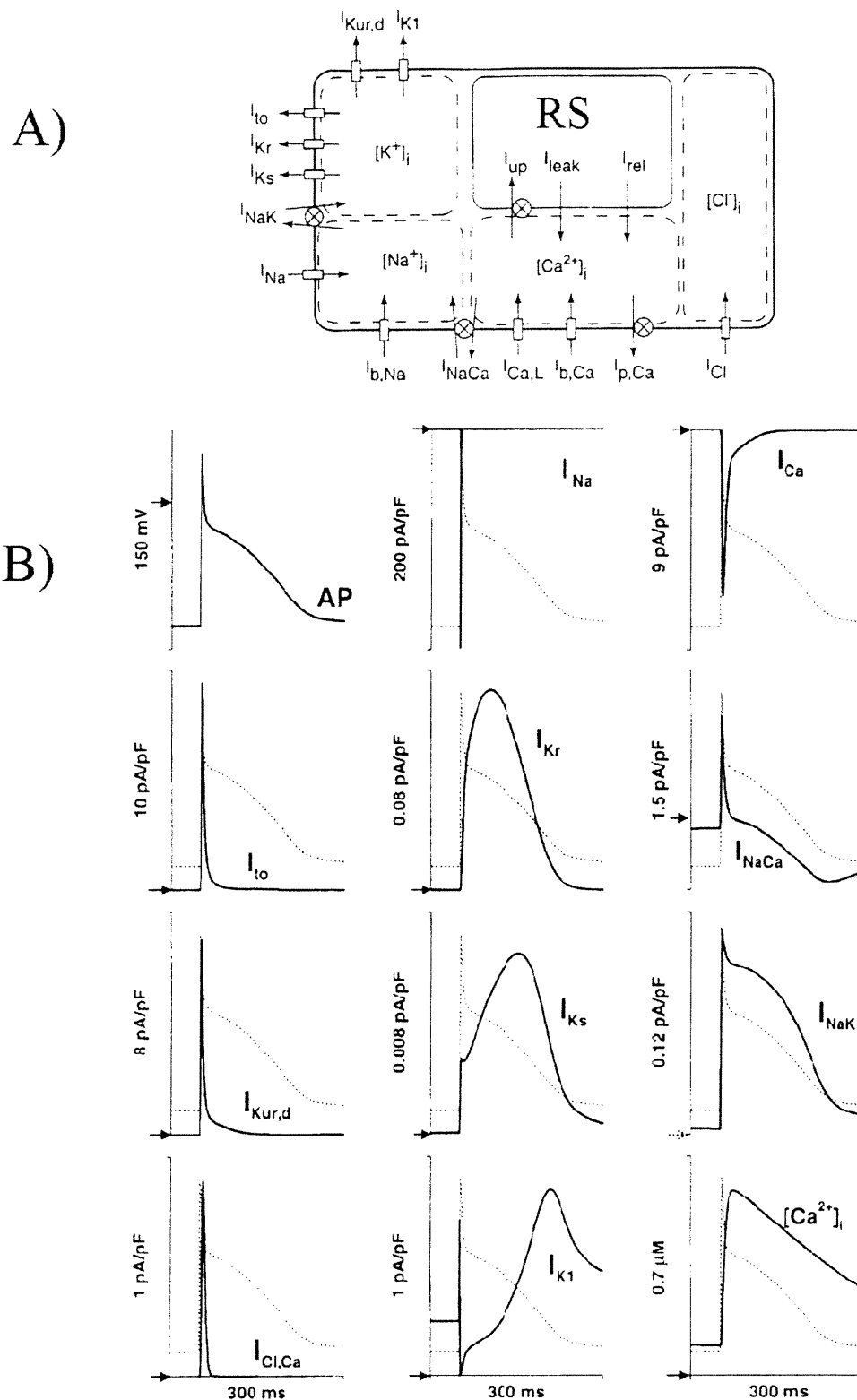


FIGURE1. 1A) Représentation schématique d'un modèle de myocyte auriculaire canin 1B) Modèle d'un potentiel d'action auriculaire canin.

1A) Les compartiments intracellulaires (en pointillés) indiquent les ions intracellulaires. La concentration des ions est affectée par les courants ioniques, les pompes et les échangeurs. Les boîtes rectangulaires indiquent les courants ioniques du sarcolemme; les cercles contenant des croix indiquent les pompes et les échangeurs. RS- réticulum sarcoplasmique, I_{K1} - courant potassique rectificateur interne, $I_{Kur,d}$ - courant potassique rectificateur externe ultra-rapide chez le chien, I_{to} - courant sortant transitoire, I_{Kr} - courant potassique rectificateur externe rapide, I_{Ks} - courant potassique rectificateur externe lent, I_{NaK} - Courant de la pompe Na^+K^+ , I_{Na} - courant sodique, $I_{b,Na}$ - courant sodique de fond, I_{NaCa} - courant de l'échangeur Na^+/Ca^{2+} , $I_{Ca,L}$ - courant calcique de type L, $I_{b,Ca}$ - courant calcique de fond, $I_{p,Ca}$ - courant de la pompe calcique sarcoplasmique, I_{Cl} - courant de chlore, I_{up} - le courant entrant calcique dans le RS, I_{leak} - courant calcique de fuite du RS, I_{rel} - courant calcique de libération du RS, $[K^+]_i$ - concentration intracellulaire de potassium, $[Na^+]_i$ - concentration intracellulaire de sodium, $[Ca^{2+}]_i$ - concentration intracellulaire de calcium, $[Cl^-]_i$ - concentration intracellulaire de chlore. **1B)** Un modèle de potentiel d'action auriculaire canin (en haut, à gauche), les courants membranaires sous-jacents (I_{Na} , I_{Ca} , I_{to} , I_{Kr} , I_{NaCa} , $I_{Kur,d}$, I_{Ks} , I_{NaK} , $I_{Cl,Ca}$, and I_{K1}), et $[Ca^{2+}]_i$ transitoire durant le potentiel d'action. Les lignes pointillées démontrent la progression du potentiel d'action dans le temps en comparant avec le courant correspondant. Les flèches solides sur l'axe des Y indiquent la référence zéro (0 mV pour le potentiel d'action, 0pA/pF pour les courants, 0 μ M pour le $[Ca^{2+}]_i$). La flèche pointillée sur l'axe des Y pour I_{NaK} indique la valeur de la ligne de fond de 0.13 pA/pF (modifié de Ramirez et coll., 2000).

les canaux I_{K1} se réactivent progressivement causant une repolarisation jusqu'au potentiel de repos. Les potentiels d'action dans l'oreillette sont de plus courtes durée que ceux du ventricule. Dans l'oreillette, I_{K1} est le courant dominant au repos même s'il est considérablement plus petit que dans le ventricule (Heidbuchel et coll., 1990). Il existe un autre canal potassique, qui est activé par l'action de l'acétylcholine sur les récepteurs muscariniques (M_2) ($I_{K,ACh}$). Avec I_{K1} , il contribue à la stabilité du potentiel de repos auriculaire et est également responsable de l'hyperpolarisation. La dépolarisation du potentiel d'action auriculaire est suivie d'une phase rapide prononcée de repolarisation et d'un petit plateau peu défini. Ceci reflète la prédominance d'un courant large I_{to} par rapport à un plus petit courant I_{Ca} (Escande et coll., 1987; Giles et Imaizumi, 1988). La phase terminale lente de la repolarisation est médiée par I_K et $I_{K,ACh}$. Ce dernier aurait un rôle majeur.

2. Le système nerveux autonome

Le cœur est sous le contrôle du système nerveux autonome (système sympathique et parasympathique) qui a des effets sur toutes les fonctions cardiaques : la chronotropie sur les cellules du nœud sinusal (pacemaker); la conduction à travers l'oreillette, le système auriculo-ventriculaire (A-V) et les ventricules; la contractilité du myocarde. Le système sympathique via la libération de l'adrénaline et la noradrénaline a des effets chronotropes positifs sur les cellules du nœud sinusal, raccourcit la vitesse de conduction à travers le nœud A-V, et augmente la contractilité du myocarde. La stimulation du système parasympathique provoque une libération de l'acétylcholine via

les terminaisons du nerf vague (Loffelholz et Pappano, 1985) qui inhibe l'activité du nœud sinusal, prolonge le temps de conduction à travers le nœud A-V et affaiblit la contraction du myocarde (surtout le myocarde auriculaire) (Jalife et coll., 1999).

Les systèmes sympathique et parasympathique agissent respectivement via des récepteurs adrénergiques et muscariniques. Au moins neuf sous-types de récepteurs adrénergiques et cinq sous-types de récepteurs muscariniques ont été décrits. (Brodde et Michel, 1999). Les récepteurs principaux cardiaque alpha1- et bêta-adrénergiques contribuent de façon similaires aux effets inotropes positif de la noradrénaline (Skomedal et coll., 1997). La réponse endogène à la noradrénaline est faite via les récepteurs alpha1 et bêta dans une proportion de 14 et 86% respectivement (Borthne et coll., 1995). Dans l'oreillette humain, le ratio des récepteurs bêta1- et bêta2-adrénergiques est de 60-70% et 40-30% respectivement (Brodde, 1991). Ces deux récepteurs se couplent à la protéine Gs pour activer l'adénylate cyclase qui va augmenter le niveau d'AMPC. Ceci va activer la protéine kinase A qui phosphorilera plusieurs protéines du sarcolemme incluant les canaux calciques de type L. En activant ce dernier, un plus grand influx de calcium augmentera la contraction (Kaumann et Molenaar, 1997). Par contre, Altschuld et coll. (1995) ont démontré dans des myocytes chez le chien, un effet inotrope positif bêta2-adrénergiques sans augmentation du niveau d'AMPC malgré une augmentation de calcium cytosolique. Cependant, des études ont démontré (Kaumann et coll., 1989; Schafers et coll., 1997) que l'augmentation de la contractilité cardiaque est stimulé de façon prédominante via les récepteurs bêta1-adrénergiques. Lorsque la noradrénaline se lie aux récepteurs alpha1 adrénergiques, la protéine Gh ou Gq se couple à la phospholipase C pour diviser la phosphatidyl inositol

en inositol triphosphate (IP₃) et 1,2-diacylglycerol. Un petit effet inotrope positif est associé avec la formation de IP₃ (Otani et coll., 1988) en stimulant la libération de calcium du réticulum sarcoplasmique.

2.1 Le système parasympathique

Chez le chien, les neurones pré-ganglionnaires efférents parasympathiques qui projettent leurs axones aux neurones post-ganglionnaires efférents sont pour la plupart situés dans le noyau ambigu (Plecha et coll., 1988). Quelques neurones parasympathiques sont localisés dans le noyau moteur dorsal et dans les régions situées entre ces deux noyaux. La localisation exacte des neurones vagues chez l'humain n'a pas encore été établie. Les fibres vagues cardiaques pré-ganglionnaires chez le chien forment le tronc vago-sympathique avec les fibres sympathiques. Les fibres vagues pré-ganglionnaires forment des contacts synaptiques avec les neurones vagues post-ganglionnaires dans les ganglions intracardiaques qui sont localisés très proches des structures qu'ils innervent (Elvan et Zipes, 1996). Les fibres du nerf vague projettent au cœur en longeant la veine cave supérieure, au-dessus de l'oreillette droite, et en passant par-dessus la jonction entre la veine cave inférieure et la surface auriculaire inférieure (Randall et coll., 1985).

La stimulation du nerf vague ou l'administration de l'acétylcholine diminue la durée du potentiel d'action des myocytes auriculaires, raccourcit la période réfractaire auriculaire, hyperpolarise la membrane durant la phase 4 (Higgins et coll., 1973), et diminuent la contractilité de l'oreillette (Ten et coll., 1976).

Chez des modèles animaux, la stimulation vagale ou l'administration de l'acétylcholine peuvent provoquer de la fibrillation auriculaire en raccourcissant les périodes réfractaires (Rensma et coll., 1988; Wu et coll., 1989; Yano et coll., 1991).

Les neurones post-ganglionnaires parasympathiques dans chaque plexus ganglionnaire cardiaque intrinsèque innervent les tissus du cœur (Yuan et coll., 1993). Les neurones situés dans les ganglions auriculaires innervent les tissus de l'oreillette et ceux des ganglions ventriculaires innervent les tissus du ventricule (Ardell, 1994).

2.2 Le système sympathique

Les neurones sympathiques pré-ganglionnaires qui projettent au cœur du chien sont localisés dans les colonnes intermédiolatérales des huit segments thoraciques supérieurs de la moelle épinière. Ces fibres pré-ganglionnaires passent au travers les communicants du rami blanc (Armour et Randall, 1975). Ils projettent leurs axones via les nerfs thoraciques crâniens droit et gauche de la moelle épinière (Norris et coll., 1997) aux neurones post-ganglionnaires qui sont les efférents sympathiques de tous les ganglions intrathoraciques. Ces neurones post-ganglionnaires sympathiques efférentes sont localisés non seulement dans les ganglions paravertébraux (ganglions stellaires et dans la chaîne de ganglions sympathiques thoraciques crâniens), mais également dans les ganglions cervicaux supérieur et moyen, les ganglions médiastinaux et les ganglions cardiaques intrinsèques (Armour, 1994). Ces neurones projettent des axones sur

différentes régions du cœur via les parties dorsales et ventrales de l'anse sous-clavière qui origine du ganglion cervical moyen. Le nerf stellaire droit émerge soit du ganglion stellaire ou du ganglion cervical moyen. Les nerfs sympathiques traversent les tissus péricardiaux, les veines pulmonaires, et la veine cave supérieure avant de se projeter vers l'oreillette droite. Les nerfs stellaires et craniovagaux ont une distribution localisée dans l'oreillette droite, avec une densité plus élevée dans la région du nœud sinusal. La distribution des fibres sympathiques dans les oreillettes a été établie en observant les différences régionales de concentration de noradrénaline dans les tissus (Randall, 1984). La concentration de la noradrénaline est plus élevée au bout de l'appendice auriculaire et plus faible dans l'oreillette gauche.

La stimulation des nerfs sympathiques ou l'administration d'agents bêta-adrénergiques diminue la période réfractaire effective (Govier et coll., 1966). Des concentrations élevées de catécholamines provoquent une diminution de la durée du potentiel d'action, et une augmentation dans le taux de dépolarisation de la phase 4 des cellules du nœud sinusal ce qui augmente l'automatisme (Mastuda et Levy, 1985).

2.3 Interactions entre les systèmes sympathique et parasympathique

Les interactions du système sympathique et vagal jouent un rôle important dans la régulation des fonctions cardiaques. Les composantes sympathiques et parasympathiques du système nerveux autonome exercent des effets semblables sur les périodes réfractaires auriculaires, et des effets différents sur le rythme sinusal et sur le

temps de conduction du noeud A-V (Furukawa et coll., 1990). Dans l'oreillette et spécialement dans la région du nœud sinusal, plusieurs terminaisons nerveuses post-ganglionnaires sympathiques et vagues sont très rapprochées. Ceci constitue un substrat anatomique pour des interactions complexes entre les deux composantes autonomes (Levy, 1971). L'effet dépresseur vagal est plus prononcé quand le niveau du tonus sympathique est augmenté. Cet antagonisme vagal qui se nomme l'antagonisme accentué peut se produire au niveau pré- et post-synaptique (Levy, 1988). Au niveau pré-synaptique, le neuropeptide Y est libéré des terminaisons nerveuses sympathiques et inhibe la libération de l'acétylcholine (Potter, 1985). L'acétylcholine libérée par les fibres nerveuses vagues inhibe la libération de la noradrénaline des terminaisons nerveuses sympathiques (Lavallée et coll., 1978). La stimulation sympathique exerce un effet chronotrope et inotrope positif qui est atténué par un tonus vagal concomitant élevé (Takahashi et Zipes, 1983).

2.4 Le système nerveux intrinsèque

Les ganglions cardiaques intrinsèques qui sont le chemin final commun impliqué dans la régulation cardiaque (Armour, 1994) sont composés de neurones post-ganglionnaires efférentes parasympathiques et sympathiques (Butler et coll., 1990), de neurones du circuit local (Gagliardi et coll., 1988), et de neurones afférentes (Ardell et coll., 1991). À l'intérieur du réseau neural intrapéricarde qui contrôle le cœur, il existe des points de convergence intracardiaque spécifiques où les influx bilatéraux autonomes se rejoignent avant de se distribuer sélectivement aux tissus du pacemaker, de conduction, et de

contraction (Pardini et coll., 1987). Chez le chien, ces points de convergence sont constitués de plusieurs ganglions de différentes tailles localisés dans du tissu adipeux situé sur l'épicarde et en association avec un ou plusieurs troncs de nerfs (Gagliardi et coll., 1988). Sept plexi ganglionnaires ont été identifiés dans le système nerveux intrinsèque canin (Yuan et coll., 1994); quatre dans l'oreillette et trois dans le ventricule.

Dans l'oreillette les plexus ganglionnaires sont (Figure 2):

- 1) **PGOD**- plexus ganglionnaire de l'oreillette droite situé dans le pannicule adipeux sur la surface ventrale du complexe commun de la veine pulmonaire droite. Celui-ci est associé au contrôle neural du nœud sinusal.
- 2) **PG(OGI-VCI)**- plexus ganglionnaire situé à la jonction de l'oreillette gauche inférieure et de la veine cave inférieure. Celui-ci module les tissus de conduction de l'oreillette inférieure et du nœud A-V (Ardell et Randall, 1986).
- 3) **PGOGd**- plexus ganglionnaire de l'oreillette gauche dorsale situé sur la surface dorsale de l'oreillette entre les veines pulmonaires communes, caudal à l'artère pulmonaire droite. Celui-ci est le principal modulateur des tissus contractiles (Yuan et coll., 1993).
- 4) **PGOGv**- plexus ganglionnaire de l'oreillette gauche ventrale qui est contenu à l'intérieure du pannicule adipeux sur l'aspect caudale-ventrale de l'oreillette gauche, adjacent au sillon AV (Armour and Hopkins, 1990). Ce plexi comprend les composantes céphaliques, intermédiaires et caudales (Yuan et coll., 1993).

Chez l'humain, dix plexi ganglionnaires ont été identifiés (Armour et coll., 1997), cinq dans l'oreillette et cinq dans le ventricule. Au moins 14 000 neurones sont associés au

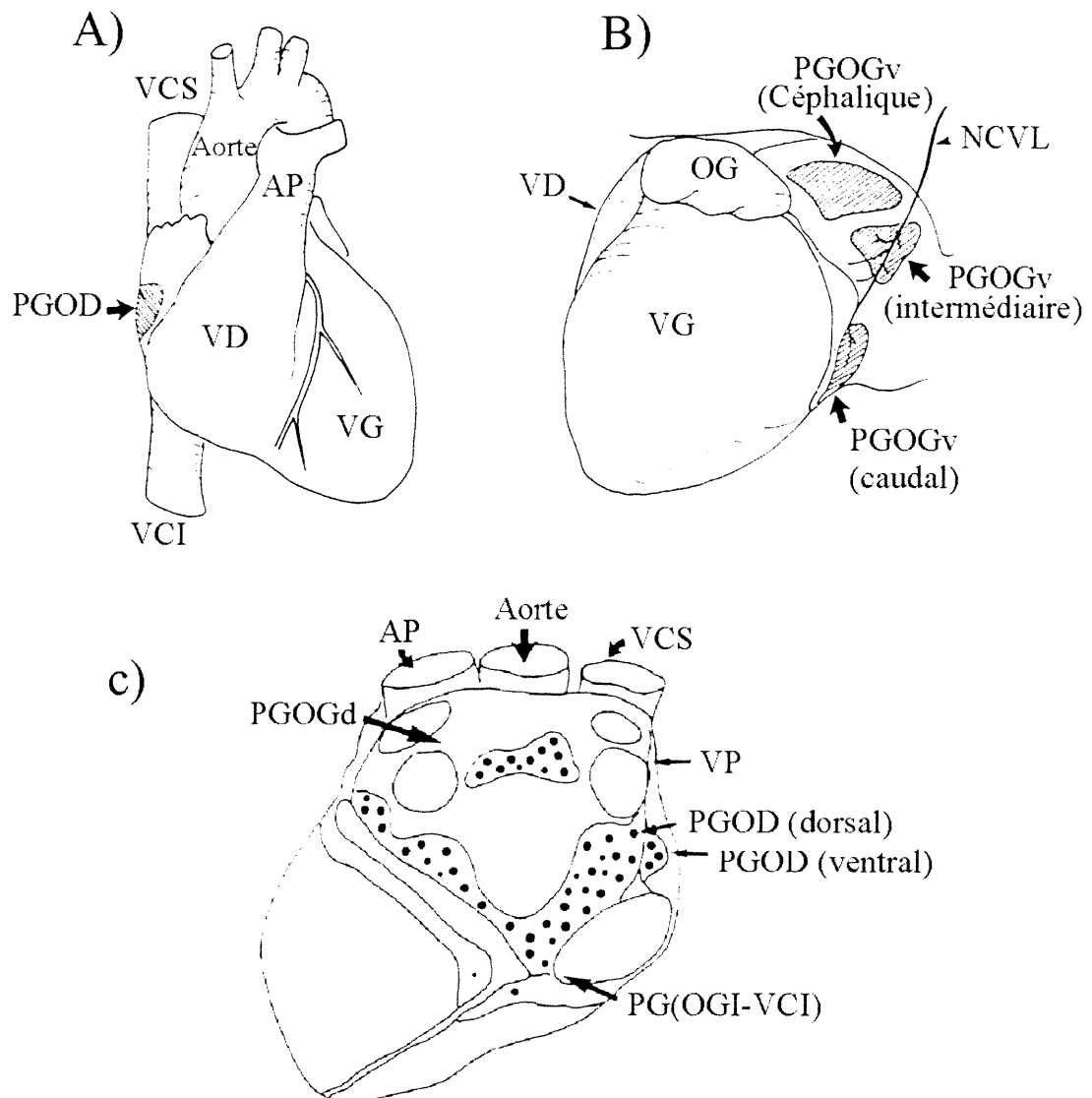


FIGURE 2. Les plexus ganglionnaires auriculaires chez le chien. Localisation anatomique des plexus ganglionnaires situés dans les pannicules adipeux des oreillettes. A) et B)- Vues ventrales du cœur C) -vue dorsale du cœur. PGOD- plexus ganglionnaire de l'oreillette droite, VCS- veine cave supérieure, VCI- veine cave inférieure, AP- artère pulmonaire, VD- ventricule droit, VG- ventricule gauche, OG- oreillette gauche, PGOGv- plexus ganglionnaire de l'oreillette gauche ventrale, NCVL- nerf cardiaque ventro-latéral, PG(OGI-VCI)- plexus ganglionnaire situé à la jonction de l'oreillette gauche inférieure et de la veine cave inférieure, PGOGd- plexus ganglionnaire de l'oreillette gauche dorsale, VP- veines pulmonaires (modifié de Yuan et coll., 1994).

cœur humain, ce qui est le double de ce qu'on trouve dans le cœur de chien (Yuan et coll., 1994). La longueur moyenne des neurones cardiaques intrinsèques chez l'humain (39 μm) est plus grande que celle mesurée chez le chien (25 μm) et distribuée de façon uniforme à travers les ganglions. Cependant, les neurones chez le chien sont plus à la périphérie des ganglions avec des projections vers le centre.

2.5 Le système nerveux autonome et les courants

2.5.1 Interaction avec une stimulation bêta-adrénergique

La régulation autonome change les propriétés des courants membranaires des cellules cardiaques et modifie les caractéristiques du potentiel d'action, ce qui affecte la performance cardiaque.

La stimulation adrénérge peut affecter une grande variété de canaux ioniques cardiaques. L'activation des récepteurs bêta-adrénérge va accroître $I_{\text{Ca,L}}$ par une voie qui implique l'activation de la protéine Gs qui augmente l'adénylate cyclase. Ceci augmente le niveau d'AMPc qui va activer une protéine kinase A et phosphoryler le canal calcique (Trautwein et Hescheler, 1990). L'augmentation de $I_{\text{Ca,L}}$ par une stimulation bêta-adrénérge des tissus auriculaires provoque une élévation du plateau (vers une valeur plus positive) du potentiel d'action (Hartzell, 1988). Cependant, la stimulation bêta-adrénérge n'a pas d'effet sur $I_{\text{Ca,T}}$ dans les cellules auriculaires chez le chien (Bean, 1985). Les effets de la stimulation bêta-adrénérge sur le courant

sodique sont très controversés. Une stimulation bêta-adrénergique par l'isoprotérénol va accroître I_{NA} cardiaque chez le rat et le lapin par un mécanisme dépendant et indépendant de la protéine G (Matsuda et Shibata, 1992; Kirstein et coll., 1996; Lu et coll., 1999). Chez l'humain, la stimulation de la PKA via l'AMPc augmente significativement la conductivité des canaux sodiques (Frohnwieser et coll., 1997). Par contre, chez le chien, des études ont démontré que l'isoprotérénol inhibe I_{NA} (Ono et coll., 1993) mais que cela dépend aussi des conditions expérimentales utilisées (Gintant et Liu, 1992). Cragun et coll. (1997) ont démontré chez le chien que la stimulation bêta-adrénergique avec l'administration de la flécainide (antiarythmique de la classe IC qui déprime I_{NA}) réduit I_{NA} plus qu'avec la flécainide seule. La stimulation bêta-adrénergique augmente aussi le courant potassique ("delayed rectifier") I_{Ks} et non I_{Kr} (Sanguinetti et coll., 1991) par un mécanisme dépendant de la protéine G (Harvey et Hume, 1989a). Cependant, Koumi et coll. (1995) ont démontré que le courant potassique I_{K1} est supprimé par une stimulation adrénergique. Un autre courant potassique, I_{Kur} , joue un rôle significatif dans la repolarisation auriculaire humaine (Wang et coll., 1993) et il est augmenté par un agoniste bêta-adrénergique (Li et coll., 1996). Chez le chien, la stimulation bêta-adrénergique augmente I_{Kur} via des protéines kinase A et C (Yue et coll., 1999). Un autre courant activé par la stimulation bêta-adrénergique est un courant de chlore (I_{Cl}) dépendant de l'AMPc (Harvey et Hume, 1989b). L'activation de ce courant aide à raccourcir le potentiel d'action. La stimulation bêta-adrénergique accroît $I(f)$ chez le mouton (Earm et coll., 1983) et l'humain (Porciatti et coll., 1997) et provoque un déplacement vers les potentiels positifs de la courbe d'activation du courant. De plus, Sorota et coll. (1999) ont démontré que

l'isoprotérénol peut également activer $I_{K,ACH}$ dans les myocytes auriculaires chez le chien, ce qui raccourcit d'avantage le potentiel d'action.

2.5.2 Interaction avec l'acétylcholine

L'acétylcholine n'a peu ou pas d'effet sur les niveaux basaux de I_{Ca} . Par contre, l'acétylcholine inhibe l'augmentation de I_{Ca} produite par une stimulation bêta-adrénergique via la protéine G_i . Cette dernière empêche la formation d'AMPC en inhibant l'adénylate cyclase (Watson et coll., 1988). L'acétylcholine seule ne modifie pas le courant potassique I_K . Cependant, l'amplification de I_K par l'isoprotérénol peut être inhibée par l'acétylcholine (Harvey et Hume, 1989b). Le courant potassique I_{K1} , qui est supprimé par l'activation des récepteurs bêta-adrénergiques, peut redevenir activé par l'acétylcholine. L'inhibition de la suppression causée par l'isoprotérénol implique des mécanismes intracellulaires et membranaires (Koumi et coll., 1995). Le courant chlore, activé par l'AMPC suite à une stimulation bêta-adrénergique, peut être supprimé par une stimulation simultanée du récepteur muscarinique (via l'acétylcholine) (Harvey et Hume, 1989b). L'acétylcholine agit aussi sur $I(f)$ en déprimant ce courant (Renaudon et coll., 1997). La stimulation vagale ou l'acétylcholine active également $I_{K,ACH}$ (Kurachi et coll., 1986) et raccourcit la durée du potentiel d'action et la période réfractaire.

2.6 Le système nerveux autonome et les arythmies

Le système nerveux autonome joue un rôle dans la genèse des arythmies ventriculaires parce que toute augmentation du tonus sympathique peut induire une arythmie. Dans la fibrillation ou le flutter auriculaire qui sont des arythmies plus communes, le système nerveux autonome joue un rôle plus complexe (Leclercq et coll., 1996). Un changement abrupt dans le tonus autonome est un facteur important pour l'initiation des tachycardies ventriculaires (Fei et coll., 1994) et de la fibrillation auriculaire paroxystique (Coumel, 1990; Coumel, 1992). Les tachycardies causent généralement une baisse initiale de la pression artérielle qui déclenche une compensation sympathique et un retrait vagal (Waxman et coll., 1982). Une fois l'arythmie déclenchée, les changements du tonus autonome peuvent exercer des effets significatifs qui dépendent de la localisation, de l'innervation et de la réponse au tonus du système nerveux autonome (Waxman et coll., 1983).

Wen et coll. (1998) ont démontré, en regardant la variabilité du rythme cardiaque, qu'une augmentation dans la modulation sympathique et/ou une diminution du tonus vagal pouvaient faciliter l'initiation du flutter auriculaire typique. Coumel (1989) a démontré deux modes de comportements différents précédant une attaque de fibrillation auriculaire paroxystique chez des patients. En observant les changements du rythme cardiaque précédant les arythmies, il a distingué une fibrillation auriculaire paroxystique d'origine vagale et une autre d'origine adrénérergique. La fibrillation auriculaire d'origine vagale est prédominante chez les hommes (4 hommes : 1 femme) et apparaît entre l'âge

de 40 et 50 ans. Cette arythmie est idiopathique et les événements se produisent surtout la nuit et se terminent le matin. D'autres facteurs prédisposants sont : le repos, les périodes de digestion (surtout après les repas), l'absorption d'alcool ou les périodes de repos suivant un stress ou un effort. Une bradycardie progressive précède l'arythmie, ce qui reflète la prédominance vagale. Les fibrillations auriculaires paroxystiques d'origine adrénergique sont moins fréquemment observées et peuvent se produire chez des patients atteints d'hyperthyroïdie, de phéochromocytome, ou de cardiomyopathie. Les palpitations se produisent exclusivement le jour, surtout le matin, pendant l'exercice ou durant un stress émotionnel. L'arythmie est précédée par une accélération sinusale rapide, durant l'exercice, par exemple.

3. Électrophysiologie du coeur

L'impulsion électrique cardiaque origine d'une dépolarisation transitoire des tissus du noeud sinusal dans le haut de l'oreillette droite proche de la veine cave supérieure . Ceci provoque un front d'activation qui traverse le tissu de conduction spécialisé des oreillettes jusqu'au noeud auriculo-ventriculaire (A-V) (Fogoros, 1997). Dans les fibres de l'oreillette, la phase 0 est rapide et le potentiel d'action a une durée assez courte. Les cellules du noeud A-V ont des potentiels d'action à réponses très lentes caractérisés par un temps de conduction long (délai du noeud AV). Le front d'activation passe par le faisceau de His vers les branches principales droite et gauche du faisceau de Purkinje qui se divisent en fibres de plus en plus petites jusqu'aux fibres terminales de Purkinje. Celles-ci sont en contact direct avec les cellules du myocarde et la réponse finale est une

excitation des cellules musculaires du ventricule. Les fibres ventriculaires ont des potentiels d'action d'une durée plus longue que les fibres auriculaires (Lathers et O'Rourke, 1992). L'impulsion crée après son passage un tissu réfractaire qui ne peut pas être excité pendant 200-400 ms. Lorsque les dernières fibres du muscle cardiaque ont été excitées, tout le tissu est réfractaire. Après une période de latence électrique, le tissu cardiaque redevient excitable et une nouvelle impulsion est générée dans le noeud sinusal. Dans un coeur normal, cette séquence d'événements est répétée 50-90 fois par minute (Wit et Cranefield, 1978) (Figure 3).

4. Les arythmies

Les arythmies cardiaques peuvent se produire suite à un dérangement dans le fonctionnement des cellules cardiaques ou à des anomalies anatomiques. Ce trouble des cellules peut être local ou généralisé, mais il produit de toute manière un fonctionnement désordonné de tout le coeur (Janse, 1993). Les arythmies cardiaques peuvent être supraventriculaires ou ventriculaires (Fogoros, 1997). Les tachycardies supraventriculaires impliquent le noeud A-V ou l'oreillette. Les types d'arythmies dans l'oreillette sont la tachycardie sinusale, la réentrée autour du noeud sinusal, la tachycardie auriculaire, le flutter auriculaire et la fibrillation auriculaire. Les arythmies impliquant le noeud A-V sont la réentrée dans le noeud A-V et la réentrée A-V (voies accessoires, par exemple le syndrome de Wolff-Parkinson-White) (Prystowsky et Klein, 1994). Des arythmies ventriculaires peuvent également se former, comme la tachycardie ventriculaire et la fibrillation ventriculaire.

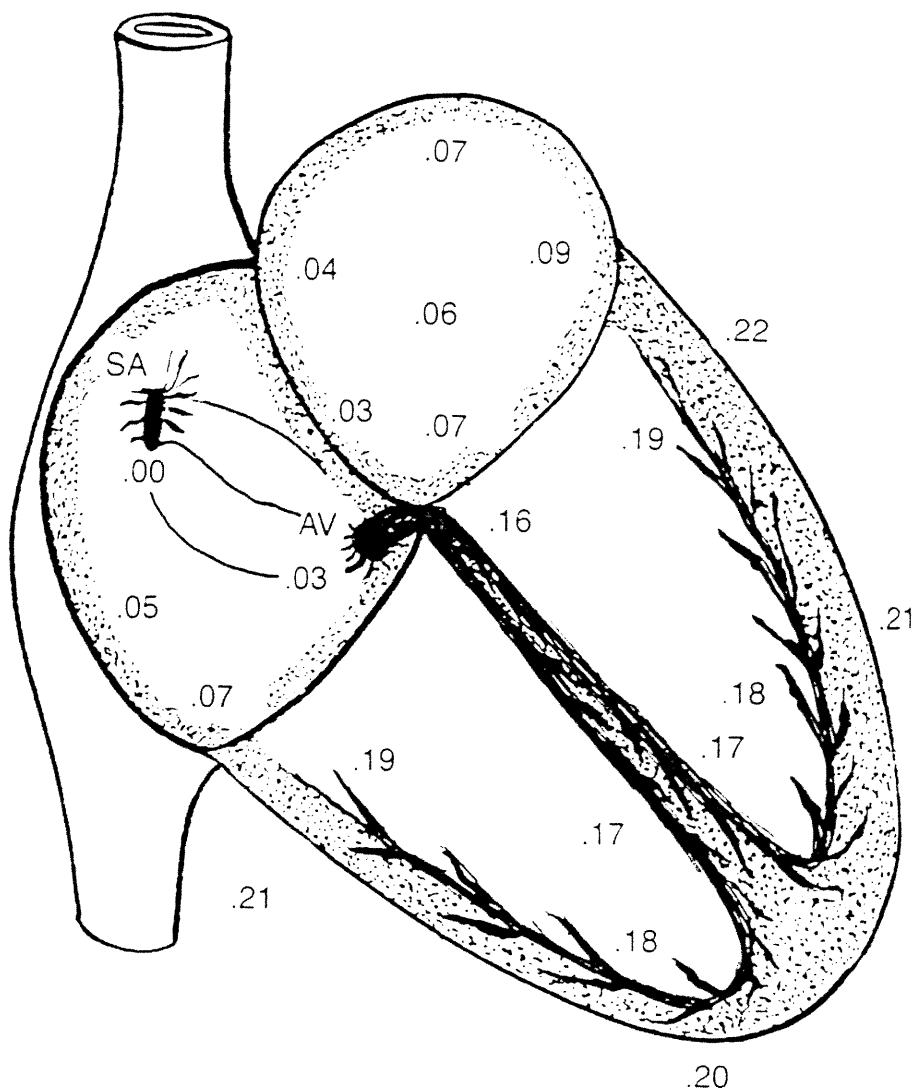


FIGURE 3. Les temps d'activation autour d'un cycle cardiaque normal. L'impulsion débute dans le nœud sinusal (SA), elle se dirige tout en traversant les oreillettes vers le nœud A-V (AV), et par la suite elle voyage par le faisceau de His, vers les deux branches de Purkinje et elle se divise en fibres de plus en plus petites jusqu'aux fibres terminales de Purkinje. (Guyton, 1991) Les chiffres indiquent le temps d'activation en secondes.

Cette dernière représente un désorganisation de dépolarisation rapide et irrégulière du myocarde qui est associé à la mort subite (Franz et coll., 1994).

4.1 Les mécanismes des arythmies

Les trois mécanismes principaux des arythmies sont: 1) l'automatisme anormale, 2) la réentrée, et 3) les post-dépolarisations. (Fogoros, 1997). Les arythmies par anomalie d'automatisme se produisent lorsque la fréquence d'activation du coeur par le noeud sinusal atteint des valeurs inférieures à la fréquence intrinsèque des pacemakers subsidiaires ou lorsque la fréquence d'activation spontanée d'un pacemaker subsidiaire augmente (Janse 1993). Il y a une accélération anormale de l'activité de la phase 4 du potentiel d'action. Par exemple, sous l'influence du système nerveux autonome, les pacemakers subsidiaires peuvent se dépolariser à des fréquences plus rapides que celui du noeud sinusal et ainsi diriger le rythme cardiaque (Lathers et O'Rourke, 1992). Le deuxième mécanisme, la réentrée, implique un bloc unidirectionnel de la conduction qui permet la circulation d'une impulsion autour d'un obstacle (voir 5.1). Le troisième mécanisme implique le mouvement d'ions à charge positive dans la cellule cardiaque. Les influx ioniques causent une post-dépolarisation vers la fin de la phase 3 ou début de la phase 4. Si les post-dépolarisations sont assez larges, ils peuvent déclencher l'ouverture des canaux sodiques et générer un nouveau potentiel d'action (Fogoros, 1997).

5. Le flutter auriculaire

Le flutter auriculaire chez l'humain est parmi les arythmies les plus difficiles à contrôler avec des thérapies pharmacologiques. Pour améliorer l'efficacité des médicaments antiarythmiques, il faut d'abord comprendre le mécanisme responsable soit une réentrée.

Le flutter auriculaire peut être souvent un rythme persistant ou paroxystique qui a une durée variable, de quelques secondes à quelques heures, et occasionnellement d'une journée ou plus. Un flutter persistant, qui est stable avec un rythme chronique, est moins fréquent parce que, avec ou sans traitement, il peut s'interrompre spontanément ou dégénérer en fibrillation auriculaire (Waldo, 1995). Dans une étude menée récemment au Wisconsin aux États-Unis par Granada et coll. (2000), il y a eu 181 nouveaux cas diagnostiqués pendant quatre ans sur 58,820 résidents. L'incidence chez l'homme était deux fois plus élevée que chez la femme. En projetant leur résultats à toute la population des États-Unis, ces investigateurs ont trouvé que l'incidence serait 88/100,000 personnes par année. Les individus ayant une histoire d'insuffisance cardiaque ou une maladie pulmonaire obstructive chronique avaient un risque plus élevé à développer le flutter auriculaire. Le flutter auriculaire est aussi très commun chez des patients dans la première semaine après une chirurgie à coeur ouvert. Dans cette population il y a une incidence de 30% de tachycardies supraventriculaires dans lequel un tiers sont des flutters auriculaires (Waldo et MacLean, 1980).

Le terme "flutter auriculaire" a été proposé par Jolly et Ritchie (1910) pour décrire une arythmie auriculaire ectopique avec une rapidité régulière, présentant typiquement des ondes en dent de scie sur l'électrocardiogramme de surface dans les dérivations inférieures II, III et aVF. Cette arythmie est divisée en deux types: 1) le flutter du type commun ou classique et, 2) le flutter du type non-commun (Wells et coll., 1979). La plupart des patients avec un flutter auriculaire souffrent d'une maladie cardiaque. L'hypertension, la maladie coronarienne athérosclérotique, la maladie de la valve mitrale, la maladie congénitale et la cardiomyopathie sont parmi les pathologies sous-jacentes les plus communes (Josephson, 1993). Le premier type de flutter a des fréquences auriculaires entre 240 et 320 battements par minute et il peut toujours être renversé par une stimulation rapide. Ce type de flutter est le résultat d'un mouvement de réentrée de l'impulsion auriculaire dans un trajet qui possède un créneau d'excitabilité. (voir 5.1.1) Le deuxième type de flutter est plus rapide que le premier avec des fréquences auriculaires entre 340 et 430 battements par minute (Waldo et coll., 1984). Celui-ci ne peut pas être renversé par une stimulation rapide et il est le résultat d'une réentrée de type "leading circle" (voir 5.1.2) où l'impulsion circule autour d'une barrière fonctionnelle dans un trajet sans créneau d'excitabilité (Allessie et coll., 1977).

5.1 Le mécanisme du flutter auriculaire

- la réentrée

Le mécanisme responsable du flutter auriculaire est la réentrée (Lewis et coll., 1920).

Pour que la réentrée se produise, les conditions suivantes sont requises:

- 1) deux voies conductrices par lesquelles une impulsion électrique peut se propager
- 2) un bloc unidirectionnel antérograde (dans le sens de l'activation normale) dans une de ces voies
- 3) une conduction rétrograde lente dans la région du bloc antérograde
- 4) la réactivation du tissu de la voie normale (Mines, 1913; Garrey, 1914).

Un bloc unidirectionnel peut se former dans du tissu cardiaque endommagé ou ischémique. Un potentiel d'action arrivant aux cellules en aval du bloc par une autre voie normale, se propage tellement lentement dans la direction rétrograde que les cellules en amont du bloc unidirectionnel sont de nouveau excitables. Les cellules en avant du front de propagation terminent leur période réfractaire effective à temps permettant la recirculation du potentiel d'action (Lathers et O'Rourke, 1992) (Figure 4).

A chaque instant pendant la propagation de l'impulsion, une partie du circuit est complètement réfractaire et ne peut pas être excitée. Cette portion est suivie d'une autre portion partiellement réfractaire et, lorsque le temps de circulation est assez long, d'une dernière portion qui contient du tissu complètement excitable. Ces deux dernières composantes constituent le créneau d'excitabilité du circuit de réentrée (Figure 5). Le flutter auriculaire commun chez l'humain résulte d'un circuit de réentrée macroscopique dans l'oreillette droite délimitée à la face antérieure par l'anneau de la valve tricuspide (Cosio et coll., 1996). Dans le flutter auriculaire humain typique circulant dans le sens inverse des aiguilles d'une montre, le front de réentrée procède dans une direction latérale vers une direction septale le long du tissu de l'isthme entre la veine cave inférieure et la valve tricuspide, passe entre l'anneau tricuspide et la crête d'Eustache

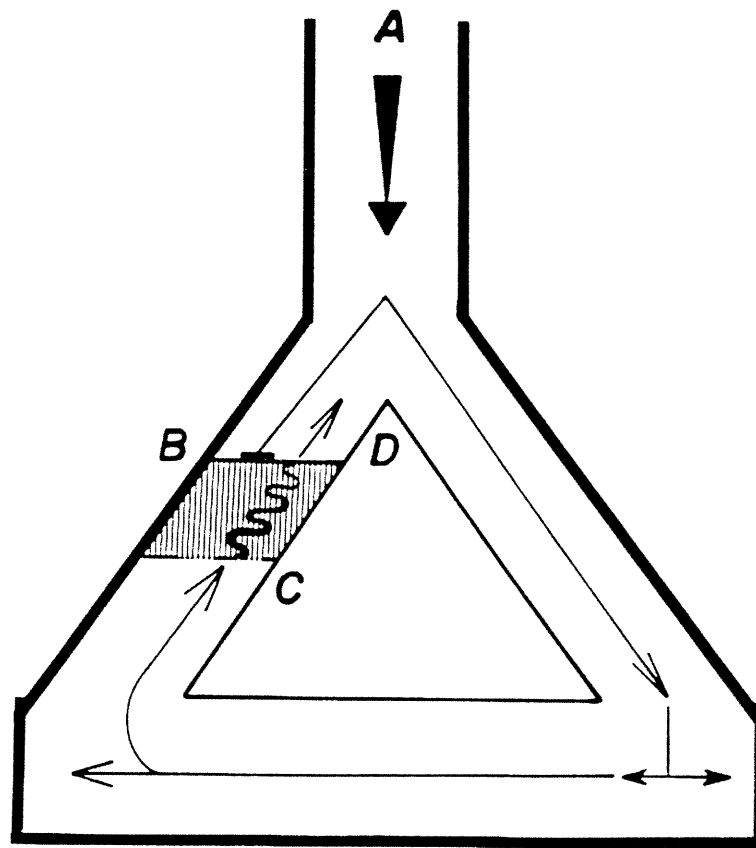


FIGURE 4. Modèle de la réentrée. Une impulsion entre dans le système (A). La propagation antérograde est bloquée (à gauche) à un site où la conduction est déprimée (B), mais elle se propage normalement à travers la voie droite. L'impulsion par la suite se propage dans la direction rétrograde de la voie gauche (C) où elle rencontre la région déprimée. Elle se propage lentement dans cette région et elle atteint du tissu normal, déjà repolarisé (D), et donc l'impulsion va réentrer dans le système conducteur (Rosen, 1981).

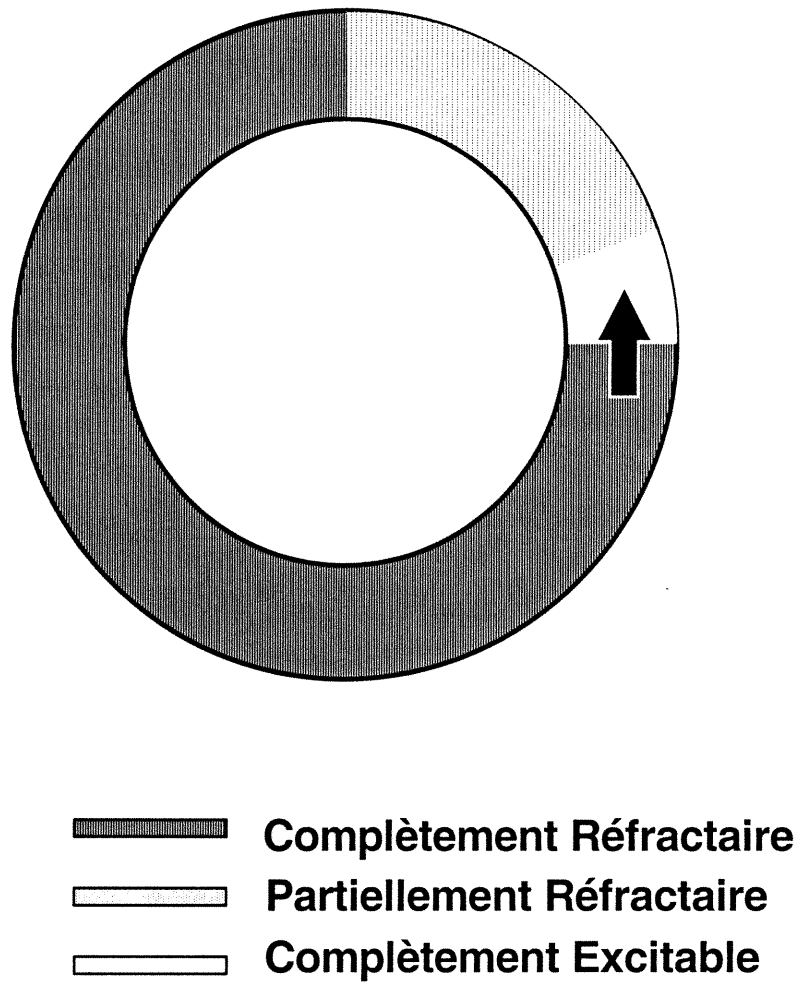


FIGURE 5. Circuit de réentrée avec son créneau d'excitabilité.

(situé entre la veine cave inférieure et l'ostium du sinus coronaire) et par la suite se propage vers le haut du septum dans une direction cranio-caudale (Nakagawa et coll., 1996) (Figure 6).

5.1.1 Réentrée autour d'un obstacle anatomique

La réentrée peut se produire autour d'un obstacle inexcitable tel qu'une cicatrice (obstacle anatomique) (Boyden, 1991). Ce type de réentrée peut se produire sur un circuit défini, si la longueur du circuit est grande, si la vitesse de conduction de l'impulsion circulante est basse, ou si la période réfractaire est courte. La longueur du chemin de l'impulsion circulante est déterminée par le périmètre de l'obstacle anatomique (Mines, 1913). Ce type de réentrée est caractérisé par: 1) une longueur et une localisation fixes du circuit, 2) l'existence d'un espace de tissu excitable entre la queue et la tête de l'onde dépolarisante, et 3) une fréquence d'arythmie qui est proportionnelle à la vitesse de conduction et inversement proportionnelle à la longueur du circuit (Figure 7A).

5.1.2 Réentrée autour d'un obstacle fonctionnel

La réentrée qui n'est pas reliée à un obstacle anatomique, circule autour d'un circuit qui est défini par les propriétés électrophysiologiques des fibres qui le composent (obstacle fonctionnel). L'impulsion dans ce type de réentrée "leading circle", prend le chemin le plus court. Dans ce cas, l'efficacité du stimulus du front circulant est suffisant pour exciter le tissu en aval qui est encore dans sa phase réfractaire relative.

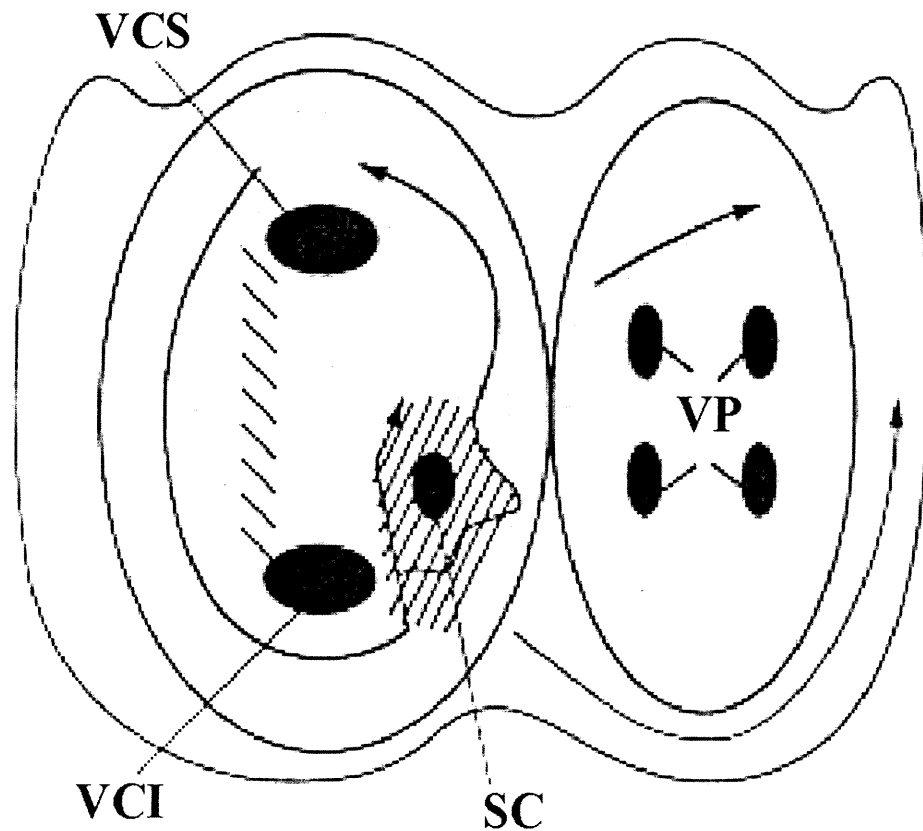


FIGURE 6. L'activation auriculaire dans le flutter auriculaire

typique humain. Schémas représentant les oreillettes dans une vue oblique antérieure gauche. L'endocarde est ombré et les ouvertures de la veine cave supérieure (VCS), la veine cave inférieure (VCI), du sinus coronaire (SC) et les veines pulmonaires (VP) sont démontrées. La direction de l'activation est indiquée par les flèches. Les régions hachurées démontrent les localisations approximatives des zones de conduction lente et de bloc (modifié de Cosio et coll., 1996; Waldo, 2000).

L'obstacle fonctionnel dans ce "leading circle" est activée par de petites vagues centripètes qui sortent du cercle et font collision dans le centre du circuit (Allessie et coll., 1977). L'impulsion se propage uniformément autour du circuit. La tête du front circulant est bloquée par sa propre queue relativement réfractaire et il n'y a pas de créneau d'excitabilité. Ce type de réentrée est caractérisé par: 1) une longueur et une localisation du circuit variable, 2) une longueur du circuit électrique égale à la longueur de l'onde dépolarisante, 3) aucun espace de tissu excitable à l'intérieur du circuit, et 4) une période d'arythmie qui est proportionnelle à la période réfractaire du tissu (Allessie et coll., 1977; Janse, 1993) (Figure 7B)

6. Le créneau d'excitabilité d'une réentrée et la méthode du

"Reset-Response"

La méthode du "reset-response" détermine les caractéristiques électrophysiologiques du créneau d'excitabilité d'un circuit de réentrée (Stamato et coll., 1989). Des stimuli prématurés déclenchés durant une réentrée soutenue peuvent interagir avec le rythme et peuvent faire avancer le battement suivant de la tachycardie (Strauss et coll., 1973).

Lorsqu'un stimulus prématuré est introduit dans le circuit de réentrée, l'intervalle de couplage, qui est la distance entre le dernier complexe de la tachycardie et la réponse au stimulus prématuré, peut être mesurée. L'intervalle entre la réponse au stimulus et le prochain battement du flutter peut aussi être mesurée, ce qui constitue le cycle de retour.

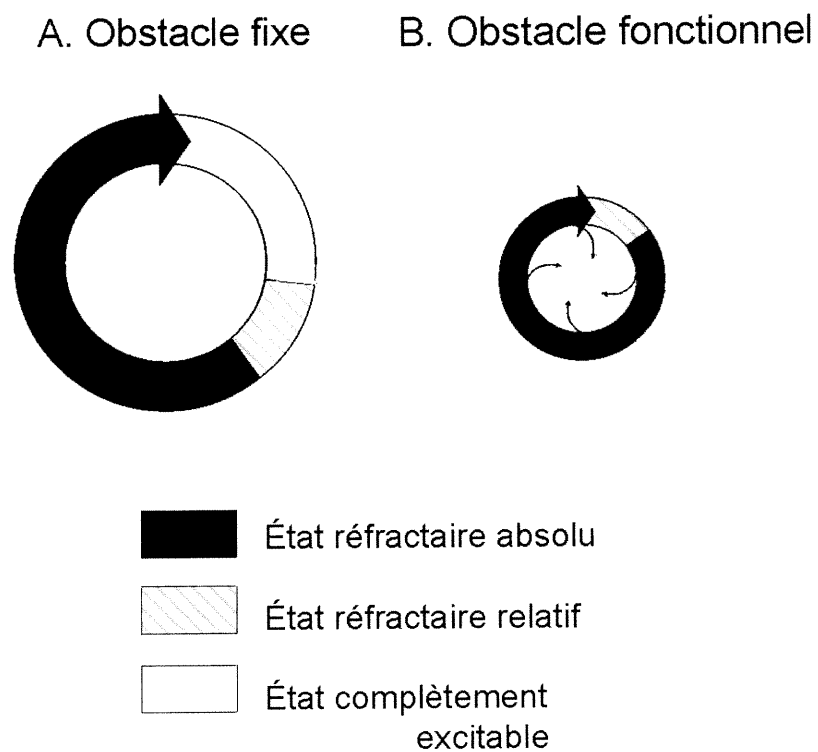


FIGURE 7. Réentrée autour d'un obstacle fixe (A) avec possibilité de tissu excitable, par rapport à une réentrée autour d'un obstacle fonctionnel (B) sans tissu excitable à l'intérieur du circuit. (Mines, 1913; Allesie et coll., 1977; modifié de Hélie et coll., 1993).

Ce stimulus prématuré a fait un "reset" de la tachycardie en déclenchant le battement suivant plus tôt qu'en absence de stimulation. Le "reset" démontre que la réponse prématurée est entrée dans le circuit et qu'elle a avancé le battement suivant de la tachycardie.

Les types de réponse obtenue durant le "reset" sont caractérisés par la relation entre le cycle de retour et l'intervalle de couplage du stimulus prématuré.

Il existe trois différentes courbes de réponse "reset-response"; la courbe plate, la courbe ascendante, et la courbe mixte (Almendral et coll., 1986). Une réponse plate démontrant le même temps de conduction du battement prématuré à différents intervalles de couplage suggère qu'à ces intervalles il y a récupération complète d'excitabilité dans le circuit de réentrée (Figure 8). Donc, une courbe plate à des intervalles de couplage long dans le créneau d'excitabilité indique que, au cycle de la tachycardie, l'impulsion du circuit de réentrée rencontre du tissu complètement excitable (Bernstein et Frame, 1987). Un stimulus émis à des intervalles de couplage plus court, prolongera le prochain cycle de la tachycardie, et la courbe sera ascendante. Cette courbe suggère que l'impulsion rencontre du tissu partiellement réfractaire dans au moins une partie du circuit. Une courbe mixte est composée d'une portion ascendante (tissu partiellement réfractaire) et d'une portion plate (tissu complètement excitable) (Frame et coll., 1986; Almendral et coll., 1986; Bernstein et Frame, 1987). Une stimulation bloquée signifie qu'elle a atteint du tissu complètement réfractaire.

Les courbes "reset-response" ont été utilisées jusqu'à présent pour estimer les caractéristiques globales du circuit de réentrée en clinique (Almendral et coll., 1986;

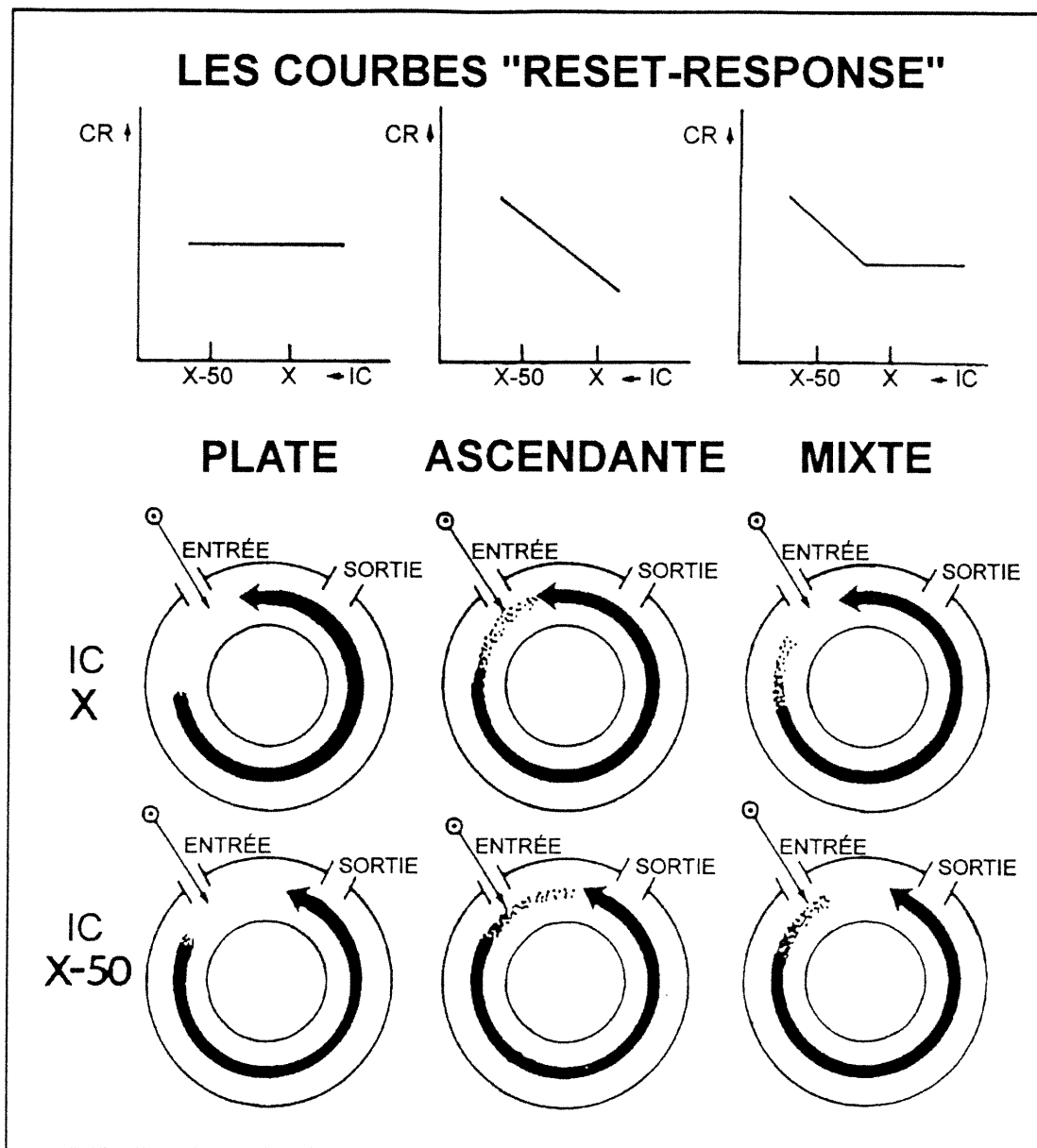


FIGURE 8. Représentation schématique des 3 courbes « Reset-Response » observées durant une tachycardie ventriculaire. En traçant point par point la relation entre l'intervalle de couplage (IC) du stimulus prématuré en abscisse et le cycle de retour (CR) en ordonnée, une courbe plate, ascendante ou mixte a été observée (en haut). En bas, des circuits de réentrée avec leur entrée et sortie sont démontrés durant une tachycardie ventriculaire. Ces diagrammes illustrent ce qui arrive lorsqu'un stimulus prématuré

entre dans le circuit à deux temps différents : à $IC = X$ et à $IC = X-50$, durant les trois courbes différentes. Dans le circuit où la courbe est plate, le stimulus prématuré a rencontré du tissu complètement excitable à $IC = X$ et à $IC = X-50$ partout dans le circuit. Dans la courbe ascendante, le stimulus a rencontré du tissu partiellement réfractaire à X et à $X = 50$ dans au moins une partie du circuit. Le stimulus prématuré dans la courbe mixte a rencontré du tissu complètement excitable à $IC = X$ et du tissu partiellement réfractaire à $IC = X-50$ (Modifié de Stamato et coll., 1989).

Della Bella et coll., 1991; Jalil et coll., 1998) et dans les modèles expérimentaux (Frame et coll., 1986; Kus et coll., 1991, Jalil et coll., 1997). Des études antérieures chez l'humain dans la tachycardie ventriculaire (Callans et coll., 1996) et le flutter auriculaire (Callans et coll., 1997) ont démontré qu'il y avait des différences dans la courbe "reset-response" selon le site de stimulation, dans la tachycardie ventriculaire chez le lapin (Boersma et coll., 1994) et chez le chien (Hanna et Coll., 2001). En présence d'une région du circuit où la conduction est intervalle-dépendante, Ingelmo et Frame (2000) ont démontré in-vitro que la forme de la courbe "reset-response" était différente quand les stimuli étaient introduits de façon distal plutôt qu'une localisation proximal à cette région. De plus, Frame et coll. (1987) ont étudié la conduction de l'impulsion de réentrée autour d'un anneau tricuspide en utilisant une matrice d'électrodes intracavitaires portant 96 électrodes bipolaires. Ces investigateurs ont démontré qu'en absence de médicament, la réentrée était uniforme et que la conduction n'était ralentie dans aucune partie du circuit de réentrée.

7. Des études antérieures du flutter auriculaire chez les animaux

Plusieurs modèles de flutter auriculaire chez des animaux ont été développés au cours des années pour produire des flutters auriculaires qui se rapprochent de celui observé chez l'humain. Frame et coll. (1986) ont modifié un modèle de réentrée auriculaire chez le chien en ajoutant à l'incision entre les deux veines caves (Rosenblueth et Garcia Ramos, 1946; Kimura et coll., 1954; Lanari et coll., 1956) une autre incision s'étendant vers l'appendice de l'oreillette droite, de telle sorte que les incisions créent un "Y". Ces

chercheurs ont plus tard découvert, en faisant de la cartographie auriculaire de la séquence d'activation, que la réentrée auriculaire circulait autour de la valve tricuspide (Frame et coll., 1987). Boyden et coll. (1989) ont aussi reproduit le modèle de Frame et coll. (1986) pour démontrer les séquences d'activations durant l'entraînement du circuit par stimulation rapide. Crijns et coll. (1993), ont également reproduit ce modèle de flutter auriculaire (Frame et coll., 1986) chez le cochon.

Boyden et Hoffman (1981) ont développé un modèle différent de flutter auriculaire chez le chien en agrandissant l'oreillette droite par une intervention chirurgicale. Dans ce modèle, il y a une dilatation progressive de l'oreillette droite qui résulte d'une insuffisance de la valve tricuspide et d'une obstruction partielle de l'artère pulmonaire. Le feuillet septal de la valve tricuspide est excisé à travers une atriectomie. Cette dilatation sensibilise l'oreillette pour induire une tachycardie qui ressemble au flutter.

Un autre modèle expérimental de flutter auriculaire chez le chien est un modèle de lésion produite en écrasant une région de l'oreillette droite (Feld et Shahandeh-Rad, 1992). Ce modèle est caractérisé par un circuit de réentrée autour d'un obstacle anatomique (la lésion) dans l'oreillette droite. Le tissu écrasé en conjonction avec l'anneau de la valve tricuspide forment un isthme de tissu auriculaire où la vitesse de conduction est plus lente que celle de l'oreillette durant le flutter auriculaire.

La péricardite stérile est un autre modèle chez le chien développé pour reproduire un flutter auriculaire en absence de lésion dans l'oreillette (Pagé et coll., 1986). Les surfaces de l'oreillette sont saupoudrées avec du talque en poudre à travers une

thoracotomie droite. Ces flutters ressemblent à ceux de patients ayant subi une chirurgie à coeur ouvert. Ce type de modèle produit souvent un flutter auriculaire très rapide ou même une fibrillation auriculaire à cause de la création d'un circuit fonctionnel plutôt qu'un circuit anatomique. Une autre forme de réentrée fonctionnelle, causant un flutter auriculaire, a été induite dans des cœurs isolés de chiens en infusant de l'acétylcholine (Allessie et coll., 1984).

De tous ces modèles de flutter auriculaire, seul le modèle de Frame et coll., (1986) produit un flutter auriculaire stable qui circule autour d'un circuit anatomique possédant un créneau d'excitabilité incluant une portion complètement excitable qui se rapproche de celles observées chez l'humain. La lésion en forme de "Y" sur l'oreillette chez le chien est donc le meilleur modèle représentatif du flutter auriculaire commun chez l'humain.

8. Les antiarythmiques

La classification des médicaments antiarythmiques proposée par Vaughan Williams (1975), regroupe les différents antiarythmiques en quatre classes, selon leurs effets électrophysiologiques prédominants sur le potentiel d'action (Dorian et Meyers, 1989; Lathers et O'Rourke, 1992). Les antiarythmiques de la classe I contiennent des bloqueurs du canal sodique qui réduisent le maximum de la phase 0 du potentiel d'action. Les antiarythmiques de la classe II sont des bloqueurs des récepteurs β -adrénergiques. Les antiarythmiques de la classe III contiennent des agents qui prolongent la période de

repolarisation et augmentent la durée du potentiel d'action. Les antiarythmiques de la classe IV sont formés de bloqueurs des canaux calciques.

Les antiarythmiques peuvent agir sur le circuit de réentrée en affectant la vitesse de conduction ou l'état réfractaire. Ces médicaments agissent en altérant les potentiels d'action transmembranaires des fibres cardiaques normales ou anormales par leurs effets sur les courants membranaires entrants et sortants ou par leurs effets sur des récepteurs (eg. adrénérgiques). Les antiarythmiques peuvent créer un bloc complet dans le circuit en transformant un bloc unidirectionnel en bloc bidirectionnel, abolissant ainsi la réentrée. Un autre mécanisme d'action des antiarythmiques pour éliminer une réentrée est d'augmenter la période réfractaire effective des fibres cardiaques (Dorian et Meyers, 1989).

En 1990, une nouvelle approche à la classification des médicaments a été proposé par le « Sicilian Gambit » (Colatsky, 1992). Le système Vaughan-Williams est basé sur l'identification des sites de la membrane cellulaire où un médicament produit son effet principal mais ne tient pas compte des autres effets de ces médicaments. Cependant, le « Sicilian Gambit » prend en considération les actions additionnels des médicaments antiarythmiques; le degré de bloc du canal, les effets agonistes et antagonistes sur les récepteurs, les effets sur la pompe sodium-potassium, le temps de liaison à un site cellulaire, les effets des seconds messagers, et l'affinité de la liaison dépendant de l'état de la cellule (activé ou inactivé). Par contre, le « Sicilian Gambit » n'est pas un véritable système de classification parce que c'est plutôt une liste de tout ce qui est

connu sur les médicaments. Néanmoins, le système de Vaughan-Williams demeure la classification la plus utile pour catégoriser les antiarythmiques (Fogoros, 1997).

8.1 La classe I

La classe I comprend les antiarythmiques qui bloquent les canaux sodiques rapides. Leurs effets cellulaires sont marqués par une dépression de la vitesse maximale de dépolarisation ($dV/dt \text{ max}$) du potentiel d'action (Franz et coll., 1994). A des concentrations cliniques, cette diminution de la phase 0 s'accompagne d'une augmentation du seuil d'excitabilité, d'une prolongation de la période réfractaire effective et d'une diminution de la vitesse de conduction. Ces médicaments de la classe I peuvent aussi diminuer la dépolarisation spontanée de la phase 4 dans les cellules pacemaker et la plupart ont des propriétés anesthésiques locales (Dorian et Myers, 1989). L'action des antiarythmiques de la classe I sur la repolarisation est variable. En se basant sur cette action et sur des données électrophysiologiques expérimentales et cliniques, cette classe peut être divisée en trois sous-groupes (Harrison, 1986).

8.1.1 Les sous-groupes de la classe I

Les agents de la classe IA agissent principalement en bloquant les canaux sodiques rapides avec une constante de dissociation entre 4-12 sec (Vaughan Williams, 1991; Grant, 1996), et donc ils diminuent la phase 0 de dépolarisation et ralentissent ainsi la vitesse de conduction. Ils augmentent aussi le temps de repolarisation, la période réfractaire et ils peuvent aussi diminuer l'automatisme. Les antiarythmiques de la classe

IA sont efficaces dans le traitement des arythmies auriculaires et ventriculaires. Dans cette classe on retrouve la quinidine, la procaïnamide et le disopyramide.

Les agents de la classe IB ont peu ou pas d'effet sur la vitesse maximale de conduction de la phase 0 des fibres normales, mais ils dépriment la conduction dans les fibres présentant une réponse déprimée rapide ou dans des fibres avec une membrane dépolarisée. Ils diminuent la durée du potentiel d'action et, à un moindre degré, ils diminuent la période réfractaire effective. Ces agents sont modérément utiles pour le traitement d'arythmies ventriculaires surtout en phase aiguë d'infarctus. Par contre, ils sont moins proarythmiques. Dans cette classe on retrouve la lidocaïne, la mexilétine, la tocainide et le phénytoïne.

Les agents de la classe IC dépriment considérablement le maximum de la phase 0 de dépolarisation, mais, contrairement aux agents de la classe IA, ils ne changent pas significativement la durée du potentiel d'action. Ces médicaments ont un effet plus prononcé sur le canal sodique que les autres sous-classes grâce à leurs cinétiques très lentes de liaison et de dissociation (entre 15-25 sec) (Vaughan Williams, 1991; Koller et Franz, 1994) au canal sodique. Dans cette classe on retrouve la flécaïnide, le propafénone et la moricizine (Lathers et O'Rourke, 1992; Franz et coll., 1994; Fogoros, 1997). Cependant, la moricizine possède des propriétés de la classe IA, IB et IC. Ce médicament n'a pas la même affinité que les autres antiarythmiques de la classe IC pour le canal sodique et donc diminue moins la vitesse de conduction que la flécaïnide et la propafénone, comme un médicament de la classe IA. De plus, la moricizine diminue les

périodes réfractaires comme un antiarythmique de la classe IB. Ce dernier est classifié un antiarythmique de la classe IC à cause des ses propriétés proarythmiques (Fogoros, 1997).

8.2 La classe II

Les antiarythmiques de la classe II sont des β -bloquants qui s'opposent aux effets de l'excitation sympathique cardiaque. Ces médicaments dépriment la phase 4 de dépolarisation et exercent leurs effets antiarythmiques par une inhibition compétitive du récepteur β -adrénergique. Parce que la stimulation adrénergique est plus prononcée dans le nœud sinusal et le nœud A-V, les β -bloqueurs ont le plus d'effets électrophysiologiques dans ces structures (Fogoros, 1997). Le propranolol est le prototype de cette classe. Le labétolol bloque non seulement les récepteurs β -adrénergiques mais également les récepteurs α adrénergiques. Le sotalol est un β -bloqueur qui possède des effets électrophysiologiques similaires à un médicament de la classe III, et il peut ainsi être catégorisé dans les deux classes. À de forte concentrations, la plupart des médicaments de cette classe démontrent des propriétés anesthésiques locales (Dorian et Meyers, 1989; Lathers et O'Rourke, 1992).

8.3 La classe III

Les médicaments antiarythmiques de la classe III agissent principalement en prolongeant la durée du potentiel d'action et des périodes réfractaires sans effet sur la vitesse

d'ascension de la phase 0 de dépolarisation et sur le potentiel membranaire de repos. Quelques exemples de médicaments de la classe III sont le sotalol, le brétylium, l'amiodarone et l'ibutilide. Cependant, quelques médicaments possèdent également des propriétés d'autres classes. Par exemple l'amiodarone a aussi des propriétés de la classe I, II et IV. Le d,l-sotalol est également un β -bloqueur (Dorian et Meyers, 1989; Lathers et O'Rourke, 1992).

8.4 La classe IV

Les antiarythmiques de la classe IV (le vérapamil et le diltiazem) bloquent sélectivement le canal lent entrant calcique se produisant durant les phases 0 à 2 du potentiel d'action cardiaque. Alors ces antiarythmiques diminuent encore l'amplitude et la vitesse d'ascension du potentiel d'action dans le noeud sinusal et le noeud A-V, et ils dépriment surtout la phase IV de la dépolarisation diastolique lente. À cause du ralentissement de la vitesse de conduction et de l'augmentation de la période réfractaire, la vitesse de conduction des impulsions supraventriculaires à travers le noeud A-V jusqu'au ventricule est réduite (Dorian et Meyers, 1989; Lathers et O'Rourke, 1992). Le vérapamil et le diltiazem sont surtout utilisés pour le traitement des arythmies cardiaques (Fogoros, 1997).

8.5 La Propafénone

8.5.1 Effets électrophysiologiques

8.5.1a Bloqueur sodique

La propafénone (2'-[2-hydroxy-3-propylamino-propoxy]-3-phenyl propiophenone hydrochloride) est un antiarythmique de la classe IC d'après la classification de Vaughan Williams (1984). Ce médicament a un effet stabilisant direct sur la membrane cellulaires du myocarde. L'effet électrophysiologique se manifeste sous forme d'une baisse de la vélocité du segment ascendant (phase 0) du potentiel d'action, accompagnée d'une dépression de l'automatisme spontané de la phase 4. La propafénone produit une réduction de la conductance sodique qui est fréquence et voltage dépendante (Kohlhardt et Seifert, 1980). Ce médicament n'a pas d'effet à l'état de repos mais se lie aux récepteurs dans les états activés et inactivés (Honjo et coll., 1989). La propafénone a un effet tonique de bloc sur le canal sodique due à sa dissociation lente du canal, avec un temps de récupération fréquence-dépendant de 6.3 secondes (Koller et Franz, 1994) à 15.5 secondes (Kohlhardt et Seifert, 1980). Alors, il y a accumulation de bloc durant des dépolarisations répétitives parce que la récupération du bloc est lente.

Les deux métabolites principaux 5-OH-propafenone (constante de dissociation entre 7-19 sec (Thompson et coll., 1988; Rouet et coll., 1989)) et N-depropylpropafenone (constante de dissociation 18 sec (Grant 1996)) possèdent aussi des propriétés de bloqueurs du canal sodique. Le métabolite 5-OH-propafenone a des effets sur le dV/dt max et sur l'amplitude du potentiel d'action similaire (80%) à celle de la propafénone

tandis que la N-depropylpropafénone a des activités de classe I plus faible, étant environ quatre fois moins active que la propafénone (Malfatto et al., 1988; Oti-Amoako et coll., 1990).

La molécule de la propafénone possède un centre chiral et peut donc exister comme 2 énantiomères. Les énantiomères R et S ont des effets comparables à la propafénone sur la conductance du sodium et déprime le dV/dt max à un degré similaire in vitro (Kroemer et coll., 1989, Oti-Amoako et coll., 1990). Ceci suggère que le site de liaison pour les canaux sodiques à l'intérieur de la molécule de propafénone soit distant du centre chiral du médicament (Bryson et coll., 1993).

8.5.1b Bêta-bloqueur

La propafénone possède une activité bêta-bloqueur dans les préparations in vitro et in vivo (Kroemer et coll., 1989; Lee et coll., 1990) et par conséquent a des actions antiarythmiques de la classe II. La liaison de la propafénone aux récepteurs bêta-adrénergiques est stéréosélective. Groschner et coll. (1991) ont démontré que l'énantiomère S était 50 fois plus puissante que le R comme bloqueur bêta-adrénergique dans le muscle du cœur de cobaye. De plus, Kroemer et coll. (1989) ont observé que l'énantiomère S était 100 fois plus puissante que le R comme bloqueur bêta-adrénergique sur les lymphocytes humains. Il en conclue que le S-propafénone est responsable des propriétés bêta-bloqueurs de la propafénone. Cependant, la puissance bêta-bloqueur in vivo de la propafénone chez des volontaires humains est environ 1/40 de celle du propranolol (McCleod et coll., 1984). Par contre, à des doses thérapeutiques,

la puissance relative fonctionnelle du bloc se rapproche à $\frac{1}{4}$ de celle du propranolol (Vaughan Williams, 1991). Les métabolites de la propafénone ne possèdent pas d'effets bêta-bloqueurs significatifs chez l'humain (Siddoway et coll., 1987; Kroemer et coll., 1989).

8.5.1c Bloqueur calcique

La propafénone diminue la force de contraction dans le muscle lisse et cardiaque, ce qui suggère un bloc des canaux calciques voltage-dépendant (Malfatto et coll., 1988; Honjo et coll., 1989; Carron et coll., 1991). Delgado et coll. (1993) ont proposé que la propafénone, à des concentrations thérapeutiques, démontre des propriétés anticalciques qui peuvent être impliquées dans son mécanisme antiarythmique.

8.5.1d Bloqueur potassique

La propafénone bloc également le courant potassique et possède donc des propriétés de la classe III. Duan et coll. (1993) ont démontré que la propafénone bloque avec une concentration inhibitrice à 50 % de $5.9 \mu\text{mol/L}$ le courant sortant transitoire (I_{to}), le rectificateur (I_{K1}), et le rectificateur externe (I_{Kr}) chez le lapin. Delpon et coll. (1995) ont démontré que ce médicament bloquait les deux rectificateurs externes (I_{Kr} et I_{Ks}) mais inhibait de façon préférentielle la composante rapide (I_{Kr}) avec $5 \mu\text{mol/L}$. De plus, la composante ultra-rapide (I_{kur}) est également inhibée par la propafénone mais seulement à une concentration inhibitrice à 50 % $>30 \mu\text{mol/L}$ (Gross et Castle, 1998). Alors la propafénone va bloquer les courants I_K à des concentrations cliniques mais ne bloquera

I_{K1} et I_{to} qu'à des niveaux supratherapeutiques (Stanton, 2000). Ces canaux sont bloqués indépendamment du voltage (Duan et coll., 1993). Inomata et coll. (1993) ont confirmé un effet bloqueur du canal potassique activé par l'acétylcholine ($I_{K,ACH}$) dans des myocytes auriculaires de cobayes. En bloquant ces courants potassiques, les périodes réfractaires, la repolarisation, et donc le potentiel d'action sont prolongés sous la propafénone.

8.5.2 Métabolisme

La propafénone est presque entièrement métabolisée. Des études pharmacocinétiques sur la propafénone chez l'humain (Hege et coll., 1984) et chez le chien (Hege et coll., 1986) ont démontré que ce médicament est métabolisé avec <4% de la dose excrétée inchangée dans l'urine et dans les fèces. Durant le traitement à long terme, la demi-vie plasmatique est de 6 hrs (Connolly et coll., 1983). Il existe 11 métabolites de la propafénone mais la 5-OH-propafénone et la N-depropypropafénone sont les plus importants (Kates et coll., 1985). Le métabolisme oxydatif de la propafénone en 5-OH-propafénone dépend d'une voie hépatique qui utilise un isoenzyme cytochrome P450 (Siddoway et coll., 1987; Kroemer et coll., 1989). Environ 7% de la population caucasienne métabolise lentement parce que cet enzyme est déficient (Borioni et coll., 1990). Chez les métaboliseurs rapides, la demi-vie d'élimination varie de 2-10 hrs, tandis que chez les métaboliseurs lents, elle varie de 10-32 hrs (Siddoway et coll., 1987). Puisque les métabolites ne possèdent pas d'activité bêta-bloquante, les métaboliseurs lents, qui ne peuvent pas métaboliser la propafénone en 5-OH-propafénone, ont une concentration de propafénone plus élevée et donc plus d'effet bêta-bloquant. Ceci implique que n'importe quelle dose administrée chez un patient à métabolisme lent va

avoir plus d'effet bêta-bloqueur que chez un patient qui métabolise rapidement (Capucci et Boriani, 1995).

8.5.3 Les arythmies

La propafénone est utilisée en clinique pour le traitement d'arythmies auriculaires et ventriculaires. Ce médicament possède des propriétés inotropes et chronotropes négatives (Ledda et coll., 1981). Chez l'humain, après une administration per os ou intraveineuse, la propafénone prolonge l'intervalle P-R et la durée du QRS. Des doses plus élevées peuvent prolonger l'intervalle Q-Tc (Connolly et coll., 1983; Dinh et coll., 1985; Schamroth et coll., 1985). De plus, la propafénone prolonge les temps de récupération du nœud sinusal, prolonge la période réfractaire effective de l'oreillette, du ventricule et du nœud A-V, et augmente la conduction dans le nœud A-V (intervalle AH) ainsi que la conduction dans le système His-Purkinje (intervalle HV) (Neuss et coll., 1983; Dinh et coll., 1985).

La propafénone a démontré une efficacité dans le traitement clinique de la fibrillation auriculaire (Connolly et coll., 1989; Suttorp et coll., 1990, Capucci et coll., 1999; Khan, 2001) et du flutter auriculaire (Doni et coll., 1995; D'este et coll., 1997; Doni et coll., 2000). Dans 5 études différentes impliquant 184 patients atteints d'une fibrillation auriculaire récente et 15 patients atteints d'un flutter auriculaire, la conversion en rythme sinusal a été réussie dans 46 à 70% des patients en fibrillation auriculaire (1 à 2 mg/kg bolus suivi d'une infusion continue) (Capucci et coll., 1987; Bianconi et coll., 1989; Carerj et coll., 1989; Goy et coll., 1991; Gentili et coll., 1992) et dans 33% des patients

en flutter auriculaire (Bianconi et coll., 1989). La propafénone semble être plus efficace pour la conversion de la fibrillation auriculaire que pour celle du flutter auriculaire (Grant, 1996). La propafénone est également efficace dans le traitement de la fibrillation auriculaire dans des patients atteints du syndrome de Wolff-Parkinson-White (Ludmer et coll., 1987; Dubuc et coll., 1989). Ce médicament est aussi administré chez des patients atteints d'une tachycardie supraventriculaire paroxystique (Shen et coll., 1986; Hammill et coll., 1987; Reimold et coll., 1998). La propafénone est maintenant moins utilisé dans le traitement de tachycardie ventriculaire (Connolly et coll., 1983; Schamroth et coll., 1985; Dinh et coll., 1985; Budde et coll., 1991). Ce médicament peut être proarythmique chez les patients possédant une maladie cardiaque sous-jacente (Fogoros, 1997) et doit être administrée avec prudence chez ces patients.

8.6 Le Sotalol

Le sotalol est un antiarythmique de la classe III (bloqueurs des canaux potassiques) possédant aussi des propriétés bêta-bloquantes (Vaughan Williams, 1984). Ce médicament est un mélange racémique des isomères D et L dans un ratio approximatif de 1 :1 (Antonaccio et Gomoll, 1990). Les actions bêta-bloquantes du sotalol sont non-sélectives (bloque β_1 et β_2) et ne sont pas associées avec une activité sympathomimétique (Singh, 1990; Antonaccio et Gomoll, 1993). La prolongation du potentiel d'action par le sotalol est causée par une réduction du courant rectificateur externe (I_K) associé avec une plus petite réduction du rectificateur interne (I_{K1}) (Carmeliet, 1985). Sanguinetti et Jurkiewicz (1990) ont démontré que le sotalol bloquait

sélectivement le courant rapide potassique (I_{Kr}) chez le cobaye. Les deux isomères du sotalol (D et L) contribuent à l'effet classe III, tandis que l'effet bêta-bloqueur est presque entièrement causé par l'isomère L et est dose-dépendant (Kato et coll., 1986, Singh, 1993). De plus, les effets du sotalol sur le potentiel d'action sont fréquence-dépendants inverses; l'effet diminue quand la fréquence du stimulus augmente (Singh, 1993). Nademanee et coll. (1985) ont étudié l'effet du sotalol chez 33 patients atteints d'une arythmie ventriculaire. Ces investigateurs ont observé une prolongation des périodes réfractaires effectives dans l'oreillette, le nœud A-V (de 25% chacun) et dans le ventricule (de 15%) reflété par une prolongation des intervalles QT et QTc (Touboul et coll., 1987). Ce dernier augmente également les périodes réfractaires dans les voies accessoires. L'effet classe II du sotalol (β -bloqueur) prolonge le temps de récupération du nœud sinusal ainsi que le temps de conduction à travers le nœud A-V. Le sotalol est approuvé pour le traitement des arythmies ventriculaires mais peut être utile dans tous les types de tachycardies (Fogoros, 1997). Par contre, le sotalol peut être proarythmique et peut produire une arythmie ventriculaire (torsades de pointes) due à la prolongation QT dans 1-4% des patients (Anderson et Prystowsky, 1999).

8.7 L'amiodarone

L'amiodarone est généralement classifié d'après Vaughan Williams (1984) comme un antiarythmique de la classe III, parce qu'il prolonge la repolarisation en inhibant les canaux potassiques (Singh et Vaughan Williams, 1970). Cependant, ce médicament a des propriétés fréquence-dépendantes de la classe I, inhibe les canaux sodiques (Mason

et coll., 1983), et possède de l'activité de la classe II. Par contre, l'effet antiadrénergique de l'amiodarone est différent des autres bêta-bloqueurs parce qu'il est non-compétitif et s'ajoute à l'effet bêta-bloqueur (Charlier, 1970). L'amiodarone déprime l'automaticité du nœud sinusal, ce qui résulte en un ralentissement du rythme cardiaque sinusal. Ce médicament diminue la conduction et augmente les périodes réfractaires du nœud A-V (Mitchell et coll., 1989) ce qui pourrait être utile dans le traitement des arythmies supraventriculaires. Après une thérapie per os à long terme, l'amiodarone a une demi-vie d'élimination jusqu'à 60 jours (Haffajee et coll., 1983). Une distribution lente aux tissus requiert une période longue de chargement du médicament, jusqu'à plusieurs mois, avant d'atteindre une concentration en état stable dans les tissus.

Le traitement à court terme avec de l'amiodarone inhibe principalement I_{Kr} , tandis que le traitement à long terme diminue I_{Ks} (Kaichiro et coll., 2001). Cette activité de la classe III résulte en une augmentation des périodes réfractaires auriculaires et ventriculaires, et d'une prolongation de l'intervalle QTc. L'amiodarone prévient souvent l'induction de la tachycardie ventriculaire mais quand la tachycardie est toujours inductible, l'amiodarone prolonge le cycle de la tachycardie de 20-25% durant la thérapie à long terme (DiCarlo et coll., 1987; Mitchell et coll., 1989). Les effets de l'amiodarone per os sur les fonctions du nœud sinusal et AV sont maximaux après moins de 2 semaines, tandis que les effets sur la tachycardie ventriculaire et les périodes réfractaires ventriculaires apparaissent graduellement durant la thérapie orale, devenant maximaux après 10 semaines (Mitchell et coll., 1989).

8.8 Effets des antiarythmiques sur le créneau d'excitabilité

Plusieurs études ont démontré la présence d'un créneau d'excitabilité en absence de médicaments antiarythmiques dans le flutter auriculaire humain (Della Bella et coll., 1991; Doni et coll., 1995; Stambler et coll., 1996; Jalil et coll., 1998) et chez le chien (Frame et coll., 1986; Wu et Hoffman, 1987; Spinelli et Hoffman, 1989; Inoue et coll., 1991; Kus et coll., 1991; Derackhchan et coll., 1994; Niwano et coll., 1994; Jalil et coll., 1997). Les antiarythmiques changent la forme du potentiel d'action en agissant sur les canaux ioniques (Fogoros, 1997) et peuvent donc agir sur le créneau d'excitabilité. En milieu clinique, la procainamide (classe IA) a significativement augmenté le créneau d'excitabilité dans le flutter auriculaire commun (Jalil et coll., 1998), mais n'a pas changé sa grandeur exprimée en pourcentage du cycle de flutter et ne l'a pas converti en créneau uniquement composé de tissu partiellement réfractaire (Stambler et coll., 1996). Doni et coll. (1995; 1996) ont démontré que la propafénone avait un effet positif sur le créneau d'excitabilité dans le flutter auriculaire facilitant sa conversion par stimulation transoesophagienne. Cependant, l'amiodarone n'a pas significativement réduit le créneau d'excitabilité dans les tachycardies ventriculaires (Naitoh et coll., 1998; Masotti et coll., 1999). Dans les modèles expérimentaux, il a été démontré que le d-sotalol (qui n'a pas de propriété bêta-bloquante) a significativement augmenté le créneau d'excitabilité dans un modèle de fibrillation auriculaire de chèvre (Wijffels et coll., 2000), et aussi dans une tachycardie ventriculaire dans des cœurs de lapin perfusés sous Langendorff (Boersma et coll., 1994). Par contre, le d-sotalol a significativement diminué le créneau d'excitabilité dans un modèle de flutter auriculaire chez le chien

(Spinelli et Hoffman, 1989; Rahme et coll., 1995), d'anneau tricuspide chez le chien (Fei et Frame, 1996), et de tachycardie ventriculaire dans le cœur de lapin perfusé sous Langendorff (Reiter et coll., 1994). Dans un modèle de réentrée chez le chien avec une lésion en forme de Y sur l'oreillette droite, Derakhchan et coll. (1994) ont démontré que la propafénone ne modifiait pas significativement le créneau d'excitabilité. Par contre, d'autres études ont démontré une prolongation du créneau d'excitabilité avec la propafénone dans le même modèle (Spinelli et Hoffman, 1989) et aussi dans un modèle d'écrasement de tissu entre les deux veines caves (Inoue et coll., 1991). Les études des antiarythmiques sur le créneau d'excitabilité sont donc très controversées et dépendent de la préparation utilisée.

8.9 Interaction du système nerveux autonome et les antiarythmiques

L'efficacité des médicaments antiarythmiques est réduite par des agonistes du système nerveux autonome dans les arythmies auriculaires et ventriculaires. Des changements dans le tonus du système nerveux autonome peuvent renverser les effets bénéfiques des médicaments antiarythmiques, rendant le médicament inefficace ou même proarythmique (Ranger et coll., 1989; Cappato et coll., 1993). Des études cliniques ont démontré que les effets des médicaments qui bloquent les canaux sodiques contre les tachycardies ventriculaires peuvent être renversés par une activation bêta-adrénergique (Morady et coll., 1988; Jazayeri et coll., 1989; Calkins et coll., 1992; Markel et coll., 1993; Sager and Behboodikhah, 1996). De plus, il a été démontré que l'isoprotérénol antagonise les actions du d-sotalol et du dofétilide dans les cardiomyocytes

ventriculaires isolés de chien (Marchang et coll., 2000), ce qui peut s'avérer désavantageux en présence de taux élevés de catécholamines. Il a aussi été démontré que les effets contre les tachycardies supraventriculaires des antiarythmiques de la classe IA et IC sont renversés par l'isoprotérénol (Dongas et coll., 1985; Dubuc et coll., 1987; Akhtar et coll., 1988; Niazi et coll., 1989; Helmy et coll., 1990; Stambler et coll., 1996). Morady et coll. (1989) ont démontré que l'adrénaline renverse partiellement ou complètement les effets du vérapamil dans les tachycardies supraventriculaires paroxystiques. De plus, dans un modèle de lésion en Y sur l'oreillette droite chez le chien, Rahme et coll. (1997a,b) ont démontré que la noradrénaline et l'acétylcholine modifient la composition du créneau d'excitabilité dans le circuit de réentrée du flutter auriculaire et renversent les effets électrophysiologiques du d-sotalol sur le créneau d'excitabilité. Alors, les agonistes du système nerveux autonome peuvent renverser les effets bénéfiques des médicaments antiarythmiques ce qui pourraient les rendre inefficaces.

9. Le traitement pharmacologique du flutter auriculaire

9.1 Le traitement aigu

Dès lors qu'un flutter auriculaire est diagnostiqué, il y a trois options disponibles : 1) administrer un médicament antiarythmique, 2) faire une cardioversion électrique, ou 3) faire une stimulation rapide de l'oreillette droite pour arrêter le flutter (Waldo, 2000). La cardioversion est le traitement de choix lorsque le flutter est associé à une situation qui requiert la restauration urgente en rythme sinusale, par exemple lorsque la

conduction auriculo-ventriculaire est 1:1 de l'oreillette au ventricule. Cependant, la cardioversion nécessite un agent anesthésique qui peut être indésirable chez un patient qui a récemment mangé ou qui est atteint d'une maladie pulmonaire chronique obstructive. La stimulation rapide ou un antiarythmique devient alors le premier choix. Pour ralentir la réponse ventriculaire, un bloqueur des canaux calciques (vérapamil, diltiazem), ou un bêta-bloqueur (esmolol, propranolol ou metoprolol) peut être utilisé. Un digitalique (digoxin), qui par son effet vagotonique sur le noeud A-V, diminue la réponse ventriculaire, est aussi acceptable. Les médicaments antiarythmiques les plus utilisés sont l'ibutilide, la flécainide et la propafénone. L'ibutilide i.v. convertit 60% des flutters auriculaires en rythme sinusal (Ellenbogen et coll., 1996). La flécainide et la propafénone peuvent aussi être utilisés par voie intraveineuse ou per os pour convertir le flutter en rythme sinusal. Les antiarythmiques peuvent être utilisés avant une cardioversion électrique ou une stimulation rapide de l'oreillette pour : 1) contrôler la fréquence de la réponse ventriculaire (avec un bêta-bloqueur, un bloqueur des canaux calciques, ou de la digitale), 2) pour accroître l'efficacité de la stimulation rapide de l'oreillette en rythme sinusal (en utilisant par exemple un antiarythmique de la classe I); ou 3) augmenter les chances que le rythme sinusal soit soutenu après une cardioversion efficace (en utilisant les médicaments antiarythmiques de la classe IA, IC ou III) (Waldo, 2000).

9.2 Le traitement à long terme

9.2.1 L'ablation par cathéter

La difficulté à obtenir une suppression chronique du flutter auriculaire avec des antiarythmiques a modifié l'approche thérapeutique à long terme du flutter. L'ablation par cathéter avec énergie à radiofréquence est maintenant utilisée comme méthode de guérison pour le traitement d'un flutter auriculaire chronique ou récurrent (Daoud et Morady, 1998; Kongsgaard et Aass, 2000; Waldo, 2000). L'amélioration des techniques d'ablation par cathéter avec énergie à radiofréquence et de la cartographie intracavitaire a amélioré l'efficacité de cette approche thérapeutique pour atteindre un taux de guérison allant jusqu'à 95% pour les patients atteints d'un flutter auriculaire commun (Cosio et coll., 1996a, Cosio et coll., 1996b). La technique nécessite une étude électrophysiologique de l'oreillette durant le flutter pour identifier la localisation du circuit de réentrée et par la suite, confirmer que le circuit de réentrée inclut un isthme critique entre la veine cave inférieure, la crête d'Eustache, l'ostium du sinus coronarien et la valve tricuspide. Une fois la région identifiée, une ligne d'ablation est créée à travers l'isthme. La conduction à travers cet isthme peut être difficile à abolir complètement (Cosio et coll., 1996a, Cosio et coll., 1996b), mais la démonstration d'un bloc bidirectionnel complet dans cet isthme signifie une ablation réussie du flutter auriculaire (Waldo, 2000).

9.2.2 Les antiarythmiques

Le flutter auriculaire est difficile à supprimer complètement avec une thérapie pharmacologique. Dans le passé, le traitement standard par médicaments antiarythmiques était les agents de la classe IA (quinidine, procainamide, ou disopyramide) pour essayer de prévenir une rechute. Par contre, des études récentes (Nabar et coll., 2001) indiquent que les antiarythmiques de la classe IC (flécainide et propafénone) sont aussi efficaces, sont mieux tolérés, et ont moins de toxicité sur les organes que les médicaments de la classe IA (Waldo, 2000). Par contre, ces médicaments sont contre-indiqués chez des patients atteints d'une maladie cardiaque structurale sous-jacente. La moricizine, un antiarythmique de la classe I possédant des propriétés A, B, et C, peut être aussi efficace dans le traitement du flutter et de la fibrillation auriculaire (Brooks et coll., 1994, Waldo, 2000; Geller et coll., 2001). De plus, les antiarythmiques de la classe III amiodarone, sotalol et dofétilide peuvent aussi être efficaces (Lenz et Hilleman, 2000; Sager, 2000, Al-Dashti et Sami, 2001). Cependant, puisque le sotalol et le dofétilide peuvent causer des torsades de pointes, une arythmie ventriculaire dangereuse, il faut éviter une prolongation de l'intervalle Q-T au-delà de 500 ms. L'amiodarone est très efficace mais peut causer des problèmes à cause de sa toxicité potentielle à long terme (Podrid, 1995). Si le flutter auriculaire récidive malgré une thérapie antiarythmique, la fréquence des ondes du flutter peut être plus lente qu'en absence de drogue. Un médicament qui ralentit la réponse ventriculaire en bloquant la conduction du nœud A-V (bêta-bloqueurs, bloqueurs des canaux calciques seuls ou en combinaison avec de la digitale) doit être administré en même temps (Waldo,

2000) pour prévenir une conduction 1:1 en présence de flutter auriculaire ralenti sous thérapie antiarythmique.

10. Hypothèse

Les transmetteurs du système nerveux autonome (noradrénaline et acétylcholine) modifient les effets des antiarythmiques sur le créneau d'excitabilité du flutter auriculaire chez le chien et chez l'humain. Le flutter auriculaire demeure un défi majeur à la thérapie pharmacologique car sa prévention et son traitement avec les médicaments antiarythmiques sont fréquemment inefficaces. Il est provoqué par la circulation d'un front d'excitation autour d'un circuit bien défini et est caractérisé par la présence d'un créneau d'excitabilité où le tissu peut avoir retrouvé partiellement ou complètement son excitabilité. En pratique clinique, la propafénone est utilisée pour le traitement du flutter et de la fibrillation auriculaire. Ce n'est pas connu si le système nerveux autonome influence les effets de la propafénone dans les tachycardies supraventriculaires.

Nous allons étudier les propriétés du circuit de réentrée chez le chien avant et après une infusion de propafénone afin de déterminer les caractéristiques de la réentrée qui sont modifiées par ce médicament. La durée et la composition du créneau d'excitabilité sont déterminées non seulement par la longueur du circuit et les caractéristiques électrophysiologiques locales, mais aussi par des influences externes comme celles du système nerveux autonome. Nous allons également étudier la modulation des effets de la propafénone sur les propriétés électrophysiologiques du circuit de réentrée induite par l'ajout de la noradrénaline (sympathique) et l'acétylcholine (parasymphatique). Chez

l'humain, nous allons étudier les propriétés électrophysiologiques du créneau d'excitabilité dans des cas de flutter auriculaire récidivant malgré une thérapie avec des antiarythmiques de la classe I et III et leur modulation par l'influence d'une activation sympathique et d'un retrait parasympathique.

10.1 Études Expérimentales

Dans une première série d'expériences, nous étudions le "resetting" dans une préparation canine in vivo. Les propriétés électrophysiologiques du circuit de flutter auriculaire sont caractérisées par le "resetting" causé par une ou plusieurs stimulations. Le "resetting" a été utilisé dans des préparations in vitro de tachycardie ventriculaire soutenue (Bernstein et Frame, 1990), dans des modèles de flutter auriculaires chez des animaux (Frame et coll., 1986; Frame et coll., 1987; Derackhchan et coll., 1994; Fei et coll., 1996; Jalil et coll., 1997) et chez l'humain (Almendral et coll., 1986a; Almendral et coll., 1986b; Stamato et coll., 1989; Arenal et coll., 1992; Callans et coll., 1993; Callans et coll., 1996; Callans et coll., 1997; Jalil et coll., 1998). Dans des études antérieures (Derackhchan et coll., 1994; Jalil et coll., 1997; Jalil et coll., 1998), le "resetting" a été déterminé au site de détection plutôt qu'au site de stimulation. Par conséquent, les propriétés du créneau d'excitabilité n'ont pas été bien estimées. Dans nos études, nous allons présenter nos résultats par rapport au site de stimulation et non par rapport au site de détection. Nous allons aussi démontrer que le "resetting" n'est pas uniquement dû à l'effet de la prématurité (où le front de réentrée antérograde produit par la stimulation circule dans la queue du potentiel d'action du flutter), mais qu'un second mécanisme,

l'effet de collision, peut lui aussi induire un ralentissement de la propagation. Ce dernier résulte de la propagation du front de réentrée antérograde stimulé à travers du tissu partiellement réfractaire à la suite de la collision entre le front de réentrée rétrograde et le front du flutter original.

Dans une deuxième étude, nous allons déterminer si une stimulation prématurée à un site prédit la gamme de prématurité à travers tout le circuit de réentrée dans un modèle canin de flutter auriculaire. La courbe "reset-response" a été utilisée jusqu'à présent pour évaluer les caractéristiques globales du circuit de réentrée. Des études ont démontré qu'il existait des différences selon la position du site de stimulation dans les courbes "reset-response" des tachycardies ventriculaires chez l'humain (Callans et coll., 1996; Callans et coll., 1997) et dans des tachycardies ventriculaires chez le lapin (Boersma et coll., 1994). Ingelmo and Frame (2000) ont démontré dans un modèle d'anneau tricuspide in vitro de chien que la forme de la courbe "reset-response" était différente suivant que la stimulation était introduite à un site distal ou proximal au site de mesure.

Dans cette étude, nous allons également étudier les effets de la propafénone sur les caractéristiques électrophysiologiques du circuit de réentrée. Frame et coll. (1987) ont étudié la conduction d'une impulsion de réentrée dans un anneau tricuspide, en utilisant un étalage intracavitaire de 96 électrodes bipolaires sur l'endocarde. Ces chercheurs ont rapporté, qu'en absence de médicament, le circuit de réentrée était relativement uniforme et qu'aucune partie du circuit ne démontrait une conduction plus lente. Callans et coll. (1991) ont démontré que la propafénone peut soit diminuer la

conduction dans un circuit de tachycardie ventriculaire qui demeure inchangé soit prolonger les barrières du circuit sans que le point de sortie du circuit soit modifié. Pour déterminer l'homogénéité spatiale de l'effet de la propafénone, nous allons étudier les temps de conduction dans différentes portions du circuit dans un flutter auriculaire en absence de stimulation, sans médicament et avec la propafénone en utilisant une ceinture contenant 16 électrodes bipolaires.

Jusqu'à présent, peu d'études ont été faites sur l'interaction des systèmes parasympathiques et sympathiques avec les antiarythmiques quant aux caractéristiques du créneau d'excitabilité dans le flutter auriculaire. Rahme et coll. (1997a,b) ont démontré que la noradrénaline et l'acétylcholine modifient la composition du créneau d'excitabilité dans le circuit de réentrée du flutter auriculaire et renversent les effets électrophysiologiques du d-sotalol sur le créneau d'excitabilité. Dans une troisième étude, nous étudions l'influence de la noradrénaline et de l'acétylcholine sur les caractéristiques électrophysiologiques du circuit de réentrée du flutter auriculaire chez le chien en présence de la propafénone. Nous examinons aussi l'homogénéité spatiale des effets de la propafénone et des neurotransmetteurs sur les caractéristiques du circuit de réentrée. Pour ce faire, les temps de conduction dans différentes sections du circuit de réentrée sont mesurés durant le flutter auriculaire en absence de stimulation prématurée avant et après l'administration de la propafénone, et suivant une infusion de noradrénaline et d'acétylcholine en utilisant une ceinture contenant 16 électrodes bipolaires.

10.2 Études Cliniques

Chez l'humain, la récurrence du flutter auriculaire avec les médicaments antiarythmiques est fréquemment observée. Pour déterminer la raison de l'inefficacité des médicaments, nous examinons dans une quatrième étude les paramètres électrophysiologiques du flutter chez des patients ne prenant aucun médicament antiarythmique, du sotalol, de la propafénone ou de l'amiodarone qui se présentent au laboratoire d'électrophysiologie pour une conversion du flutter en rythme sinusal par stimulation rapide de l'oreillette. Des études antérieures ont démontré que les effets de la propafénone sur le cycle de la fibrillation auriculaire et la fréquence de la réponse ventriculaire sont renversés en position debout, un état associé à un retrait vagal et une activation sympathique (Leather et al., 1994). Pour déterminer l'effet de l'activation sympathique sur les paramètres électrophysiologiques du flutter auriculaire, nous allons étudier l'effet d'un changement de position (couché vs debout) sur le créneau d'excitabilité du flutter auriculaire. Une inclinaison sur une table basculante va causer un pooling veineux et une réduction du retour veineux, du débit cardiaque et de la taille du cœur. La diminution du débit cardiaque va stimuler une augmentation dans le tonus sympathique et un retrait vagal. Comme résultat, la fréquence cardiaque et la pression artérielle diastolique vont augmenter. Les barorécepteurs qui sont situés sur le côté artériel de la circulation dans le sinus carotidien et l'arche aortique répondent à l'étirement des vaisseaux. En réponse à une hypotension, il y a une diminution dans la pression de distension des barorécepteurs, ce qui va diminuer la fréquence de décharge, une diminution de signaux au centre vasomoteur, et par conséquent une augmentation du tonus sympathique et une inhibition du tonus vagal. Ceci va avoir comme réflex de stimuler les récepteurs alpha1-

adrénergiques qui va augmenter la contractilité et la fréquence cardiaque pour avoir une hausse du débit cardiaque. De plus, la rénine va être libéré par les reins en réponse à une pression rénale basse ce qui va augmenter l'angiotensine II et avoir un effet vasoconstricteur et donc augmenter l'effet adrénérique .

CHAPITRE II

INFLUENCE OF PROPAFENONE ON RESETTING AND TERMINATION OF CANINE ATRIAL FLUTTER

Contribution de l'étudiante

La candidate a exécuté les chirurgies expérimentales, a contribué à l'analyse des données et à la rédaction de l'article.

Influence of Propafenone on Resetting and Termination of Canine Atrial Flutter

BOUALEM MENSOUR, ELISE JALIL, ALAIN VINET, and TERESA KUS

From the Research Center of Sacré-Coeur Hospital and the Institute of Biomedical Engineering of Université de Montréal, Québec, Canada

MENSOUR, B. ET AL.: Influence of Propafenone on Resetting and Termination of Canine Atrial Flutter. Previous studies on atrial flutter (AF) presumed that resetting was due to the prematurity effect (PE) in which the stimulated antegrade wavefront travels in the tail of the AF preexisting wavefront. We studied the collision effect (CE) between the AF and the stimulated retrograde wavefronts, its contribution to resetting, and its relationship to AF termination and how they are affected by the Class IC agent propafenone (PPF). A canine model of AF was created using a Y-shaped lesion in the right atrium in 14 dogs (33 ± 3 kg). Five atrial bipolar electrodes were positioned around the tricuspid valve. In a subsequent set of 11 dogs, we used 16 bipolar electrodes for recording. AF was induced by burst pacing. Single and multiple stimuli were applied to measure conduction time and reset-response curves (RRCs). This was repeated after the administration of PPF (1 mg/kg loading dose for 10 minutes, followed by 1.8 mg/kg/per hour infusion). Three distinct mechanisms were found to contribute to the RRC: the PE, the CE, and heterogeneity. PPF stabilized the RRC, increased significantly the cycle length (CL), the duration of the effective refractory period, as well as the duration of the excitable gap. However, PPF did not alter the duration of the fully excitable portion. We studied 36 annihilations without and 48 with PPF. Transient fibrillation was found in 75% of the episodes without, compared to 22% with PPF. Other types of termination such as conduction block, CL oscillations, and reversal of activation were found for 25% of the episodes without and 78% with PPF. In many cases, conduction block and CL oscillations were associated with a failure of propagation of the stimulated antegrade wavefront in the region of collision. Termination by reversal of activation suggests that propagation was two dimensional and could not be represented by a one dimensional movement. The average coupling interval (in percent of CL), that induced fibrillation was not significantly different from that at which conduction block occurred. This suggests that transient fibrillation is associated with a weak CE rather than with rapid pacing. The CE is amplified by multiple stimuli and PPF. The incidence of transient fibrillation in AF annihilation diminishes with PPF as the CE becomes more important. This suggests that the evaluation of PE and CE in AF may be an indication of the risk of atrial fibrillation. (*PACE* 2000; 23:1200-1219)

atrial flutter, propafenone, resetting, termination

Introduction

Atrial flutter (AF) is a reentrant rhythm in the right atrium. In experimental animal models with a Y-shaped lesion in the right atrium, AF has been shown to be a circus movement around the tricuspid valve annulus.^{1,2} The electrophysiological properties of the AF circuit can be characterized by resetting, a programmed stimulation with one or more stimuli that advances the tachycardia. Resetting has been used in sustained ventricular tachycardia in vitro preparations,³ in animal AF

models,^{1,2,4-6} and in humans.⁷⁻¹⁴ In previous studies,⁴ resetting was determined at the recording site instead of the pacing site. As a result, the duration of the excitable gap (EG) was underestimated, while the effective refractory period (ERP) and the fully excitable portion were overestimated. In this article, we present our results in reference to the pacing site and show that the old definition of resetting should be reexamined to account for tissue heterogeneity. We also show that resetting is due not only to prematurity effect (PE), in which the stimulated antegrade wavefront travels in the tail of the AF action potential, but also to collision effect (CE). The latter results from the propagation of the stimulated antegrade wavefront through partially refractory tissue left by the collision between the stimulated retrograde and the flutter wavefronts.

Propafenone (PPF), a Class IC agent, has a pronounced effect on the rapid sodium channel and a

Supported by the DeSève foundation and the Medical Research Council of Canada.

Address for reprints: Alain Vinet, Ph.D., Sacré-Coeur Hospital Research Center, 5400 Boulevard Gouin Ouest, Montréal, Québec, QC, Canada, H4J 1C5. Fax: (514) 338-2694; e-mail: vineta@crhsc.umontreal.ca

Received June 30, 1999; revised December 11, 1999; accepted January 14, 2000.

weak effect on repolarization. It significantly slows conduction velocity by decreasing the upstroke velocity of action potential.¹⁵ The effects of PPF on the duration of the EG and on AF termination have been studied in several models: Y-shaped incision^{1,16} and intercaval crush.¹⁷ The composition and the duration of the EG was studied by Derakhchan et al.⁴ However, the relationship between PPF and CE and how the latter can affect resetting and termination of the flutter have not been studied yet.

Method

Surgical Technique

Fourteen mongrel dogs of either sex (33 ± 3 kg) were studied in the postabsorptive state. General anesthesia was induced with sodium thiopental (30 mg/kg intravenously [IV]) and maintained with chloralose (80 mg/kg IV bolus supplemented by 15 mg/kg per hour maximum as needed). The dogs were intubated endotracheally and ventilated (Harvard Pump, Holliston, MA, USA) with room air (10 breaths/minute, tidal volume to achieve a maximum inspiratory pressure of 20 cm of water) to maintain arterial pH 7.35–7.45 and pO₂ > 80 mmHg. Arterial and venous cannulae were inserted in the left femoral artery and vein by direct cutdown for blood pressure monitoring and drug administration, respectively. An additional venous cannula was inserted in the right internal jugular vein for blood sampling. Muscular relaxation was then induced with gallamine triethiodide (Flaxedil 100), 3 mg/kg IV. A right thoracotomy was performed via the fourth or fifth intercostal space and the pericardium was incised to provide access to the vena cava and the right atrium. Based on the procedure developed by Frame et al.,¹ a lesion was created by sewing in a line extending from the superior to the inferior vena cava. A second line, extending from the first two-thirds of the way to the tip of the right atrial appendage and parallel to but 1–2 cm above the atrioventricular groove was similarly sewn. Both sewed lines were also crushed to assure an anatomic barrier. Previous studies¹⁸ have shown that in this model, reentry occurs in a clockwise or counterclockwise direction around the tricuspid valve. Five close (2–4 mm) bipolar, teflon coated, stainless steel wire electrodes were inserted using a 26-gauge needle around the base of the right atrium for stimulating or recording from the endocardial atrial surface. In a subsequent set of 11 dogs, eight close (2–4 mm) bipolar stimulation electrodes were inserted around the base of the right atrium, and 16 bipolar electrodes were mounted on a belt for recording. The latter were uniformly distributed around the tricuspid valve to get a better resolution on the conduction times in the circuit.

Measurement of Electrophysiological Parameters

A single lead (II) surface electrocardiogram, atrial electrograms from each of the five bipolar electrodes and femoral arterial pressure were monitored using a Nihon Kohden (Tokyo, Japan) polygraph (model RM6008). The atrial electrograms were stored on a digital 8 track, Sony Instrumentation Cassette Recorder PC-108M (Tokyo, Japan). Diastolic stimulation threshold at 2-ms pulse width was measured in milliamperes at each of the five endocardial electrode recording sites at pacing cycle lengths (CLs) of 300 and 200 ms. Stimulation for determination of refractory periods was performed at twice the diastolic threshold measured at these sites by using a programmable cardiac stimulator (Bionova PCS80, Institut de Génie Biomédical, Ecole Polytechnique de Montréal, Montréal, Québec, Canada) and an isolation unit (CCSIU, Bloom Associates, Ltd., Reading, PA, USA). Atrial ERP was determined at a constant pacing CL of 300 ms (S₁S₁) by interpolating a single premature stimulus (S₂) after every 15th paced beat at a coupling interval (S₁S₂) initially within the absolute refractory period at the electrode site. This coupling interval (S₁S₂) was incremented progressively by 10 ms until S₂ resulted in atrial capture (A₂) as recorded at adjacent sites. This procedure was repeated by using 2-ms increments to better define refractoriness. Atrial ERP at each site was thus defined as the longest S₁S₂ interval at which S₂ failed to result in A₂. This procedure was repeated at a paced CL of 200 ms. After determination of ERP, AF was induced by burst stimulation (30–80 beats at CLs of 90–170 ms). Flutter induction was achieved most easily at the recording site with the shortest ERP, but when this failed, other sites were also tried. In a set of 11 dogs with 16 bipolar recording electrodes, atrial electrograms were monitored and stored using homemade software (PAM, Centre de Recherche, Hôpital Sacré-Coeur de Montréal, Montréal, Québec, Canada). Atrial ERP at each site was not performed in this set of dogs. The stimulation electrode closer to the recording site that gave a better signal was used. If resetting didn't occur at this recording site, other sites were also used.

Pacing Protocol During AF

During stable AF (CL variations < 3 ms), single and multiple stimuli were performed. Single stimuli were applied after every 20th spontaneous beat detected at the next distal electrode in the direction of wavefront propagation. Initially, the premature stimulus was introduced late in diastole and the coupling interval (CI) was progressively decreased by 2 ms until the stimulus failed to capture or the flutter was terminated. The inter-

val between a spontaneous beat (T_0) and the premature stimulus (S) ($CI = T_0S$) and the interval between the premature stimulus and the subsequent n^{th} tachycardia beat (ST_n) were measured (peak to peak) at the recording site M closest to the stimulation (in the direction of wavefront propagation) (Fig. 1). Graphs describing the relationship $ST_n - (n - 1) CL$ versus T_0S or reset-response curve (RRC) were constructed. The number $(n - 1) CL$ was subtracted from ST_n to assess if dissipation of the resetting effect was completed after $(n - 1)$ rotations. The CL was obtained by averaging the intervals between the two last spontaneous beats before each stimulation over the whole range of CIs. A three-parameter nonlinear function $y^f(x) = a_1[\tanh(-a_2 x + a_3) - \tanh(-a_2 + a_3)]$ with $y(1) = 0$ was used to fit the data $y^d = ST_n/CL - (n - 1)$ vs T_0S/CL . The stability of the resetting effect before and during drug infusion was estimated from the mean quadratic error between the data y_i^d and the

fit y_i^f ($i = 1, \dots, N$) as

$$\frac{1}{N} \sqrt{\sum_{i=1}^N (y_i^d - y_i^f)^2}$$

Multiple stimuli composed of m stimulations were delivered in the following manner: The first $(m - 1)$ stimuli were fixed premature enough to induce a significant resetting. The test stimulus (i.e., the m^{th} stimulus) was introduced at a CI longer than the flutter CL to account for the influence of the $(m - 1)$ stimuli. This CI was then decreased by 2 ms until refractoriness was encountered or the flutter was terminated.

PPF was administered during AF in a loading dose of 1 mg/kg infused over 10 minutes. This was followed by a maintenance infusion of 1.8 mg/kg per hour to achieve therapeutic plasma levels as described in Derakhchan et al.⁴ The protocol to determine the RRC was repeated following the bolus administration and again at 10-minute intervals up to a maximum of 60 minutes. Blood samples for drug plasma levels were drawn during each curve determination. If the AF was terminated during drug infusion, burst pacing was used to reinitiate it. At the end of the protocol, overdrive pacing was performed by introducing 5 or 20 successive stimulations after every 20 spontaneous beats, beginning with a pacing cycle equal to the flutter CL and decreasing by 10 ms with each attempt until the flutter was terminated.

This research protocol and care of the animals conforms to the Guiding Principles for Animal Experimentation as described by the Canadian Council on Animal Care and was reviewed by the committee for Animal Experimentation at the Research Center of Sacré-Coeur Hospital (Université de Montréal). At the end of the experimental protocol, ventricular fibrillation was induced by direct current application to the heart.

Data Analysis

The data were retrieved from the tape using axotape software and then stored on a silicon graphics computer for further analysis. The signals were automatically or manually timed using homemade software (Mact, Centre de Recherche, Hôpital Sacré-Coeur de Montréal, Montréal, Québec, Canada).

Statistical Analysis

The data were expressed as mean \pm SD. Statistical comparison between control and drug in the same animals were performed by the t -test for paired data. Values of $P < 0.05$ were considered significant.

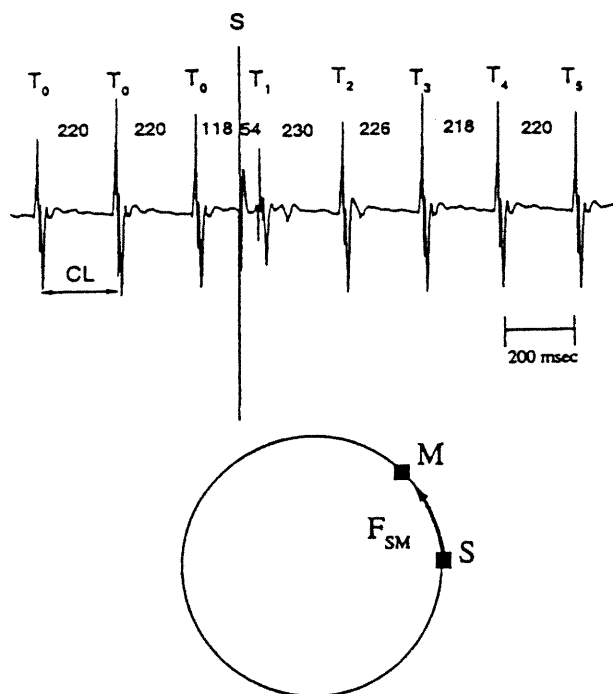


Figure 1. Endocardial bipolar recording at site M during atrial flutter. A premature stimulus is introduced after every 20 beats of atrial flutter at site S . T_0 is a spontaneous beat, S is the activation of the stimulation, and T_1, T_2, \dots are the response beats following the stimulation. T_0S is the coupling interval, ST_1 is the propagation time from S to M , ST_2 is the first return cycle, ST_3 is the second return cycle, etc. In this example, the flutter has a cycle length of 220 ms. The premature stimulus is introduced at a coupling interval T_0S of 118 ms. T_1 is advanced by 48 ms, T_2 by 38 ms, and T_3, \dots, T_n by 32 ms.

ATRIAL FLUTTER RESETTING AND TERMINATION

Numerical Simulations

To gain insight into the mechanisms responsible for resetting and to illustrate their dynamics, we have performed numerical simulations of a simple mathematical model of reentry. The latter depicts a continuous and homogeneous one-dimensional ring of cardiac cells, in which the evolution of the membrane potential V is given by the cable equation:

$$\frac{1}{\rho} \frac{\partial^2 V}{\partial x^2} = S \left(C_m \frac{\partial V}{\partial t} + I_{ion} \right)$$

$$V(0, t) = V(L, t)$$

$$\frac{\partial V}{\partial x}(0, t) = \frac{\partial V}{\partial x}(L, t)$$

where ρ (200 Ω cm) is the intracellular resistance per unit length, C_m (1 μ f/cm²) is the membrane capacitance, S (4 10^3 cm⁻¹) is the surface to volume ratio of the intracellular medium, t is the time (in milliseconds) and L is the length of the ring (in centimetres). I_{ion} (μ A/cm²) is the membrane ionic current, represented by a Beeler-Reuter type model of the cardiac myocytes. The characteristics of the model and the calculation method were described in a previous study.¹⁹

Sustained reentry was induced on a ring of 23 cm that was temporarily opened to initiate unidirectional propagation. Simulation was continued until a stable reentry was obtained, corresponding to a fixed waveform traveling at constant speed around the ring. Single and multiple stimuli were then applied, consisting of square current pulses of 2.5 ms with an amplitude of 60 A/cm² injected over a length of 450 μ m. In the model, the sodium ionic current I_{Na} is responsible for the propagation. It is expressed as $I_{Na} = g_{Na} m^3 h j (V - E_{Na})$, where $m \in [0,1]$ is a fast V dependent activation gate variable, h and j are slow inactivation gate variables. The product $h*j$ provides an appropriate measure of local state excitability¹⁹ and is used to picture the evolution of the EG during reentry.

Results

Hints From a Simple Model

It is known that the reentry circuit in common AF consists of a refractory region of tissue behind the propagating wavefront, and of an EG consisting of a partially and possibly a fully excitable region just ahead of the propagation wavefront.^{4,7} In a common representation to explain and model this phenomena, the reentry is pictured as a fixed waveform with the EG traveling at constant speed around a ring of excitable tissue.^{20,21} A stimulus applied in the EG may induce uni- or bidirectional propagation. Annihilation may take place when

the external stimulus is applied just at the limit of the EG, in the vulnerable window where only a retrograde activation wavefront is created.²² When a stimulus is applied beyond the vulnerable window, a second antegrade activation wavefront is also created by which reentry is maintained. Initially, this wavefront may travel through partially recovered tissue, such that the propagation is slower and CL prolonged. After a number of rotations, all effects of the premature stimulation are dissipated and the reentry returns to its stable regime. Numerical simulations show that this description of the dynamics following a stimulation is incomplete even for the simplified model of reentry around a homogeneous one-dimensional ring, described in the Numerical Simulation section.

A stable reentry with a CL of 325 ms was established on a ring of 23 cm. Figure 2 displays the spatiotemporal evolution of membrane potential (V , solid line) and excitability ($h*j$, dotted line) following a stimulation applied at locus S. Panel a (from top to bottom) shows the spatial profile of V and $h*j$ every 20 ms starting at the end of stimulation S_1 . S_1 was applied 225 ms (69% of the CL) after the last passage of the reentry wavefront at this location. The excitability at locus S was then at 20% ($h*j = 0.2$) of its maximum value 1 (corresponding to complete recovery). The preexisting wavefront (F) moves front left to right. The stimulation S_1 produces an antegrade (A) and a retrograde (R) activation wavefronts. Since A is premature and travels in the tail of F, it moves slowly and gives rise to a short action potential. However, the collision of R and F produces a long strip of depolarized tissue in which recovery of excitability is delayed. As a consequence, there is a long time interval from 60 to 260 ms, during which two disjoint EGs exist, one ahead of wavefront A and one behind it, separated by the region of collision where repolarization is delayed. We call this phenomenon *collision effect* (CE). Depending on the length of the circuit, wavefront A may reach the region of collision before the tissue has completely recovered its excitability and then experiences a slowing of propagation.

Panel b shows that the CE may be amplified by applying a second stimulus S_2 , which was applied 200 ms after S_1 (panel a). The spatial profile of V and $h*j$ are shown every 20 ms from the end of S_2 . A second collision takes place that delays repolarization. The EG of wavefront A diminishes as it approaches the collision region, and its propagation speed decreases as it reaches partially recovered tissue. The reentry returns to its stable regime after a few CL oscillations. Thus, the CE may produce local decrease of propagation velocity in a perfectly homogeneous tissue.

With S_2 more premature ($S_1-S_2 = 180$ ms, panel c), the dynamics become more complex. The retrograde wavefront R stops at the border of the collision region produced by S_1 . The preexisting wavefront F travels through the collision region but dies out when it reaches the tail of refractoriness left by R. Finally, the antegrade wavefront A travels around the ring and stops near the last point reached by F in the region of collision. Thus, the CE provides an alternative mechanism to an-

nihilate reentry, different from unidirectional block. The interval of prematurity for this form of termination is at least 20 ms since the same scenario was also obtained for a S_1-S_2 interval of 160 ms. This is much larger than the usual few millisecond duration for the vulnerable window, in which unidirectional block can be obtained.

The simulation results in a simple one-dimensional model of reentry show that CE exists, is amplified by multiple stimuli, and may lead to

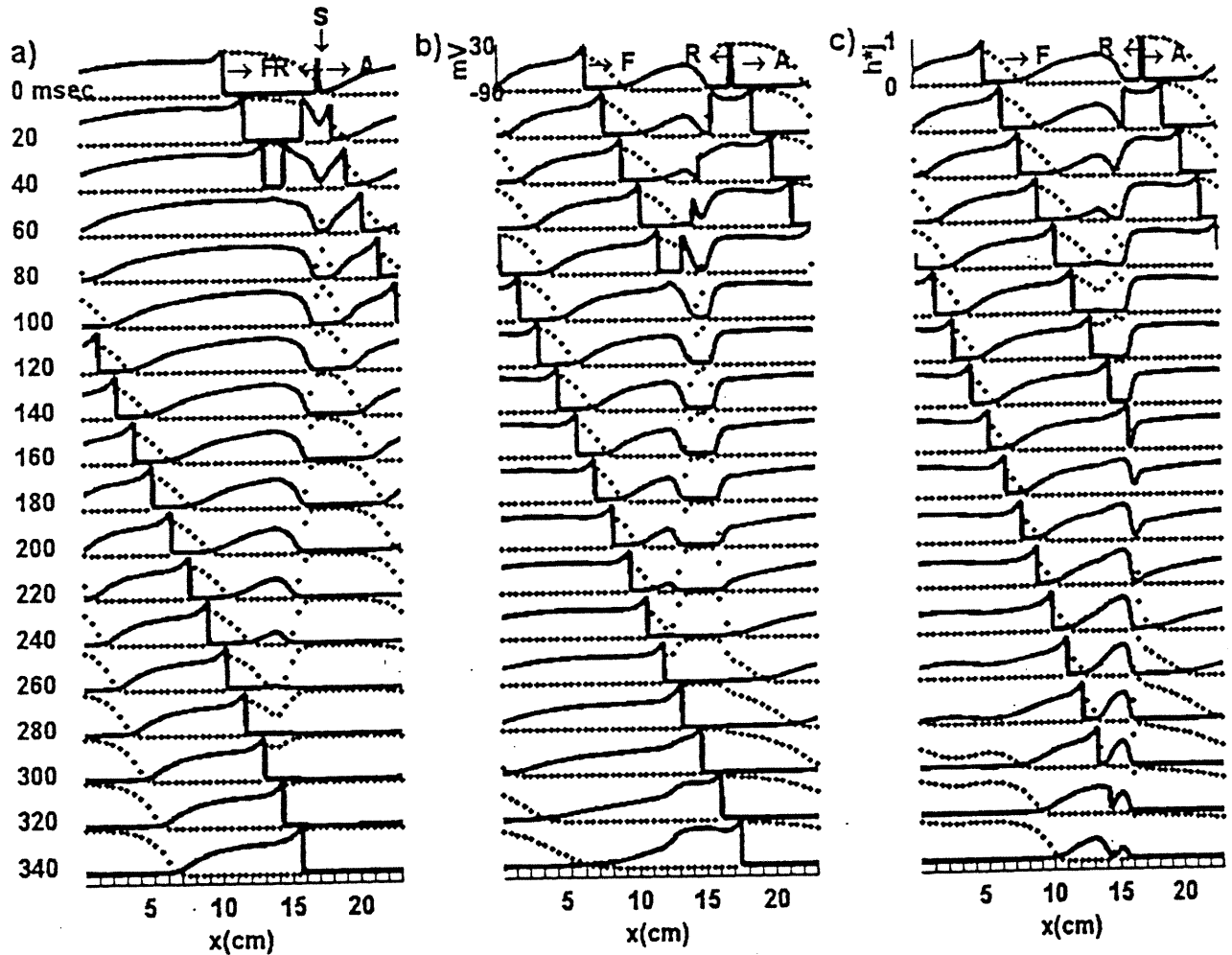


Figure 2. Reentry on a ring model of 23 cm in length and cycle length of 325 ms. Each panel displays the spatial pattern of V (solid line) and excitability h^*j (dotted line) along the ring for every 20 ms from the time of the stimulation $t = 0$. The point $x = 0$ and $x = 23$ cm are connected together to form the ring. (A) The stimulus S_1 was applied at locus S , 225 ms after the last passage of the wavefront of reentry. Two wavefronts are created by the stimulation, the antegrade A and the retrograde R that collides with the preexisting wavefront F at about 60 ms. When wavefront A reaches the site of collision, it slows down due to incomplete recovery of excitability. (B) The stimulus S_2 was applied at locus S , 200 ms after S_1 . The spatial profile at the beginning of the stimulation is indicated at 200 ms in panel a. A second collision occurs that delays repolarization and induces cycle length oscillations, which become stable after few turns (results not shown). (C) The stimulus S_2 was applied at locus S , 180 ms after S_1 . The spatial profile at the beginning of the stimulation is indicated at 180 ms in panel a. Wavefront R is terminated in the region of refractoriness left by S_1 . Wavefront F dies out because it reaches the tail of refractoriness left by R . Finally, wavefront A reaches the region of collision and stops because of refractoriness left by F .

ATRIAL FLUTTER RESETTING AND TERMINATION

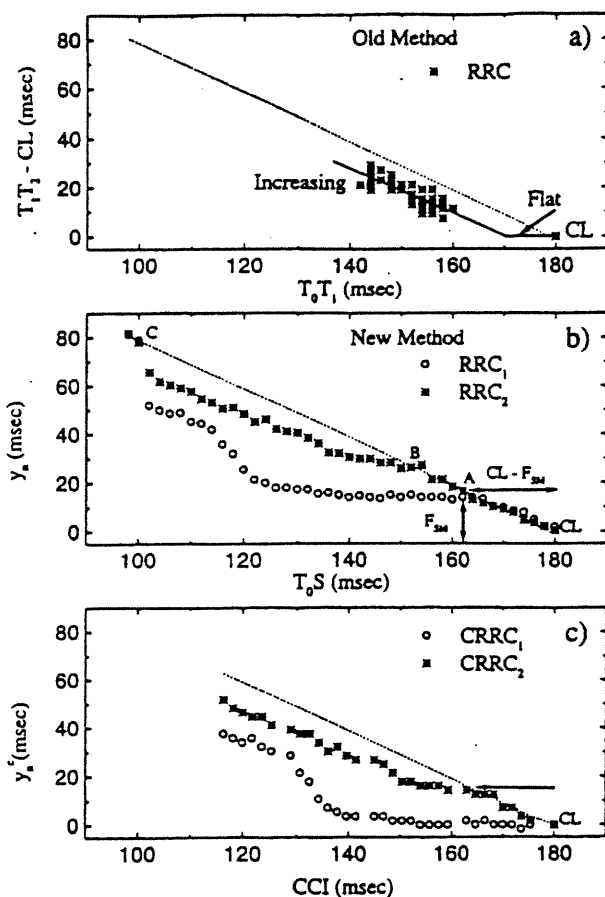


Figure 3. Comparison of the reset response curves (RRCs) obtained with the standard and the corrected methods without propafenone. (A) The RRC obtained by the standard method $T_1T_2 - CL$ (cycle length) vs T_0T_1 . A linear regression was used to fit the increasing portion of the RRC. The flat portion was obtained from the intersection of the fitted line with the horizontal line drawn from the CL. (B) The RRCs, $y_1 = ST_1$ versus T_0S (RRC_1 , open circle) and $y_2 = ST_2 - CL$ vs T_0S (RRC_2 , stars). The dashed line $CL - T_0S$ with $T_2 - T_0 = 2 CL$ represents a refractory tissue or propagation in partially refractory tissue that is fully compensated. The first part of the curve between CL and point A is refractory because the wavefront activation is already beyond S. In the second part, between A and B, RRC_1 is fully excitable but RRC_2 is partially refractory and compensates for the resetting of RRC_1 . In the third part, between B and C, resetting occurs without full compensation. At point C, the tissue is refractory indicating the end of the EG and the beginning of the ERP. The full excitable portion in RRC_1 represents the propagation time in a free running flutter F_{SM} between S and M. (C) The corrected reset response curves (CRRCs) obtained by expressing the measurements at the stimulation site, $y_1^c = ST_1 - F_{SM}$ versus corrected coupling interval (CCI) ($CRRC_1$, open circle), and $y_2^c = ST_2 - CL - F_{SM}$ versus CCI ($CRRC_2$, stars), where CCI is the corrected coupling interval $T_0S + F_{SM}$. The width of $CRRC_1$ represents the duration of the excitable gap. In this example, the effective refractory period (ERP) was 116 ms, the excitable gap (EG) was 64 ms, and the flat portion was 0 ms. With the standard method, the ERP was 142 ms, the EG was 38 ms, and the flat portion was 10 ms. Thus, the standard method overestimated the ERP and the flat portion, and underestimated the EG.

complex resetting behavior and an alternative scenario of termination.

Construction of the RRC

The reset-response method, which consists of introducing a premature stimulus during flutter, is a standard technique to determine the characteristics of the EG. The premature stimulus is applied at a single site in the circuit at coupling intervals varying from the flutter CL progressively down to the refractory period. The RRC describes the relationship between the CI of the premature beat (abscissa) versus the return cycle (RC) of the subsequent beat (ordinate). A flat portion of this curve at long CIs indicates the presence of fully excitable tissue, while an increasing portion at progressively shorter CIs reveals the presence of partially refractory tissue. Thus, the width of the RRC represents the entire EG. In most studies, the stimulating electrodes (S) and the recording electrode (M), whose signals were used to evaluate the CI

and the RC, were located at different points in the circuit.^{4,6} The CI was calculated as the time interval between the last free beat (T_0) and the first activation after the stimulus at site M (T_1) (Fig. 1). The RC was calculated as the time between the first and second poststimulus activation T_1T_2 . Only the points in which $T_0T_2 < 2 CL$ by more than 3 ms were retained for the construction of the RRC (Fig. 3a). The points with $T_0T_2 \geq 2 CL$, shown in the new method (Fig. 3B between points A and B, stars), were not retained. This procedure may introduce some inconsistencies in the results. First, as shown in Figure 1, the CI is the sum of two separate time intervals: T_0S , from the last free beat to the time of stimulation, and ST_1 which is the time needed for the captured beat to travel from S to M. The prematurity of the stimulation at site S is $T_0S + F_{SM}$, where F_{SM} is the conduction time of the flutter wavefront between S and M. As long as ST_1 remains equal to F_{SM} , $CI = T_0S + ST_1$ provides a correct measure of the prematurity.

However, as shown in Fig. 3B (ST_1 , open circles), the propagation between S and M becomes progressively slower with prematurity (i.e., $ST_1 > F_{SM}$ for smaller T_0S). Therefore, CI is overestimated by the amount $ST_1 - F_{SM}$, which increases with prematurity. Thus, the interval T_0T_1 may increase, and stimuli with different prematurities (i.e., $T_0S + F_{SM}$) may end up with the same value of CI (T_0T_1). This is shown in Fig. 3A and B, where the points associated with T_0S between 100 and 130 ms (Fig. 3B, stars) are overlapped with the ones with T_0S between 130 and 150 msec when T_0T_1 is used as abscissa (Fig. 3A).

Second, since $ERP = CI_{min}$, where CI_{min} is the shortest CI (T_0T_1) which resets the flutter, the overestimation of CI also results in the overestimation of the ERP and the underestimation of the $EG = CL - ERP$.

To avoid these pitfalls, it would be more appropriate to time the CI and the RC at the stimulation site. This would require an experimental setup with a fast switching amplifier to commute from stimulation to recording mode with the same electrode, or to avoid saturation of the recording electrode in case of close stimulation and recording sites. Since these devices were not available to us, we devised a method to approximate the measure of CI and RC at the stimulation site.

What is needed is an approximation of F_{SM} . The interval T_0S is decremented by 2 ms from the CL to the ERP, and the points $y_n = ST_n - (n - 1)CL$ ($n = 1, 2, \dots$) are plotted as a function of T_0S (Fig. 3B). A number $(n - 1)CL$ is subtracted from ST_n to see if the effects of stimulation are dissipated after $(n - 1)$ rotations. Consider first y_1 (open circle in Fig. 3B). For $CL - F_{SM} \leq T_0S \leq CL$, the activation wavefront is already beyond S, the stimulation has no effect and y_1 falls on the line $CL - T_0S$ (dashed line in Fig. 3B). For T_0S slightly shorter than $CL - F_{SM}$, the antegrade wavefront created by the stimulation travels in fully excitable tissue, and $y_1 = F_{SM}$ just as for the free running flutter. The ordinate at which y_1 leaves the line $CL - T_0S$ and becomes a flat line thus corresponds to F_{SM} (≈ 15 ms, point A in Fig. 3B). The corrected coupling interval (CCI) expressed with respect to S is thus $CCI = F_{SM} + T_0S$. It measures the time elapsed since the crossing of the last free beat at site S. The corrected reset response curve (CRRC), $y_1^c = ST_1 - F_{SM}$ versus CCI (CRRC₁) measures the increase of the propagation time from S to M relative to the free running flutter (Fig. 3C open circles). Propagation in fully excitable tissue corresponds to $y_1^c = 0$. Since stimuli applied in the ERP also fall on the dashed line $ST_1 = CL - CI$ (point C, Fig. 3B), the shortest CCI that resets the AF defined the end of the ERP and the beginning of the EG.

The comparison of CRRC₁ and CRRC₂ ($y_2^c = ST_2 - F_{SM} - CL$ vs CCI, Fig. 3C, stars) may also reveal some additional properties of the circuit. In the case illustrated in Fig. 3C, CRRC₂ falls on the line $CL - CCI$ at long coupling intervals between points A and B. Considering CRRC₂ alone, this would suggest that stimuli applied at these coupling intervals did not induce propagation. Comparison with CRRC₁ shows that the stimuli were indeed successful and that propagation from S to M was as in fully recovered tissue. The difference between CRRC₁ and CRRC₂ indicates that the wavefront has traveled in partially recovered tissue in some part of the circuit beyond site M (horizontal arrow in Fig. 3C), which fully compensates the resetting between S and M at long CCIs, and increases the delay at shorter CCIs. Since the flat portion is meant to measure full recovery over the entire circuit, it was defined from CRRC₂. For calculation purposes, we have defined the flat portion as the range of CCIs with $CRRC_2 \leq 1.67$ standard deviation (95% confidence interval) of the free running cycle. The flat portion was considered to exist if its width was > 4 ms, which represented the maximum sampling error between two activations. With this criterion, the flat portion was 0 ms in Fig. 3C, CRRC₂ being purely increasing, and 26 ms in Fig. 4B (without PPF) and 4D (with PPF) where CRRC₂ was mixed with a flat portion at long CCIs followed by an increasing portion at short CCIs.

This procedure also helps to correct another possible imprecision in the standard method of analysis of the reset-response. In the standard method, the duration of the flat portion was obtained from the intersection of the line that fit the increasing portion of the RRC (i.e., $T_1T_2 - CL$ vs T_0T_1) with a horizontal line drawn from the CL (solid lines, Fig. 3A). This procedure overestimated the flat portion. The latter had a duration of 10 ms with the standard method (Fig. 3A), compared to 0 ms with the corrected method (Fig. 3C) where the CRRC₂ was purely increasing. In this example, the corrected ERP and EG were 116 ms and 64 ms, respectively. (Fig. 3C), compared to 142 ms and 38 ms in the standard method (Fig. 3A). As shown in Fig. 4B and 4D, there were cases where CRRC₁ and CRRC₂ had the same flat portions. In such cases, the standard and the corrected methods would give similar results.

Effects of PPF on the EG and the CRRC

The effects of PPF on AF and on the characteristics of the EG as determined by CRRC₁ (EG, ERP) and CRRC₂ (flat portion) are given in Table IA. Propafenone prolonged AF CL from 136 ± 16 ms to 178 ± 27 ms ($P < 0.0001$). The ERP, evalu-

ATRIAL FLUTTER RESETTING AND TERMINATION

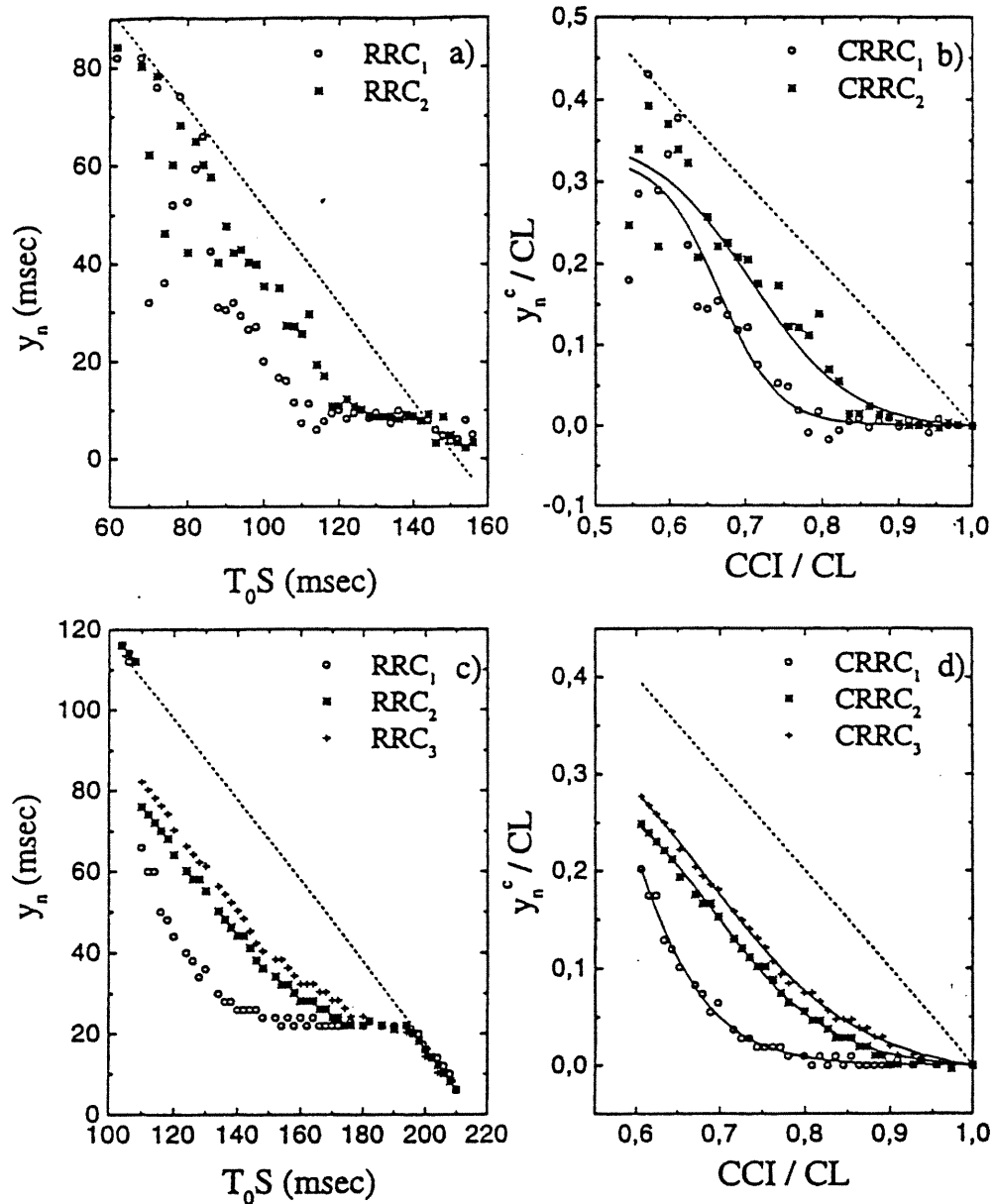


Figure 4. The reset response curves (RRCs) and their corresponding corrected reset response curve (CRRCs) before and after drug infusion, (A and B) without PPF and (C and D) with PPF. In this example, the tissue is not completely recovered after one rotation, compare CRRC₂ (stars) and CRRC₃ (plus). A nonlinear function of the form $y(x) = a_1[\tanh(-a_2 \times +a_3) - \tanh(-a_2 + a_3)]$ with $y(1) = 0$ is used to fit the CRRCs, expressed in percent of the cycle length. The mean quadratic error between the fit and the data is reduced with propafenone, indicating stability of the circuit.

ated from RRC₁, was also increased from 82 ± 15 ms to 112 ± 21 ms ($P < 0.0001$). However, the proportion of the ERP to the CL remained constant, $60 \pm 8\%$ without PPF compared to $63 \pm 5\%$ with PPF ($P = 0.22$) (results not shown). The EG was also increased from 54 ± 12 ms to 66 ± 12 ms ($P = 0.01$). In proportion to the CL, the EG stayed constant ($40 \pm 8\%$) without PPF compared to $37 \pm 5\%$ with PPF ($P = 0.22$) (results not shown). The increase

in the EG may be represented by the following equation:

$$EG = \alpha CL - \beta ERP$$

Where α and β are the proportion of increase in CL and ERP, respectively. We found that $\alpha \approx \beta = 1.3$, which suggests the presence of both Class I and Class III effects. PPF did not affect the overall du-

Table I.
Effects of Propafenone on Atrial Flutter Using the Corrected Method

| Dog | A CL (ms) | | EG (ms) | | ERP (ms) | | FEP (ms) | | Mean Quadratic Error | |
|-----------|------------|----------|----------|---------|-----------|----------|------------|-------|----------------------|-------------|
| | C | PPF | C | PPF | C | PPF | C | PPF | C | PPF |
| 1 | 132 ± 2 | 214 ± 7 | 55 | 70 | 77 | 144 | 7 | 14 | 0.077 | 0.035 |
| 2 | 142 ± 1 | 196 ± 2 | 56 | 78 | 86 | 118 | 6 | 0 | 0.080 | 0.046 |
| 3 | 135 ± 1 | 196 ± 2 | 41 | 57 | 94 | 139 | 0 | 11 | 0.012 | 0.021 |
| 4 | 152 ± 3 | 218 ± 1 | 74 | 86 | 78 | 132 | 26 | 22 | 0.045 | 0.005 |
| 5 | 135 ± 1 | 141 ± 1 | 67 | 57 | 68 | 84 | 0 | 7 | 0.062 | 0.078 |
| 6 | 124 ± 1 | 165 ± 1 | 34 | 56 | 90 | 109 | 0 | 0 | 0.041 | 0.018 |
| 7 | 127 ± 1 | 144 ± 1 | 59 | 66 | 68 | 78 | 0 | 0 | 0.061 | 0.030 |
| 8 | 130 ± 4 | 170 ± 1 | 45 | 62 | 85 | 108 | 0 | 0 | 0.016 | 0.017 |
| 9 | 140 ± 1 | 173 ± 1 | 73 | 61 | 67 | 112 | 0 | 0 | 0.050 | 0.028 |
| 10 | 112 ± 1 | 140 ± 2 | 49 | 54 | 63 | 86 | 0 | 0 | 0.023 | 0.027 |
| 11 | 147 ± 1 | 203 ± 2 | 43 | 91 | 104 | 112 | 0 | 0 | 0.020 | 0.011 |
| 12 | 179 ± 1 | 206 ± 2 | 63 | 72 | 116 | 134 | 0 | 0 | 0.012 | 0.008 |
| 13 | 119 ± 2 | 175 ± 2 | 47 | 55 | 72 | 120 | 0 | 0 | 0.009 | 0.014 |
| 14 | 129 ± 1 | 156 ± 1 | 55 | 60 | 74 | 96 | 0 | 0 | 0.010 | 0.009 |
| Mean ± SD | 136 ± 16 | 178 ± 27 | 54 ± 12 | 66 ± 12 | 82 ± 15 | 112 ± 21 | 3 ± 7 | 4 ± 7 | 0.04 ± 0.03 | 0.02 ± 0.02 |
| T test | P < 0.0001 | | P = 0.01 | | P < 0.001 | | P = 0.8636 | | P = 0.0361 | |

A CL = atrial flutter cycle length; EG = excitable gap; ERP = effective refractory period; C = control; PPF = propafenone; FEP = fully excitable portion.

Table II.
Effects of Propafenone on Atrial Flutter using the Standard Method

| Dog | EG (ms) | | ERP (ms) | | FEP (ms) | |
|-----------|------------|---------|------------|----------|------------|--------|
| | C | PPF | C | PPF | C | PPF |
| 1 | 58 | 47 | 76 | 172 | 17 | 28 |
| 2 | 48 | 59 | 94 | 136 | 3 | 21 |
| 3 | 39 | 25 | 96 | 172 | 6 | 25 |
| 4 | 50 | 56 | 102 | 162 | 25 | 27 |
| 5 | 39 | 33 | 96 | 108 | 9 | 11 |
| 6* | 33 | — | 92 | — | 10 | — |
| 7 | 47 | 50 | 80 | 94 | 12 | 7 |
| 8 | 35 | 25 | 98 | 146 | 10 | 12 |
| 9 | 57 | 33 | 84 | 140 | 5 | 10 |
| 10 | 31 | 23 | 82 | 118 | 10 | 13 |
| 11 | 34 | 50 | 112 | 154 | 15 | 10 |
| 12 | 37 | 47 | 142 | 160 | 9 | 14 |
| 13 | 32 | 24 | 88 | 152 | 9 | 8 |
| 14 | 47 | 21 | 82 | 136 | 8 | 8 |
| Mean ± SD | 43 ± 9 | 38 ± 14 | 95 ± 17 | 142 ± 27 | 11 ± 6 | 15 ± 8 |
| T test | P = 0.2219 | | P < 0.0001 | | P = 0.0625 | |

* The criteria of resetting were not satisfied with propafenone.
EG = excitable gap; ERP = effective refractory period; FEP = fully excitable portion; C = control;
PPF = propafenone.

ATRIAL FLUTTER RESETTING AND TERMINATION

ration of full excitability (i.e., the flat portion, evaluated from $CRRC_2$), 3 ± 7 ms without PPF compared to 4 ± 7 ms with PPF. It was also observed that 9 of 14 dogs had $CRRC_2$ without flat portions in the absence and presence of drugs. In summary, propafenone increased CL, ERP, and the EG nearly in the same proportions, but did not change the width of the flat portion.

Table II shows the results obtained with the standard method. As expected, the estimated ERP was much longer than that obtained by the corrected method. As for the corrected method, the estimated ERP was significantly increased by PPF (from 95 ± 17 ms to 142 ± 27 ms $P < 0.0001$), but the difference expressed in percent of the CL also remained significant ($69 \pm 7\%$ vs $79 \pm 7\%$, $P = 0.0013$) (results not shown), an effect of the overestimation of the ERP. The EG stayed constant (from 43 ± 9 ms to 38 ± 14 ms, $P = 0.22$), but the difference became significant when expressed in percent of CL (from $31 \pm 7\%$ to $21 \pm 7\%$, $P = 0.001$) (results not shown). The flat portions, determined by the standard method, were longer than those of the corrected method, but PPF did not significantly change their duration (11 ± 6 ms without PPF compared to 15 ± 8 ms with PPF, $P = 0.06$). In comparison with the revised method, the ERP and the flat portion were overestimated, while the EG was underestimated. With the standard method, PPF appears to induce a larger relative increase in the ERP than in CL, and the RRCs were mixed in all dogs and no purely increasing curves were observed.

PPF did not affect the stability of the CL (i.e., the standard deviation, Table I). However, it did affect the stability of the RRC. This is illustrated for one dog in Figure 4A (without PPF) and 4C (with PPF), which shows that the variation of resetting as a function of T_0S is much smoother and continuous in the presence of the drug. To quantify this change in stability, the $CRRCs$, expressed in percent of CL (Figs. 4B and 4D), were fitted by a nonlinear function and the mean quadratic error was calculated (see Pacing Protocol During AF). Results for $CRRC_2$, given in Table I, show a significant drop of the mean quadratic error with PPF.

Mechanism of Resetting

Single Stimulus

As discussed above, the difference between $CRRC_1$ and $CRRC_2$ indicates incomplete recovery of excitability in part of the circuit beyond the locus M. Depressed excitability between S and M (i.e., $CRRC_1 > 0$) is expected to persist for some distance beyond M such that $CRRC_2 > CRRC_1$. In this case, slowing of conduction occurs because the antegrade wavefront travels in the tail of the

flutter wavefront (PE). $CRRC_2 > 0$ at CCI values where $CRRC_1 = 0$ may indicate a heterogeneity embedded in the tissue. However, it may also reflect a dynamic heterogeneity induced by the stimulation. As shown by numerical simulations (Fig. 2, Hints From a Simple Model), the stimulus induces a retrograde wavefront that collides with the activation wavefront of the flutter and defines a region where recovery of excitability might be delayed (CE). In general, resetting might come from a mix of PE, CE, and heterogeneity. In some cases, the relative contribution of each effect could be assessed by measuring the conduction time in the different portions of the circuit and by plotting the relative conduction time (RCT), (i.e., the ratio of conduction time post-to-prior the stimulation) versus the CCI expressed in percent of CL in each region.

Figure 5 shows the RCT in the different portions of the circuit whose $CRRCs$ are given in Figure 3C. The flat portion of $CRRC_1$ corresponds to $RCT = 1$ between S and M (panel a). It is followed by a pronounced slowing of propagation in the second portion of the circuit between electrodes M and the following site N (panel b), which explains why $CRRC_2$ does not have a flat portion and shows that there is spatial heterogeneity in the recovery of excitability. At short CCIs, the abrupt increase of RCT between S and M (panel a) is partially compensated by a drop of RCT in the second portion of the circuit (panel b). The delay ($RCT > 1$) takes place in the first (panel a) and the second portion of the circuit (panel b). Collision takes place in the last portion of the circuit between sites N and S, but CE is absent or is undetectable. The latter may have been dissipated before the stimulated antegrade wavefront reaches the region of collision.

Figure 6 shows the RCT in the circuit whose $CRRCs$ are given in Figure 4D. In this case, both PE and CE effects are present in the circuit. First, we observe the PE between sites S and M (panel a), which is dissipated completely between sites M and N (i.e., RCT returns to one) (panel b). The RCT increases again in the final portion between sites N and S (panel c), which is consistent with a CE. Both effects contribute to the $CRRC$ at short CCIs. When CE is important, it may take more than a turn to dissipate completely such that a difference between the $CRRC_2$ (stars) and $CRRC_3$ (plus) still exists (Fig. 4D). With a single stimulus, propagation was always stabilized after the second cycle (i.e., $CRRC_n = CRRC_3$, $n > 3$).

The low number of recording sites, their uneven distribution around the circuit, and CL and conduction time fluctuations have precluded the distinction between the CE and PE in some cases. We used the following criteria to identify the existence of CE:

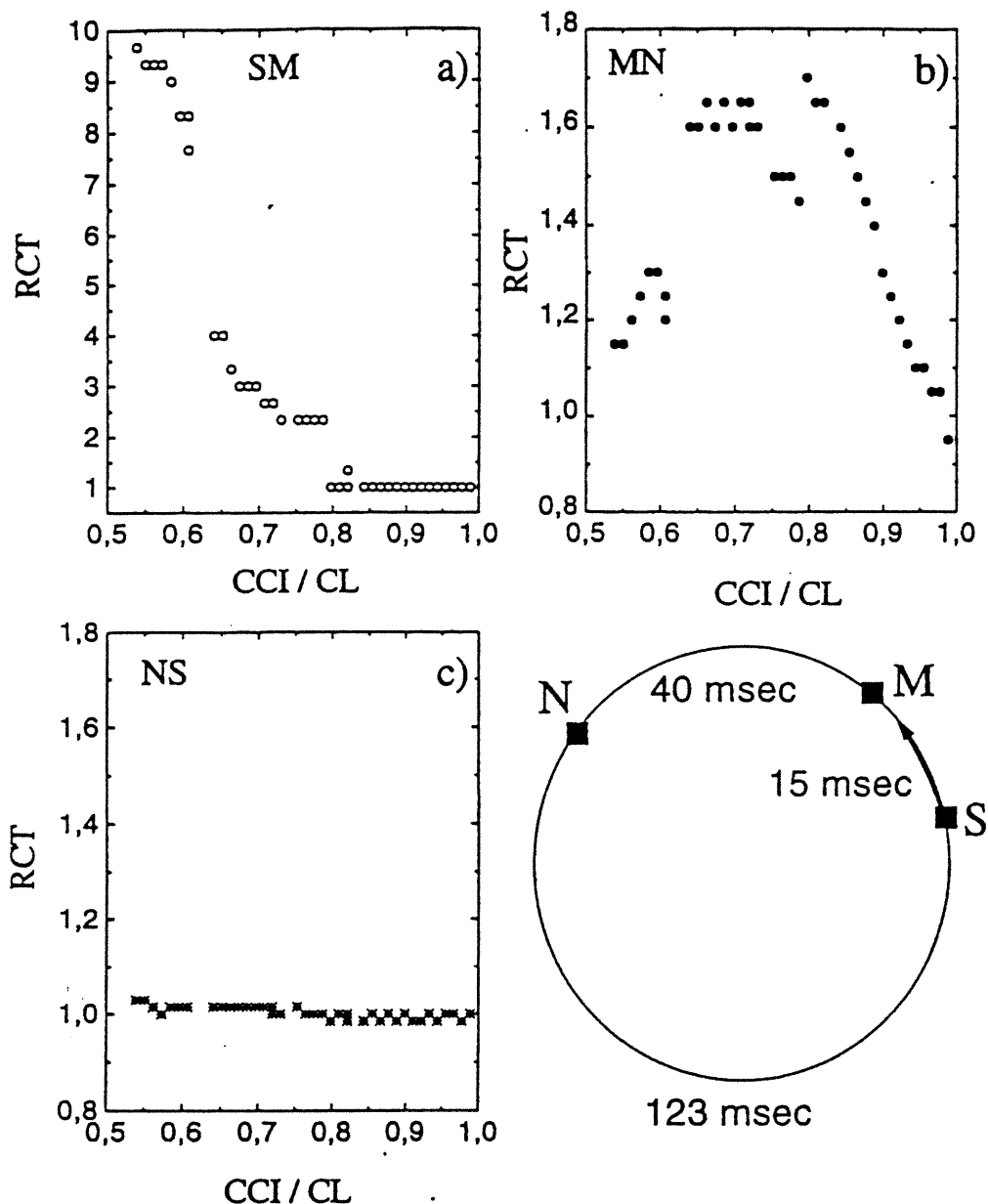


Figure 5. Relative conduction time (RCT) versus corrected coupling interval ($CCI = T_{oS} + F_{SM}$, expressed in percent of the cycle length) in the different regions of atrial flutter (AF) circuit, corresponding to the corrected reset response curve (CRRCs) in Fig. 3C (A) In the first portion of the circuit between sites S and M, $RCT = 1$ in the range $(0.8, 1)$ indicating fully excitable tissue, and $RCT > 1$ in the range $(0.54, 0.8)$ indicating partially refractory tissue. (B) In the second portion, between sites M and N, RCT increases in the range $[0.8, 1]$ indicating partially refractory tissue, and decreases in the range $[0.54, 0.8]$ to compensate for prematurity in A. Full compensation of excitability occurs in the range $[0.9, 1]$, corresponding to the first portion in $CRRC_2$ (horizontal arrow in Fig. 3C). (C) In the last portion of the circuit between sites N and S, the tissue is fully excitable ($RCT = 1$) in the whole range $[0.54, 1]$.

ATRIAL FLUTTER RESETTING AND TERMINATION

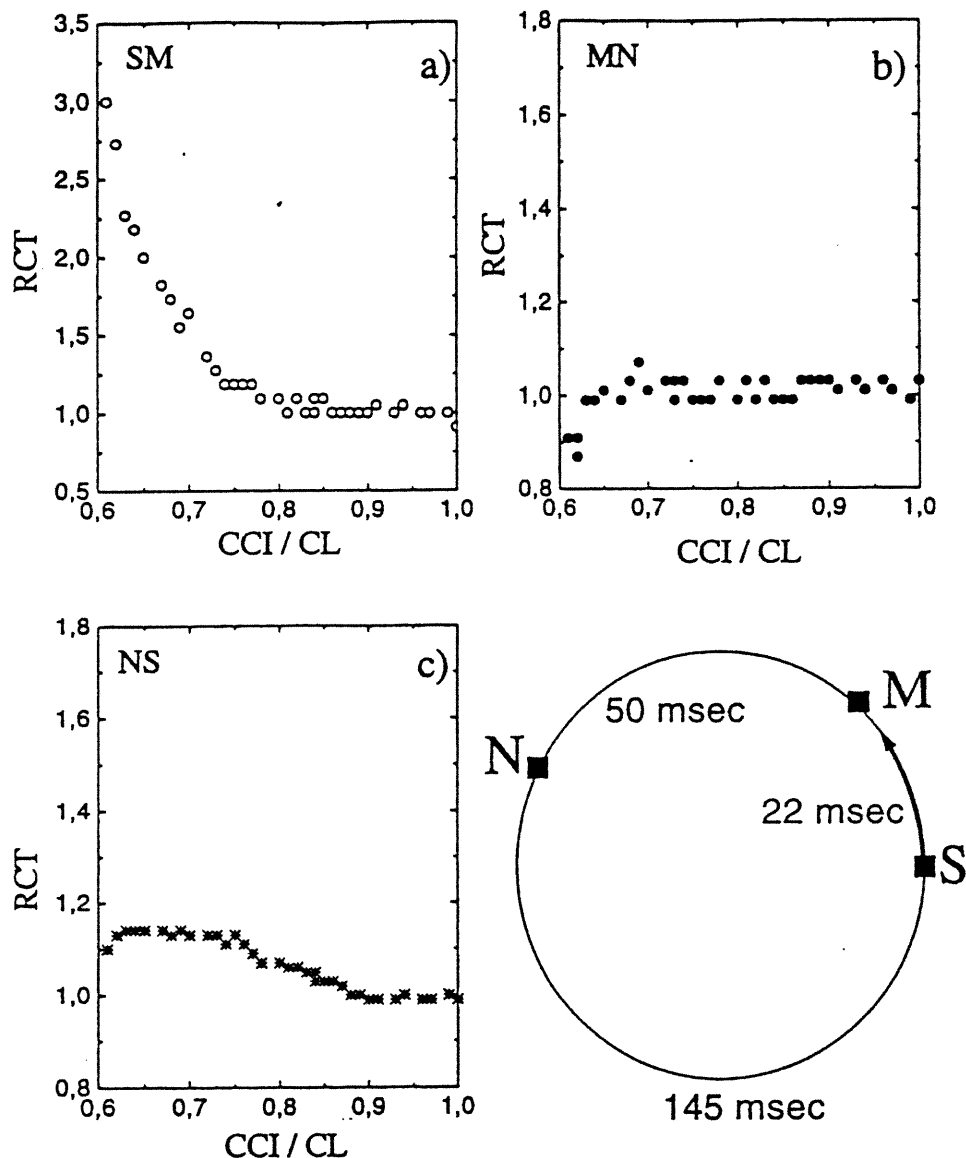


Figure 6. Relative conduction time (RCT) versus corrected coupling interval (CCI) ($CCI = T_{oS} + F_{SM}$, expressed in percent of the cycle length) in the different regions of the atrial flutter (AF) circuit corresponding to Figure 4D. (A) The RCT between sites S and M is constant ($RCT = 1$) in the range $[0.8, 1]$, indicating fully excitable tissue, but it increases ($RCT > 1$) in the range $[0.6, 0.8]$ indicating partially refractory tissue. The increase in RCT in this region is due to the prematurity effect (PE). (B) The RCT between sites M and N is constant ($RCT = 1$) in the whole range $[0.6, 1]$ indicating complete dissipation of the PE. (C) The RCT in the collision region between sites N and S is constant ($RCT = 1$) in the range $[0.9, 1]$, indicating fully excitable tissue, but it increases ($RCT > 1$) in the range $[0.6, 0.9]$, indicating partially refractory tissue. The increase of RCT in this region is attributed to the collision effect (CE). In this example, the tissue is fully excitable in the range $[0.9, 1]$ in all part of the circuit, indicating homogeneity of the tissue.

1. If $RCT > 1$ in the last portion of the circuit where collision had taken place, and $RCT = 1$ (i.e., PE was dissipated) in the portion of the circuit adjacent to this last portion, then the increase of RCT in the last portion was attributed to the CE (Fig. 6).

2. If the dissipation of the PE was not complete in the portion of the circuit adjacent to the collision region, but the increase in RCT in the collision region was of the same order of magnitude or higher than in the adjacent zone, then this increase of RCT was attributed to the CE (Fig. 10).

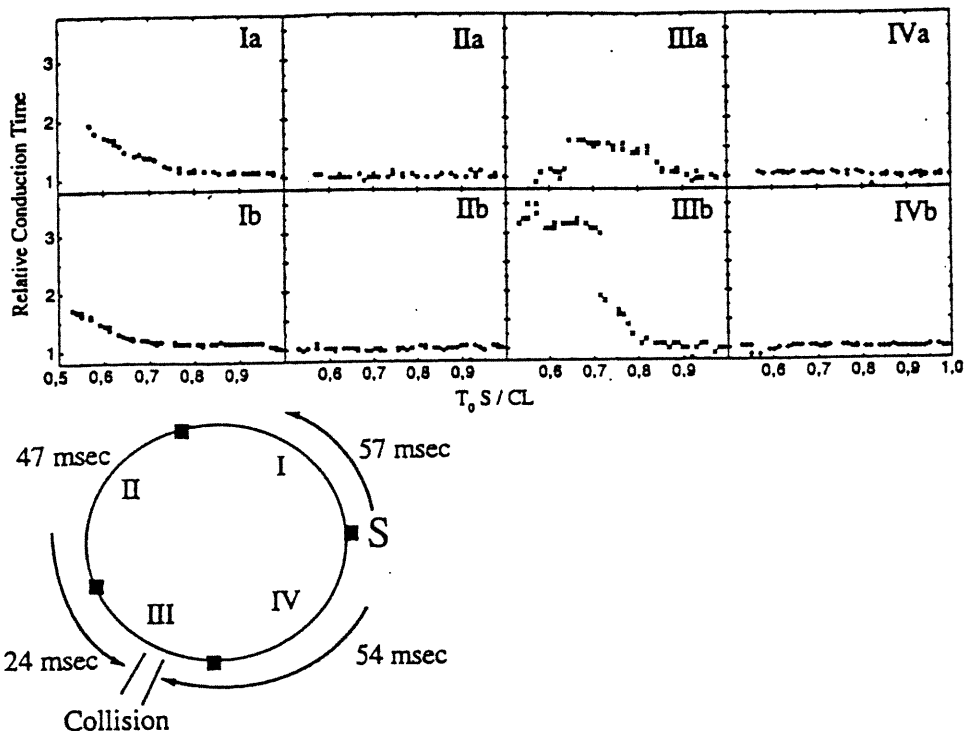


Figure 7. Relative conduction time (RCT) versus corrected coupling interval ($CCI = T_0S + F_{SM}$, expressed in percent of the cycle length [CL]) for one (top panels) and three stimulations (bottom panels) in the different regions of the atrial flutter (AF) circuit with propafenone, using 16 recording sites. Regions I, II, III, and IV have durations of 57, 47, 24, and 54 ms, respectively. The RCT in region I (panel Ia) is constant ($RCT = 1$) in the range $[0.8, 1]$, indicating fully excitable tissue, but it increases ($RCT > 1$) in the range $[0.55, 0.8]$ indicating partially refractory tissue. The increase in RCT in this region is due to the prematurity effect (PE), which is dissipated completely in region II (panel IIa). The RCT in the collision region (panel IIIa) is constant ($RCT = 1$) in the range $[0.9, 1]$ and $[0.55, 0.65]$, indicating fully excitable tissue, but it increases ($RCT > 1$) in the range $[0.65, 0.9]$, indicating partially refractory tissue. The increase in RCT in this region is attributed to the collision effect (CE), which is dissipated completely in region IV (panel IVa). In this example, the tissue is fully excitable in the range $[0.9, 1]$ in all parts of the circuit, indicating tissue homogeneity. The bottom panels (Ib, IIb, IIIb, IVb) represent the RCT of the test stimulus in a set of three stimulations with the first two applied at 82% of the CL. Regions I, II, and IV remained unaffected except for the prolongation of the EG in region I (panel Ib) due to the shortening of action potential duration. In region III, the CE is amplified by multiple stimuli (panel IIIb) due to depression of the tissue by successive collisions.

3. When there was no dissipation of PE in the portion adjacent to the collision region and no increase of RCT in the collision region, then the CE was considered absent or undetectable (Fig. 5).

With these criteria, the CE was identified in 11 (11%) of 103 CRRCs without PPF compared to 34 (27%) of 127 CRRCs with PPF. PPF facilitated the identification of CE because it changed the recovery of excitability in the substrate and reduced the fluctuations in RCT along the circuit.

The criteria used to identify the CE were not stringent enough to exclude the effects of delayed refractoriness due to structural heterogeneity in the region of collision. The uncertainty was enhanced by the poor spatial resolution of the collision region provided by the low number of electrodes. To improve the distinction between

the different types of propagation delay, we performed a series of experiments using a set of 16 electrodes distributed uniformly around the reentry circuit. In Figure 7 for example, PE was observed in region I (panel Ia), while CE was observed in region III (panel IIIa) after a complete recovery of excitability in region II (panel IIa). In region IV (panel IVa), excitability was restored. The increase in RCT occurred in the region of collision, representing only 13% of the free running flutter, and was not observed in the adjacent portions of the circuit, suggesting a true CE.

Multiple Stimuli

With a single stimulus, the CE could not be observed in all preparations. To see the effect of

ATRIAL FLUTTER RESETTING AND TERMINATION

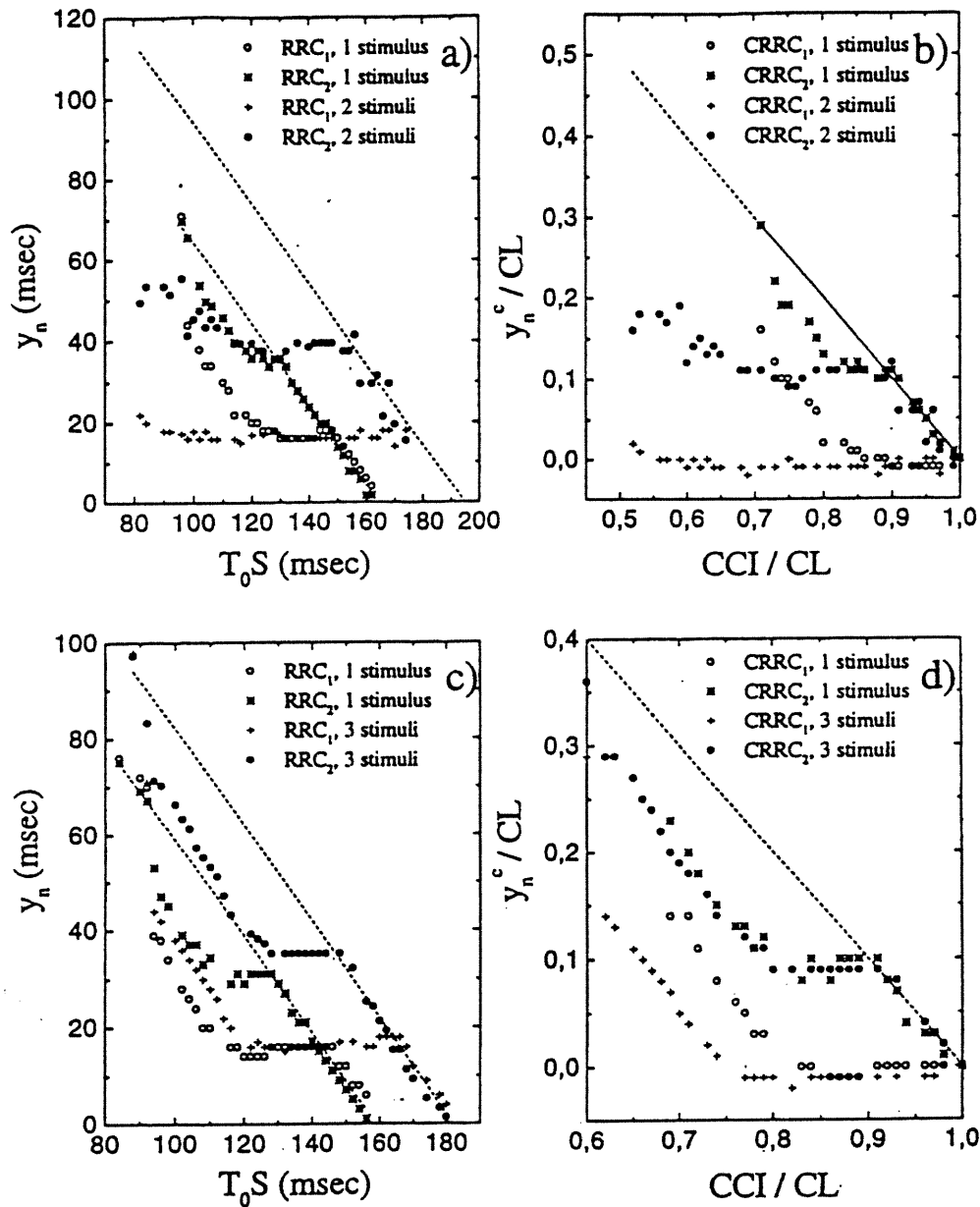


Figure 8. The reset response curves (RRCs) and their corresponding corrected reset response curve (CRRCs) for single and double stimuli with propafenone. (A) RRC_1 (open circle) and RRC_2 (stars) for a single stimulus, and RRC_1 (plus) and RRC_2 (solid circle) for double stimuli. (B) Their corresponding CRRCs, expressed in percent of the cycle length (CL), for single stimulus, and in percent of the corrected cycle length (CCL) for double stimuli. In the latter, the first stimulus was introduced at $T_0S = 102$ ms (61% of CL), prolonging the next return cycle (i.e., CCL) by 18%. The CCL was obtained from the data on the dashed line in RRC_1 (plus) as $CCL = T_0S + ST_1$. The excitable gap (EG) was prolonged with double stimuli due to the shortening of action potential duration, (C and D) same as (A and B) but for single and triple stimuli. The first stimulus was introduced at $T_0S = 112$ ms (68% of CL), the second stimulus was introduced at 164 ms later, prolonging the next return cycle (i.e., CCL) by 15%. The EG was also prolonged with triple stimuli due to the shortening of action potential duration.

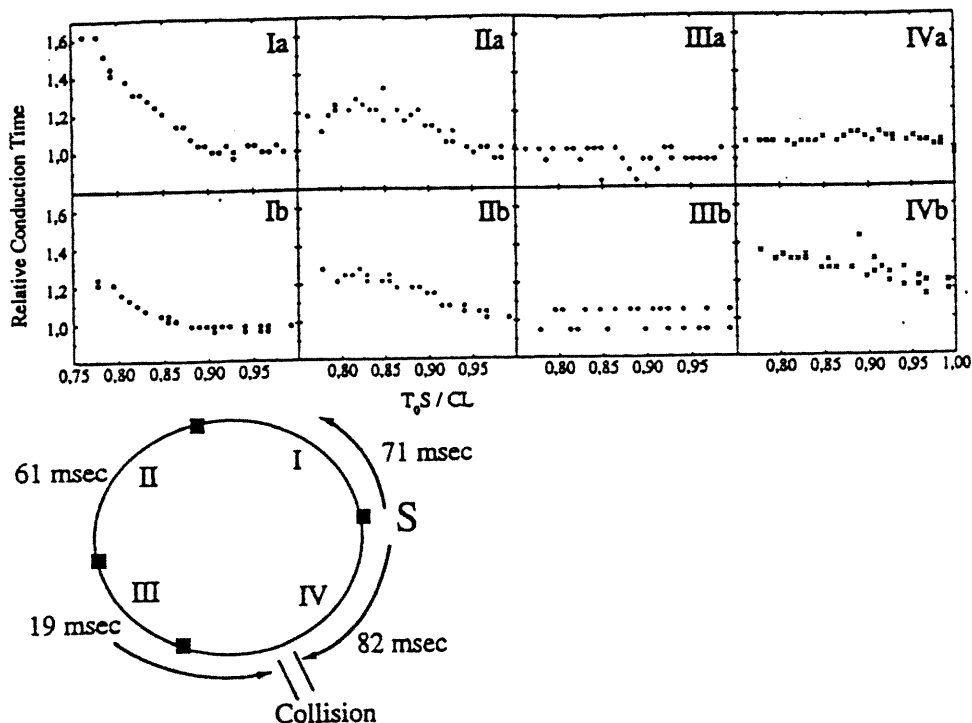


Figure 9. Relative conduction time (RCT) versus corrected coupling interval (CCI) ($CCI = T_0S + F_{SM}$, expressed in percent of the cycle length [CL] for one (top panels) and five stimulations (bottom panels) in the different regions of the atrial flutter (AF) circuit with propafenone (PPF), using 16 recording sites. Regions I, II, III, and IV have durations of 71, 61, 19, and 82 ms, respectively. The RCT in region I (panel Ia) is constant ($RCT = 1$) in the range [0.9,1], indicating fully excitable tissue, but it increases ($RCT > 1$) in the range [0.75,0.9] indicating partially refractory tissue. The increase in RCT in this region is due to the prematurity effect (PE). The RCT in region II (panel IIa) is constant ($RCT = 1$) in the range [0.95,1] indicating fully excitable tissue. It increases ($RCT > 1$) in the range [0.8,0.95] due to heterogeneity but decreases in the range [0.75,0.8] to compensate for prematurity in region I. In regions III (panel IIIa) and IV (panel IVa), the tissue is completely recovered. The bottom panels represent the RCT of the test stimulus in a set of five stimulations with the first four applied at 90% of the CL. Regions I (panel Ib), II (panel IIb), and III (panel IIIb) remain unaffected except for the prolongation of the flat portion in region I (panel Ib) due to the shortening of the action potential duration. In this region, the flutter is terminated before reaching the effective refractory period. Thus, the EG is underestimated. The increase in RCT in the region of collision (panel IVb) is attributed to the collision effect, which is due to depression of the tissue by successive collisions.

multiple stimuli on the CE, we performed multiple stimulations and overdrive pacing. Regardless of the low number of recording sites, multiple stimuli and PPF facilitated the distinction between the CE and PE. For 1 or 2 extrastimuli or sustained pacing, this distinction was possible in 4 (20%) of 20 CRRCs without PPF compared to 12 (36%) of 33 CRRCs with PPF.

When one or two extrastimuli (S_1) were used prior to the test stimulus (S), the S_1 stimulations were always applied at a coupling interval premature enough to induce a significant resetting. The test stimulus (S) scanned the CI to construct the RRC. Figure 8A and C compare RRC_1 and RRC_2 obtained with single (S) (open circle, stars) and double stimuli (S_1 -S) (plus, solid circle), and triple stimuli (S_1 - S_1 -S) (plus, solid circle). Figure 8B and

D show the corresponding $CRRC_1$ and $CRRC_2$ after normalization by CL. In the case of one and two S_1 stimuli, the CL was corrected to account for the influence of the S_1 s. The corrected cycle length (CCL) corresponded to the time needed for the wavefront, produced by the last S_1 , to complete a rotation. The data points corresponding to long T_0S were used to draw the line $T_0S + ST_1$ vs T_0S (dash lines in 8a and c). ST_1 must be 0 for a stimulation applied at the moment when the front reached M and had completed a rotation, CCL was estimated as the value where the line crossed the abscissa.

In Figure 8B, the extrastimulus was applied at 61% of the CL ($T_0S = 102$ ms), prolonging the next return cycle (i.e., CCL) by $\approx 18\%$. In Figure 8D, the first S_1 was applied at 68% of the CL ($T_0S =$

ATRIAL FLUTTER RESETTING AND TERMINATION

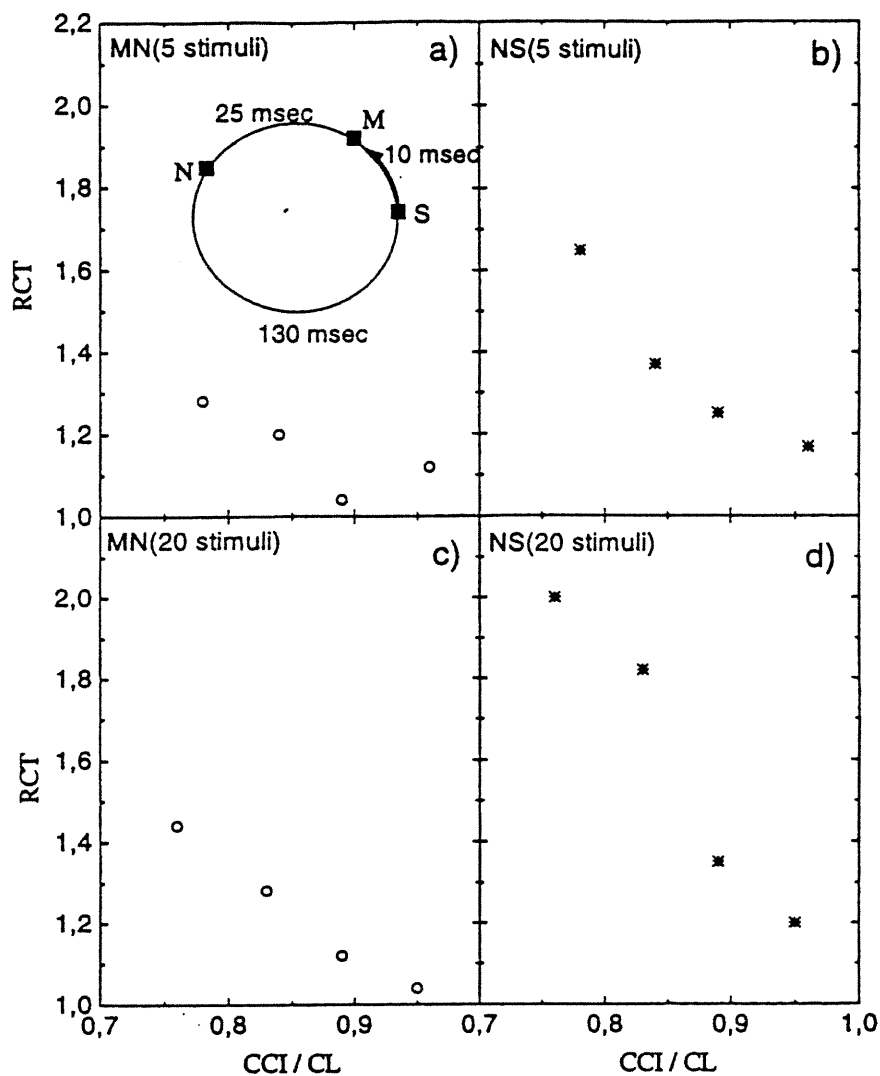


Figure 10. Relative conduction time (RCT) versus the corrected coupling interval (CCI), expressed in percent of the cycle length (CL), for the last stimulus in pacing with 5 or 20 stimuli after drug infusion (A and B). The RCT for 5 pacing stimuli increases between sites M and N due to prematurity effect (PE). It also increases in the region of collision between sites N and S. This increase is attributed to the collision effect (CE), (C and D) same as (A and B) but for 20 pacing stimuli. The CE with 20 stimuli is much greater than with 5 stimuli.

112 ms). The second S_1 , which was applied 164 ms later, prolonged the return cycle (i.e., CCL) by $\approx 15\%$. The test stimulus in double and triple stimuli protocol could induce propagation in a larger range of CCIs (plus, solid circle), indicating an extended EG. Furthermore, the conduction time from S to M (CRRC₁, plus) was close to that of the free running flutter over a wide range of CCIs, indicating a full recovery of excitability in this portion of the circuit as expected from the shortening of the action potential due to prematurity.

Multiple stimuli could increase the CE without affecting the PE. This is shown in Figure 7 which compares the results obtained with one (top row panels) using 16 recording sites. In three stimuli protocol, the first two stimuli had fixed prematurities (82% of the free running CL). The amplitude of RCT of the test stimulus due to PE remained the same (panels Ia and Ib), but the amplitude of RCT ascribed to CE was much higher with multiple stimuli (panels IIIa and IIIb). The increase of RCT produced by the extrastimuli occurred only in the region of collision.

Spatial heterogeneity was also observed using single and multiple stimulations as shown in Figure 9 for one (top row panels) and five stimulations (bottom row panels) using 16 recording sites. The four S_1 stimuli had fixed prematurity (90% of the CL). The amplitude of RCT of the test stimulus due to PE (panels Ia and Ib) and heterogeneity (panels IIa and IIb) remained the same for 1 and 5 stimulations. The difference in RCT between Ia and Ib at short coupling intervals was due to an incomplete RRC in Ib because the flutter stopped before reaching the ERP. An increase in RCT due to multiple stimuli was observed in the region of collision (panels IVa and IVb) after a complete dissipation in region III (panels IIIa and IIIb). Again, this increase was consistent with a CE since it occurred always in the region of collision. In few cases, we did observe an increase in heterogeneity due to multiple stimuli (results not shown).

The increase of RCT due to the collision may be amplified by adding more stimuli at increasing prematurities, as shown in Figure 10 for overdrive pacing with 5 or 20 stimuli. In this figure, the CE in region N-S increased with the number of stimuli (panels b and d), while the PE in region M-N remained unaffected (panels a and c).

Termination of AF

The incidence of termination increased with the number of stimuli. Single stimuli resulted in termination of AF in 26 (25%) of 103 RRCs without PPF and in 31 (24%) of 127 RRCs with PPF. Double stimuli resulted in termination in 7 (50%) of 14 RRCs without PPF and in 8 (53%) of 15 RRCs with PPF. Overdrive pacing attempted in seven

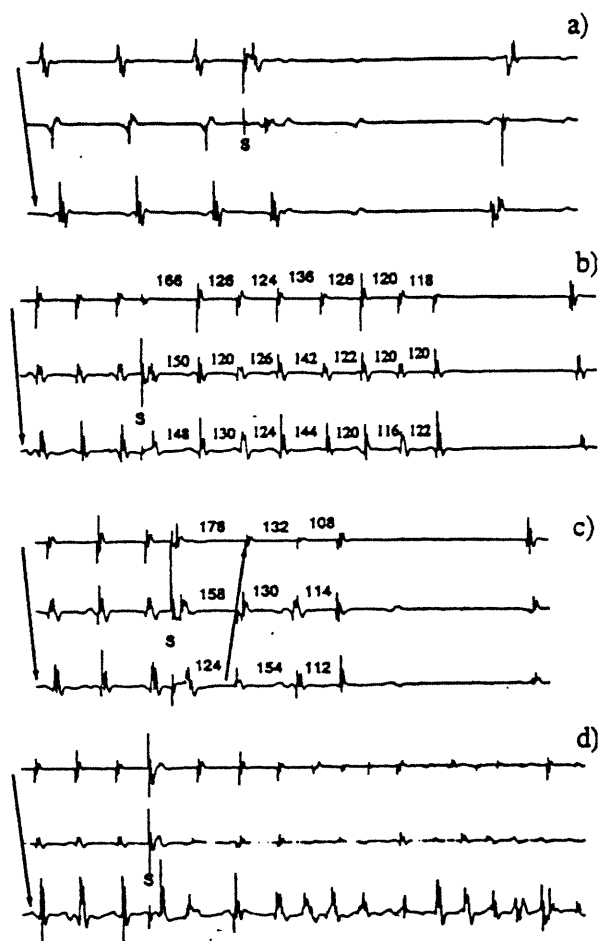


Figure 11. The different types of atrial flutter (AF) termination. (A) Abrupt termination due to the collision effect, which depressed the tissue to a critical point such that the stimulated antegrade wavefront couldn't propagate. (B) Cycle length oscillations with the last cycle short. (C) Changing the direction of rotation in the region of collision from clockwise to counterclockwise. (D) Fibrillation.

animals on PPF resulted in termination in all 7 (100%). Overdrive pacing without drugs was not performed. Overall, multiple stimuli increased the efficacy of termination over single stimuli. Our results are consistent with previous studies in ventricular tachycardia.⁹ Four mechanisms of AF termination were observed: (1) abrupt AF termination, (2) termination preceded by CL oscillations, (3) reversal of activation or changing path, and (4) transient fibrillation. Each mechanism is described as follows:

1. Abrupt termination of AF was observed in cases for which a large CE was detected. The flut-

ATRIAL FLUTTER RESETTING AND TERMINATION

ter was then terminated within one cycle. It was not unidirectional block since the antegrade wavefront was detected in all segments before the region of collision where propagation failed (Fig. 11A). This mode of termination was consistent with the block of propagation reported in the mathematical model of reentry (Fig. 2), which was due to depression of the tissue in the region of collision.

2. CL oscillations have been described to be associated with interval dependant changes in conduction velocity and in action potential duration and atrial refractoriness.²³⁻²⁵ We observed AF annihilation following CL alternations or more complex forms of CL fluctuations (e.g., Fig. 11B). In all cases, failure of propagation was observed with a short last cycle. Large amplitude CL variations led to early termination, while small variations led to late termination. Annihilation of AF occurred when the antegrade wavefront arrived early after a short cycle and collided with tissue that had not recovered its excitability. In many cases, annihilation was observed in the region of collision, which suggests that CE might also be involved in this type of termination.

3. Reversal of activation or changing path is another mechanism of termination (Fig. 11C). It could occur many times before terminating the AF. Each reversal was preceded by a sequence of CL oscillations ending with a block after a short cycle, or changing the path and blocked. This suggests that propagation was two dimensional and could not be approximated by a one-dimensional movement.

4. Transient fibrillation occurred when the AF circuit was unstable because of CL and/or conduction time fluctuations. Wavefronts from the outside could easily invade the AF circuit and then desynchronized it. Fibrillation could start after a premature activation or after a few complex CL oscillations (Fig. 11D).

We have estimated the risk of transient fibrillation with and without PPF in 36 annihilations without (including single, double, and triple stimuli) and 48 with PPF (including single, double, triple, and overdrive pacing). Transient fibrillation was found in 75% of the episodes without PPF, compared to 22% with PPF. Termination by scenarios 1, 2, or 3 was found in 25% of the episodes without PPF and 78% with PPF. Termination by conduction block (i.e., scenario 1) was associated with a failure of propagation of the stimulated antegrade wavefront in the region of collision. When termination occurred following CL oscillations (i.e., scenario 2), variation in conduction time was observed in the region of collision, suggesting that CE might also be involved in this type of termination.

The presence of PPF may facilitate the depression of the tissue in the region of collision and prevent "short-circuiting." These results are in agreement with previous studies,^{16,17,26} which showed that PPF terminated the flutter by depressing conduction to a critical point beyond which propagation of the circulating impulse becomes impossible.

Our results showed that with PPF, an EG with a flat portion favoured abrupt termination of AF while a partially EG favoured termination by CL oscillations with or without reversal of activation. In dog 4, which had the largest flat portion, seven of nine episodes terminated abruptly (scenario 1) without CL variability. In the other dogs with a small flat portion or purely increasing RRC, termination occurred by CL oscillations, reversal of activation, or fibrillation.

Discussion

This study showed that a better estimation of the ERP, the EG, and the fully excitable portion can be obtained by expressing both the CI and the RC in reference to the stimulation site. The standard method,⁴ which expressed the CI and the RC in reference to the electrode distal to the stimulating site (in the direction of wave propagation), overestimated the ERP and underestimated the EG. This method also overestimated the flat portion due to the removal of data points at longer CIs, which corresponded to full compensation (i.e. $T_1T_2 = 2 \text{ CL}$), and failed to meet the criteria of resetting. Our analysis of the RRCs RRC_1 and RRC_2 showed that resetting could occur at these data points, but could also be fully compensated because of heterogeneity in the circuit. The wavefront propagated in fully excitable tissue in the first portion of the circuit (RRC_1), but in partially excitable tissue in the remaining portions (RRC_2). Such compensation was also previously observed,¹¹ but the authors argued that this phenomenon occurred for only one CI, and seemed unlikely to occur for a range of CIs.

The analysis of conduction time between electrodes in the different regions of the circuit revealed a slowing of conduction due to prematurity, CE, or spatial heterogeneity that may come from change in recovery of excitability or in wavefront curvature due to anatomic constraints. In the latter, the wavefront may detach from the obstacle near sharp edges and propagate around a circular area, thus increasing local conduction time.²⁷ The propagation delay in the region of collision was attributed to the collision effect rather than tissue heterogeneity. The results suggested that the CE was more readily amplified by multiple stimuli than PE or heterogeneity effects.

This study also showed that Class IC-PPF prolonged the CL, the ERP, and the EG in similar proportions, but didn't affect the flat portion. PPF stabilized the reentry circuit by reducing conduction time fluctuations in the different regions of the circuit. This results in smoother and more continuous RRCs. PPF also reduced the risk of transient fibrillation prior to termination. Our findings are in agreement with previous studies on PPF in the same model,¹⁶ and in the intercaval crush model,¹⁷ which demonstrated the prolongation of the ERP and the EG. Those models used the extrastimulus technique at a basic pacing CL of 300 ms to calculate the ERP during AF. They also determined the EG by subtracting the ERP from the CL.

Multiple stimuli were found to increase resetting and termination in AF. The duration of the flat portion between sites S and M was prolonged due to the shortening in action potential duration, caused by the prematurity of the first stimulus. Previous studies on ventricular tachycardia^{9,9,28} also showed that the EG was increased with double and triple stimuli. In those studies, the first stimulus was always fixed such that it didn't reset the tachycardia. The role of that stimulus was to "peel back" refractoriness such that the test stimulus could enter the circuit and reset the tachycardia over a broad range of coupling intervals. Contrary to the PE and heterogeneity, the slowing of conduction due to the CE was found to increase as the number of stimuli was increased. This suggests that the RRC of a sequence of pacing stimuli cannot be predicted from the RRC of one stimulus due to the increase in the CE.

Finally, the incidence of AF termination due to depression of conduction in the region of collision was increased by PPF. The EG wasn't abolished by PPF, in agreement with previous studies in animal models^{16,17} and in humans.²⁶ Termination occurred abruptly without CL oscillation, with CL variability, by fibrillation, or by changing the direction of rotation. The latter indicates that AF cannot always be approximated by a one-dimensional propagation, as in a ring. There was no significant change between the average coupling interval (in percent of the CL) that induced fibrillation and conduction block, 0.66 ± 0.1 versus 0.63 ± 0.14 ($P = 0.56$) without PPF and 0.59 ± 0.08 versus 0.64 ± 0.1 ($P = 0.14$) with PPF. This suggests that transient fibrillation is more likely to occur when the CE is small and not because of rapid pacing.

Limitation of the Studies

Our studies were limited for the following reasons:

1. Difficulties in distinguishing between the PE and the CE, and also between the different

types of termination due to the low number of recording sites and their uneven distributions. In a subsequent set of 11 dogs, we used 16 recording sites distributed uniformly around the circuit. This allowed us to reduce the uncertainty in distinguishing between PE, CE, and heterogeneity.

2. Difficulties in measuring the EG and the flat portion due to the variability of CL and/or conduction time in some cases.

3. The plasma levels of PPF have not been analysed yet. Our analysis was based on the plasma levels given in Derakhchan et al.⁴ where the same drug administration protocol was used. We measured the EG around a 60-minute infusion of PPF. Steady-state plasma levels might not have been reached in some cases.

4. Only one dose of PPF was used in each dog. Higher doses may have given different results.

Conclusion

We have studied the effects of PPF on resetting and termination of AF using single, multiple stimuli, and overdrive pacing. Our results are expressed at the pacing site and not the recording site as in previous studies. An improved representation of the RRC has been then obtained. We have found that PPF prolonged significantly not only the CL and the ERP as in Derakhchan et al.,⁴ but also the duration of the EG. However, the duration of the flat portion was not affected. Propafenone also stabilized the conduction time and the RRC. We have shown that resetting was not only due to the PE and heterogeneity, but also to the CE. The latter was found to increase with the number of stimuli and with PPF. We have also studied the relationship between the CE and AF termination with and without PPF. The flutter was more likely to be terminated by conduction block due to the depression of the tissue by the CE and PPF. The conduction block occurred abruptly without CL variability, with CL oscillations, or with reversal of activation. The incidence of transient fibrillation in AF diminished under the effects of PPF as well as CE. This suggests that the evaluation of PE and CE in AF may be an indication of the risk of atrial fibrillation.

Our findings demonstrate the relevance of studying the CE with other antiarrhythmic drugs with Class I and III effects to estimate the possible risk of transient fibrillation. These studies may be useful in the clinical setting by identifying drugs with little potential for transforming AF to fibrillation but whose use increases the chances of successful overdrive of AF.

Acknowledgment: The authors thank Ms. Caroline Bouchard for her technical support.

ATRIAL FLUTTER RESETTING AND TERMINATION

References

1. Frame LH, Page RL, Hoffman BF. Atrial reentry around an atomic barrier with a partially refractory excitable gap: A canine model of atrial flutter. *Circ Res* 1986; 58:495-511.
2. Frame LH, Page RL, Boyden PA, et al. Circus movement in the canine atrium around the tricuspid ring during experimental atrial flutter and during reentry in vitro. *Circulation* 1987; 76:1155-1175.
3. Bernstein RC, Frame LH. Ventricular reentry around a fixed barrier: Resetting with advancement in an in vitro model. *Circulation* 1990; 81:267-280.
4. Derakhchan K, Page P, Lambert C, et al. Effects of procainamide and propafenone on the composition of the excitable gap in canine atrial reentry tachycardia. *J Pharmacol Exp Ther* 1994; 270:47-54.
5. Fei H, Hanna MS, Frame LH. Assessing the excitable gap in reentry by resetting. *Circulation* 1996; 94:2268-2277.
6. Jalil E, Laflamme M, Kus T. Effects of procainamide on the excitable gap composition in a canine model of atrial flutter. *Can J Physiol Pharmacol* 1997; 75:1-8.
7. Jalil E, Le Franc P, Lebeau R, et al. Effects of procainamide on the excitable gap composition in common human atrial flutter. *PACE* 1998; 21:528-535.
8. Almendral JM, Stamato NJ, Rosenthal ME, et al. Resetting response patterns during sustained ventricular tachycardia: Relationship to the excitable gap. *Circulation* 1986; 4:722-730.
9. Almendral JM, Rosenthal ME, Stamato NJ, et al. Analysis of the resetting phenomenon in sustained uniform ventricular tachycardia: Incidence and relation to termination. *J Am Coll Cardiol* 1986; 8:294-300.
10. Stamato NJ, Frame LH, Rosenthal ME, et al. Procainamide-induced slowing of ventricular tachycardia with insights from analysis of resetting response patterns. *Am J Cardiol* 1989; 63:1455-1461.
11. Arenal A, Almendral JM, San Roman D, et al. Frequency and implications of resetting and entrainment with right atrial stimulation in atrial flutter. *Am J Cardiol* 1992; 70:1292-1298.
12. Callans DJ, Hook BG, Josephson ME. Comparison of resetting and entrainment of uniform sustained ventricular tachycardia: Further insights into the characteristics of the excitable gap. *Circulation* 1993; 87:1229-1238.
13. Callans DJ, Zardini M, Gottlieb CD, et al. The variable contribution of functional and anatomic barriers in human ventricular tachycardia: An analysis with resetting from two sites. *J Am Coll Cardiol* 1996; 27:1106-1111.
14. Callans DJ, Schwartzman D, Gottlieb CD, et al. Characterization of the excitable gap in human type I atrial flutter. *J Am Coll Cardiol* 1997; 30:1793-1801.
15. Dukes I, Vaughan Williams EM. The multiple modes of action of propafenone. *Eur Heart J* 1984; 5:115-125.
16. Spinelli W, Hoffman BF. Mechanisms of termination of reentrant atrial arrhythmias by class I and class III antiarrhythmic agents. *Circ Res* 1989; 65:1565-1579.
17. Inoue H, Yamashita T, Nozaki A, et al. Effects of antiarrhythmic drugs on canine atrial flutter due to reentry: Role of prolongation of refractory period and depression of conduction to excitable gap. *J Am Coll Cardiol* 1991; 18:1098-1104.
18. Boyden PA, Frame LH, Hoffman BF. Activation mapping of reentry around an anatomic barrier in the canine atrium: Observations during entrainment and termination. *Circulation* 1989; 79:406-416.
19. Vinet A, Roberge FA. The dynamics of sustained reentry in a ring model of cardiac tissue. *Ann Biomed Eng* 1994; 22:568-591.
20. Ito H, Glass L. Theory of reentrant excitation in a ring of cardiac tissue. *Physica D* 1992; 56:84-106.
21. Della Bella P, Maenzi G, Tondo C, et al. Usefulness of excitable gap and pattern of resetting in atrial flutter for determining reentry circuit location. *Am J Cardiol* 1991; 68:492-497.
22. Shaw RM, Rudy Y. The vulnerable window for unidirectional block in cardiac tissue: Characterization and dependence on membrane excitability and intercellular coupling. *J Cardiovasc Electrophysiol* 1995; 6:115-131.
23. Frame LH, Simpson MB. Oscillations of conduction, action potential duration, and refractoriness: A mechanism for spontaneous termination of reentrant tachycardias. *Circulation* 1988; 78:1277-1287.
24. Frame LH, Rhee EK. Spontaneous termination of reentry after one cycle or short nonsustained runs: Role of oscillations and excess dispersion of refractoriness. *Circ Res* 1991; 68:493-502.
25. Ortiz J, Igarashi M, Gonzalez X, et al. Mechanism of spontaneous termination of stable atrial flutter in the canine sterile pericarditis model. *Circulation* 1993; 88:1866-1877.
26. Tai CT, Chen SA, Feng AN, et al. Electropharmacologic effects of class I and class III antiarrhythmic drugs on typical atrial flutter. *Circulation* 1998; 97:1935-1945.
27. Fast VG, Kléber AG. Role of wave curvature in propagation of the cardiac impulse. *Cardiovasc Res* 1997; 33:258-271.
28. Stamato NJ, Rosenthal ME, Almendral JM, et al. The resetting response of ventricular tachycardia to single and double extrastimuli: Implications for an excitable gap. *Am J Cardiol* 1987; 60:596-601.

CHAPITRE III

**EFFECTS OF PROPAFENONE ON THE SPATIO-
TEMPORAL ELECTROPHYSIOLOGICAL
CHARACTERISTICS OF THE REENTRY CIRCUIT
IN A CANINE MODEL OF ATRIAL FLUTTER**

**EFFECTS OF PROPAFENONE ON THE SPATIO-TEMPORAL
ELECTROPHYSIOLOGICAL CHARACTERISTICS OF THE REENTRY
CIRCUIT IN A CANINE MODEL OF ATRIAL FLUTTER**

Elise Jalil ^{a,c}, Boualem Mensour ^c, Caroline Bouchard ^c, Alain Vinet ^{b,c} and Teresa Kus ^{a,c}

^a Department of Pharmacology, Université de Montréal, Montréal, Québec, Canada

^b Department of Physiology, Université de Montréal, Montréal, Québec, Canada

^c Research Centre, Hôpital du Sacré-Coeur de Montréal, Montréal, Québec, Canada.

Address for corresponding author:

Teresa Kus, MD, PhD

Sacré-Coeur Hospital Research Center

5400 Boulevard Gouin Ouest

Montréal, Québec, Canada

H4J 1C5

Tel.:(514) 338-2222 ext. 2571 Fax:(514) 338-2694

E-mail: kust@crhsc.umontreal.ca

**Effects of propafenone on the spatio-temporal electrophysiological characteristics
of the reentry circuit in a canine model of atrial flutter**

Elise Jalil, Boualem Mensour, Caroline Bouchard, Alain Vinet, Teresa Kus

Objective: The reset-response curve (RRC) has been used to assess global electrophysiological properties of the reentry circuit (ReC) in atrial flutter (AFl). In this study, we use RRC to characterise the ReC and determine if premature stimulation at one site predicts the range of prematurity throughout the ReC. Further, we assess the spatial homogeneity of the effect of the class IC antiarrhythmic propafenone (PPF) on the ReC.

Methods: A Y-shaped lesion was created between the superior and inferior vena cava and the right atrial appendage in 10 dogs. For stimulation and recording, 7 bipolar electrodes were inserted at the right atrial base. AFl was induced by burst pacing. The duration and composition of the excitable gap (EG) were determined by premature stimuli during AFl. PPF was administered intravenously during AFl in a loading dose (1 mg/kg) over 10 min followed by an infusion (1.8 mg/kg/hr) for a maximum of 2 hrs. RRCs were constructed with and without PPF. **Results:** PPF prolonged AFl cycle length (CL) and effective refractory period but had a variable effect on EG composition. In 6 dogs, a 16 bipolar electrode belt was then placed around the right atrium for recording. Conduction times (CT) in different portions of the ReC were measured in free running AFl without and with drug. In all 6 dogs, the CL prolongation on PPF was due to a marked increase of CT localised in one or two sections of the ReC. The CT were then plotted against the local prematurity for each portion of the ReC. The range of effective prematurity was large in one or two portions of the ReC adjacent to the stimulation site in the direction of propagation. **Conclusions:**

The tonic effect of PPF was spatially inhomogeneous. The variability of CT was inhomogeneous in different sections of the ReC with no consistent relation to PPF effects. RRCs obtained by single site stimulation demonstrates the EG in the region or adjacent section prematurely stimulated. However, since the range of prematurity is significantly less in the remainder of the ReC, it is not a reliable measure of EG on other regions of the ReC.

KEY WORDS: **Discipline:** experimental; **Object of study:** heart; **Level:** organism; **Field of study:** electrophysiology

Supraventricular arrhythmia, Antiarrhythmic agents, Arrhythmia (mechanisms)

INTRODUCTION

Atrial flutter (AFI) is a macroreentrant arrhythmia in the right atrium. The reset-response curve (RRC) has been used to assess the global characteristics of the reentry circuit in clinical [1-3] and in experimental [4-6] models. Previous studies have demonstrated site-dependent differences in the RRCs in human [7,8] and in rabbit [9] ventricular tachycardia. Ingelmo and Frame [10] have shown that the shape of the RRC was different when stimuli were delivered distal as compared with proximal to a single site of interval-dependant conduction in canine in vitro tricuspid rings. In this study, we determine if a premature stimulation at one site predicts the range of prematurity throughout the entire reentry circuit.

Propafenone (PPF), a class IC antiarrhythmic agent [11], produces a frequency- and voltage-dependent reduction in the sodium conductance but also possesses significant potassium channel, mild beta-adrenergic and weak calcium channel blocking activities [12]. To determine the spatial homogeneity of PPF effect, the conduction times (CT) in different portions of the reentry circuit were measured in a free running AFI both before and after the administration of the drug using a belt containing 16 bipolar electrodes. Callans et al. [13] have shown that PPF either decreases conduction in an unchanged ventricular tachycardia circuit or lengthens the circuit barriers without changing the exit point of the circuit. Frame et al. [14] have studied the conduction of the reentrant impulse around a tricuspid ring, using intracavitary electrode arrays from 96 endocardial bipolar electrodes. These investigators found that without drug, the reentry was relatively uniform and no single part

of the pathway displayed markedly slower conduction. Lidocaine slowed conduction in all parts of the reentrant pathway. In the present study, we examine the effects of PPF on the electrophysiological characteristics of the reentry circuit in a canine model of AFL.

METHODS

Surgical technique

10 mongrel dogs of either sex (mean weight \pm SD; 33 ± 3 kg) were studied in the post absorptive state. General anesthesia was induced with sodium thiopental (30 mg/kg i.v.) and maintained with chloralose (80 mg/kg i.v. bolus supplemented by 15 mg/kg/hr maximum as needed). The dogs were intubated endotracheally and ventilated (Harvard pump, Millis, MA) with room air (10 breaths/min, tidal volume to achieve a maximum inspiratory pressure of 20 cm of water) to maintain arterial pH 7.35 to 7.45 and $pO_2 > 80$ mm Hg. Arterial and venous cannulae were inserted in the left femoral artery and vein by direct cutdown for blood pressure monitoring and blood sampling, respectively. An additional venous cannula was inserted in the right internal jugular vein for drug administration. Muscular relaxation was then induced with 3 mg/kg i.v. of gallamine triethiodide (Flaxedil 100). A right thoracotomy was performed via the fourth or fifth intercostal space and the pericardium was incised to provide access to the vena cava and the right atrium. Based on the procedure developed by Frame *et al.* [4], a lesion was created by sewing in a line extending from the superior to the inferior vena cava. A second line,

extending from the first two-thirds of the way to the tip of the right atrial appendage and parallel to but 1 to 2 cm above the atrioventricular groove was similarly sewn. Both sewn lines were also crushed in order to assure an anatomical barrier. In 4 of these dogs, five close (2-4 mm) bipolar, teflon coated (except for the tips), stainless steel wire electrodes were inserted using a 26 gauge needle around the base of the right atrium for stimulating or recording from the endocardial atrial surface. In the other 6 dogs, 7 close (2-4 mm) bipolar endocardial stimulation electrodes were inserted around the base of the right atrium (Fig. 1), and, in the same area, a belt on which 16 bipolar electrodes were mounted was placed around the right atrium for epicardial recording. These electrodes were uniformly distributed around the tricuspid valve (except for the septal region). Recordings were obtained from electrodes which were in contact with the right atrium. In some animals with smaller hearts, the belt extended beyond the right atrium and 1-5 electrode pairs on this part of the belt, were therefore not used for recording.

Measurement of electrophysiological parameters

In the first 4 dogs, a single lead (II) surface electrocardiogram, atrial electrograms from each of the five bipolar electrodes and femoral arterial pressure were monitored and recorded using a Nihon Kohden (Tokyo, Japan) polygraph (model RM6008) and data also were stored on a digital 8 track, Sony Instrumentation Cassette Recorder PC-108M (Tokyo, Japan). In the 6 dogs in which 7 bipolar stimulation electrodes were inserted around the base of the atrium and a 16 bipolar electrode recording belt was used, atrial electrograms were recorded using a multi-channel recording system (Electrophysiological Data Interface,

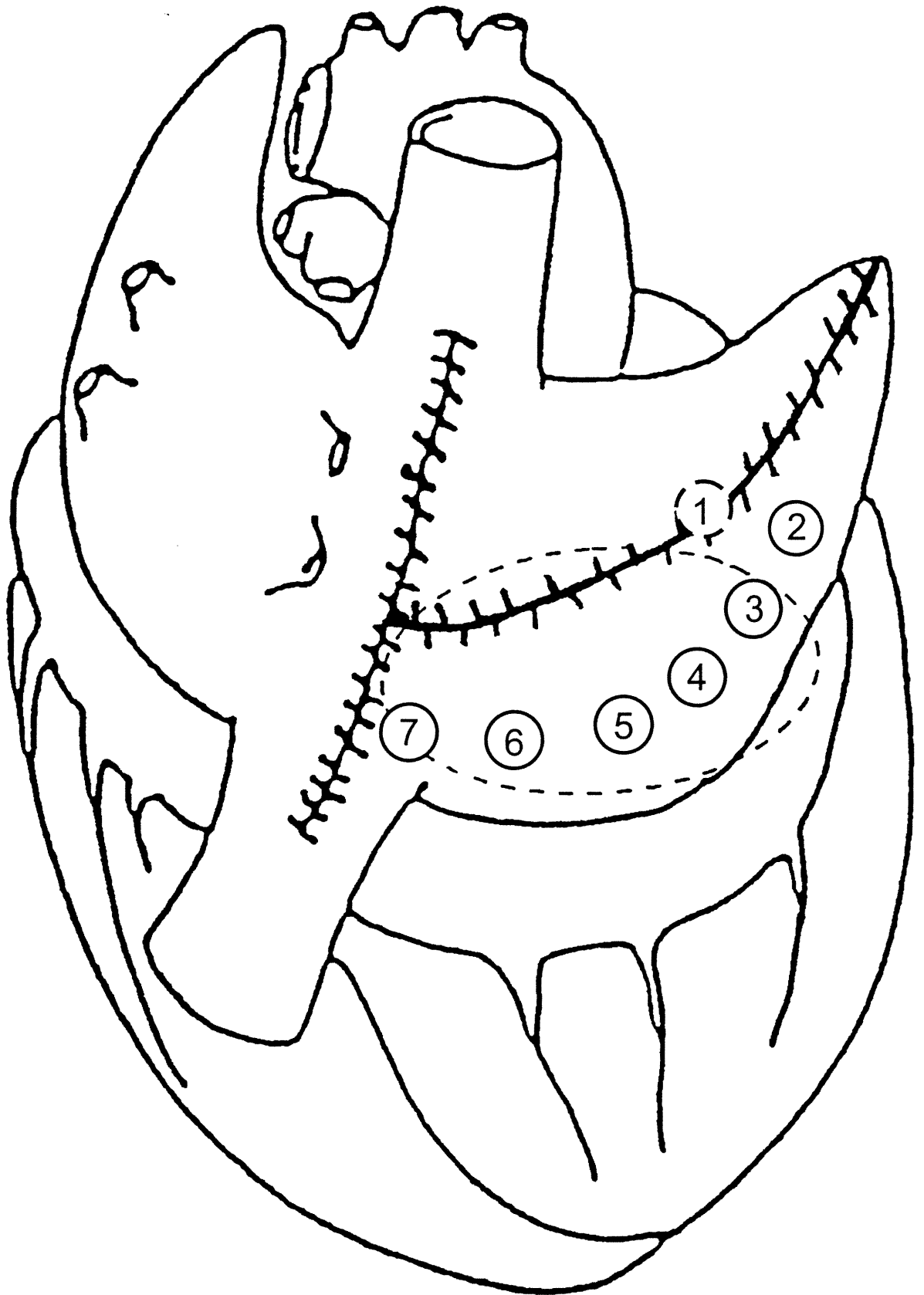


FIGURE 1 The right posterior view of the heart

Institut de Génie Biomédical, École Polytechnique de Montréal) and PC compatible computer (Prosys-Tec Inc., Canada). The bipolar electrograms were amplified by programmable-gain analog amplifiers (0.05-225 Hz) and converted to a digital format at 500 sample/channel/sec.

AFI was induced by burst stimulation (50 beats at CLs of 90-170 ms). The stimulation electrode closest to the recording site which gave the clearest signal was used. If AFI induction did not occur at this site, other stimulation sites were also used. During stable AFI [Cycle length (CL) variations of less than 3 ms], a premature stimulus was applied after every 20th spontaneous beat detected at the next distal electrode in the direction of wavefront propagation. The choice of adjacent stimulating and recording electrode site was based on the quality of the recorded signal and the occurrence of reset as described below. Initially, the premature stimulus was introduced late in diastole and the coupling interval was progressively decreased by 2 ms until the stimulus failed to capture. The interval between a spontaneous beat (T) and the premature stimulus (S) (interval TS), the interval between the premature stimulus and the response (SR) as well as the interval between the premature stimulus and the subsequent tachycardia beat ($ST1=SR+RT1$) were measured (peak to peak) at the electrode distal to the stimulating site (in the direction of wavefront propagation) as shown in Figure 2. Since the stimulation electrode (S_E , insert in Figure 3) is located at a different point in the circuit than the recording electrode (R_E), the method introduced by Mensour et al. [15] was used to estimate the coupling interval and the return cycle at the stimulation site. As shown in Figure 3, the range of TS values for which SR falls on the line $CL - [TS]$ can be used to estimate τ , the time needed for the free flutter to

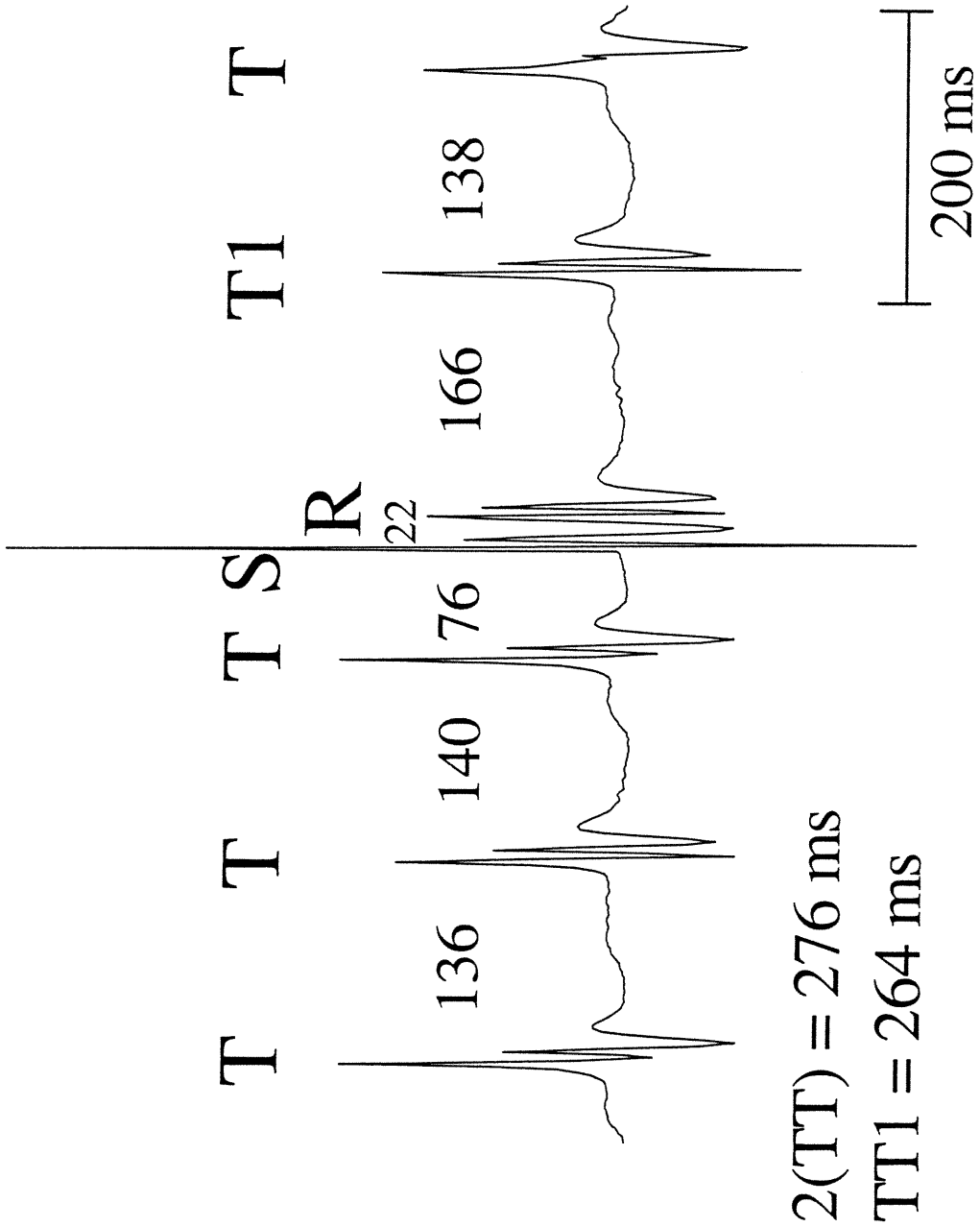


FIGURE 2 Epicardial bipolar recording during atrial flutter.

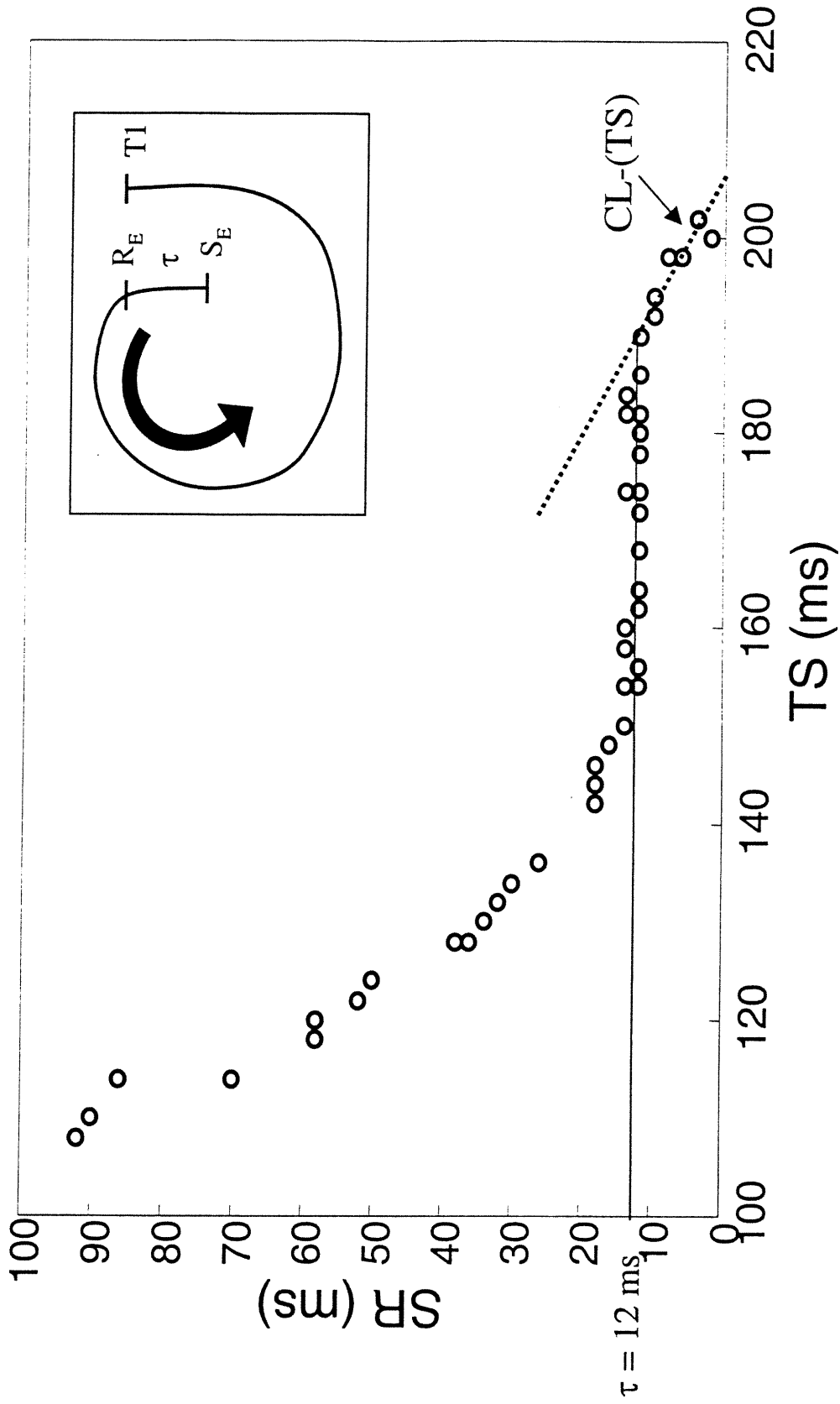


FIGURE 3 Method to approximate the measure of the coupling interval and return cycle at the stimulation site

travel from S_E to R_E . The coupling interval (CI) and the return cycle (RC) of the premature stimulus with respect to the last passage of the front at S_E are respectively estimated as $CI = \tau + TS$ and $RC = ST1 - \tau$. Graphs describing the relationship RC vs CI, i.e. the RRCs, were constructed using points for which $TT1 < 2 CL$ by more than twice the standard deviation of the AFl CL (i.e. when the premature beat reset the tachycardia). It was pointed out in Mensour et al. [15] that this criterion, standard in the literature, could sometimes lead to an underestimation of the duration of the excitable gap (EG). In fact, $TT1 = TS + SR + RT1$ for any stimulus applied in the EG. For a very premature stimulus capturing near the limit of the EG, it may happen that $TT1 > 2*CL$, because of significant conduction delay of the propagating stimulated wavefront. Nevertheless, we have decided to follow the standard criterion of reset to be consistent with the method most commonly used in the literature. The flat portion of the EG composed of fully excitable tissue was estimated from that portion of the RRC where the RC values were within one standard deviation of the CL. The ascending portion of the RRC where RC was greater than the $CL + SD(CL)$ thus represented that part of the EG composed of partially refractory tissue. A nonlinear function of the form $RC = a1 + a2 \tanh(a3 CI + a4) = F(CI)$ was fitted to the data. The value of the $F(CI)$ at the lower limit of the EG was taken as an estimate of the maximum resetting [15].

PPF was administered via the jugular vein during AFl in a loading dose of 1 mg/kg infused over 10 minutes. This was followed by a maintenance infusion of 1.8 mg/kg/hr which has been previously shown to achieve stable therapeutic plasma levels between 1-3 hrs of

infusion time as described in Derakhchan et al.[16]. The protocol to determine the RRC was repeated following the bolus administration and again at 10 minute intervals during the infusion as the AFL CL prolonged to a maximum of 2 hrs. Blood samples (5-7 ml) for drug plasma levels were obtained from the femoral vein during RRC determination.

To determine the spatial homogeneity of PPF effect, the CTs in different portions of the circuit were measured for free running AFI both before and after the administration of the drug. This was done for the 6 dogs in which the electrode recording belt was used. Using the free running AFI before drug administration as a reference, the electrodes whose activation times were not consistent with a continuous progression of the activation front around the circuit were discarded as bystanders. The CTs were computed between each successive pair of remaining electrodes and averaged over 15 beats. Sections of the AFI circuit were defined such that the CT through each section under control conditions was at least 5 ms. The CTs in each section 60 and 120 min after the onset of the PPF infusion were expressed relative to control.

This research protocol and care of the animals conform to the Guiding Principles for Animal Experimentation as described by the Canadian Council on Animal Care and was reviewed by the committee for Animal Experimentation at the Research Centre of Sacré Coeur Hospital (Université de Montréal). At the end of the experimental protocol, ventricular fibrillation was induced by direct current application to the heart.

Data analysis

In four animals, the data was digitalised using a TL-2 data acquisition interface (Axon instruments, Foster City, California) and all data were further analysed by a Silicon Graphics computer. The signals were manually timed using software developed by our group (MACT, Centre de Recherche, Hôpital du Sacré-Coeur de Montréal, Montréal, Québec, Canada).

Statistical analysis

The data are presented as means \pm SD. For a group of 10 dogs, measures were taken both 60 min and 120 min after the beginning of PPF infusion. Comparisons between control (Ctrl) and data collected 60 (P60) and 120 min. (P120) after PPF administration were done using one way ANOVA with repeated mesures. Two orthogonal contrasts were tested: Control vs [P60,P120], to assess the global effect of the drug and, P60 vs P120, to assess whether the effect was already stabilized after the first 60 min. Some measurements (e.g. Maximum Resetting, local CT, see results) were found to be correlated to other variables that were not uniformly distributed among the groups. These confounding variables was used as covariate in the analysis of variance (ANCOVA).

RESULTS

Drug plasma levels

Drug plasma levels were monitored during the performance of the stimulation protocol. In 5 dogs, the plasma concentrations (PIC) at 60 minutes (measures obtained between 48 and 64 min) of PPF was $0.837 \pm 0.175 \mu\text{g/ml}$. At 120 min (measures between 83 and 122 min), the plasma concentration in 7 dogs was $1.090 \pm 0.426 \mu\text{g/ml}$. These levels were within the recommended therapeutic plasma concentrations ($0.1\text{-}2.0 \mu\text{g/ml}$) (Campbell, 1994).

In 4 of these dogs, the PIC were obtained both around 60 and at 120 min of PPF. The PIC at 60 minutes was $0.819 \pm 0.197 \mu\text{g/ml}$ which did not correlate with the distribution of the time measurements (from 48 to 64 min, $R = -0.3$). However, there was a strong correlation between the difference in plasma concentrations (ΔPIC) and the time between the two repeated measurements (Δt from 35 to 65 min, $R = 0.8$). The difference between the measurements of 120 and 60 min (ΔPIC_{60}) was therefore estimated by the model $\Delta\text{PIC} = \Delta\text{PIC}_{60} + \beta (t_{m2} - 120)$, where t_{m2} is the time of the second measurement. We found $\Delta\text{PIC}_{60} = 0.15 \mu\text{g/ml}$ (CI at 95 % = $0.038\text{-}0.27 \mu\text{g/ml}$). The increase of the PIC, occurring during the first hour, was thus followed by a slow rising drift of the concentration during the second hour. The major metabolite, 5-hydroxy propafenone, was undetectable.

Global effects of propafenone on the excitable gap characteristics and reset-response curve

The AFl characteristics measured before and during a PPF infusion administered to a maximum of 2 hours are shown in Table I. AFl CL was found to be significantly prolonged by PPF (Ctrl vs [P60,P120], $P < .001$), and the effect was enhanced by continued infusion ([P60 vs P120], $p < .001$). PPF prolonged AFl CL from 144 ± 9 ms at baseline to 192 ± 24 ms at 45 to 64 min of drug infusion, and then to 204 ± 26 ms at 80 to 122 min of infusion. Despite this prolongation of AFl CL, reentry was never interrupted by PPF administration.

RRCs were determined without drug, at 60 min and again at 120 min of PPF infusion. Under control conditions, the atrial effective refractory period (ERP) during reentry (or the shortest coupling interval that resets the tachycardia during determination of the RRC) was 95 ± 18 ms resulting in an EG duration of 48 ± 14 ms or $34 \pm 10\%$ of the AFl CL. In all dogs, the control EG was composed predominantly of partially excitable tissue, defined as the portion of the RRC in which resetting was increasing with prematurity. However, in 9 of 10 dogs, at long coupling intervals approaching the AFl CL, the RRC was flat over a range of 10 ± 7 ms or $20 \pm 11\%$ of the EG duration, indicating fully excitable tissue ahead of the wavefront.

TABLE I – Effects of propafenone on atrial flutter and excitable gap parameters

| Dog | Cycle Length (ms)† | | | Effective Refractory Period (ms)† | | | Excitable Gap (ms) | | | % Excitable Gap (%) | | | Fully Excitable Portion (ms) | | | % Fully Excitable Portion (%) | | |
|------|--------------------|---------|-------------------|-----------------------------------|---------|----------|--------------------|---------|----------|---------------------|---------|----------|------------------------------|---------|----------|-------------------------------|---------|----------|
| | Ctrl | PPF 60' | PPF 120' | Ctrl | PPF 60' | PPF 120' | Ctrl | PPF 60' | PPF 120' | Ctrl | PPF 60' | PPF 120' | Ctrl | PPF 60' | PPF 120' | Ctrl | PPF 60' | PPF 120' |
| 1 | 148 | 167 | 174 | 80 | 88 | 86 | 68 | 79 | 88 | 46 | 48 | 50 | 0 | 0 | 0 | 0 | 0 | 0 |
| 2 | 147 | 203 | 218 | 118 | 170 | 180 | 29 | 33 | 38 | 20 | 16 | 17 | 3 | 4 | 4 | 12 | 11 | 10 |
| 3 | 148 | 205 | 209 | 106 | 160 | 156 | 42 | 45 | 53 | 28 | 22 | 25 | 4 | 12 | 13 | 9 | 27 | 24 |
| 4 | 150 | 217 | 231 | 114 | 172 | 192 | 36 | 45 | 39 | 24 | 21 | 17 | 11 | 6 | 5 | 30 | 14 | 12 |
| 5 | 130 | 173 | 189 | 77 | 142 | 156 | 53 | 31 | 33 | 41 | 18 | 17 | 4 | 5 | 9 | 7 | 15 | 28 |
| 6 | 154 | 212 | 225 | 124 | 182 | 182 | 31 | 30 | 43 | 20 | 14 | 19 | 10 | 7 | 16 | 31 | 24 | 37 |
| 7 | 144 | 193 | 195 | 92 | 104 | 98 | 52 | 89 | 97 | 36 | 46 | 50 | 13 | 6 | 8 | 24 | 7 | 8 |
| 8 | 135 | 190 | 217 | 82 | 138 | 156 | 53 | 52 | 61 | 39 | 27 | 28 | 8 | 20 | 9 | 16 | 38 | 15 |
| 9 | 152 | 218 | 230 | 84 | 130 | 182 | 68 | 88 | 48 | 45 | 40 | 21 | 27 | 25 | 23 | 39 | 28 | 48 |
| 10 | 127 | 144 | 153 | 76 | 80 | 94 | 51 | 64 | 59 | 40 | 44 | 39 | 8 | 0 | 0 | 15 | 0 | 0 |
| Mean | 144 | 192* | 204* ¹ | 95 | 137* | 148* | 48 | 56 | 56 | 34 | 30 | 28 | 9 | 8 | 9 | 18 | 16 | 18 |
| ±SD | ±9 | ±24 | ±26 | ±18 | ±36 | ±40 | ±14 | ±23 | ±21 | ±10 | ±13 | ±13 | ±8 | ±8 | ±7 | ±12 | ±13 | ±16 |

Ctrl – control; PPF – propafenone † - ANOVA p < 0.0001

* paired Student t-test compared to Ctrl p < 0.001

¹ paired Student t-test compared to PPF 60 min p = 0.0003

PPF induced a significant prolongation of the ERP to 137 ± 36 ms after 60 min and to 148 ± 40 ms after 120 min compared to 95 ± 18 ms at control (Ctrl vs [PPF-60.PPF-120], $P < .001$). Most of the prolongation occurred in the first 60 min of infusion, since the additional change in the last 60 min of infusion was just outside the level of significance (PPF-60 vs PPF-120, $P = .06$). The change of ERP expressed as a percentage of the AFI CL (control: $66 \pm 10\%$, PPF-60: $69 \pm 13\%$, PPF-120: $71 \pm 13\%$) was not significant because it was highly non-homogeneous amongst the preparations (e.g. $\%ERP_{ctrl} - \%ERP_{PPF60}$ range: $[-20\% - +10\%]$). This explains why no significant changes were found in the EG (CL-ERP), either in duration or $\%$ of the CL.

PPF did not modify the duration of full excitability which remained 8 ± 8 ms after 60 min and 9 ± 7 ms after 120 min or $16 \pm 13\%$ and $18 \pm 16\%$ of the EG respectively. Neither did it significantly modify the flat portion expressed as $\%$ of the CL (ctrl $6 \pm 5\%$, $4 \pm 4\%$ at 60 min; $4 \pm 3\%$ at 120 min, Ctrl vs [PPF-60.PPF-120], $P = .124$). It seems paradoxical that the flat portion does not show significant change both in duration and in $\%$ of the CL since the latter was demonstrated to increase. In fact, this is a result of the heterogeneous effect of PPF on the flat portion (from dog to dog) that can be seen in Table I.

PPF shifted the RRC upward and to the right, a direct consequence of the prolongation of the AFI CL (fig 4. A,C). However, the resetting curves expressed as a percentage of the CL were almost superimposed (fig. 4.B,D), which indicates that resetting was also increased by the same proportions as the CL at all CI.

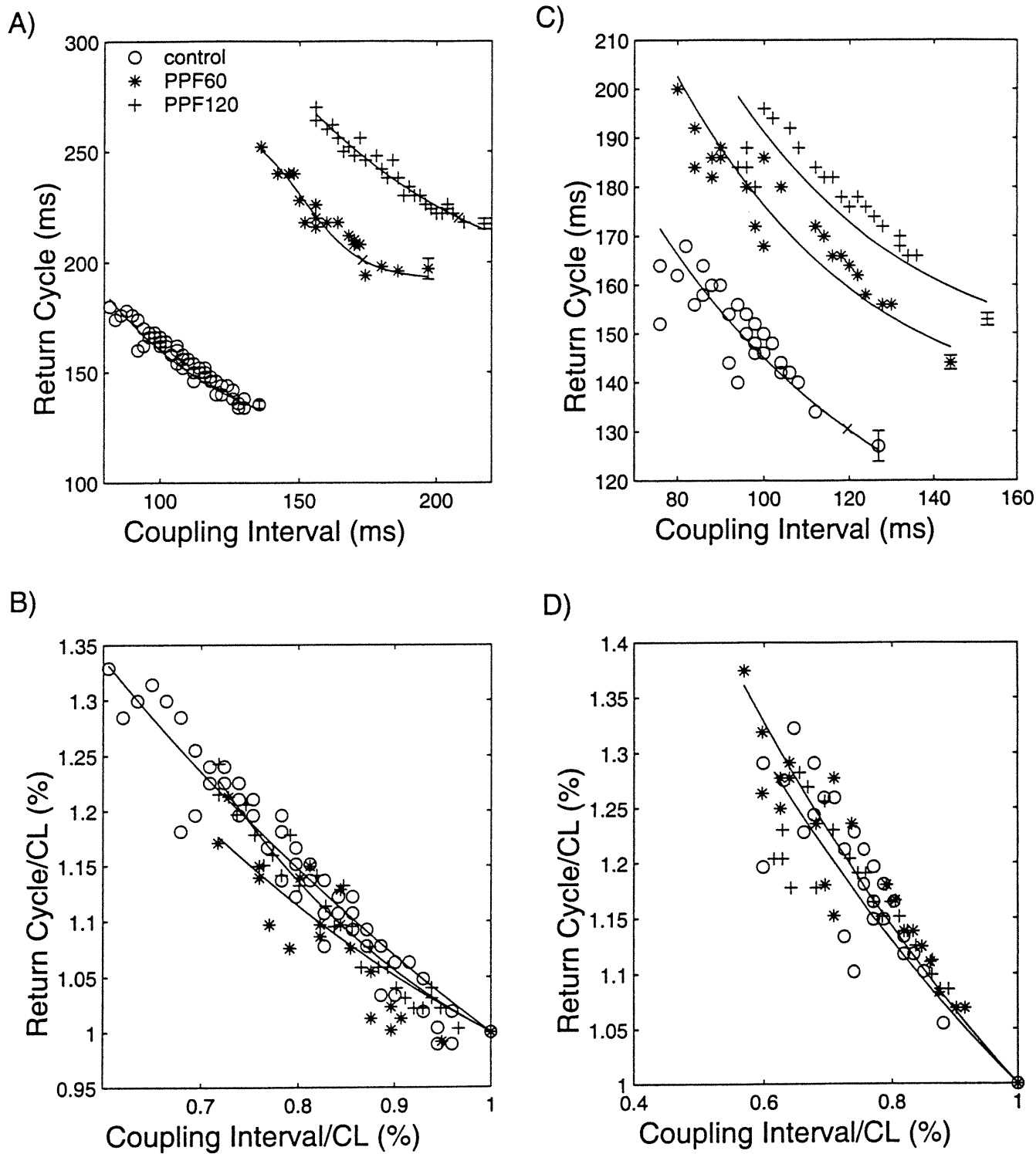


FIGURE 4 Two examples of the effects of propafenone on the reset-response curve.

The prolongation of the ERP by PPF can result both from the class III and/or class I effect of the drug (see discussion). In an attempt to find an indicator that can be directly associated to the class I effect of PPF, the maximum resetting (MR= maximum RC - mean CL, see Method) was analysed. PPF induced a slight but non-significant increase of both the net (Ctrl: 38.9 ± 11 ms, PPF-60 min: 45.9 ± 21 ms, PPF-120 min: 45.9 ± 21 ms) and relative (i.e. MR/CL, Ctrl: $21 \pm 8\%$, PPF-60: $22 \pm 10\%$, PPF-120, $23 \pm 12\%$) maximum resetting. However, the MR was linked to the ERP (see fig. 5) since under both control and drug conditions, greater MR was observed in preparations with a shorter ERP. To get a measure of the effect of PPF on the relative MR, corrected for the change in ERP, we have fitted a model using an analysis of covariance (ANCOVA):

$$Y_{\text{ctrl}}^d = \mu_d - \Delta_{\text{ctrl-PPF}}/2 + \beta X_{\text{ctrl}}^d + \epsilon$$

$$Y_{\text{PPF60}}^d = \mu_d + \Delta_{\text{ctrl-PPF}}/2 - \Delta/2_{\text{PPF60-PPF120}} + \beta X_{\text{PPF60}}^d + \epsilon$$

$$Y_{\text{PPF120}}^d = \mu_d + \Delta_{\text{ctrl-PPF}}/2 + \Delta/2_{\text{PPF60-PPF120}} + \beta X_{\text{PPF120}}^d + \epsilon$$

where $Y_{\text{ctrl,PPF60,PPF120}}^d$ and $X_{\text{ctrl,PPF60,PPF120}}^d$ are respectively the % relative MR and relative ERP in each dog (d) under control conditions (ctrl), at 60 min of PPF (PPF60) and at 120 min of PPF (PPF120); μ_d is the mean MR of each dog; $\Delta_{\text{ctrl-PPF}}$ is the contrast between drug and control; $\Delta_{\text{PPF60-PPF120}}$ is the contrast between the effect of PPF at 60 and 120 min; β is the slope between the relative MR and the relative ERP; and ϵ is the error term used to evaluate the significance of the effects. We found both β (-89.3, 95% Conf. Int: [-113.71, -64.89]) and $\Delta_{\text{ctrl-PPF}}$ (6.4%, 95% Conf. Int: [3.4-9.3] %) to be significant. $\Delta_{\text{ctrl-PPF}}$ indicates an increase of the relative MR by PPF, independent of its effect on the ERP. This means that a stimulus applied with the same relative prematurity with PPF and under control will

induce more resetting with drug. We considered this to be indicative of the class-I action of the drug.

Spatial characteristics of the effects of Propafenone

In the 6 dogs (dogs 1- 6 of Table I) in which a 16 bipolar electrode recording belt was used, CTs between electrode sites were measured under control conditions, and at 60 and 120 min after the beginning of the PPF infusion. In all cases, the prolongation of the CL on PPF was due to a marked increase of the CT mainly localised in one or two sections of the circuit (fig6. A-F). The regions of slowed conduction were different from one dog to another and were not related to any specific anatomical structure. It is noteworthy that the direction of propagation in the presence of PPF (both at 60 and 120 min) was different from control in 4 out of 6 dogs. In another animal, the direction of propagation for control and 60 min of PPF were the same whereas at 120 min propagation was in the opposite direction. However, in this animal, the portion in which conduction was slowed by PPF remained the same, irrespective of the direction of rotation.

Since the portions of the circuit sensitive to PPF were specific to each preparation, we tried to determine if they could be related to some characteristics of AFI under control conditions. Our first guess was that the sensitivity to PPF might be linked to an altered time course in the recovery of excitability that would be indicated by a higher beat-to-beat variability of the local CT (CT) under control conditions. We found that the variability of

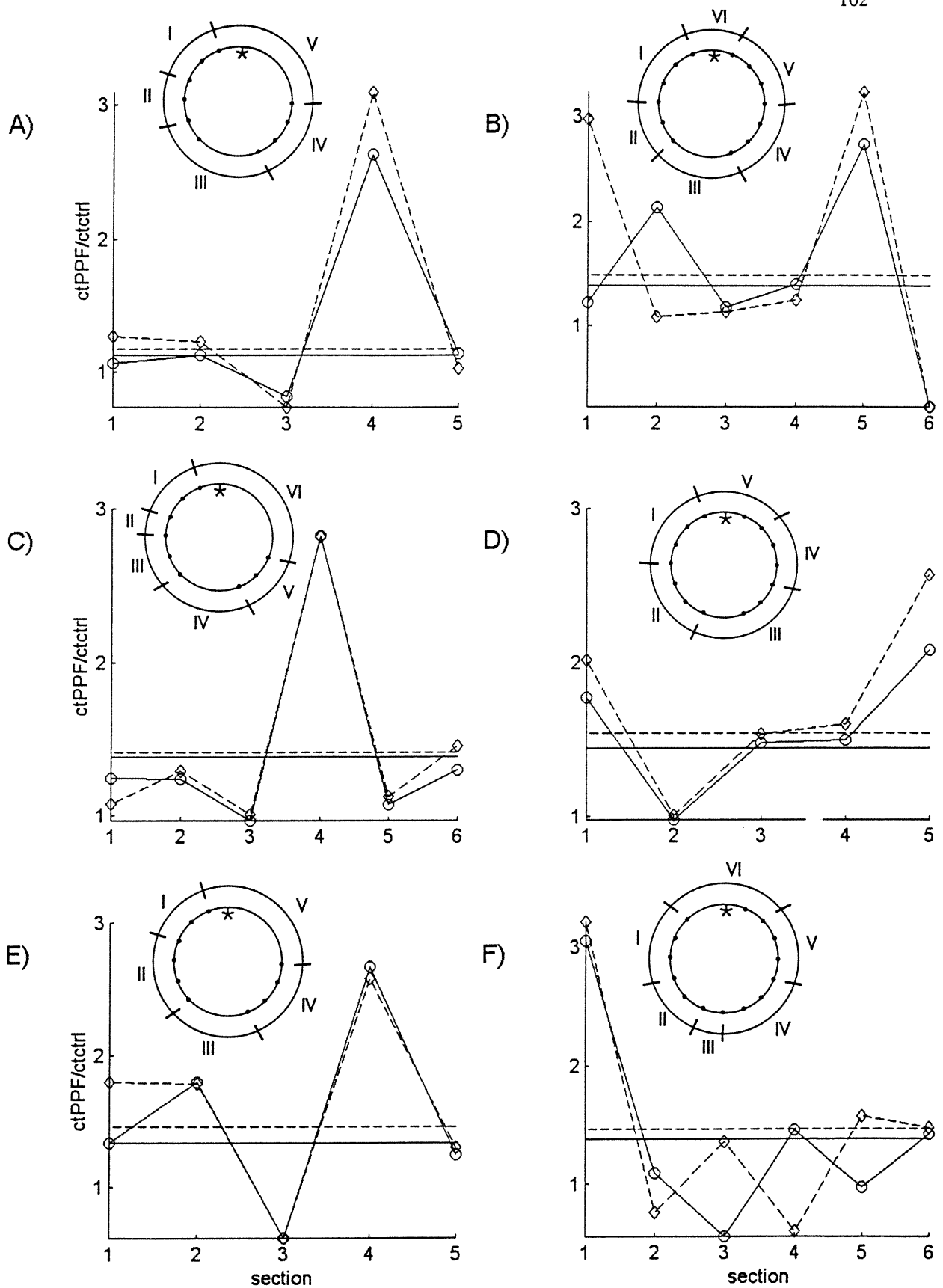


FIGURE 6 Inhomogeneity of propafenone effect on conduction time around the atrial flutter circuit in free running flutter.

the CT ($\text{std}(\text{CT})/\text{mean}(\text{CT})$, fig. 7A-F) was indeed very inhomogeneous among the different sections of the circuit, but that in general there was no consistent relation with the localization of PPF effect. For one dog (dog 1, fig 8A), the PPF effect was significantly correlated with the CT variability (section 4 of dog 1, fig 7A). This dog (dog 6, Table I) also had the longest EG (68 ms, 46% of CL) and no flat portion whereas the other animals had shorter EG ranging from 29-53 ms. In general, there was higher correlation in animals with a longer EG and shorter flat portion.

Fluctuations in the local CT could result either from an intrinsic local instability or from variations of local CL (i.e. measured at the entrance of each section) caused by a change of propagation in other parts of the circuit. Fig. 9A-F shows that there were indeed large fluctuations of the local CL in different parts of the circuit. The local CL was in general correlated with the beat-to-beat changes in local CT. To remove the effects of the local CL variability on the CT, the data in each portion of the circuit under control conditions were fitted with the model:

$$CT_i = CT_m + \beta CL_i + \epsilon$$

where CT_i , $i=1:N$ are the free beats used to evaluate the CT in each section, CT_m is the mean CT if the CL = 0, CL_i is the CL interval measured at the entrance of each section, and ϵ is the error term measuring the fluctuation of CT that cannot be explained by the changes of CL. The mean square ϵ was then correlated to the PPF effect. In general, the correlations were higher than those obtained with the standard deviation of CT. However, with the exception of dog 1, they remained above the $P = 0.05$ level of significance.

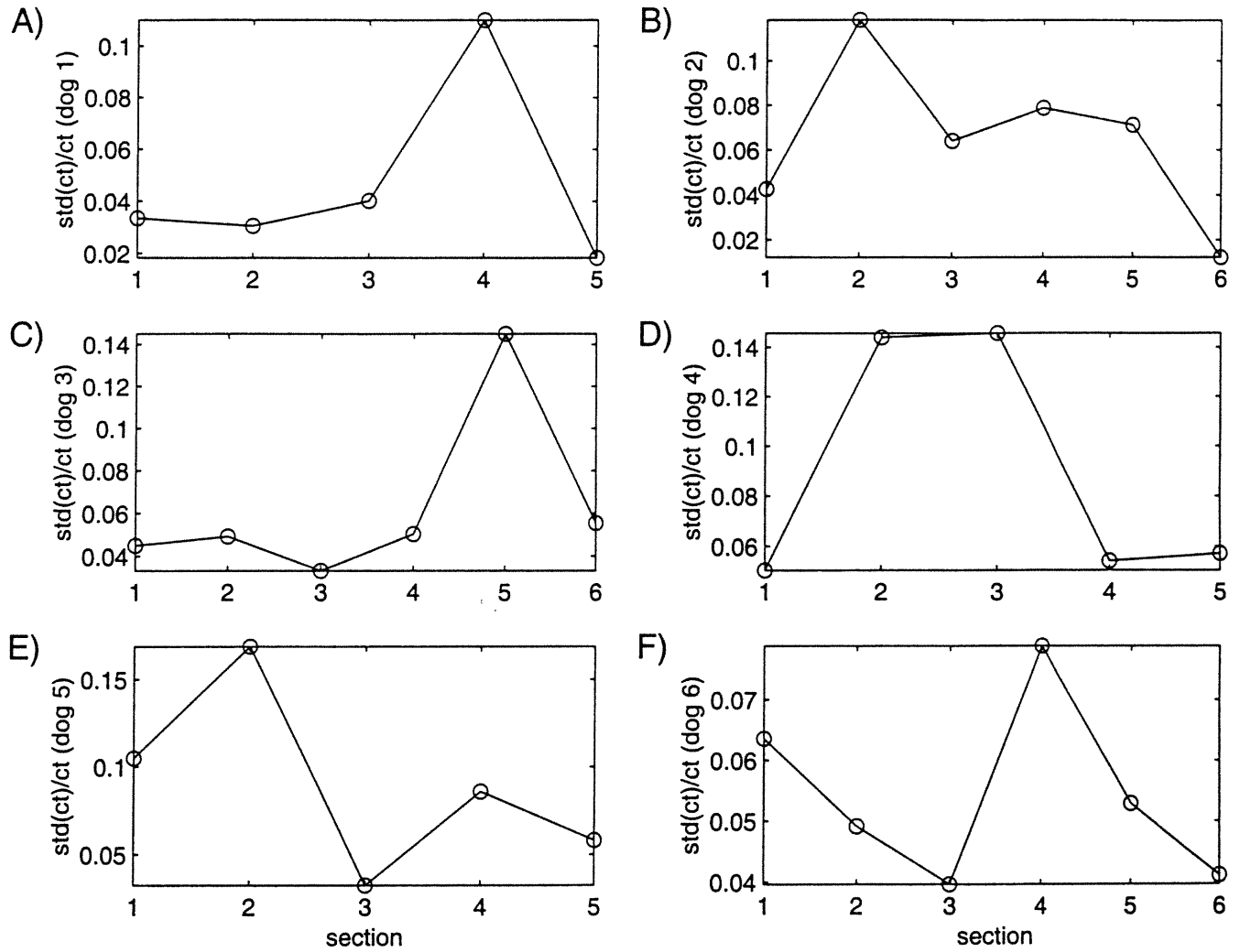


FIGURE 7 Variability on the conduction time for each section.

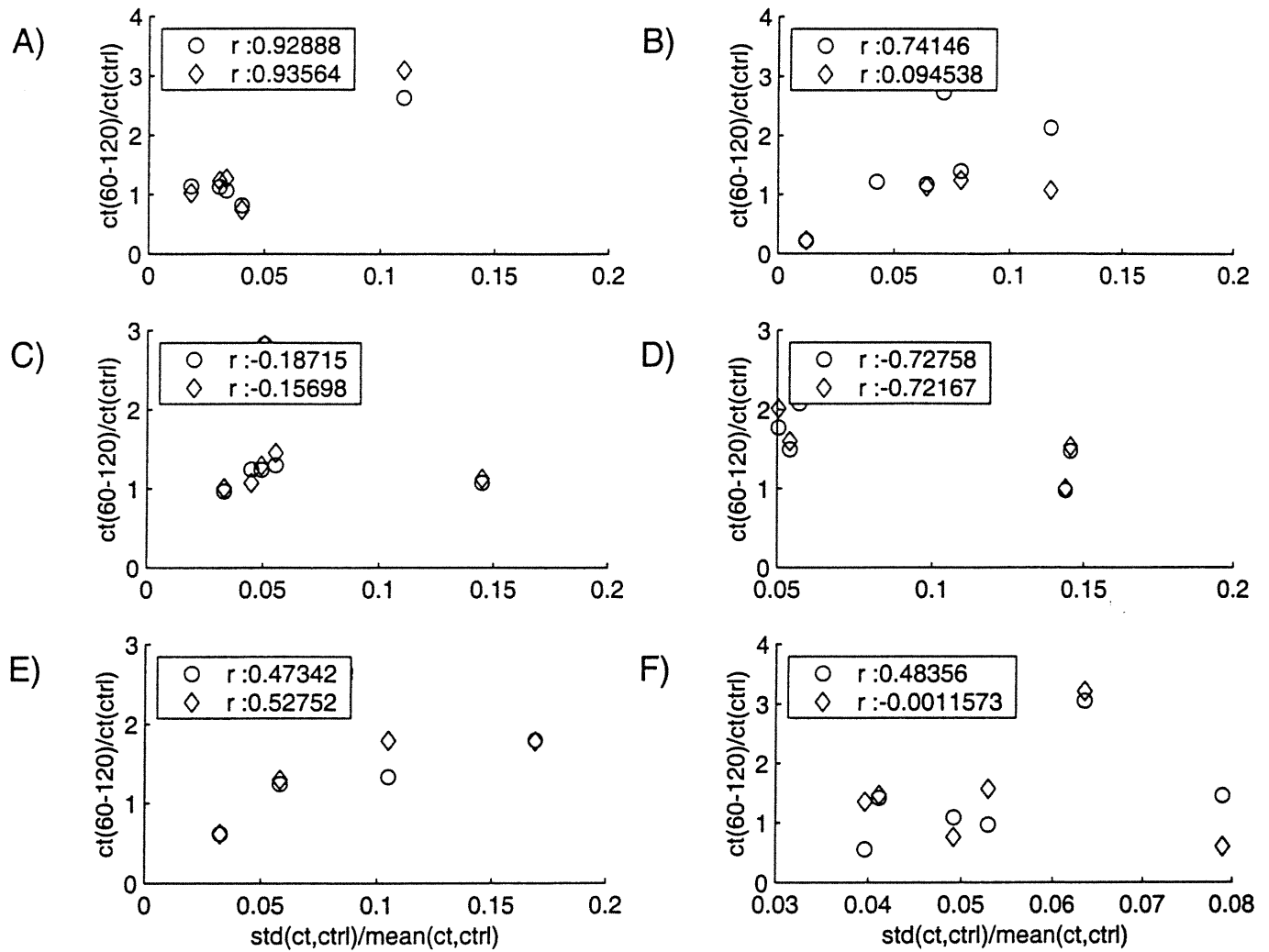


FIGURE 8 Effect of the variability of the conduction time on the effect of propafenone on conduction time.

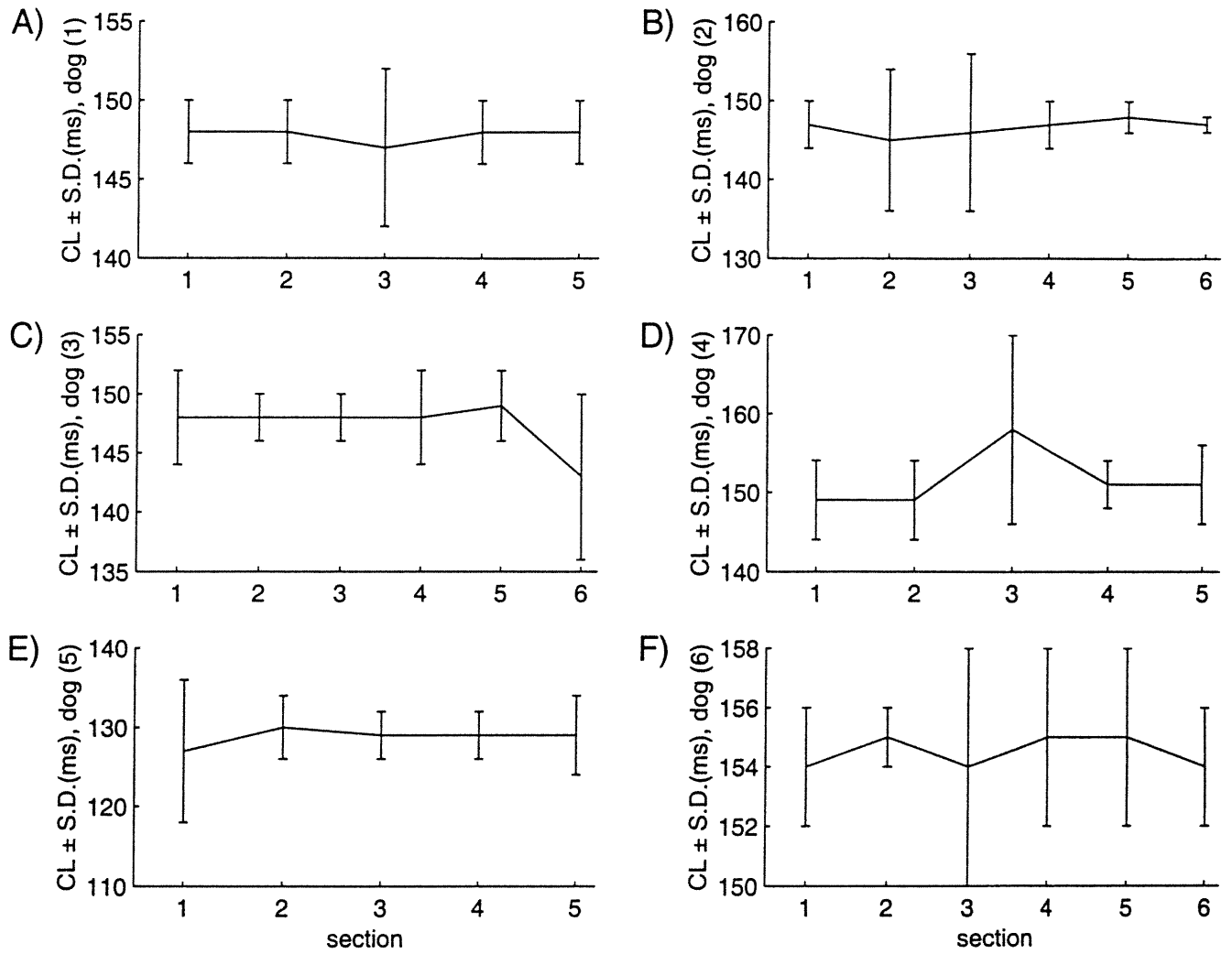


FIGURE 9 Cycle length fluctuations for each section

Prematurity effect

The data collected in the protocol to construct RRCs were also used to assess the variation of the CT as a function of prematurity in each portion of the circuit. The CT of the anterograde flutter beat produced by each premature stimulus was measured in each portion of the circuit. The effective local prematurity was computed as the time between the anterograde front and the preceding free flutter beat at the entrance of each portion of the circuit. The CTs were then plotted against the local prematurity for each portion of the circuit. As shown in the example displayed in fig. 10, the range of effective prematurity experienced in the different portions of the circuits was very different. In all 6 dogs, the range of effective prematurity was large only in the first one or two portions adjacent to the stimulation site in the direction of propagation. The increase of CT in these portions of the circuit was so large that the range of effective prematurity for the portions beyond these first sections was 10 ms or less, with minimal change of CT. Thus, a protocol with premature stimulation at one site does not produce a wide range of prematurity in each individual portion of the circuit.

DISCUSSION

This study demonstrated that PPF significantly prolonged the AFl CL and ERP, but had a variable effect on the total duration of the EG and also on the fully excitable portion ahead of the wavefront even after a 2 hour infusion. These results are in accordance with those

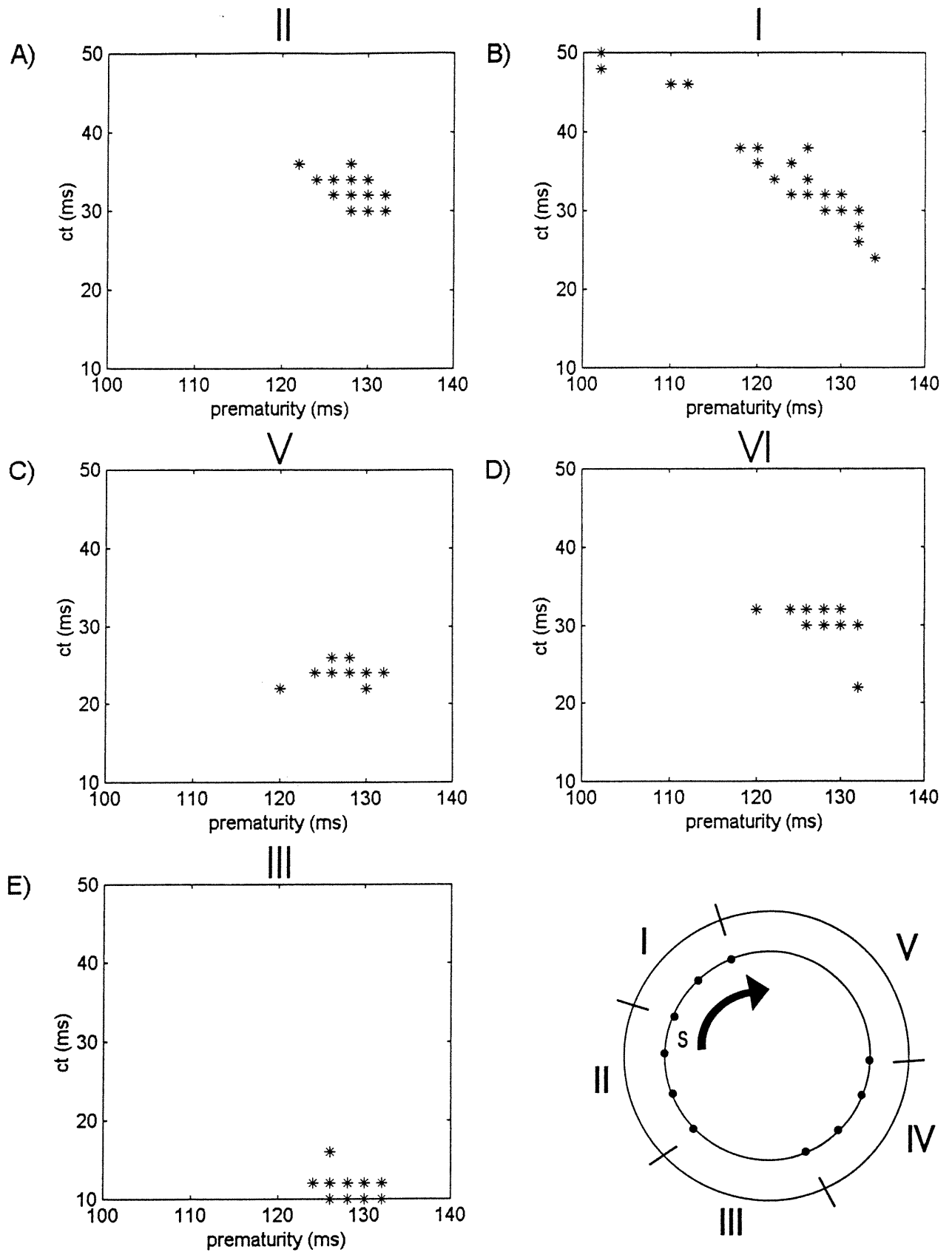


FIGURE 10 Effect of prematurity on the different sections of the reentry circuit.

found by Derakhchan et al. [16] after a one hour infusion in the same model. However, our findings differ from previous studies which demonstrated a prolongation of the EG on PPF in the same model [17] and in an intercaval crush model [18]. The persistence of fully excitable tissue with PPF therapy can be explained by the drug dynamic. PPF has no effect on the sodium channel in the resting state but binds to both activated and inactivated sodium channels [19]. PPF has a very pronounced tonic sodium current block due to its slow dissociation from the sodium channel, as reflected in a time constant recovery of upstroke velocity from use-dependant block of 6.3 seconds [20] to 15.5 seconds [21]. Our studies demonstrate that both the CL and ERP increase with PPF. This increase in the ERP can be explained by an indirect effect of the CL prolongation due to the direct class I action of the drug. An alternative explanation is that PPF inhibits the atrial transient outward current (I_{to}), the inward rectifier current (I_{K1}), the delayed rectifier (I_{Kr} and I_{Ks}) [22,23] and also the ultra-rapidly activating delayed rectifier (I_{Kur}) [24]. All these actions could directly prolong action potential duration and therefore the ERP. In order to get a direct indication of class I effect, the maximum reset was analysed. Since a link was observed between the maximum reset and the ERP, it was corrected for the difference in the ERP of all dogs. An increase in the relative max reset by PPF was found, independent of its effects on the ERP, that was interpreted as a class I effect of the drug. This marked class I effect likely contributes to prolong the ERP of atrial tissue.

PPF has been shown to either decrease conduction in an unchanged ventricular tachycardia circuit or lengthen the circuit barriers without changing the exit point of the circuit [13]. Our

study examined the spatial characteristics of the effects of PPF by analysing the CTs between electrode sites without drug, and at 60 min and 120 min of PPF infusion. The prolongation of the CL was mainly due to a marked increase in the CT mainly localised to one or two sections of the reentry circuit demonstrating that the tonic effect of PPF was spatially inhomogeneous. In one dog, the portion in which conduction was slowed by PPF remained the same, irrespective of the direction of rotation on drug suggesting that the effect of PPF may be characteristic of the substratum of the reentry. However, the regions of slowed conduction did not correspond to any anatomical fixed reference point. This is interesting because previous investigators [14] have shown that conduction velocity around a tricuspid ring to be relatively uniform with no region accounting for a major fraction of the CT around the reentrant pathway. From the overall pattern of activation in two dogs, they have reported that there was no localized area of slow conduction in the absence of drug, with lidocaine and methacholine. This contradicts the wide spatial heterogeneity of the PPF effect that we have found in our study, and suggests that spatial homogeneity/heterogeneity of action could be drug specific.

Gaspo et al.[25] have shown that rapid atrial activation causes a time-dependent decrease in ERP, conduction velocity, and wavelength, which, along with increased regional heterogeneity, provides a substrate for atrial fibrillation. PPF has been demonstrated to reduce the likelihood of atrial fibrillation [26-28], which is consistent with the increase of ERP that it induces. On the other hand, spatial heterogeneity of the PPF action should have the opposite effect, unless it acts specifically to counterbalance the heterogeneity in

recovery of excitation and/or repolarisation that could exist in the substratum under control conditions. Further studies are needed to determine how the preferential sites of PPF action are linked to the properties of the substratum and its susceptibility to AF under control conditions.

To determine if the regions of the reentry circuit sensitive to PPF might be related to some characteristics of AF1 without drug, the variability in the local CT was analysed. In general, the variability of the CT was inhomogeneous in the different sections of the circuit with no consistent relation to the effects of PPF. However, in the dog where AF1 had the largest EG and no fully excitable portion, the site of greatest variation in CT was identified to be the site of greatest PPF effect. Large fluctuations of the local CL in different parts of the circuit along with the possibility of an intrinsic local instability can account for the fluctuations in the local CT. Indeed, a correlation was found between the local CL with the beat to beat changes in the local CT. Although the fluctuations in the CT had a higher correlation with the PPF effect when the local CL variability on the CT was removed, it remained below the level of significance with the exception of the dog with the largest EG and no flat portion. In general, there was a greater correlation in dogs with a longer EG and shorter flat portion. This suggests that the sections displaying instability during free AF1 may predict the drug site of action only when there is no fully excitable portion present or when there is a long enough EG. The absence of a flat portion indicates that the action potential during flutter is impinging on the tail of the prior action potential, such that propagation becomes sensitive to small spontaneous local fluctuation of CL. In this context, the area with some

delay in the recovery of excitability could be more easily detected. In contrast, when a flat portion is present, CT in all portions of the circuit becomes less sensitive to small spontaneous CL fluctuations .

To assess the variation of the CT as a function of prematurity in each section of the circuit, the CT of the anterograde flutter beat produced by each premature stimulus was measured in each portion of the circuit. In all 6 dogs, the range of effective prematurity was large in the first one or two sections adjacent to the stimulation site in the direction of propagation. The sections beyond these portions had a range of prematurity of 10 ms or less and showed only minimal change in CT. Therefore, premature stimulation at one site does not predict the range of prematurity throughout the entire reentry circuit.

Previous studies have demonstrated site-dependent differences in the RRCs in human [7] and in rabbit [9] ventricular tachycardia. Ingelmo and Frame [10] have shown that the shape of the RRC was different when stimuli were delivered distal as compared with proximal to a single site of interval-dependant conduction delay in canine in vitro tricuspid rings. These investigators found that the length of the flat portion of the RRCs accurately reflects the duration of the fully EG for proximal RRCs, but may overestimate the fully EG from distal stimulation sites. Our study shows that the RRCs obtained by stimulating at only one site will most likely predict the EG in the region of the premature stimulus or adjacent section. However, it may not predict the global characteristics of the EG for the entire circuit as it is presently being reported in most studies[2,3,15,16]. Indeed, previous

studies have also shown that the window of reset by itself does not measure the local EG or reflect the EG at any point in the circuit [29-31]. However, our results suggest that, with reentry circuit divided into 5-6 sections, when stimuli are applied at 3 or 4 sites these measurements should be sufficient to provide a reasonable representation of the reset properties around the circuit.

Acknowledgements: The authors wish to thank Pierre Rocque, Philippe Comtois and Pierre Fortier for the excellent technical help.

References:

1. Almendral JM, Stamato N, Rosenthal M, Marchlinski F.E., Miller J.M., Josephson M.E. Resetting Response patterns during sustained ventricular tachycardia: relationship to the excitable gap. *Circulation* 1986; 74: 722-730.
2. Della Bella P, Marenzi G, Tondo C, Cipolla CM, Doni F, Grazi S et al. Usefulness of excitable gap and pattern of resetting in atrial flutter for determining reentry circuit location. *Am J Cardiol* 1991; 68(5): 492-497.
3. Jalil E, Le Franc P, Molin F, Lebeau R, Molin F, Costi P. Effects of procainamide on the excitable gap composition in common human atrial flutter. *PACE* 1998; 21: 528-535.
4. Frame LH, Page RL, Hoffman BF: Atrial reentry around an anatomic barrier with a partially refractory excitable gap. *Circ. Res* 1986; 58: 495-511.
5. Kus T, Derakhchan K, Bouchard C, Pagé P. Effects of procainamide on refractoriness, conduction, and excitable gap in canine atrial reentrant tachycardia. *PACE* 1991; 14(Part II): 1707-1713.
6. Jalil E, Laflamme M, Kus T: Effects of procainamide on the excitable gap in canine model of atrial flutter. *Can J Physiol Pharmacol* 1997; 75: 1-8.

7. Callans DJ, Zardini M, Gottlieb CD, Josephson ME. The variable contribution of functional and anatomic barriers in human ventricular tachycardia: an analysis with resetting from two sites. *J Am Coll Cardiol* 1996; 27(5): 1106-1111.

8. Callans DJ, Schwartzman D, Gottlieb, Dillon SM, Marchlinski FE. Characterization of the excitable gap in human type I atrial flutter. *J Am Coll Cardiol* 1997; 30: 1793-801.

9. Boersma L, Brugada J, Kirchhof C, Allessie M. Mapping of reset of anatomic and functional reentry in anisotropic rabbit ventricular myocardium. *Circulation* 1994; 89(2): 852-862.

10. Ingelmo C, Frame LH: Mechanism for site-dependent differences in the shape of the resetting response curve in fixed barrier reentry. *J Cardiovasc Electrophysiol* 2000; 11: 981-989.

11. Vaughan Williams EM: A classification of antiarrhythmic actions reassessed after a decade of new drugs. *J Clin Pharmacology* 1984; 24(4): 129-147.

12. Dukes ID, Vaughan Williams EM: The multiple modes of action of propafenone. *Eur Heart J* 1984; 5(2): 115-125.

13. Callans DJ, Hook BG, Josephson ME: The mechanism of propafenone-induced slowing of ventricular tachycardia in man as defined by analysis of resetting response patterns. *PACE* 1991; 14(pt II): 2035-2041.

14. Frame LH, Page RL, Boyden PA, Fenoglio JJ Jr, Hoffman BF. Circus movement in the canine atrium around the tricuspid ring during experimental atrial flutter and during reentry in vivo. *Circulation* 1987; 76(5): 1155-1175.

15. Mensour B, Jalil E, Vinet A, Kus T. Influence of propafenone on resetting and termination of canine atrial flutter. *PACE* 2000; 23(8): 1200-1219.

16. Derakhchan K, Pagé P, Lambert C, Kus T. Effects of procainamide and propafenone on the composition of the excitable gap in canine atrial reentry tachycardia. *J Pharmacol Exp Ther* 1994; 270: 47-54.

17. Spinelli W, Hoffman BF. Mechanisms of termination of reentrant atrial arrhythmias by Class I and Class III antiarrhythmic agents. *Circ Res* 1989; 65: 1565-1579.

18. Inoue H, Yamashita T, Nozaki A, Sugimoto T. Effects of antiarrhythmic drugs on canine atrial flutter due to reentry: role of prolongation of refractory period and depression of conduction to excitable gap. *J Am Coll Cardiol* 1991; 18: 1098-1104.

19. Honjo H, Watanabe T, Kamiya K, Kodama I, Toyama J. Effects of propafenone on electrical and mechanical activities of single ventricular myocytes isolated from guinea-pig hearts. *British J Pharmacol* 1989; 97: 731-738.
20. Koller B, Franz MR. New classification of moricizine and propafenone based on electrophysiologic and electrocardiographic data from isolated rabbit heart. *J Cardiovasc pharmacol* 1994; 24(5): 753-760.
21. Kohlhardt M, Seifert C. Inhibition of V_{max} of the action potential by propafenone and its voltage-, time- and pH dependence in mammalian ventricular myocardium. *Naunym-Schmiedeberg's Archives of Pharmacology* 1980; 315: 55-62.
22. Duan D, Fermini B, Nattel S. Potassium channel blocking properties of propafenone in rabbit atrial myocytes. *J Pharmacol Exp Ther* 1993; 264: 1113-1123.
23. Delpon E, Valenzuela C, Pérez O, Casis O, Tamargo J. Propafenone preferentially blocks the rapidly activating component of delayed rectifier K^+ current in guinea pig ventricular myocytes. *Circ Res* 1995; 76(2): 223-235.
24. Gross GJ, Castle NA. Propafenone inhibition of human atrial myocyte repolarizing currents. *J Mol Cell Cardiol* 1998; 30: 783-793.

25. Gaspo R, Bosch RF, Talajic M, Nattel S. Functional mechanisms underlying tachycardia-induced sustained atrial fibrillation in a chronic dog model. *Circulation* 1997; 96: 4027-4035.
26. Connolly SJ, Hoffert DL. Usefulness of propafenone for recurrent paroxysmal atrial fibrillation. *Am J Cardiol* 1989; 63: 114-116.
27. Pritchett ELC, McCarthy EA, Wilkinson WE. Propafenone treatment of symptomatic paroxysmal supraventricular arrhythmias. *Ann Intern Med* 1991; 114: 539-544.
28. Reimold SC, Cantillin CO, Friedman PL, Antman EM. Propafenone versus sotalol for suppression of recurrent symptomatic atrial fibrillation. *Am J Cardiol* 1993; 71: 558-563.
29. Fei H, Hanna MS, Frame LH. Assessing the excitable gap in reentry by resetting. *Circulation* 1996; 94: 2268-2277.
30. Peters NS, Coromilas J, Hanna MS, Josephson ME, Costeas C, Wit AL. Characteristics of the temporal and spatial excitable gap in anisotropic reentrant circuits causing sustained ventricular tachycardia. *Circ Res* 1998; 82: 279-293.
31. Hanna MS, Coromilas J, Josephson ME, Wit AL, Peters NS. Mechanisms of resetting reentrant circuits in canine ventricular tachycardia. *Circulation* 2001; 103: 1148-1156.

Figure Legends:

Figure 1: The right posterior view of the heart. A Y-shaped anatomical barrier is produced (based on the model of Frame et al., 1986) extending from the superior to the inferior vena cava and to the tip of the right atrial appendage. Seven bipolar electrodes were inserted around the base of the right atrium for stimulating. Electrode position 1 is on the endocardial surface of the right atrium facing the aorta, whereas positions 2-7 are on the right atrial endocardial surface below the incision. Subsequently, 16 bipolar electrodes were mounted on a belt placed around the right atrium for recording. Electrodes 1-8 were placed on the anterior surface and electrodes 9-16 positioned on the posterior surface of the right atrium facing the aorta. The dashed line represents the tricuspid annulus.

Figure 2: Epicardial bipolar recording during atrial flutter. A premature stimulus was introduced after every 20th beat of atrial flutter by an adjacent endocardial stimulating electrode. TT, atrial flutter cycle length; TS, coupling interval of the premature stimulus, ST1, return cycle; and R, response to the premature stimulus. At the recording electrode shown, a coupling interval (TS) of 76 ms was observed. The subsequent return cycle (ST1) was prolonged to 188 ms. Because TT1 (264 ms) was shorter than twice TT (276 ms) by at least twice the standard deviation of the atrial flutter cycle length (276 ms), reset of the tachycardia was considered to have occurred.

Figure 3: Method to approximate the measure of the coupling interval and return cycle at the stimulation site. SR, conduction time between the stimulation site and the site at which the premature beat was recorded (see Figure 2). The flat portion of the curve indicates the presence of fully excitable tissue through which the propagation time is the same as in a free running flutter (without premature stimuli) between the stimulating (S_E) and recording (R_E) electrodes. Extrapolating the value of the flat portion to the ordinate approximates τ , the time needed for the free running flutter to travel from S_E to R_E . The value τ is then subtracted from the overestimated return cycle (ST1 of Figure 2) and added to an underestimated coupling interval (TS of Figure 2) to correct the data for the conduction delay from S_E to R_E in order to construct the reset-response curves of Figure 4.

Figure 4: Two examples of the effects of propafenone on the reset-response curve. A) The first example of a RRC shows an excitable gap (53 ms) under control conditions consisting of an increasing and flat portion demonstrating partially and fully excitable tissue (8 ms). A bolus of 1 mg/kg for 10 min followed by 1.8 mg/kg/hr of propafenone (PPF) was infused for 2 hours. At 57 min of PPF infusion the curve was shifted upward and to the right but the duration of the excitable gap (52 ms) remained the same and a region of the fully excitable tissue (20 ms) ahead of the wavefront remained present. Even at 118 min of PPF infusion, there was still presence of fully excitable tissue (9 ms) in the excitable gap (61 ms). Atrial flutter cycle length \pm SD: \circ control (135 ± 1); * 57 min PPF (190 ± 2); + 118 min PPF (217 ± 1). B) The same RRCs as in A) expressed as a percentage of the cycle length (CL). C) A second example of reset-response under control conditions

showing a mixed curve (excitable gap - 51 ms) with a flat portion of 7 ms. Following 58 min of PPF infusion, the RRC was purely increasing demonstrating an excitable gap (51 ms) consisting only of partially excitable tissue. The excitable gap (59 ms) after 83 minutes of PPF still remained without fully excitable tissue. Atrial flutter cycle length \pm SD: o control (127 ± 2); * 58 min PPF (144 ± 1); + 83 min PPF (153 ± 1). D) The same RRCs as in C) expressed as a percentage of the CL.

Figure 5: Maximum resetting corrected for the change in effective refractory period (ERP). The relative max reset (max reset/CL) vs ERP (ERP/CL). There is a strong correlation between the max reset and ERP. Since the dogs do not have the same ERP, the effects of propafenone (PPF) on the relative max reset were corrected for the change in ERP. There is an increase in the max resetting with drug independent of its effect on the ERP. A) without drug, B) at 60 min of PPF and C) at 120 min of PPF.

Figure 6: Inhomogeneity of propafenone (PPF) effect on conduction time (ct) around the atrial flutter circuit in free running flutter. The conduction times between electrodes around the atrial flutter circuit were measured in the 6 dogs in which a 16 bipolar electrode recording belt was used. A plot describing the ratio of conduction times between electrodes on PPF (ctPPF) at 60 and 120 min over control conduction times (ctctrl) is shown at most electrode sites. Electrode sites were discarded as bystanders if the electrode's activation times were not consistent with a continuous progression of the activation front around the atrial flutter reentry circuit. In order to keep the control propagating time at an acceptable

value, the conduction times were combined to create sections in which the total ct was above 5 ms.

A-F) - dogs 1 to 6

In all dogs, the prolongation of the CL on PPF was due to a marked increase in the ct mainly localised in one or two sections of the circuit. The regions of slowed conduction were clearly different from one dog to another and were not related to any specific anatomical structure. For each dog, a reentry circuit is shown indicating the different sections and their corresponding electrodes.

* represents electrode 1 which was always placed as a reference point at the junction of the inferior vena cava and the right atrium.

○ ctPPF/ctctrl at 60 min of PPF; ◇ ctPPF/ctctrl at 120 min of PPF; straight solid line (-) absolute value of the cycle length (CL) on PPF at 60 min over the CL at control; straight dashed line (---) absolute value of the CL on PPF at 120 min over the CL at control.

Figure 7: Variability of the conduction time (ct) for each section: To determine if a relationship exists between the variability of the ct and the effects of PPF on the reentry circuit, the variability deviation of the ct ($\text{std(ct)}/\text{ct}$) was plotted for each section in dogs 1 to 6 (panels A-F).

std(ct) = standard deviation of ct.

Figure 8: Effect of the variability of the conduction time (ct) on the effect of propafenone (PPF) on conduction time: The ratio of ct on PPF (ct(60-120)) at 60 and 120 min over control ct (ct(ctrl)) and the variability of the ct (std(ct,ctrl) over the mean (mean(ct,ctrl)) under control were plotted to determine if the PPF effect correlated with the variability of the ct. A strong correlation was found only in dog 1 (Panel A) for both PPF 60 and 120 min. In the other dogs 2-6 (Panels B-F), only weak correlations were observed. ○ 60 min of PPF; ◇ 120 min of PPF.

Figure 9: Cycle length (CL) fluctuations for each section: Since there was a large variation in the ct, the fluctuations of the local CL were measured in each section for all 6 dogs under control conditions. The different sections of the circuit clearly indicate large fluctuations of the local CL in different parts of the circuit which correlated with the beat to beat changes in local conduction time under control conditions.

Figure 10: Effect of prematurity on the different sections of the reentry circuit: The conduction time (ct) through each section of the anterograde flutter beat produced by premature stimulation was plotted against the effective local prematurity which was computed as the time between the anterograde front and the preceding free flutter beat at the entrance of each section. Section I, which is adjacent to section II (the site of stimulation), has the greatest range of prematurity. The other sections had a range of 10 ms or less with minimal change in ct of the anterograde flutter. The reentry schematic

represents the different sections of the circuit and the direction of rotation. The premature stimulus (S) (bottom right panel) was introduced between electrodes 4 and 5 of section II.

CHAPITRE IV

**INTERACTIONS OF THE AUTONOMIC NERVOUS
SYSTEM WITH PROPAFENONE ON THE
EXCITABLE GAP COMPOSITION IN A CANINE
MODEL OF ATRIAL FLUTTER**

**INTERACTIONS OF THE AUTONOMIC NERVOUS SYSTEM
WITH PROPAFENONE ON THE EXCITABLE GAP COMPOSITION
IN A CANINE MODEL OF ATRIAL FLUTTER**

Elise Jalil ^{a,c}, Boualem Mensour ^c, Caroline Bouchard ^c, Alain Vinet ^{b,c} and Teresa Kus ^{a,c}

^a Department of Pharmacology, Université de Montréal, Montréal, Québec, Canada

^b Department of Physiology, Université de Montréal, Montréal, Québec, Canada

^c Research Centre, Hôpital du Sacré-Coeur de Montréal, Montréal, Québec, Canada.

Address for corresponding author:

Teresa Kus, MD, PhD

Sacré-Coeur Hospital Research Center

5400 Boulevard Gouin Ouest

Montréal, Québec, Canada

H4J 1C5

Tel.:(514) 338-2222 ext. 2571 Fax:(514) 338-2694

E-mail: kust@crhsc.umontreal.ca

**Intercations of the autonomic nervous system with propafenone on the excitable gap
composition in a canine model of atrial flutter**

Elise Jalil, Boualem Mensour, Caroline Bouchard, Alain Vinet, Teresa Kus

Objective: Norepinephrine (NE) and Acetylcholine (ACh) are known to influence the excitable gap (EG) composition in atrial flutter (AFI). In this study, we determine whether this effect modifies the actions of the class IC antiarrhythmic drug propafenone (PPF). Further, we assess the spatial homogeneity of the effect of PPF and of these neurotransmitters on the reentry circuit.

Methods: A Y-shaped lesion was created between the superior and inferior vena cava and the right atrial appendage in 10 dogs. For stimulation and recording, 7 bipolar electrodes were inserted at the right atrial base. AFI was induced by burst pacing. The duration and composition of the excitable gap (EG) were determined by premature stimuli during AFI. PPF was administered intravenously during AFI in a loading dose of 1 mg/kg over 10 min followed by an infusion of 1.8 mg/kg/hr. RRC's were determined without drug, on PPF alone, then with an infusion of NE (15 μ g/min) into the right coronary artery, and finally with an intracoronary ACh infusion (1-3 μ g/min) but only after recovery from NE effects. **Results:** PPF significantly prolonged the cycle length (CL) and ERP but had a variable effect on the fully excitable portion (FEP) ahead of the wavefront. NE ($p < 0.05$) but not ACh ($p = 0.8$) slightly reversed the effects of PPF on the CL and the ERP. In contrast to their known significant prolongation of the EG in the absence of drug, on PPF neither neurohormones significantly affected the EG duration. However, ACh slightly increased the absolute duration of the FEP ($p = 0.03$) and significantly increased the % of the gap which was fully excitable ($p = 0.005$). In 6 of these dogs, a 16 bipolar electrode belt was then placed around the right atrium for recording. Conduction times (ct) in different portions of the reentry circuit were measured in free running AFI without and with drug. In all 6 dogs, the prolongation of CL on PPF was due to a marked increase of ct mainly localised in one or two

sections of the circuit. The change in CL with the neurotransmitters was not due to an homogeneous effect on cts in all part of the circuits. **Conclusions:** PPF and the neurotransmitters have a heterogeneous effect on the cts in the reentry circuit. Despite prolongation of ERP, in the presence of PPF there is persistence of the EG and the FEP. This is unchanged in the presence of NE or ACh thus confirming the known beta-blocking properties of PPF but also demonstrating a significant anticholinergic effect of the drug.

KEY WORDS: **Discipline:** experimental; **Object of study:** heart; **Level:** organism; **Field of study:** electrophysiology

Supraventricular arrhythmia, Autonomic nervous system, Antiarrhythmic agents, Neurotransmitters, Arrhythmia (mechanisms)

INTRODUCTION

Antiarrhythmic drug efficacy both in atrial and ventricular arrhythmia has been shown to be reversed by exposure to autonomic nervous system agonists. Sympathetic stimulation or changes in autonomic tone may reverse the beneficial effects of conventional antiarrhythmic agents resulting in inefficacy or even proarrhythmia [1,2]. Clinical studies have demonstrated that sodium channel blocking drug effects against ventricular tachycardia can be reversed by beta-adrenoceptor activation [3-7]. Furthermore, isoproterenol has been described to antagonize the actions of d-sotalol and dofetilide in ventricular isolated canine cardiomyocytes [8] which might prove disadvantageous in high catecholamine states. The effects of Class IA and IC antiarrhythmic drugs against supraventricular tachycardias have also been shown to be reversed by isoproterenol [9-14]. In addition, Morady et al. [15] demonstrated that epinephrine partially or completely reversed all of verapamil's effects in paroxysmal supraventricular tachycardias.

Propafenone (PPF), a class IC antiarrhythmic agent [16], produces a frequency- and voltage-dependent reduction in the sodium conductance but also possesses significant potassium channel, mild beta-adrenergic and weak calcium channel blocking activity [17]. Isoproterenol has been shown to reverse PPF's effects on the accessory pathway in patients with Wolff-Parkinson-White Syndrome [18,19].

In current clinical practice, PPF is used in atrial fibrillation and atrial flutter (AFL). Whether the autonomic nervous system influences the effects of PPF in supraventricular tachycardia

is not known. In the present study, we examine the influence of norepinephrine (NE) and acetylcholine (ACh) on the electrophysiological effects of PPF in a canine model of AFl. Previous studies in this model have already demonstrated that NE and ACh significantly alter the excitable gap (EG) composition of the reentry circuit and reverse the electrophysiological effects of the class III drug D-sotalol on the EG [20].

In this study, we also determine the spatial homogeneity of the effects of PPF and the neurotransmitters on the reentry circuit. The conduction times (ct) in different portions of the reentry circuit were measured in a free running AFl both before and after the administration of PPF, and then following the administration of NE and ACh using a belt containing 16 bipolar electrodes. Callans et al. [21] have shown that PPF either decreases conduction in an unchanged ventricular tachycardia circuit or lengthens the circuit barriers without changing the exit point of the circuit. Frame et al. [22] have studied the conduction of the reentrant impulse around a tricuspid ring, using intracavitary electrode arrays from 96 endocardial bipolar electrodes. These investigators have found that, without drug, the reentry was relatively uniform and that no single part of the pathway displayed markedly slower conduction. Lidocaine slowed conduction in all parts of the reentrant pathway. We have previously shown [23] that the tonic effect of PPF was spatially inhomogeneous and that, in general, the variability of ct was inhomogeneous in the different sections of the circuit with no consistent relation to the effects of PPF.

METHODS

Surgical technique

10 mongrel dogs of either sex (mean weight \pm SD; 33 ± 4 kg) were studied in the post absorptive state. General anesthesia was induced with sodium thiopental (30 mg/kg i.v.) and maintained with chloralose (80 mg/kg i.v. bolus supplemented by 15 mg/kg/hr maximum as needed). The dogs were intubated endotracheally and ventilated (Harvard pump, Millis, MA) with room air (10 breaths/min, tidal volume to achieve a maximum inspiratory pressure of 20 cm of water) to maintain arterial pH 7.35 to 7.45 and $pO_2 > 80$ mm Hg. Arterial and venous cannulae were inserted in the left femoral artery and vein by direct cutdown for blood pressure monitoring and blood sampling, respectively. An additional venous cannula was inserted in the right internal jugular vein for drug administration. Muscular relaxation was then induced with 3 mg/kg i.v. of gallamine triethiodide (Flaxedil 100). A right thoracotomy was performed via the fourth or fifth intercostal space and the pericardium was incised to provide access to the vena cava and the right atrium. Based on the procedure developed by Frame *et al.*, [24], a lesion was created by sewing in a line extending from the superior to the inferior vena cava. A second line, extending from the first two-thirds of the way to the tip of the right atrial appendage and parallel to but 1 to 2 cm above the atrioventricular groove was similarly sewn. Both sewn lines were also crushed in order to assure an anatomical barrier. In 4 of these dogs, five close (2-4 mm) bipolar, teflon coated (except for the tips), stainless steel wire electrodes were inserted using a 26 gauge needle around the base of the right atrium for stimulating

or recording from the endocardial atrial surface. In the other 6 dogs, 7 close (2-4 mm) bipolar endocardial stimulation electrodes were inserted around the base of the right atrium (Fig. 1), and, in the same area, a belt on which 16 bipolar electrodes were mounted was placed around the right atrium for epicardial recording. These electrodes were uniformly distributed around the tricuspid valve (except for the septal region). Recordings were obtained from electrodes which were in contact with the right atrium. In some animals with smaller hearts, the belt extended beyond the right atrium and 1-5 electrode pairs were not used for recording. A polyethylene catheter (Abbocath-T 24 Gauge, Abbott Ireland) was also inserted in the right coronary artery for neurohormone administration.

Measurement of electrophysiological parameters

In the first 4 dogs, a single lead (II) surface electrocardiogram, atrial electrograms from each of the five bipolar electrodes and femoral arterial pressure were monitored and recorded using a Nihon Kohden (Tokyo, Japan) polygraph (model RM6008) and data also were stored on a digital 8 track, Sony Instrumentation Cassette Recorder PC-108M (Tokyo, Japan). In the 6 dogs in which 7 bipolar stimulation electrodes were inserted around the base of the atrium and a 16 bipolar electrode recording belt was used, atrial electrograms were recorded using a multi-channel recording system (Electrophysiological Data Interface, Institut de Génie Biomédical, École Polytechnique de Montréal) and PC compatible computer (Prosys-Tec Inc., Canada). The bipolar electrograms were amplified by programmable-gain analog amplifiers (0.05-225 Hz) and converted to a digital format at 500 sample/channel/sec.

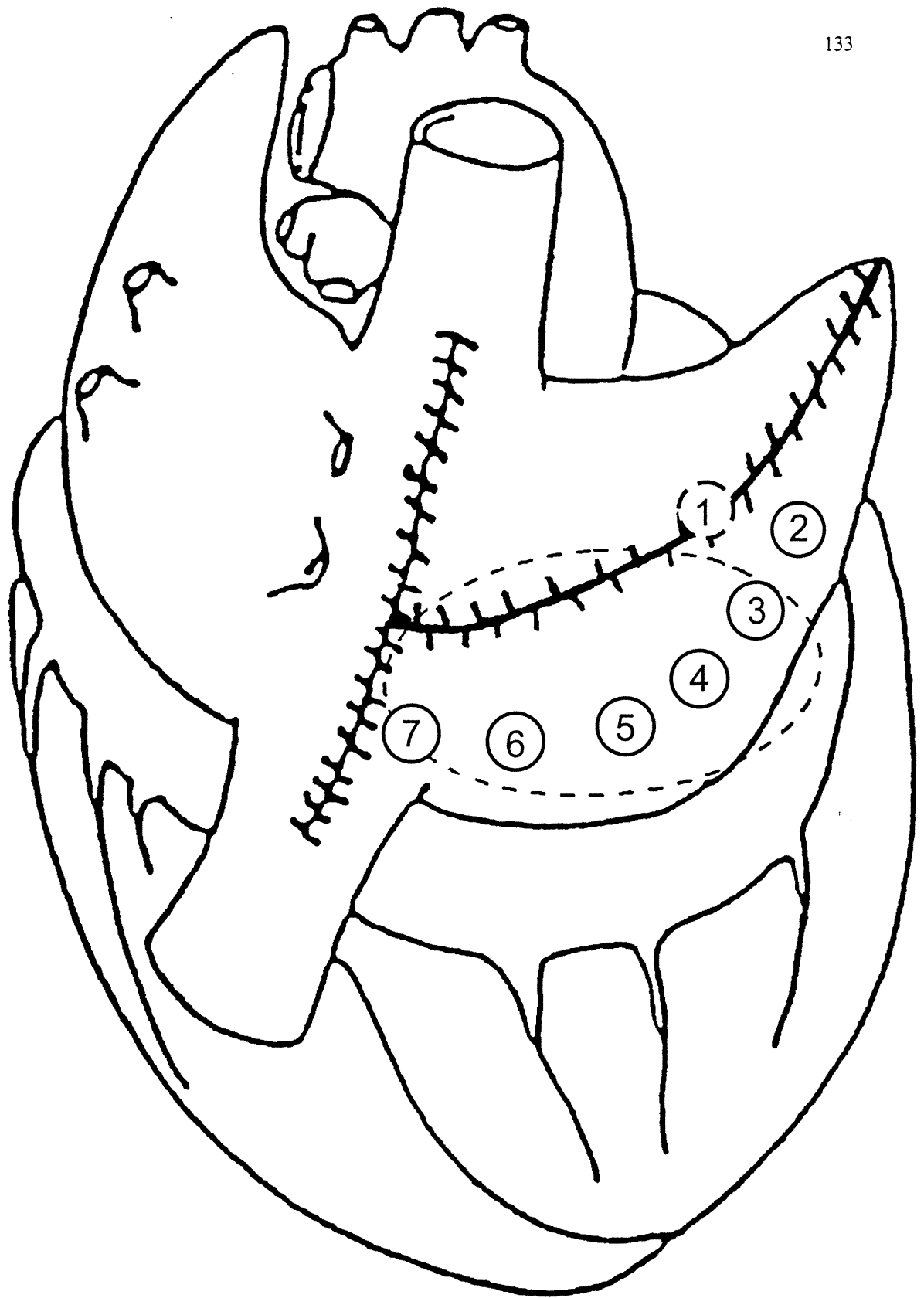


FIGURE 1 The right posterior view of the heart

AFI was induced by burst stimulation (50 beats at CLs of 90-170 ms). The stimulation electrode closest to the recording site which gave the clearest signal was used. If AFI induction did not occur at this site, other stimulation sites were also used. During stable AFI [CL variations of less than 3 ms], a premature stimulus was applied after every 20th spontaneous beat detected at the next distal electrode in the direction of wavefront propagation. The choice of adjacent stimulating and recording electrode site was based on the quality of the recorded signal and the occurrence of reset as described below. Initially, the premature stimulus was introduced late in diastole and the coupling interval was progressively decreased by 2 ms until the stimulus failed to capture. The interval between a spontaneous beat (T) and the premature stimulus (S) (interval T-S), the interval between the premature stimulus and the response (S-R) as well as the interval between the premature stimulus and the subsequent tachycardia beat ($S-T_1 = S-R + R-T_1$) were measured (peak to peak) at the electrode distal to the stimulating site (in the direction of wavefront propagation) as shown in Figure 2. Since the stimulation electrode (S_E , insert in Figure 3) was located at a different point in the circuit than the detecting electrode (R_E), the method introduced by Mensour et al. [25] was used to estimate the coupling interval and the return cycle at the stimulation site. As shown in Figure 3, the range of T-S values for which S-R falls on the line $CL - [T-S]$ gives an estimate of τ , the time needed for the free flutter to travel from S_E to R_E . The coupling interval (CI) and the return cycle (RC) of the premature stimulus with respect to the last passage of the front at S_E are estimated respectively as $CI = \tau + T-S$ and $RC = S-T_1 - \tau$. Graphs describing the relationship (RC vs CI), or RRCs, were

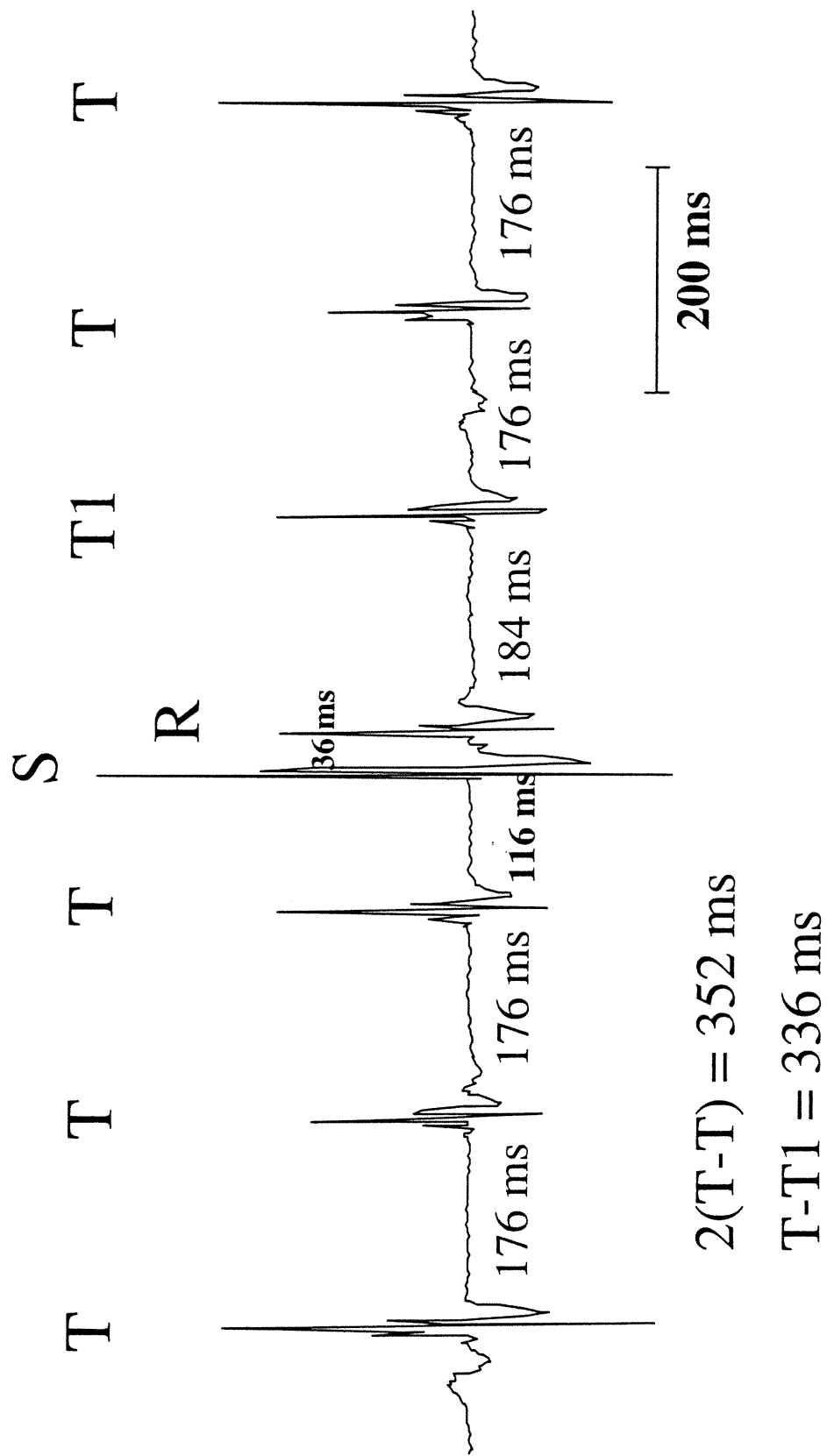


FIGURE 2 Epicardial bipolar recording during atrial flutter.

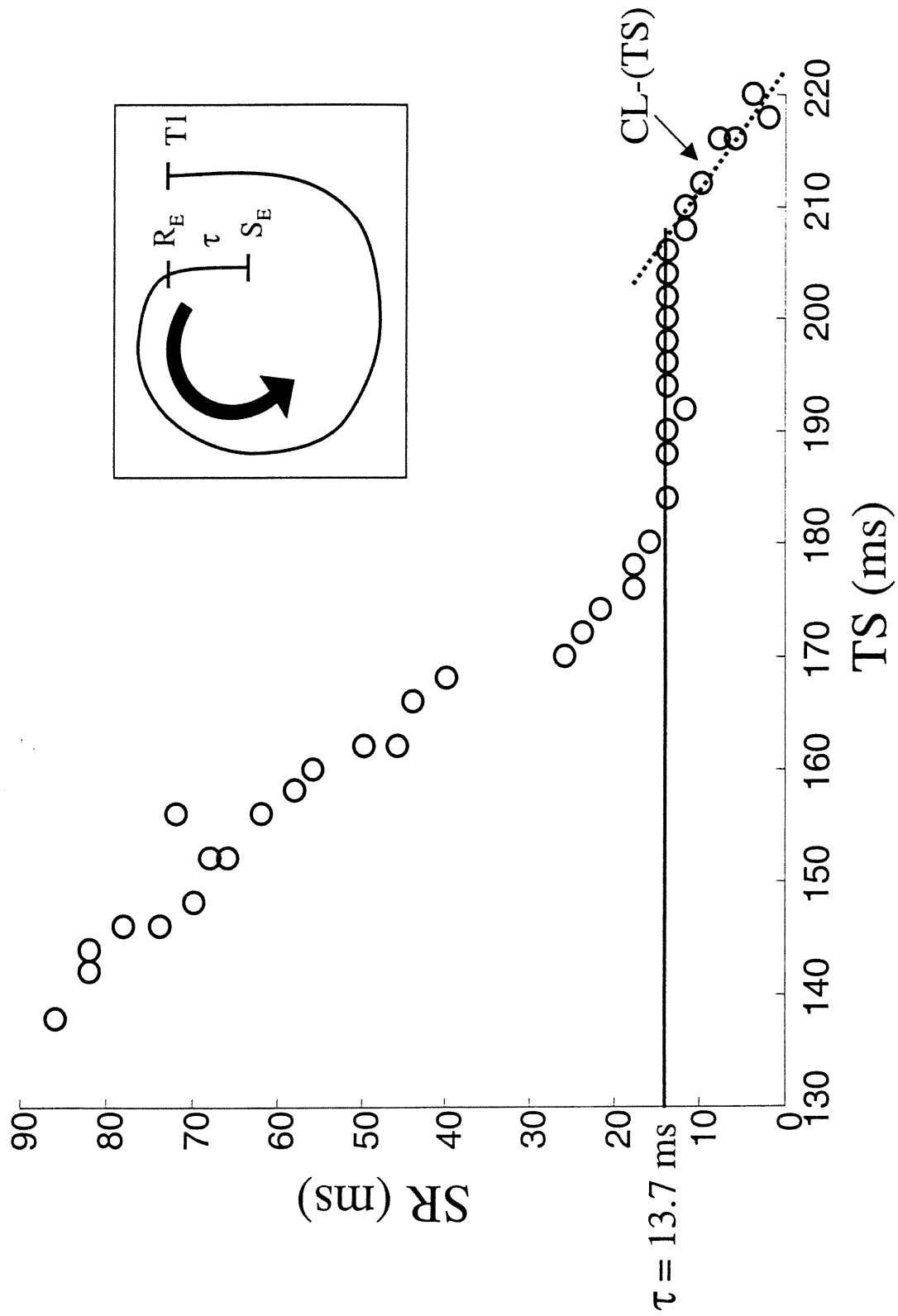


FIGURE 3 Method to approximate the measure of the coupling interval and return cycle at the stimulation site

constructed using points for which $T-T1 < 2 CL$ by more than twice the standard deviation of the AFI CL (i.e. when the premature beat reset the tachycardia). It was pointed out in Mensour et al. [25] that this criterion, standard in the literature, could sometimes lead to an underestimation of the duration of the EG. In fact, $T-T1=T-S + S-R + R-T1$ for any stimulus applied in the EG. For a very premature stimulus capturing near the limit of the EG, it may happen that $T-T1 > 2*CL$, because of significant conduction delay of the propagating stimulated wavefront. Nevertheless, we have decided to follow the standard criterion to be consistent with the method most commonly used in the literature. The flat portion of the EG composed of fully excitable tissue was estimated from that portion of the RRC where the RC values were within one standard deviation (SD) of the CL. The ascending portion of the RRC where RC was greater than the $CL +SD$ thus represented the portion of the EG composed of partially refractory tissue. A nonlinear function of the form $RC = a1 + a2 \tanh(a3 CI + a4) = F(CI)$ was fitted to the data. The value of the $F(CI)$ at the lower limit of the EG was taken as an estimate of the maximum resetting. The mean residual between the fit and the data was taken as a measure of the stability of the RRC [25].

PPF was administered via the jugular vein during AFI in a loading dose of 1 mg/kg infused over 10 minutes. This was followed by a maintenance infusion of 1.8 mg/kg/hr which has been previously shown to achieve stable therapeutic plasma levels between 0.1-2.0 $\mu g/ml$ [26]. The protocol to determine the RRC was repeated following the bolus administration and again at 10 minute intervals during the infusion. Following a minimum of 60 minutes of PPF infusion, 15 $\mu g/min$ of NE was also infused into the right coronary artery. RRCs

were repeated on PPF during the NE infusion. A saline solution was then infused into the right coronary artery for at least 15 min to permit recovery from NE effects. RRCs were repeated on PPF alone (during the saline infusion) and then on PPF with simultaneous ACh infusion (1-3 $\mu\text{g}/\text{min}$). Blood samples (5-7 ml) for drug plasma levels were obtained from the femoral vein during RRC determination.

To determine the spatial homogeneity of PPF effect, the cts in different portions of the circuit were measured during free running AFI both before and in the presence of the drug and neurohormones. This was done for the 6 dogs in which the 16 electrodes recording belt was used. Using the free running AFI before drug administration as a reference, the electrodes whose activation times were not consistent with a continuous progression of the activation front around the circuit were discarded as bystanders. The cts were computed between each successive pair of remaining electrodes and averaged over 15 beats. Sections of the AFI circuit were defined such that the ct through each section under control conditions was at least 5 ms. The cts in each section with PPF alone, PPF+NA, PPF+saline and PPF+ACh infusion were expressed relative to control.

This research protocol and care of the animals conform to the Guiding Principles for Animal Experimentation as described by the Canadian Council on Animal Care and was reviewed by the committee for Animal Experimentation at the Research Centre of Sacré Coeur Hospital (Université de Montréal). At the end of the experimental protocol, ventricular fibrillation was induced by direct current application to the heart.

Data analysis

In four animals, the data was digitalised using a TL-2 data acquisition interface (Axon instruments, Foster City, California) and all data were analysed on a Silicon Graphics computer. The signals were manually timed using software developed by our group (MACT, Centre de Recherche, Hôpital du Sacré-Coeur de Montréal, Montréal, Québec, Canada).

Statistical analysis

The data are presented as means \pm SD. For the ten dogs, the infusion of PPF was complemented with the successive administration of NE, saline and ACh, comparison among the five modalities (control, PPF alone, PPF+NE, PPF+saline, PPF+ACh) was done using one way repeated measures ANOVA. Each modality was also compared to its predecessor by the Student-Newman-Keuls test. Some measurements (e.g. Maximum Resetting, local ct, see results) were found to be correlated to other variables that were not uniformly distributed among the groups. These confounding variables was used as covariate in the analysis of variance (ANCOVA). A Pearson correlation was used to determine a relationship between NE and saline effects on ct. Regarding the plasma concentrations, two orthogonal contrasts were tested: PPF alone vs [NE+PPF, saline+PPF, ACh+PPF], to assess the effect of time on the plasma concentrations of the drug and, NE+PPF vs [saline+PPF, ACh+PPF], to assess whether the effect was already stabilized

after the NE infusion.

RESULTS

Drug plasma levels

Drug plasma levels were monitored during the protocol. In 9 dogs, the mean plasma PPF concentrations at 80 min (measured after 40 to 116 min of PPF) were $1.037 \pm 0.422 \mu\text{g/ml}$. It was significantly higher ($1.160 \pm 0.451 \mu\text{g/ml}$; $p=0.030$) during the step of the protocol in which NE was added (measured after 73 to 155 min of PPF).

In 5 of these dogs, the mean plasma concentrations were measured at every step of the protocol (Table I). The continuous infusion of PPF was associated with a slow rising drift of the concentration (PPF 80 min vs [PPF+NE, PPF+saline, PPF+ACh]; $p<0.05$, PPF+NE vs [PPF+saline, PPF+ACh]; $p<0.05$) which saturated after two hours of infusion (PPF+saline vs PPF+ACh; $p=0.70$). The same effect, suggesting achievement of an equilibrium state between the infusion rate, metabolism and distribution of PPF, was found in our previous studies [23]. The major metabolite, 5-hydroxy propafenone, was undetectable. These levels were within the recommended therapeutic plasma concentrations ($0.1\text{-}2.0 \mu\text{g/ml}$) [27].

TABLE I – Effects of neurotransmitters on the mean plasma concentrations of propafenone

| Dog | PPF at 80 min ($\mu\text{g/ml}$) | PPF+NE ($\mu\text{g/ml}$) | PPF+saline ($\mu\text{g/ml}$) | PPF+ACh ($\mu\text{g/ml}$) |
|--|---------------------------------------|--------------------------------|------------------------------------|---------------------------------|
| 3 | 1.968 | 2.259 | 2.792 | 2.343 |
| 4 | 1.126 | 0.970 | 1.290 | 1.440 |
| 5 | 1.116 | 1.155 | 1.110 | 1.332 |
| 6 | 0.794 | 0.843 | 1.064 | 0.877 |
| 7 | 0.778 | 1.008 | 1.058 | 1.071 |
| Mean plasma concentration (\pm S.D.) | $1.156 \pm 0.484^*$ | $1.247 \pm 0.576^{**}$ | $1.463 \pm 0.749^\dagger$ | 1.413 ± 0.565 |

PPF = propafenone
NE = norepinephrine
ACh = acetylcholine

*PPF 80 min vs [PPF+NE, PPF+saline, PPF+ACh]; $p < 0.05$

** PPF+NE vs [PPF+saline, PPF+ACh]; $p < 0.05$

† PPF+saline vs PPF+ACh; $p = 0.70$

Global effects of propafenone and the autonomic neurohormones on excitable gap composition and reset-response curve

Global Effect of PPF

The effects of PPF on AFI are shown in the second column of Table II. PPF shifted the RRCs upward and to the right (Fig 4A) increasing the AFI CL from 138 ± 17 ms to 188 ± 33 ms ($p < 0.0001$) and the ERP (i.e. the shortest coupling interval that resets the tachycardia during determination of the RRC) from 92 ± 22 ms to 138 ± 40 ms ($p < 0.0001$). Since CL and ERP augmentations were the same ($\Delta CL = 50 \pm 20$ ms, $\Delta ERP = 46 \pm 24$ ms), ERP/CL was increased from $66 \pm 10\%$ to $72 \pm 11\%$ ($p=0.033$). As a correlate, the EG duration remained unchanged and thus decreased when expressed as a percentage of the CL (from $34 \pm 9\%$ to $28 \pm 11\%$, $p=0.031$). In all dogs, the control EG was composed predominantly of partially excitable tissue, but in 9 of 10 dogs (except dog 2, table III) a flat portion was present. In these 9 dogs, the duration of the flat portion was not changed under PPF.

Global effect of NE

Infusion of NE ($15 \mu\text{g}/\text{min}$) into the right coronary artery during PPF administration NE decreased the CL (PPF vs [PPF+ NE]: 188 ms vs 174 ms, $p = 0.004$). As a consequence, the RRC was shifted downward and to the left (Fig 4A). NE also reduced the ERP (138 ms

TABLE II – Effects of neurotransmitters and propafenone on atrial flutter and excitable gap parameters

| | <i>Control</i> | <i>PPF</i> | <i>NE + PPF</i> | <i>Saline + PPF</i> | <i>ACh + PPF</i> |
|--------------|----------------|------------|-----------------|-----------------------|-----------------------|
| AFI CL (ms)† | 138 ± 17 | 188 ± 33* | 174 ± 26** | 194 ± 31 [‡] | 194 ± 35 |
| ERP (ms)† | 92 ± 22 | 138 ± 40* | 112 ± 30** | 138 ± 44 [‡] | 140 ± 43 |
| % ERP (%)†† | 66 ± 10 | 72 ± 11* | 64 ± 9** | 70 ± 14 | 71 ± 13 |
| EG (ms) | 46 ± 12 | 50 ± 16 | 62 ± 14 | 56 ± 20 | 54 ± 22 |
| % EG (%)†† | 34 ± 9 | 28 ± 11* | 36 ± 9** | 30 ± 14 | 29 ± 13 |
| FEP (ms) | 6 ± 3 | 7 ± 6 | 7 ± 7 | 5 ± 4 | 9 ± 7 ^{‡‡} |
| %FEP (%) | 14 ± 9 | 20 ± 16 | 14 ± 15 | 12 ± 9 | 21 ± 14 ^{‡‡} |

AFI CL – atrial flutter cycle length; ERP – effective refractory period; EG – excitable gap; FEP – fully excitable portion; PPF – propafenone; NE – norepinephrine; ACh -acetylcholine

† ANOVA = $p < 0.0001$

†† ANOVA = $p < 0.02$

Paired Student t-test
 $p < 0.05$

* compared to Control

**compared to PPF

[‡] compared to NE + PPF

^{‡‡} compared to Saline + PPF

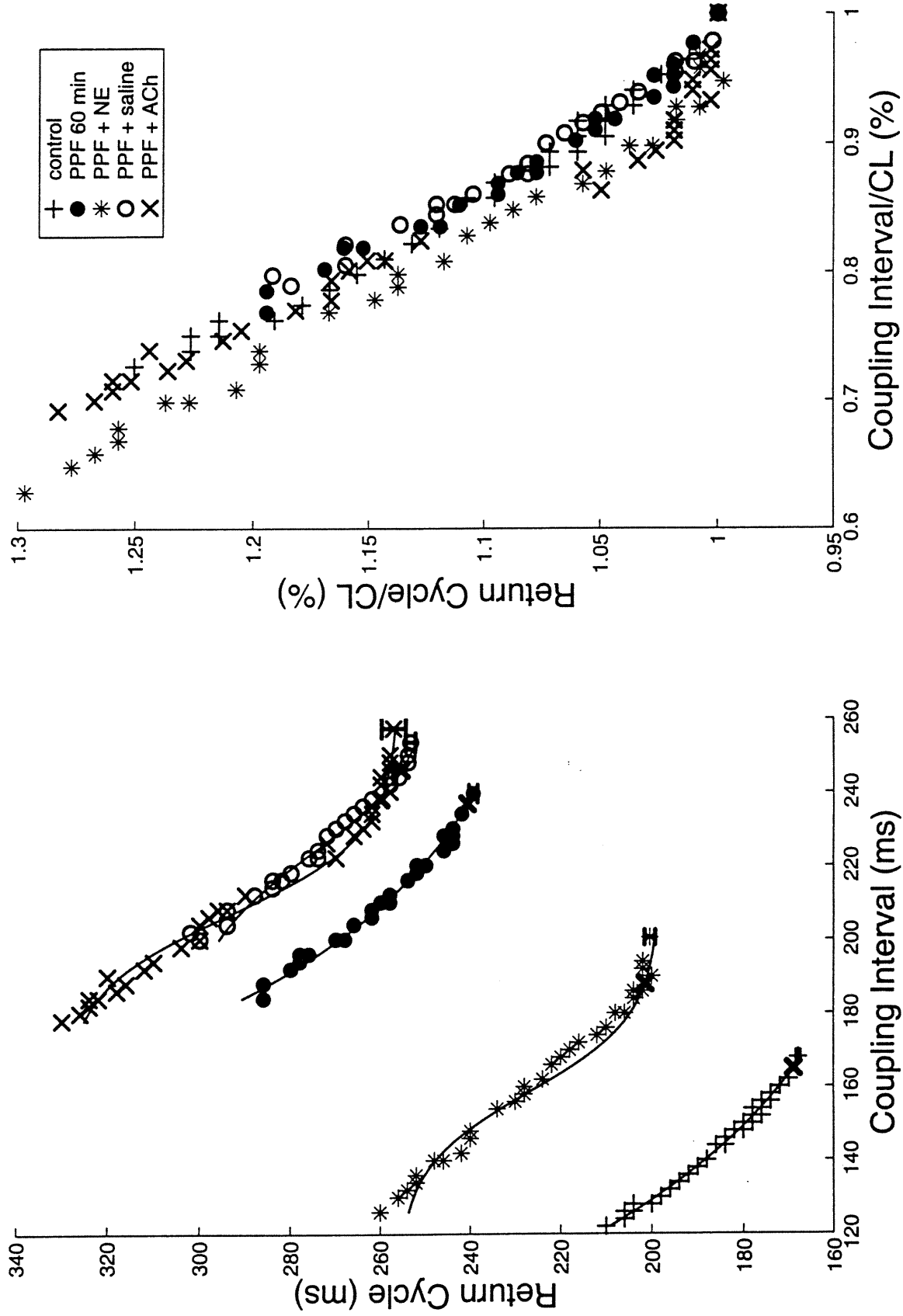


FIGURE 4 Effects of norepinephrine and acetylcholine on the reset-response curve during an infusion of propafenone.

TABLE III – Effects of neurotransmitters and propafenone on the fully excitable portion of the excitable gap

| Dog | Control | | PPF | | NE + PPF | | Saline + PPF | | ACh + PPF | |
|-----------|----------|-----------|----------|-----------|----------|-----------|--------------|-----------|-----------|-----------|
| | FEP (ms) | % FEP (%) | FEP (ms) | % FEP (%) | FEP (ms) | % FEP (%) | FEP (ms) | % FEP (%) | FEP (ms) | % FEP (%) |
| 1 | 4 | 7 | 9 | 28 | 0 | 0 | 7 | 13 | 10 | 23 |
| 2 | 0 | 0 | 0 | 0 | 0 | 0 | 0 | 0 | 0 | 0 |
| 3 | 10 | 31 | 3 | 5 | 7 | 16 | 8 | 22 | 20 | 48 |
| 4 | 3 | 12 | 4 | 10 | 3 | 5 | 6 | 24 | 7 | 30 |
| 5 | 3 | 6 | 3 | 5 | 12 | 17 | 7 | 14 | 19 | 24 |
| 6 | 9 | 22 | 17 | 36 | 18 | 42 | 11 | 23 | 8 | 27 |
| 7 | 7 | 14 | 0 | 0 | 0 | 0 | 0 | 0 | 0 | 0 |
| 8 | 7 | 15 | 4 | 9 | 9 | 19 | 5 | 5 | 10 | 14 |
| 9 | 7 | 18 | 14 | 36 | 5 | 6 | 3 | 7 | 9 | 15 |
| 10 | 7 | 13 | 8 | 37 | 18 | 37 | 6 | 14 | 10 | 27 |
| Mean ± SD | 6 ± 3 | 14 ± 9 | 6 ± 6 | 17 ± 16 | 7 ± 7 | 14 ± 15 | 5 ± 4 | 12 ± 9 | 9 ± 7* | 21 ± 14* |

FEP – fully excitable portion; PPF – propafenone; NE – norepinephrine; ACh – acetylcholine

* Paired Student t-test $p < 0.05$ compared with Saline + PPF

vs 112 ms, $p = 0.011$). However, the decrease of ERP ($\Delta\text{ERP} = 26 \pm 26$ ms) was almost twice that of the CL ($\Delta\text{CL} = 15 \pm 12$ ms), such that ERP/CL decreased from $72 \pm 11\%$ to $64 \pm 9\%$ ($p=0.035$) and EG /CL increased from $28 \pm 11\%$ to $36 \pm 9\%$ ($p=0.034$). There was however no significant change in the duration of the fully excitable portion.

In our previous study, we have proposed that the increase of relative maximum resetting ($\text{RMR} = (\text{maximum RC} - \text{mean CL})/\text{CL}$) corrected for the change of ERP was an indicator of the class I effect of PPF [23]. This correction is made because AFl with a shorter ERP (and longer EG) always have a larger RMR. The rationale is that the corrected RMR measures the depression of excitability which should be increased when sodium current is blocked by a class-I effect. Accordingly, an analysis of covariance (ANCOVA), using ERP/CL as covariate, was done to compare the RMR in the PPF and [PPF+NE] conditions. NE induced a slight but not significant increase in the RMR (raw data [NE+PPF]-[PPF]= $(30 \pm 9\%) - (22 \pm 9\%)$; corrected for ERP = $[0.5 \pm 2.5\%, p = 0.8]$). This indicates that the difference of RMR is completely accounted for by the decrease in ERP induced by NE, which we consider as a counter effect to the class III action of PPF, and that the effect of NE on the tonic class-I effect of PPF is minimal.

Global effect of ACh

Following washout of NE with saline for at least 15 min, the CL was increased to 194 ± 31 ms, a value close but slightly higher than observed with PPF alone. This is consistent with

the slow increasing drift in PPF concentration observed in the second hour of infusion. However, overall, there was no significant difference between PPF and PPF+saline for all measures given in Table II and Table III, as well as for the RRCs (fig. 4).

Subsequent intracoronary infusion of ACh (1-3 $\mu\text{g}/\text{min}$) during continued infusion of PPF did not affect the RRC curves (Fig 4A). Neither CL (PPF+saline vs PPF+ACh: 194 ± 31 ms vs 194 ± 35 ms, $p = 0.832$), ERP (PPF+saline vs PPF+ACh: 138 ± 44 vs 140 ± 43 ms, $p = 0.664$), nor EG were modified by ACh in the presence of PPF. However, the fully excitable portion of the EG increased slightly from 5 ± 4 ms to 9 ± 7 ms ($p = 0.031$) which, expressed as a percentage of the EG, represented a significant increase from $12 \pm 9\%$ to $21 \pm 14\%$ ($p = 0.005$; Table III). Furthermore, all the resetting curves expressed as a percentage of the CL were almost superimposed (fig. 4B).

Spatial characteristics on the effects of norepinephrine and acetylcholine

In the 6 dogs (dogs1-6 Table III) in which a 16 bipolar electrode recording belt was used, cts between electrode sites were measured under control conditions and then 80 min after the beginning of the PPF infusion. In all cases, the prolongation of the CL on PPF alone was due to a marked increase of the ct mainly localised in one or two sections of the circuit (Fig 5 A-F), a condition that was also seen in our previous studies [23]. The regions of slowed conduction were different from one dog to another and were not related to any specific anatomical structure. Moreover, in 3 of these dogs, the direction of propagation

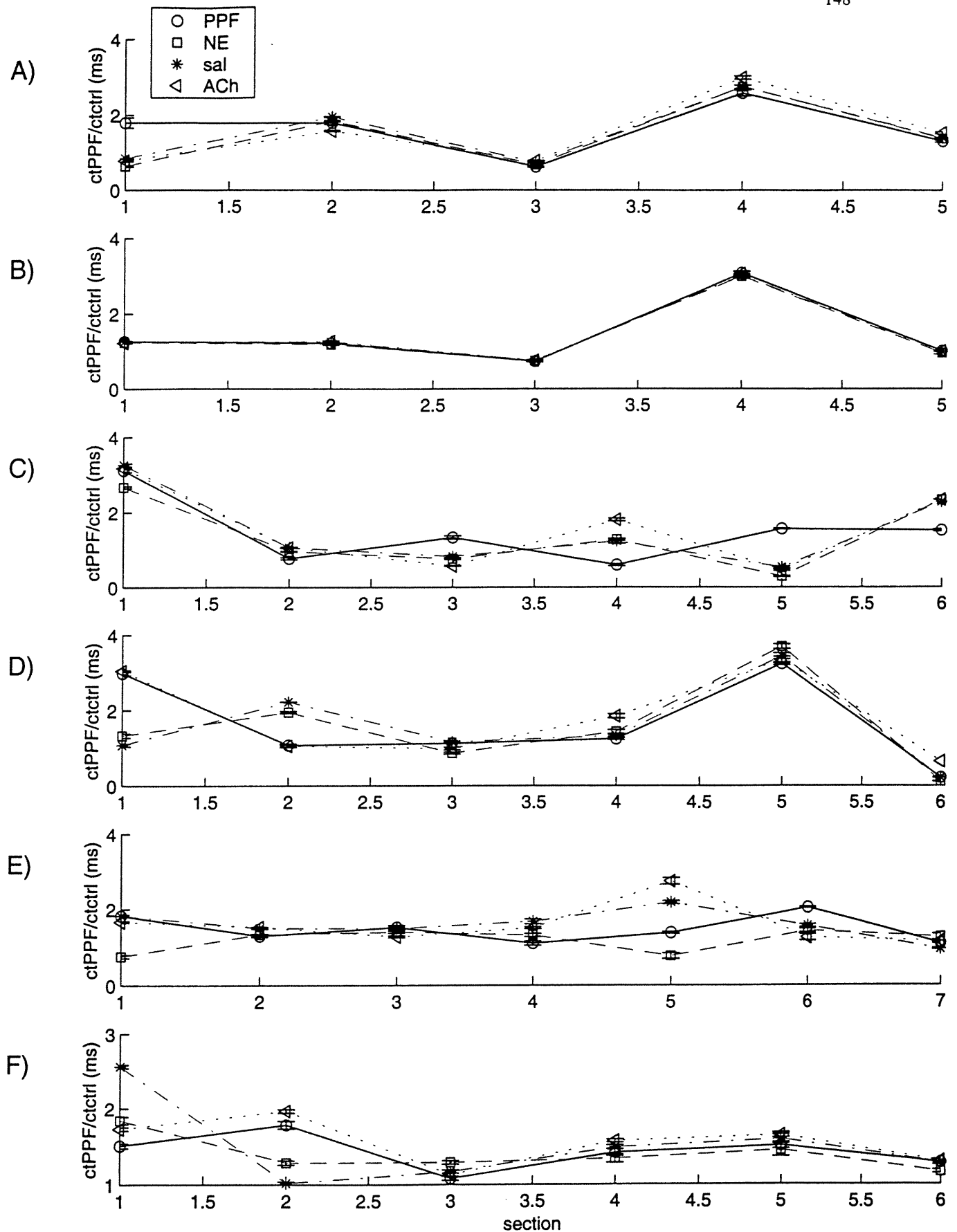


FIGURE 5 Inhomogeneity of propafenone effect on conduction time around the atrial circuit in free running flutter.

on PPF was the same as in control suggesting that the action of PPF depended on some local characteristic of the tissue, and not on the direction of the wavefront.

The cts with PPF and subsequent infusion of NE were also measured. In all 6 dogs, the decrease of CL with PPF+NE was not due to an homogeneous reduction of the cts in all part of the circuits. On the contrary (Fig 5 A-F), the effect of NE was localised in a few portions of the circuits and propagation was even found to be slower in some sections. For each dog, the non-homogeneity of the NE effect between the sections was verified by performing an ANOVA on the difference in ct ($\Delta ct = ct_{PPF}/ct_{CTRL} - ct_{NE}/ct_{CTRL}$). For all dogs, a significant difference between sections was found. Moreover, the sections where the action of NE was significant were different from dog to dog, and were not related to the action of PPF (Δct and ct_{PPF}/ct_{CTRL} were not correlated; $r = -0.31$) It is noteworthy that the direction of propagation in the presence of both PPF and NE+PPF were the same in five animals.

An intracoronary saline infusion was given for at least 20 min to washout the effects of NE. Even though all the global characteristics were indicating a complete washout of NE and a reversal to the situation existing before the NE administration, examination of the ct in the different portions of the circuit revealed that the reversal was not complete all over the reentry circuit (Fig 5 A-F). The CL prolongation was due to an inhomogeneous increase in the cts mainly localised in a few sections of the circuit. In fact, cts were even decreased in some sections of the circuit. The spatial inhomogeneity of the reversal was verified using

ANOVA on the difference in ct on PPF and saline+PPF (ctPPF/CTRL vs saline+PPF/CTRL). A significant difference between sections was found in all dogs. In addition, the sections which were not completely reversed with saline correlated with the sections which were the most affected by NE ($r = 0.782$; $p=0.01$).

Following the washout with saline, ACh was infused into the right coronary artery. In all 6 dogs, the addition of ACh had a heterogeneous effect on the ct and did not slow or accelerate the same regions as saline+PPF (Fig 5 A-F). This is interesting because, again, all the global characteristics were similar for ACh+PPF compared with saline+PPF. Therefore, the cts in the different sections were not affected in the same way but reached the same end result. The regions of slowed conduction were different from one dog to another and did not correspond to any fixed anatomical reference point. In five dogs, the direction of propagation on ACh+PPF was the same as on saline+PPF. However, in three of these dogs, the direction of propagation was different from control.

Prematurity effect

To assess the variation of the ct as a function of prematurity on PPF and with NE+PPF, the ct of the anterograde flutter beat produced by each stimulus was measured in each portion of the circuit. The effective local prematurity was computed as the time between the anterograde flutter beat produced by the premature stimulus and its preceding beat for every

entrance of each section. The cts between the sections were then plotted against the local prematurity of each section (Fig 6 A-F). In general, as previously reported with PPF [23] the sections adjacent to the stimulation had a larger range of effective prematurity. The variation of the ct as a function of prematurity was also assessed on saline+PPF and ACh+PPF. As with NE+PPF, the sections adjacent to the site of stimulation also had a larger range of effective prematurity. Since the section adjacent to the stimulation was the only one that was consistently affected, the ct of this section after stimulation was divided by the ct in the free flutter for each drug condition. These normalised cts were then plotted against the local prematurity expressed as a percentage of the CL. In 4 of 6 dogs, the curves were superimposed as previously seen when the RRCs were expressed as a percentage of the CL (Figure 4B), which is consistent with the fact that the resetting was concentrated in this first section. In 1 of two remaining dogs, the PPF curve was displaced from the superimposable curves of the other 3 conditions indicating a longer conduction time on PPF. This could be due to the fact that the direction of propagation was different for PPF. In the last remaining dog, the curves were different in all the drug conditions. In this case, the direction of propagation was the same. However, the second section in the direction of propagation also demonstrated significant resetting suggesting that depressed excitability and/or delay in recovery was more accentuated in this preparation than in the others making it more sensitive to spatial and temporal fluctuations.

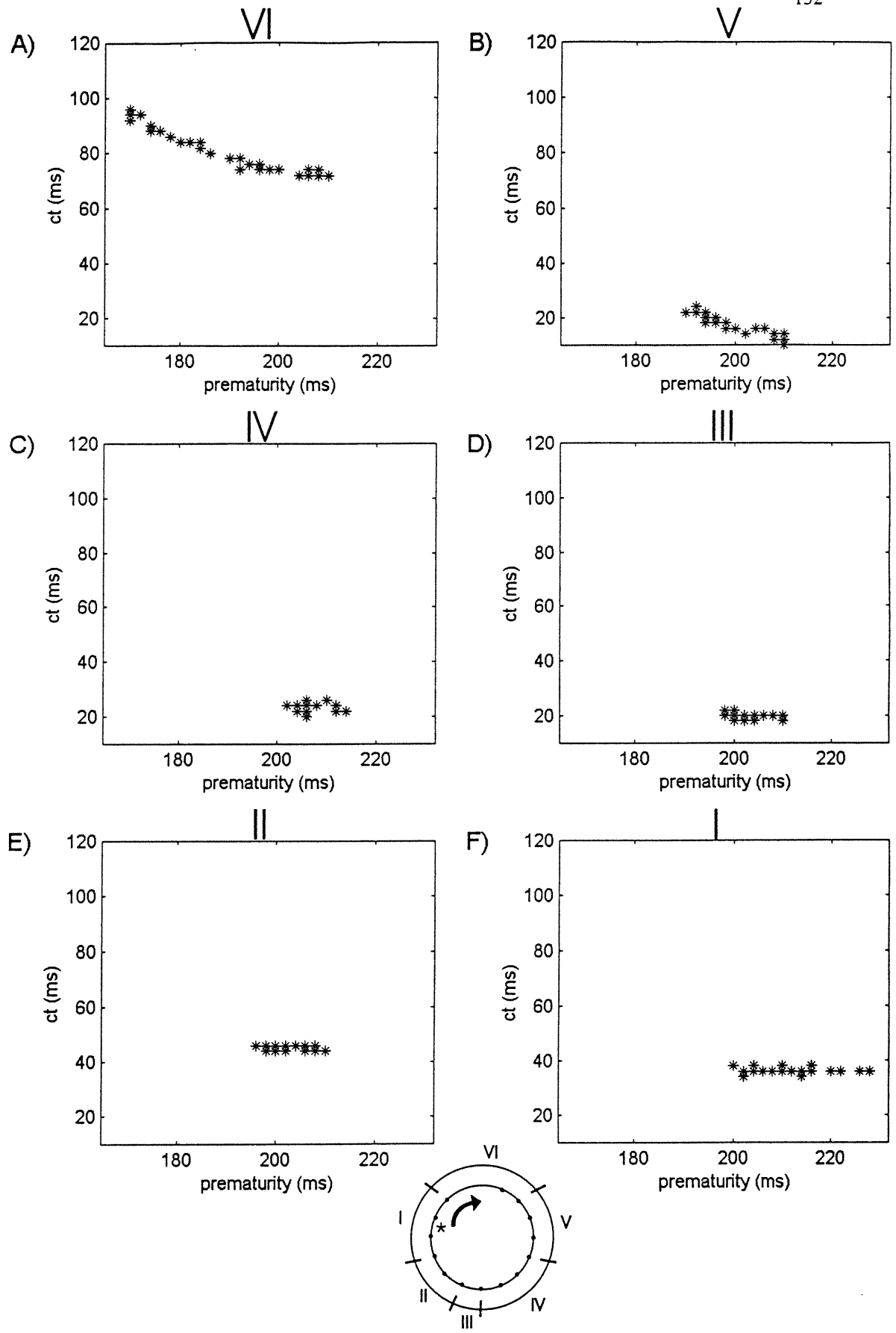


FIGURE 6 Effect of prematurity on the different sections of the reentry circuit.

DISCUSSION

This study examined the influence of the autonomic nervous system's neurotransmitters on the EG composition in AFl in the presence of PPF. This and previous studies done in our laboratory [23] demonstrated that PPF significantly prolonged the AFl CL and ERP, but had a variable effect on the fully excitable portion ahead of the wavefront. PPF increased the CL and ERP by the same amount. This increase in the ERP can be explained 1) by a direct potassium blocking effect, 2) by a direct tonic class I action of the drug which reduces the excitability and 3) by an indirect class I action of the drug which prolongs CL and results in longer action potential [23]. Previous studies have shown that PPF inhibits the atrial transient outward current (I_{to}), the inward rectifier current (I_{K1}), the delayed rectifier (I_{Kr} and I_{Ks}) [28,29] and also the ultra-rapidly activating delayed rectifier (I_{Kur}) [30].

The spatial characteristics of the effects of PPF were examined by analysing the cts between electrode sites without drug and with PPF infusion. As previously seen in our studies [23] the prolongation of the CL was mainly due to a marked increase in the ct mainly localised to one or two sections of the reentry circuit demonstrating that the tonic effect of PPF was spatially inhomogeneous. Since the effective range of prematurity obtained by stimulation at one site was important only in the portion of the circuit adjacent to the stimulation electrode, it was not possible to evaluate if the variation of the resetting properties induced by PPF was also inhomogeneous.

Previous studies have demonstrated that NE significantly decreases the ERP in the atria [31] and that sympathetic nerve stimulation during AFl slightly shortens the CL and ERP [32]. Further, Rahme et al. [33] have demonstrated that NE shortens the AFl CL and markedly decreases ERP resulting in significant prolongation of the total EG and of the fully excitable portion. In the present study, administration of NE into the right coronary artery during a simultaneous infusion of PPF slightly decreased the CL and the ERP, but had a variable effect on the fully excitable portion. Since, NE decreased the ERP by almost twice as much as the CL, this indicated that NE had a greater counter effect on the class III actions of PPF. This was confirmed by analysing the maximum resetting (to get a direct indication of class I effect) in which there was no difference independent of the ERP reduction.

The cts between electrode sites with PPF and subsequent infusion of NE were also measured. The reduction of CL with PPF+NE was not due to a homogeneous reduction of the cts in all parts of the circuit. In fact, the effect of NE was localised in a few portions of the circuit and propagation was even found to be slower in some sections. Moreover, the sections where the action of NE was significant were different from dog to dog, and were not related to the action of PPF.

These observations confirmed the incomplete beta-blocking effects of PPF. Indeed, isoproterenol infusion has been shown to partially or completely reverse the electrophysiological effects of intravenous [18] and oral [19] PPF by decreasing the refractory periods of the accessory pathway in patients with pre-excitation syndrome.

When sympathetic influence was removed by infusing saline, the CL and ERP again significantly increased with values slightly higher than observed with PPF alone. This is consistent with the slow increasing drift in PPF concentrations observed during the second hour of infusion and previously seen in our studies [23]. However, the CL reversal on saline was not homogeneous on the cts in all sections of the reentry circuit. In addition, the sections which were most affected by NE did not completely reverse with the saline infusion. Despite the incomplete local reversal on the cts in certain sections, globally the saline infusion reversed the effects of NE on the CL.

The effect of parasympathetic stimulation was produced in our experiments by infusing ACh into the right coronary artery. Previous studies have shown that, in the absence of drug, ACh shortens the wavelength in the atria by 30-40% mainly because of refractory period shortening [34]. During AFI, vagal stimulation reduces considerably the CL and ERP [32] and ACh shortens the monophasic action potential in the canine atrium [35]. Furthermore, an infusion of ACh into the right coronary artery during AFI has been shown to significantly shorten the CL, ERP, and therefore to lengthen the EG and especially the fully excitable portion. These effects were quantitatively greater than seen with NE infusion [33]. However, in our experiments in the presence of PPF, ACh did not affect the CL, ERP nor the EG. Nevertheless, the fully excitable region ahead of the wavefront was slightly increased (even when expressed as a percentage of the EG). This suggests a significant anticholinergic effect of PPF.

The addition of ACh had a heterogeneous effect on the ct and did not slow or accelerate the same regions as saline+PPF. This is interesting because ACh+PPF did not modify the CL when compared with saline+PPF. Therefore, the cts in the different sections were not affected in the same way but reached the same end result. The regions of slowed conduction were different from one dog to another and did not correspond to any fixed anatomical reference point.

A number of reports exist [36-38] which describe the occurrence of AFl with 1:1 AV conduction. This is a recognized atrial proarrhythmic effect of PPF therapy. It has been explained to directly result from the decrease in AFl rate produced by class IC use-dependent sodium channel blockade and decrease in wavefront velocity. The contribution of cholinergic blocking effects of PPF on the A-V node have not been cited as contributing to facilitated 1:1 A-V node conduction. However, previous studies have demonstrated that PPF has a significant vagolytic effect on sinus nodal automaticity in patients [39] and in dogs [40]. A vagolytic activity has also been demonstrated in conscious intact dogs on sinus rate and sinus recovery time as well as in AV-blocked dogs [41] and also in AV-blocked dogs given atropine before PPF [42]. Inomata et al. [43] have confirmed an anti-ACh effect of PPF in guinea-pig atrial myocytes and suggested that the mechanism underlying this effect is by blockade of the ACh activated K⁺ channel in its open state rather than by interaction with the muscarinic receptor.

Prematurity effect

To assess the variation of the ct as a function of prematurity on PPF and with NE+PPF in each section of the circuit, the ct of the anterograde flutter beat produced by each premature stimulus was measured in each portion of the circuit. In all 6 dogs, the range of effective prematurity was large in the first one or two sections adjacent to the stimulation site in the direction of propagation. The same was also seen with saline+PPF and ACh+PPF, which concurs with our previous findings [23] that premature stimulation at one site does not predict the range of prematurity throughout the entire reentry circuit. When the region adjacent to the stimulation site was examined and expressed as a percentage, most curves were superimposed as previously seen when the RRCs were expressed as a percentage of the CL. This confirms that the RRC obtained at one site will only predict the EG obtained at the site adjacent to the stimulation and not for the entire reentry circuit.

Clinical implications

PPF does not eliminate the EG nor does it shorten the region of full excitability ahead of the wavefront in AFL. Therefore, the wavefront will continue to circulate albeit at a slower rate. Sympathetic stimulation in the presence of PPF slightly decreases the CL and ERP thus partly reversing the effects of PPF. However, the EG and the fully excitable portion do not increase with NE confirming significant beta-blocking properties of the parent drug. Exposure to ACh does not modify the CL, ERP nor the EG. This could be beneficial since

without drug the EG significantly increases with ACh [33] and could especially promote the continued circulation of the wavefront during flutter. This vagolytic property could hypothetically be of use in preventing paroxysmal vagal atrial fibrillation [44]. However, the anticholinergic effects of PPF could also be detrimental in atrial arrhythmias by increasing AV node conduction [41] and thereby accelerating the ventricular response to a 1:1 conduction [36,38]. The major metabolite of PPF, 5-hydroxypropafenone, possesses a similar potency of sodium channel blocking activity to the parent compound [45]. However, 5-hydroxy propafenone dissociates more slowly from inactivated sodium channels than PPF [46], and also has little beta-blocking properties [47]. PPF's incomplete beta-blocking properties along with its significant anticholinergic effects have important clinical significance which may lead to proarrhythmia. Concomitant A-V node blockade using beta-blockers or calcium channel blockers is therefore strongly recommended. Previous studies have demonstrated that the proarrhythmic effects due to the interactions with the autonomic nervous system by either class IA and IC antiarrhythmic drugs can be diminished by the coadministration of propranolol [48-50].

Limitations of the study

The Y-shaped lesion which is used in this AFl model significantly denervated the region of the reentry circuit [51]. Therefore, the neurotransmitters used in this study were infused into the right coronary artery supplying the region of reentry. This has been demonstrated

by methylene blue injection which was distributed to the right atrium including the region of the reentry circuit above the tricuspid valve [33]. However, the ACh and NE infusions did not necessarily reproduce the synaptic cleft concentrations which occur with the stimulation of the autonomic nervous system. Han and Moe [52] have described NE to be more uniformly distributed during intravenous infusion than during nerve stimulation. Therefore, autonomic fibres may be nonhomogeneously distributed in the atrium and the effects observed during the NE and ACh infusion do not reproduce quantitatively the effects of autonomic activity.

At therapeutic doses the functional relative blocking potency of orally administered PPF is close to one-quarter that of propranolol [53]. Since the metabolite, 5-hydroxy propafenone, also possesses sodium channel blocking properties but not beta-blocking properties characteristic of the parent compound, our data using IV PPF which for the duration of the experiment is not significantly metabolised likely demonstrates stronger beta-blocking properties than when administered orally.

Acknowledgements: The authors wish to thank Pierre Rocque, Philippe Comtois and Pierre Fortier for the excellent technical help.

References:

1. Ranger S, Talajic M, Lemery R, Roy D, Nattel S. Amplification of flecainide-induced ventricular conduction slowing by exercise. *Circulation* 1989; 79: 1000-1006.
2. Cappato R, Alboni P, Codeca L, Guardigli G, Toselli T, Antonioli GE. Direct and autonomically mediated effects of oral quinidine on RR-QT relation after an abrupt increase in heart rate. *J Am Coll Cardiol* 1993; 22(1): 99-105.
3. Morady F, Kou WH, Kadish AH, Nelson SD, Toivonen LK, Kushner JA et al. Antagonism of quinidine's electrophysiologic effects by epinephrine in patients with ventricular tachycardia. *J Am Coll Cardiol* 1988; 12: 388-94.
4. Jazayeri MR, Vanwyhe G, Avitall B, McKinnie J, Tchou P, Akhtar M. Isoproterenol reversal of antiarrhythmic effects in patients with inducible sustained ventricular tachyarrhythmias. *J Am Coll Cardiol* 1989; 14: 705-11.
5. Calkins H, Sousa J, El-Atassi R, Schmaltz S, Kadish A, Morady F. Reversal of antiarrhythmic drug effects by epinephrine: quinidine versus amiodarone. *J Am Coll Cardiol* 1992; 19: 347-52.

6. Markel ML, Miles WM, Luck JC, Klein LS, Prystowsky EN. Differential effects of isoproterenol on sustained ventricular tachycardia before and during procainamide and quinidine antiarrhythmic drug therapy. *Circulation* 1993; 87: 783-792.

7. Sager PT, Behboodikhah M, Frequency-dependent electrophysiologic effects of d,l-sotalol and quinidine and modulation by beta-adrenergic stimulation. *J Cardiovasc Electrophysiol* 1996, 7: 102-112.

8. Marchang H, Brachmann J, Karolyi L, Kubler W, Schols W. Isoproterenol specifically modulates reverse rate-dependent effects of d,l-sotalol, d-sotalol, and dofetilide. *J Cardiovasc Pharmacol* 2000; 35: 443-450.

9. Dongas J, Tchou P, Mahmud R, Lehmann MH, Denker S, Akhtar M. Catecholamine-mediated reversal of procainamide induced retrograde block in paroxysmal supraventricular tachycardias: possible cause of treatment failures (abstr). *Circulation* 1985; 72(suppl III): III-126.

10. Dubuc M, Kus T, Fromer M, Primeau R, Shenasa M. Reversibility of the electrophysiologic effects of antiarrhythmic drugs by isoproterenol in patients with paroxysmal supraventricular tachycardia (PSVT). *Circulation* 1987; 76(suppl IV): IV-69 (abstract).

11. Akhtar M, Niazi I, Naccarelli GV, Tchou P, Rinkenberger R, Dougherty AH, et al. Role of adrenergic stimulation by isoproterenol in reversal of effects of encainide in supraventricular tachycardia. *Am J Cardiol* 62(19): 45L-49L, 1988.
12. Niazi I, Naccarelli G, Dougherty A, Rinkenberger R, Tchou P, Akhtar M. Treatment of atrioventricular node reentrant tachycardia with encainide: reversal of drug effect with isoproterenol. *J Am Coll Cardiol* 13(4): 904-910, 1989.
13. Helmy I, Scheinman MM, Herre JM, Sharkey H, Griffin JC. Electrophysiologic effects of isoproterenol in patients with atrioventricular reentrant tachycardia treated with flecainide. *J Am Coll Cardiol* 1990; 16(7): 1649-1655.
14. Stambler BS, Wood MA, Ellenbogen KA. Pharmacologic alterations in human type I atrial flutter cycle length and monophasic action potential duration. Evidence of a fully excitable gap reentrant circuit. *J Am Coll Cardiol* 1996; 27 (2): 453-61.
15. Morady F, Kou WH, Kadish AH, Toivonen LK, Kushner JA, Schmaltz S. Epinephrine-induced reversal of verapamil's electrophysiologic and therapeutic effects in patients with paroxysmal supraventricular tachycardia. *Circ* 1989; 79: 783-790.
16. Vaughan Williams EM. A classification of antiarrhythmic actions reassessed after a decade of new drugs. *J Clin Pharmacology* 1984; 24(4): 129-147.

17. Dukes ID, and Vaughan Williams EM. The multiple modes of action of propafenone. *Eur Heart J* 1984; 5: 115-125.
18. Goy J-J, Metrailler J-C, Humair L, de Torrente A, Restoration of sinus rhythm in atrial fibrillation of recent onset using intravenous propafenone. *Am Heart J* 1991; 122(6):1788-90.
19. Manolis AS, Katsaros C, and Cokkinos DV. Electrophysiological and electropharmacological studies in pre-excitation syndromes: results with propafenone therapy and isoproterenol infusion testing. *Eur Heart J* 1992; 13: 1489-1495.
20. Rahme M, Feracci A, Kus T. Effects of D-Sotalol on excitable gap composition in canine atrial reentry tachycardia. *Pacing Clin Electrophys* 1995;18(Part II): 905(abstract).
21. Callans, D.J., Hook, B.G., Josephson, M.E., The mechanism of propafenone-induced slowing of ventricular tachycardia in man as defined by analysis of resetting response patterns. *PACE* 1991; 14(pt II): 2035-2041.
22. Frame LH, Page RL, Boyden PA, Fenoglio JJ Jr, Hoffman BF. Circus movement in the canine atrium around the tricuspid ring during experimental atrial flutter and during reentry in vitro. *Circulation* 1987; 76(5): 1155-1175.

23. Jalil E, Mensour B, Bouchard C, Vinet A, Kus T. Effects of propafenone on the spatio-temporal electrophysiological characteristics of the reentry circuit in a canine model of atrial flutter. (Submitted to *Cardiovasc Res*, 2001).

24. Frame LH, Page RL, Hoffman BF. Atrial reentry around an anatomic barrier with a partially refractory excitable gap. *Circ. Res.* 1986; 58:495-511.

25. Mensour B, Jalil E, Vinet A, Kus T. Influence of propafenone on resetting and termination of canine atrial flutter. *PACE* 2000; 23(8): 1200-1219.

26. Derakhchan K, Pagé P, Lambert C, Kus T. Effects of procainamide and propafenone on the composition of the excitable gap in canine atrial reentry tachycardia. *J Pharmacol Exp Ther* 1994; 270:47-54.

27. Campbell TJ. Sodium channel blockers. In: Singh BN, Dzau VJ, Vanhoutte PM, Woosley RL, eds. *Cardiovascular Pharmacology and Therapeutics*. Churchill Livingstone, New York, 1994:645-663.

28. Duan D, Fermini B, Nattel S. Potassium channel blocking properties of propafenone in rabbit atrial myocytes. *J Pharmacol Exp Ther* 1993; 264: 1113-1123.

29. Delpon E, Valenzuela C, Pérez O, Casis O, Tamargo J. Propafenone preferentially blocks the rapidly activating component of delayed rectifier K⁺ current in guinea pig ventricular myocytes. *Circ Res* 1995; 76(2): 223-235.
30. Gross GJ, Castle NA. Propafenone inhibition of human atrial myocyte repolarizing currents. *J Mol Cell Cardiol* 1998; 30: 783-793.
31. Govier WC, Mosal NC, Whittington P, Broom AH. Myocardial alpha and beta adrenergic receptors as demonstrated by atrial functional refractory-period changes. *J Pharmacol Exp Ther* 1966; 154(2): 255-263.
32. Yano K, Hirata T, Hirata M, Hano O, Matsumoto Y, Mitsuoka T, et al. Effects of sympathetic and parasympathetic stimulation on the induction of atrial flutter in dogs with aseptic pericarditis. *Jap Heart J* 1991; 32 : 811-825.
33. Rahme M, Jalil E, Laflamme M, Kus T. Effect of autonomic neurotransmitters on excitable gap composition in canine atrial flutter. *Can J Phys Pharmacol* 2001; 79: 13-17.
34. Rensma PL, Allessie MA, Lammers WJEP, Bonke FIM, Schlij MJ. Length of excitation wave and susceptibility to reentrant atrial arrhythmias in normal conscious dogs. *Circ Res* 1988; 62: 395-410.

35. Wu K-M, Ross S, Hoffman BF. Monophasic action potentials during reentrant atrial flutter in the dog: Effects of clofilium and acetylcholine. *J Cardiovasc Pharm* 1989; 13: 908-914.
36. Kauffmann R, Goich J, Parra C, Ayala A, Manzur F. Efficacy of propafenone in supraventricular arrhythmias. *Rev Med Chil* 1989; 117(4):401-5.
37. Botto GL, Bonini W, Broffoni T, Cappelletti G, Falcone C, Lombardi R, et al. Regular ventricular rhythms before conversion of recent onset atrial fibrillation to sinus rhythm. *Pacing Clin Electrophysiol* 1994; 17(11 Pt 2):2114-7.
38. El-Harari MB, Adams PC. Atrial flutter with 1:1 atrioventricular conduction caused by propafenone. *Pacing Clin Electrophysiol* 1998; 21(10):1999-2001.
39. Alboni P, Pirani R, Paparella N, Candini GC, Tomasi AM, Masoni A. A method for evaluating different modes of action of an antiarrhythmic drug in man. The effects of propafenone on sinus nodal functions. *Int J Cardiol* 1985; 7: 255-265.
40. Katoh T, Karagueuzian HS, Sugi K, Ohta M, Mandel WJ, Thomas P. Effects of propafenone on sinus nodal and ventricular automaticity: In vitro and in vivo correlation. *Am Heart J* 1987; 113: 941-952.

41. Boucher M, Chassaing C, Hamel J-D, Poirier J-M. Cardiac electrophysiological effects of propafenone and its 5-hydroxylated metabolite in the conscious dog. *Eur J Pharmacol* 1996;315: 171-177.
42. Li JH, Boucher M, Carpentier A, Duchêne-Marullaz P. Propafenone in the conscious dog with chronic atrioventricular block: Mechanisms of chronotropic cardiac effects and plasma concentration-response relationships. *J Cardiovasc Pharmacol* 1986; 8: 885-891.
43. Inomata N, Ohno T, Ishihara T, Akaike N. Antiarrhythmic agents act differently on the activation phase of the Ach-response in guinea-pig atrial myocytes. *Br J Pharmacol* 1993; 108: 111-115.
44. Coumel P. Fibrillation auriculaire paroxystique; le rôle du système nerveux autonome. *Arch Mal Coeur* 1994; 87 (III): 55-62.
45. Malfatto G, Zaza A, Forster M, Sadowick B, Danilo Jr P, Rosen MR. Electrophysiologic, inotropic and antiarrhythmic effects of propafenone, 5-hydroxypropafenone and N-depropylpropafenone. *J Pharmacol Exp Ther* 1988; 246(2): 419-26.

46. Rouet R, Libersa CC, Broly F, Caron JF, Adamantidis MM, Honore E, et al. Comparative electrophysiological effects of propafenone, 5-hydroxy-propafenone, and N-depropylpropafenone on guinea pig ventricular muscle fibers. *J Cardiovasc Pharmacol* 1989;14(4):577-84.
47. Lee JT, Kroemer HK, Silberstein DJ, Funck-Brentano C, Lineberry MD, Wood AJ et al. The role of genetically determined polymorphic drug metabolism in the beta-blockade produced by propafenone. *N Engl J Med* 1990; 322(25): 1764-1768.
48. Myerburg RJ, Kessler KM, Cox MM, Huikuri H, Terracall E, Interian A Jr, et al. Reversal of proarrhythmic effects of flecainide acetate and encainide hydrochloride by propranolol. *Circulation* 1989; 80: 1571-1579.
49. Friehling TD, Lipshutz H, Marinchak RA, Stohler JL, Kowey PR. Effectiveness of propranolol added to a type I antiarrhythmic agent for sustained ventricular tachycardia secondary to coronary artery disease. *Am J Cardiol* 1990; 65: 1328-1333.
50. Stramba-Badiale M, Lazzarotti M, Facchini M, Schwartz PJ. Malignant arrhythmias and acute myocardial ischemia: Interaction between flecainide and the autonomic nervous system. *Am Heart J* 1994; 28: 973-82.

51. Pagé P, Dandan N, Do QB, Cardinal R. The right atrial Y-shaped incision model of atrial flutter affects atrial vagal innervation. *Eur J of Cardiac Pacing and Electrophysiol* 1996; 6 (Suppl. 5): 31.

52. Han J, Moe GK. Nonuniform recovery of excitability in ventricular muscle. *Circ Res* 1964; 14: 44-60.

53. Vaughan Williams EM. Significance of classifying antiarrhythmic actions since the Cardiac Arrhythmia Suppression Trial. *J Clin Pharmacol* 1991; 31: 123-135.

Figure Legends:

Figure 1: The right posterior view of the heart. A Y-shaped anatomical barrier is produced (based on the model of Frame et al., 1986) extending from the superior to the inferior vena cava and to the tip of the right atrial appendage. Seven bipolar electrodes were inserted around the base of the right atrium for stimulating. Electrode position 1 is on the endocardial surface of the atria facing the aorta, whereas positions 2-7 are on the atrial endocardial surface below the incision. Subsequently, 16 bipolar electrodes were mounted on a belt placed around the right atrium for recording. Electrodes 1-8 were placed on the anterior surface and electrodes 9-16 positioned on the posterior surface of the right atrium facing the aorta. The dashed line represents the tricuspid annulus.

Figure 2: Epicardial bipolar recording during atrial flutter. A premature stimulus was introduced after every 20th beat of atrial flutter by an adjacent endocardial stimulating electrode. TT, atrial flutter cycle length; TS, coupling interval of the premature stimulus, ST1, return cycle; and R, response to the premature stimulus. At the recording electrode shown, a coupling interval (TS) of 116 ms was observed. The subsequent return cycle (ST1) was prolonged to 220 ms. Because TT1 (336 ms) was shorter than twice TT (352 ms) by at least twice the standard deviation of the atrial flutter cycle length (176 ms), reset of the tachycardia was considered to have occurred.

Figure 3: Method to approximate the measure of the coupling interval and return cycle at the stimulation site. SR, conduction time between the stimulation site and the site at which the premature beat was recorded (see Figure 2). The flat portion of the curve indicates the presence of fully excitable tissue through which the propagation time is the same as in a free running flutter (without premature stimuli) between the stimulating (S_E) and recording (R_E) electrodes. Extrapolating the value of the flat portion to the ordinate approximates τ , the time needed for the free running flutter to travel from S_E to R_E . The value τ is then subtracted from the overestimated return cycle (ST1 of Figure 2) and added to an underestimated coupling interval (TS of Figure 2) to correct the data for the conduction delay from S_E to R_E in order to construct the RRCs of Figure 4.

Figure 4: Effects of norepinephrine and acetylcholine on the reset-response curve during an infusion of propafenone. A) The RRC without drug consisted of a fully EG demonstrating partially and fully excitable tissue. Following 80 min of PPF infusion, the curve shifted upward and to the right, with a variable effect on the duration and composition of the EG. A simultaneous infusion of 15 $\mu\text{g}/\text{min}$ of NE significantly reversed the effects of PPF by shifting the curve downward and to the left without significantly affecting the composition of the EG. Replacing the NE with a saline infusion significantly shifted the curve upward and to the right without modulating the EG. ACh (3 $\mu\text{g}/\text{min}$) simultaneously infused with PPF did not significantly affect the RRC and therefore did not reverse the effects of the drug. However, a slight significant increase in the fully excitable portion was observed. B) The same RRCs as in A) expressed as a percentage of the cycle length (CL).

Atrial flutter cycle length \pm SD: + control (168 ± 0.21); • 80 min PPF (240 ± 0.59); * PPF + NE (200 ± 0.72); ° PPF + saline (253 ± 0.65); x PPF + ACh (257 ± 1.6).

Figure 5: Inhomogeneity of propafenone (PPF) effect on conduction time (ct) around the atrial flutter circuit in free running flutter. The conduction times between electrodes around the atrial flutter circuit were measured in the 6 dogs in which a 16 bipolar electrode recording belt was used. A plot describing the ratio of conduction times between electrodes on PPF alone (ctPPF), PPF+NE (ctPPF+NE), PPF+saline (ctPPF+saline) and PPF+ACh (ctPPF+ACh) over control conduction times (ctctrl) are shown at most electrode sites. Electrode sites were discarded as bystanders if the electrode's activation times were not consistent with a continuous progression of the activation front around the atrial flutter reentry circuit. In order to keep the control propagating time at an acceptable value, the conduction times were combined to create sections in which the total ct was above 5 ms.

A-F) - dogs 1 to 6

In all dogs, the prolongation of the CL on PPF was due to a marked increase in the ct localised in a few sections of the circuit. The regions of slowed conduction were clearly different from one dog to another and were not related to any specific anatomical structure.

° ctPPF alone/ctctrl; x ctPPF+NE/ctctrl; * ctPPF+saline; + ctPPF+ACh

Figure 6. Effect of prematurity on the different sections of the reentry circuit: The conduction time (ct) through each section of the anterograde flutter beat produced by premature stimulation was plotted against the effective local prematurity which was computed as the time between the anterograde front and the preceding free flutter beat at the entrance of each section. Section VI, which is adjacent to section I (the site of stimulation), has the greatest range of prematurity. The reentry schematic represents the different sections of the circuit and the direction of rotation. The premature stimulus (S) (bottom) was introduced between electrodes 4 and 5 of section I .

CHAPITRE V

**EXCITABLE GAP COMPOSITION IN THE
PRESENCE OF ANTIARRHYTHMIC DRUGS IN
COMMON HUMAN ATRIAL FLUTTER**

EXCITABLE GAP COMPOSITION IN THE PRESENCE
OF ANTIARRHYTHMIC DRUGS IN COMMON HUMAN
ATRIAL FLUTTER

Elise Jalil, MSc, Boualem Mensour, PhD, Alain Vinet, PhD, and Teresa Kus, MD, PhD

Running title:

ANTIARRHYTHMIC DRUGS ON EXCITABLE GAP COMPOSITION IN ATRIAL
FLUTTER

The Research Centre of Sacré-Coeur Hospital, Montréal, Québec, Canada.

This research was supported by the Medical Research Council of Canada.

Address for correspondence:

Teresa Kus, MD, PhD

Sacré-Coeur Hospital Research Center

5400 Boulevard Gouin Ouest

Montréal, Québec, Canada

H4J 1C5

Tel.:(514) 338-2222 ext. 2571 Fax:(514) 338-2694

E-mail: kust@crhsc.umontreal.ca

SUMMARY

Recurrence of atrial flutter on antiarrhythmic drugs is frequently observed. To determine the reasons for drug inefficacy, the electrophysiological parameters of atrial flutter were studied in patients without drug, on sotalol, on amiodarone and on propafenone. Upright tilt in 3 of these patients was performed to determine the effects of sympathetic activation on the excitable gap composition. Atrial flutter recurrence on these drugs is associated with the continued presence of an excitable gap and fully excitable portion. Upright tilting accelerates atrial flutter with a variable effect on the excitable gap characteristics. These findings explain the persistent viability of the atrial flutter circuit despite drug therapy in these patients.

ABSTRACT

Background and objective: Recurrence of atrial flutter (AFI) on antiarrhythmic drugs is frequently observed. To determine the reasons for drug inefficacy, the electrophysiological parameters of AFI were studied in 8 patients without drug, 6 patients on sotalol (Sot), 8 patients on amiodarone (Amio) and 4 patients on propafenone (PPF) who presented to the electrophysiology laboratory for conversion of recurrent AFI by rapid atrial pacing. Upright tilt was performed in 3 of these patients to determine the effects of sympathetic activation and vagal withdrawal on the excitable gap (EG) composition. **Methods:** . The duration and composition of the excitable gap (EG) were determined by premature stimuli delivered during AFI through a quadripolar electrode catheter positioned in the right atrium in the pathway of the AFI circuit. In 3 patients referred for ablation, this was done using a duodecapolar catheter. Studies were done at rest (supine) and with upright tilt (70°). **Results:** The EG in AFI recurring on Sot (80 ± 25 ms), Amio (78 ± 13 ms) and PPF (83 ± 26 ms) was not significantly different from that without drug (88 ± 14 ms). Furthermore, a fully excitable portion was present whether with or without drug. An upright tilt decreased the AFI CL in all 3 patients but produced variable effects on the EG and fully excitable portion. **Conclusions:** AFI recurrence on Amio, PPF or Sot is associated with the continued presence of an EG and fully excitable portion. Upright tilting accelerates the atrial flutter with a variable effect on the EG and fully excitable portion. These findings explain the persistent viability of the AFI circuit despite drug therapy in these patients.

KEY WORDS: atrial flutter, antiarrhythmia agents, re-entry

Introduction

Common (type I) human atrial flutter (AFl) is due to a macroreentrant circuit in the right atrium (1-3) with a counterclockwise reentrant wavefront (1). The wavefront proceeds in a lateral to septal direction along the isthmus of tissue between the inferior vena cava and tricuspid valve, passes between the tricuspid annulus and Eustachian ridge, and then propagates up the septum in a caudocranial direction to return to the isthmus via the lateral atrial wall (4).

The excitable gap (EG) represents the portion of the reentry circuit that has partially and possibly fully recovered excitability. It is measured by the reset-response method, which consists of the introduction of a premature stimulus during AFl. This premature beat interacts with the reentry circuit, causing a pause that is not fully compensatory (5).

The resetting technique was first used to determine the EG in human ventricular tachycardia (6-11) usually slowed by antiarrhythmic drug. In common human AFl, a fully EG has been demonstrated in the absence of antiarrhythmic drug (12) and with the administration of procainamide (13).

Recurrence of AFl on antiarrhythmic drugs is frequently observed. To determine the reasons for drug inefficacy, the electrophysiological parameters of AFl were studied in patients without drug, on Sotalol (Sot), on Amiodarone (Amio) and on Propafenone (PPF) who presented to the electrophysiology laboratory for conversion of recurrent AFl by rapid atrial pacing.

Further, we also examine in 3 patients the effects of upright tilting on the electrophysiological parameters of AFI in order to determine if sympathetic activation and vagal withdrawal influence the duration and properties of the EG in common human AFI.

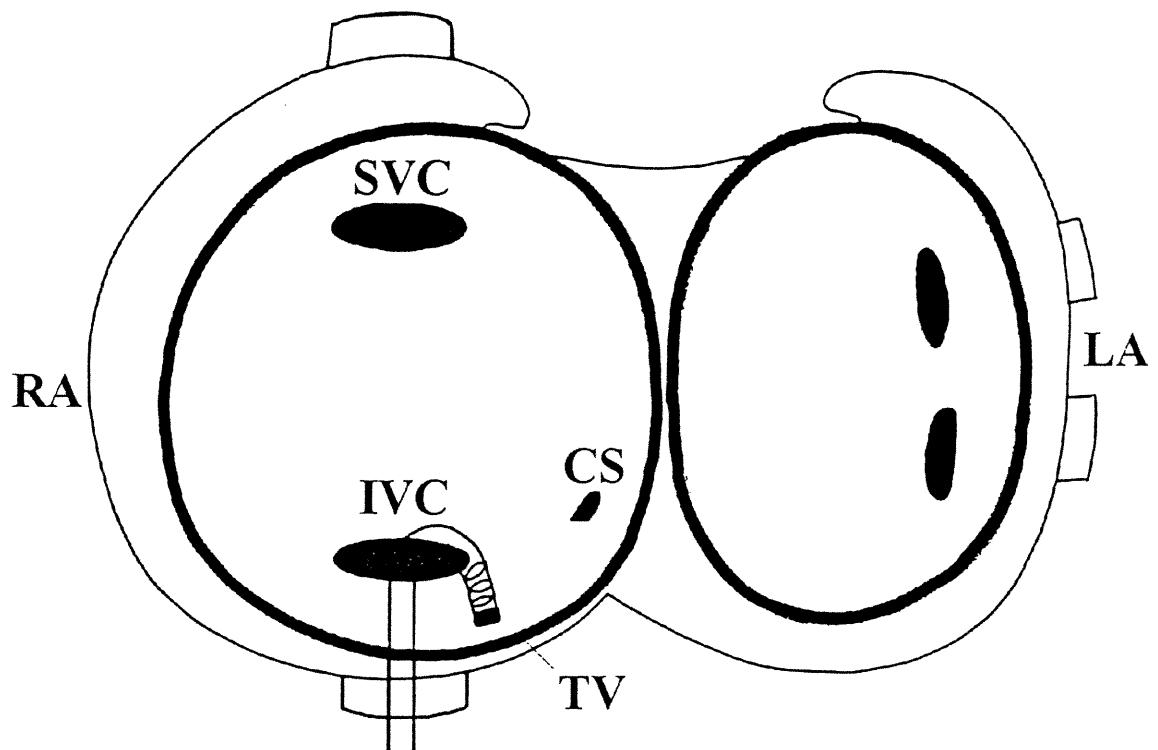
Methods

Population

Twenty six patients (21 men and 5 women; mean age 65 ± 14 years) with common (type I) AFI were referred to the invasive electrophysiological laboratory, either for clinically indicated catheter overdrive pacing (23 patients) or ablation of the AFI isthmus (patients 5, 13 and 20; Table 1). As shown in Table 1, cardiac pathologies included coronary artery disease, sick sinus syndrome, mitral or aortic valve stenosis, arterial hypertension, cardiomyopathy and pericarditis. Informed consent was obtained according to usual clinical practice and the protocol was approved by the review committee of the Sacré-Coeur Hospital in Montreal (Quebec, Canada). A quadripolar electrode catheter with a deflectable tip (6 French (Cordis-Webster)) was inserted via the right femoral vein under local anaesthesia, and the tip was positioned in the right atrium at the AFI isthmus between the inferior vena cava and the tricuspid valve (Figure 1). In the 3 patients undergoing ablation, 3 catheters were inserted via the right femoral vein: a quadripolar electrode catheter at the apex of the right ventricle (6 French (Daig)), a duodecapolar catheter in the right atrium around the tricuspid valve (7 French (Daig)) and a radiofrequency ablation catheter with thermistor (7 French (Cordis Webster)) which was positioned at the isthmus between the inferior vena cava and the tricuspid valve.

TABLE 1 – Population characteristics

| Patient | Age | Sex | Antiarrhythmic Drug Therapy | Cardiac Diagnosis |
|---------|-----|-----|-----------------------------|---|
| 1 | 54 | M | none | Coronary artery disease |
| 2 | 73 | M | none | Sick sinus syndrome |
| 3 | 73 | M | none | Coronary artery disease |
| 4 | 72 | M | none | Arterial hypertension |
| 5 | 65 | M | none | None |
| 6 | 54 | M | none | Arterial hypertension |
| 7 | 54 | M | none | Mitral valve stenosis |
| 8 | 86 | F | none | None |
| 9 | 52 | M | Amiodarone | Sick sinus syndrome |
| 10 | 50 | M | Amiodarone | Coronary artery disease |
| 11 | 66 | M | Amiodarone | Mitral valve replacement |
| 12 | 50 | M | Amiodarone | Coronary artery disease |
| 13 | 53 | M | Amiodarone | Coronary artery disease |
| 14 | 80 | F | Amiodarone | Coronary artery disease, Arterial Hypertension, Valvular cardiomyopathy |
| 15 | 85 | F | Amiodarone | Aortic stenosis |
| 16 | 78 | M | Amiodarone | None |
| 17 | 39 | M | Propafenone | Pericarditis |
| 18 | 68 | M | Propafenone | Dilated cardiomyopathy |
| 19 | 63 | M | Propafenone | None |
| 20 | 78 | F | Propafenone | None |
| 21 | 37 | M | Sotalol | None |
| 22 | 72 | M | Sotalol | Arterial hypertension |
| 23 | 81 | M | Sotalol | Coronary artery disease |
| 24 | 65 | M | Sotalol | Coronary artery disease, Arterial hypertension |
| 25 | 54 | M | Sotalol | Arterial hypertension, Sick sinus syndrome, dilated cardiomyopathy |
| 26 | 78 | F | Sotalol | None |



- RA - Right Atrium
- LA - Left Atrium
- SVC - Superior Vena Cava
- IVC - Inferior Vena Cava
- CS - Coronary Sinus
- TV - Tricuspid Valve

FIGURE 1: Schematic representation of the atria in a left anterior oblique view, from the tricuspid (left) and mitral rings.

Measurement of Electrophysiological Parameters

The EG during AFI was determined by introducing a premature stimulus (through the distal electrode pair; pulse duration 2 ms, amplitude 2-5 mA) after every 20th spontaneous beat (detected by the proximal electrode pair). Initially, the premature stimulus was introduced late in diastole and the coupling interval was progressively decreased by 2-4 ms until the stimulus failed to capture. The interval between a spontaneous beat (T) and the premature stimulus (S) (interval T-S), the interval between the premature stimulus and the response (S-R) as well as the interval between the premature stimulus and the subsequent tachycardia beat ($S-T_1 = S-R + R-T_1$) were measured (peak to peak) as shown in Figure 2. Since the stimulation electrode was located at a different point in the circuit than the detecting electrode, the method introduced by Mensour et al. (14) was used to estimate the coupling interval and the return cycle at the stimulation site (S_E). As shown in Figure 3, the range of T-S values for which S-R falls on the line CL- T-S gives an estimate of τ , the time needed for the free flutter to travel from the stimulating to the detecting electrode. The coupling interval (CI) and the return cycle (RC) of the premature stimulus with respect to the last passage of the front at S_E are respectively estimated as $CI = \tau + T-S$ and $RC = S-T_1 - \tau$. Graphs describing the relationship (RC vs CI), or RRCs, were constructed using points for which $T-T_1 < 2 CL$ by more than twice the standard deviation of the AFI CL (i.e. when the premature beat reset the tachycardia). It was pointed out in Mensour et al. (14) that this criterion, standard in the literature, could sometimes lead to an underestimation of the duration of the EG. In fact, $T-T_1 = T-S + S-R + R-T_1$ for any stimulus applied in the EG. For a very premature stimulus capturing near the limit of the EG, it may happen that T-T1

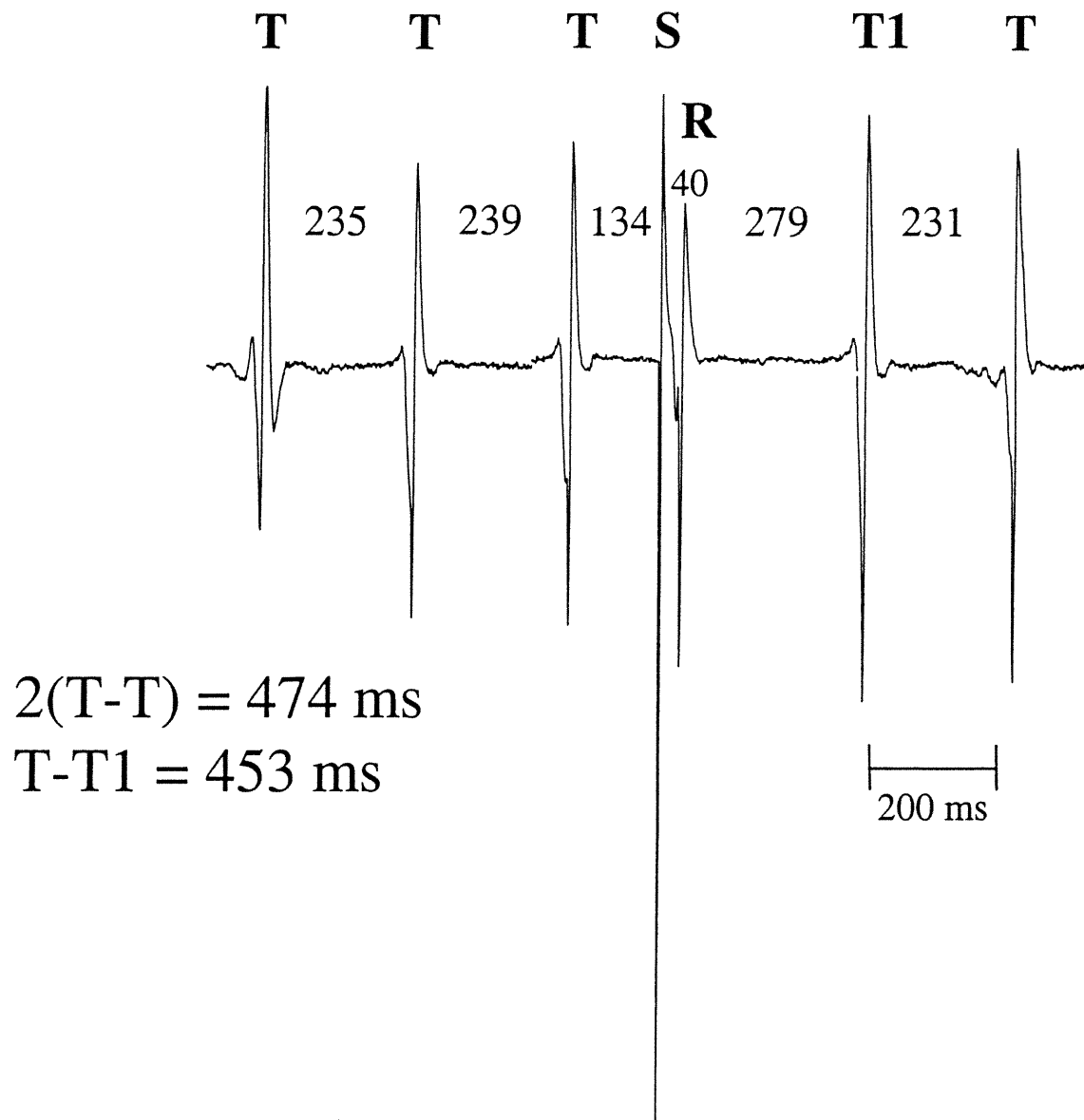


Figure 2: Bipolar recording during atrial flutter.

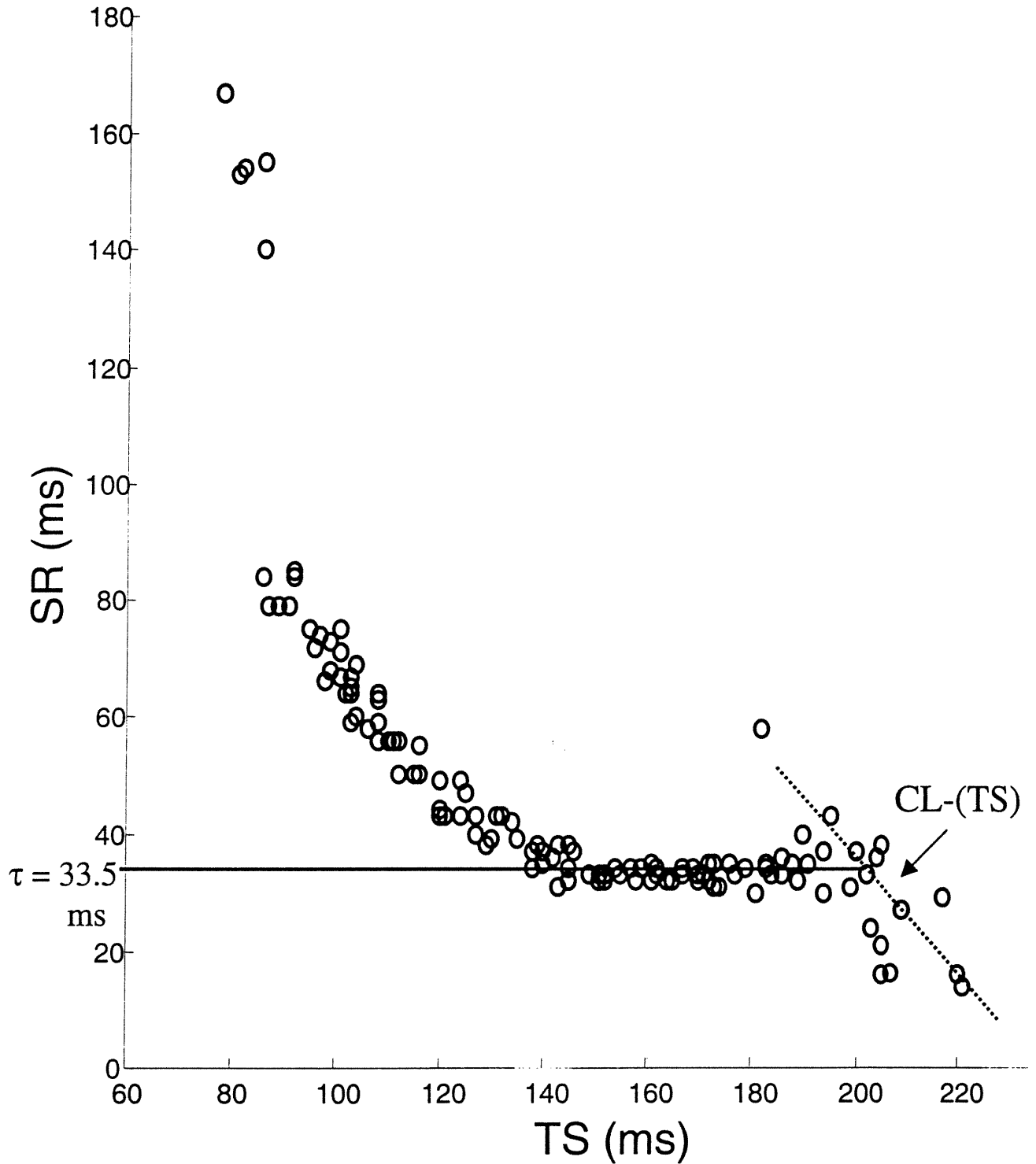


Figure 3: Method to approximate the measure of the coupling interval and return cycle at the stimulation site.

> 2*CL, because of significant conduction delay of the propagating stimulated wavefront. Nevertheless, we have decided to follow the standard criterion to be consistent with the method most commonly used in the literature. The flat portion of the EG composed of fully excitable tissue was estimated from that portion of the RRC where the RC values which were within one standard deviation (SD) of the CL. The ascending portion of the RRC where RC was greater than the CL +SD thus represented the portion of the EG composed of partially refractory tissue.

RRCs were determined using the same technique as described above by introducing premature stimuli through a duodecapolar catheter positioned in the right atrium for multiple electrode recording in the AFL circuit in patients referred to the electrophysiology service for ablation of AFL refractory to antiarrhythmic drugs. Studies were done at rest (supine) and after 10 minutes in the upright (70°) position to allow time for stabilization of sympathetic activation and vagal withdrawal. Three patients: one without antiarrhythmic drug, one on Amio and one on PPF at recommended therapeutic doses which had not prevented recurrence of AFL were studied after having obtained informed consent for testing in the upright position. Blood pressure (Ohmeda impedance digital plethysmograph [Ohmeda Medical Systems, Madison, WI, USA]) and heart rate were monitored continuously.

Data analysis

In all patients, the data was digitalised using a Cardio Lab 4.0 computerized recording

system (Prucka Engineering Inc., SugarLand, Texas) and all data were further analysed by a Silicon Graphics computer. The signals were manually timed using software developed by our group (MACT, Centre de Recherche, Hôpital du Sacré-Coeur de Montréal, Montréal, Québec, Canada).

Statistical analysis

The data are presented as means \pm SD. Comparison among the four groups of patients (Drug free, Amio, PPF and Sot) was done using one way ANOVA. An orthogonal contrast was tested: [Drug free group vs (Amio, Sot, PPF)], to assess global effects of drug. Since significant global difference was diagnosed by the ANOVA ($p < 0.05$), each group was compared to the Drug free group by the Student-Newman-Keuls test.

Results

Global effects of drug on the excitable gap characteristics and reset-response curve

The effects of Amio, Sot and PPF on AFI and EG characteristics compared to Drug free are shown in Table 2. The AFI CL was found to be significantly longer on drug than without (Ctrl vs [Sot, Amio, PPF], $p = 0.002$). Whether on Sot (267 ± 13 ms; $p = 0.033$), Amio (264 ± 30 ms; $p = 0.037$) or PPF (296 ± 36 ms; $p = 0.002$), AFI CL was longer in patients on drug than in those without antiarrhythmic therapy (231 ± 35 ms).

TABLE 2 – Effects of drug on atrial flutter and excitable gap parameters

| Drug | AFI (ms)† | ERP (ms)† | % ERP (%)† | EG (ms) | % EG (ms)† | FEP (ms) | % FEP (%)† |
|-------------|-----------|-----------|------------|-----------|------------|-----------|------------|
| Drug free | 231 ± 35 | 143 ± 38 | 61 ± 8 | 87.6 ± 14 | 38.2 ± 8 | 23.9 ± 16 | 27.4 ± 19 |
| Amiodarone | 264 ± 30* | 186 ± 25* | 71 ± 4* | 77.5 ± 13 | 29.4 ± 4* | 28.2 ± 12 | 36.2 ± 15 |
| Sotalolol | 267 ± 13* | 188 ± 26* | 70 ± 9* | 79.7 ± 25 | 29.7 ± 9* | 44.8 ± 20 | 57.2 ± 23* |
| Propafenone | 296 ± 36* | 213 ± 17* | 72 ± 5* | 83.4 ± 26 | 27.5 ± 5* | 34.3 ± 12 | 43.8 ± 20 |

AFI CL = Atrial Flutter Cycle Length

ERP = Effective Refractory Period

EG = Excitable Gap

FEP = Fully Excitable Portion

† ANOVA = p < 0.05

* p < 0.05 when compared with Drug free

A RRC was determined in all patients during AFI. Under drug free conditions, the atrial effective refractory period (ERP) during reentry (or the shortest coupling interval that resets the tachycardia during determination of the RRC) was 143 ± 38 ms resulting in an EG duration of 88 ± 14 ms or $38 \pm 10\%$ of the AFI CL. In the patients without antiarrhythmic therapy, the drug free EG was composed predominantly of partially excitable tissue, defined as the portion of the RRC in which resetting was increasing with greater prematurity. However, at long coupling intervals approaching the AFI CL, the RRC was flat over a range of 24 ± 16 ms or $27 \pm 19\%$ of the EG duration, indicating fully excitable tissue ahead of the wavefront.

An example of the RRC in 4 different patients (without drug, on Sot, PPF, or Amio) is shown in Figure 4. As shown in Table 2, patients on Sot (188 ± 26 ms; $p = 0.009$), Amio (186 ± 25 ms; $p = 0.007$) and PPF (213 ± 17 ms; $p = 0.001$) had a significantly longer ERP when compared to patients without drug (Drug free vs [Sot, Amio, PPF], $p < 0.001$). Because the increase in ERP were equal or greater than the increase of CL, the ERP were also significantly longer, when expressed as a percentage of the CL: Sot ($70 \pm 9\%$; $p = 0.025$), Amio ($71 \pm 4\%$; $p = 0.013$) and PPF (72 ± 5 ; $p = 0.017$) when compared with drug free patients ($61 \pm 8\%$; (Drug free vs [Sot, Amio, PPF], $p = 0.003$). As a consequence, the EG in all patients on drug was significantly shorter when expressed as a percentage of the CL (Sot ($30 \pm 9\%$; $p = 0.029$), Amio ($29 \pm 4\%$; $p = 0.016$) and PPF ($28 \pm 5\%$; $p = 0.018$)) when compared to patients without antiarrhythmic drug therapy ($38 \pm 8\%$) (Drug free vs [Sot, Amio, PPF], $p = 0.004$). However, the absolute duration of the EG remained

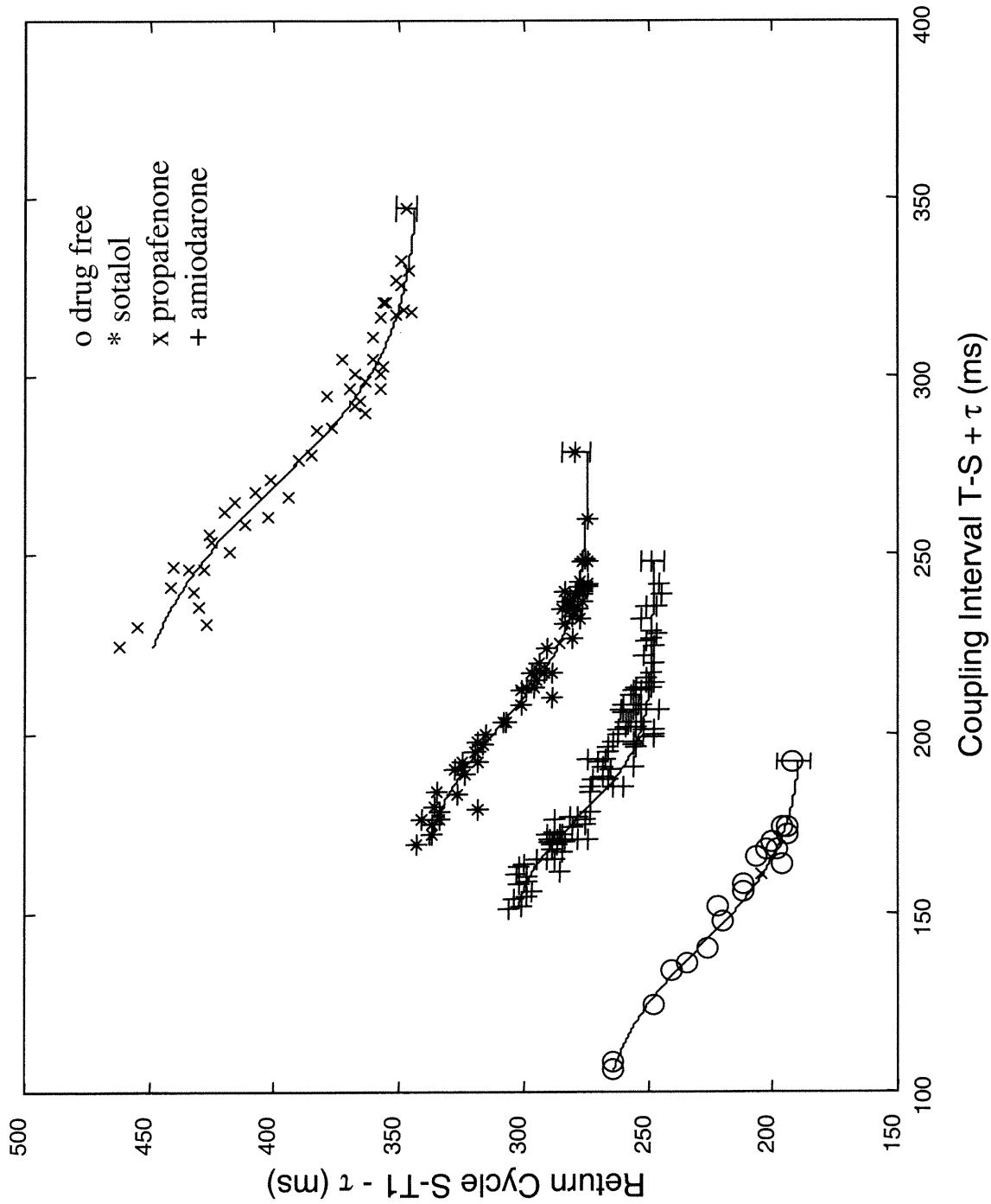


Figure 4: Effects of sotalol, propafenone and amiodarone on the reset-response curve

unchanged. In all patients, whether on drug or without, the EG was composed of both partially excitable tissue and a fully excitable portion ahead of the wavefront. This fully excitable portion when expressed as a percentage of the EG was even longer on drug when compared with drug free (Drug free vs [Sot, Amio, PPF], $p = 0.034$).

Effects of tilt on the excitable gap characteristics and reset-response curve

In 3 of these patients, one on Amio, one on PPF and one patient without antiarrhythmic therapy, an upright tilt (70°) which produces sympathetic activation and vagal withdrawal was performed (15) (Table 3). In all 3 patients, the CL decreased but there was little change in the ERP or EG in 2 patients (Drug free, Amio) but a marked change in ERP and EG in the patient on PPF as seen in Table 3.

Discussion

This study examined the composition of the EG in AFI in the presence of antiarrhythmic drug. The AFI CL and ERP were significantly longer in patients on Amio, Sot and PPF when compared to the patients without antiarrhythmic therapy. However, the EG was not significantly shorter but the difference became significant when expressed as a percentage of the CL. This is in accordance with clinical studies in ventricular tachycardia which have demonstrated that amiodarone slightly reduced but did not significantly change the EG (16-17). Callans et al. (18) have shown the presence of an EG in patients treated with PPF for

TABLE 3 - Effects of tilt on atrial flutter and excitable gap parameters

| | Control | Control (Tilt) | Amio | Amio (Tilt) | PPF | PPF (Tilt) |
|-------------|---------|----------------|---------|-------------|---------|------------|
| AFI CL (ms) | 235 ± 5 | 221 ± 3 | 261 ± 3 | 246 ± 3 | 263 ± 3 | 255 ± 3 |
| ERP (ms) | 120 | 124 | 198 | 190 | 188 | 109 |
| % ERP (%) | 51 | 56 | 76 | 77 | 71 | 42 |
| EG (ms) | 115 | 97 | 63 | 56 | 75 | 146 |
| % EG (%) | 49 | 44 | 24 | 23 | 28 | 57 |
| FEP (ms) | 23 | 16 | 31 | 39 | 32 | 15 |
| % FEP (%) | 20 | 17 | 49 | 70 | 43 | 10 |

AFI CL = Atrial Flutter Cycle Length

ERP = Effective Refractory Period

EG = Excitable Gap

FEP = Fully Excitable Portion

Amio = Amiodarone

PPF = Propafenone

ventricular tachycardia. PPF has also been shown to convert type II AF1 into type I by slowing conduction and therefore prolonging the AF1 CL. This facilitates capture and termination of AF1 due to the presence of an EG (19-20). In our study, only type I AF1 was seen and thus all patients had an EG.

We have previously shown in our laboratory (13), that procainamide significantly prolonged the AF1, ERP and EG without significantly affecting the fully excitable portion of the reentry circuit. In the present study, patients on antiarrhythmic drug had a flat portion which was significantly longer when expressed as a percentage of the EG compared to the control patients. The persistence of an EG with a fully excitable portion despite drug therapy explains the persistent viability of the AF1 circuit in these patients and is likely the reason for antiarrhythmic drug inefficacy.

More recently, class III drugs ibutilide and dofetilide have been found effective in the conversion of AF1 to sinus rhythm. Studies have shown that an intravenous infusion of ibutilide was more effective than intravenous sotalol in converting AF1 (70% vs 19%) or atrial fibrillation (44% vs 11%) to sinus rhythm (21). Norgaard et al. (22) studied the efficacy of dofetilide for acute termination of atrial fibrillation and AF1. Pharmacological conversion with dofetilide was seen in 64% of those with AF1 and in 24% of those with atrial fibrillation in contrast to 0% and 4% in the placebo group. However, both drugs dramatically prolonged ventricular repolarisation, and consequently the Q-T interval, associated with a small incidence of torsades de pointes (22-23).

In addition, advances in both electrophysiologic mapping and radiofrequency catheter ablation techniques have improved the efficacy of this therapeutic approach to about a 95% cure rate for patients with AF1 (3,24). Radiofrequency ablation of AF1 is safe and the highest success rate is achieved with radiofrequency energy applied in the isthmus between the inferior vena cava orifice and tricuspid valve (25-26). For these reasons, antiarrhythmic drug use as prevention therapy is decreasing at the expense of invasive ablation procedure.

Effect of tilt

Sympathetic stimulation has been shown to reverse the beneficial effects of conventional antiarrhythmic agents resulting in inefficacy or even proarrhythmia (27-28). Clinical studies have demonstrated that sodium channel blocking drug effects against ventricular tachycardia can be reversed by beta-adrenoceptor activation (29-33). Previous studies have shown that the AF1 cycle length without antiarrhythmic therapy (34) and the atrial fibrillation cycle length on PPF (15) can be shortened by passive upright tilting. In addition, isoproterenol has been shown to shorten the mean of 100 consecutive atrial fibrillation intervals in patients on PPF (35). In this study, sympathetic activation and vagal withdrawal by upright tilting was affected on the electrophysiological parameters of AF1 in 3 patients: one without drug, one on Amio and one on PPF. Our study has shown that tilting accelerated the AF1 CL in all 3 patients but decreased the ERP in only the patients on PPF, suggesting an interaction between the drug and the sympathetic activation. Sympathetic activation had a variable effect on the EG and the fully excitable portion ahead of the

wavefront. Therefore, changes in the electrophysiological parameters of AFL can occur with upright tilt.

Limitations of the study

In this study, comparison of EG characteristics was not done in the same patient without and in the presence of drug. Thus, we do not show the effect of drug on the EG but rather demonstrate the continued presence of fully EG when drug is ineffective in preventing AFL. In addition, it is impossible to generalize about the effects of upright tilt on the characteristics of the EG in the presence or absence of different antiarrhythmic drugs as only a very small number of patients were studied.

Measurement of the RRC was performed using an electrode catheter with the distal stimulation electrode positioned on the common pathway of the reentry circuit, which is the target site for current techniques of catheter ablation. Thus, we consider that premature stimuli were introduced directly into the reentry circuit. Therefore, conduction delay or block in tissue outside the circuit should not be a factor in our measurements. In the protocol, stimulations as well as measurements were done at one site, and the data were considered representative of the global properties of the circuit. The spatial inhomogeneity of the EG and resetting properties could not be evaluated (36,37).

References:

1. Feld GK, Fleck RP, Chen PS et al. Radiofrequency Catheter Ablation for the Treatment of Human Type I Atrial Flutter: Identification of a Critical Zone in the Reentrant Circuit by Endocardial Mapping Techniques. *Circulation* 1992; 86:1233-1240.
2. Cosio FG, Arribas F, López-Gil M, Goicolea A. Endocardial Catheter Mapping of Atrial Arrhythmias. In: Shenasa M, Borggreffe M, Breithardt G, eds. *Cardiac Mapping*, New York: Mount Kisco, Futura Publishing Co. Inc., 1993: 443-459.
3. Cosio, FG, Arribas, F, Lopez-Gil, M, Palacios, J. Atrial flutter mapping and ablation, I: studying atrial flutter mechanisms by mapping and entrainment. *Pacing Clin Electrophysiol* 1996; 19: 841-853.
4. Nakagawa, H, Lazzara, R, Khastgir, T et al. Role of the tricuspid annulus and the eustachian valve/ridge on atrial flutter: relevance to catheter ablation of the septal isthmus and a new technique for rapid identification of ablation success. *Circulation* 1996; 94: 407-424.
5. Strauss HC, Saroff AL, Bigger JT Jr, Giardina EGV. Premature atrial stimulation as a key to the understanding of sinoatrial conduction in man: presentation of data and critical review of the literature. *Circulation* 1973; XLVII: 86-93.

6. Almendral JM, Stamato NJ, Rosenthal ME, Marchlinski FE, Miller JM, Josephson ME. Resetting Response patterns during sustained ventricular tachycardia: relationship to the excitable gap. *Circulation* 1986; 74:722-730.

7. Rosenthal ME, Stamato NJ, Almendral JM et al. Influence of the site of stimulation on the resetting phenomenon in ventricular tachycardia. *Am J Cardiol* 1986; 58(10): 970-976.

8. Stamato NJ, Rosenthal ME, Almendral JM, Josephson ME. The Resetting Response of Ventricular Tachycardia to Single and Double Extrastimuli: Implications for an Excitable Gap. *Am J Cardiol* 1987; 60:596-601.

9. Stamato NJ, Frame LH, Rosenthal ME, Almendral JM, Gottlieb CD, Josephson ME. Procainamide-induced slowing of ventricular tachycardia with insights from analysis of resetting response patterns. *Am J Cardiol* 1989; 63: 1455-1461.

10. Callans DJ, Hook BG, Josephson ME. Comparison of resetting and entrainment of uniform sustained ventricular tachycardia. Further insights into the characteristics of the excitable gap. *Circulation* 1993; 87(4):1229-1238.

11. Sarter BH, Schwartzman D, Callans DJ, Gottlieb CD, Marchlinski FE. Bundle branch reentry ventricular tachycardia: an investigation of the circuit with resetting. *J Cardiovasc Electrophysiol* 1996; 7(11):1082-1085.

12. Della Bella P, Marenzi G, Tondo C et al. Usefulness of excitable gap and pattern of resetting in atrial flutter for determining reentry circuit location. *Am J Cardiol* 1991; 68(5):492-497.
13. Jalil E, Kus T, Le Franc P, Lebeau R, Molin F, Costi P. Effects of procainamide on the excitable gap composition in common human atrial flutter. *PACE* 1998; 21: 528-535.
14. Mensour B, Jalil E, Vinet A, Kus T. Influence of propafenone on resetting and termination of canine atrial flutter. *PACE* 2000; 23(8): 1200-1219.
15. Leather RA, Klein GJ, Murdoch C, Yee R, Leitch JW. The inefficacy of intravenous propafenone for rate control in atrial fibrillation. *Can J Cardiol* 1994; 10 (4): 433-438.
16. Naitoh N, Waschizuka T, Takahashi K, Aizawa Y. Effects of class I and III antiarrhythmic drugs on ventricular tachycardia-interrupting critical paced cycle length with rapid pacing. *Jpn Circ J* 1998; 62(4): 267-273.
17. Masotti CS, Pierangeli A. Na⁺ channel blockers vs class III antiarrhythmic drugs in treating sustained ventricular tachycardia: reversing and preventing as different electrophysiological mechanisms. *Panminerva Med* 1999; 41(4): 295-306.

18. Callans DJ, Hook BG, Josephson ME. The mechanism of propafenone-induced slowing of ventricular tachycardia in man as defined by analysis of resetting response patterns. PACE 1991; Vol 14(Part II): 2035-2041.

19. Doni F, Della Bella P, Kheir A et al. Atrial flutter termination by overdrive transesophageal pacing and the facilitating effect of oral propafenone. Am J Cardiol 1995; 76: 1243-1246.

20. Doni F, Staffiere E, Manfredi M et al. Type II Atrial flutter interruption with transesophageal pacing: Use of Propafenone and possible change of the substrate. PACE 1996; 19(Pt II): 1958-1961.

21. Vos MA, Golitsyn SR, Stangl K et al. Superiority of ibutilide (a new class III agent) over DL-sotalol in converting atrial flutter and atrial fibrillation. The Ibutilide/Sotalol Comparator Study Group. Heart 1998; 79(6): 568-575.

22. Norgaard BL, Wachtell K, Christensen PD et al. Efficacy and safety of intravenously administered dofetilide in acute termination of atrial fibrillation and flutter: a multicenter, randomized, double-blind, placebo-controlled trial. Danish Dofetilide in Atrial Fibrillation and Flutter Study Group. Am Heart J 1999; 137(6):92-995.

23. Stambler BS, Wood MA, Ellenbogen KA, Perry KT, Wakefield LK, VanderLugt JT. Efficacy and safety of repeated intravenous doses of ibutilide for rapid conversion of atrial flutter or fibrillation. Ibutilide Repeat Dose Study Investigators. *Circulation* 1996; 94(7): 1613-1621.

24. Cosio FG, Arribas F, Lopez-Gil M, Gonzalez HD. Atrial flutter mapping and ablation II. Radiofrequency ablation of atrial flutter circuits. *Pacing Clin Electrophysiol* 1996; 19(6): 965-975.

25. Fischer B, Haissaguerre M, Garrugues S et al. Radiofrequency catheter ablation of common atrial flutter in 80 patients. *J Am Coll Cardiol* 1995; 25: 1365-72.

26. Schwartzman D, Callans DJ, Gottlieb CD, Dillon SM, Movsowitz C, Marchlinski FE. Conduction block in the inferior vena caval-tricuspid valve isthmus: Association with outcome of radiofrequency ablation of type I atrial flutter. *J Am Coll Cardiol* 1996; 28: 1519-31.

27. Ranger S, Talajic M, Lemery R, Roy D, Nattel S. Amplification of flecainide-induced ventricular conduction slowing by exercise. *Circulation* 1989; 79: 1000-1006.

28. Cappato R, Alboni P, Codeca L, Guardigli G, Toselli T, Antonioli GE. Direct and autonomically mediated effects of oral quinidine on RR-QT relation after an abrupt increase in heart rate. *J Am Coll Cardiol* 1993; 22(1): 99-105.
29. Morady F, Kou WH, Kadish AH et al. Antagonism of quinidine's electrophysiologic effects by epinephrine in patients with ventricular tachycardia. *J Am Coll Cardiol* 1988; 12: 388-94.
30. Jazayeri MR, Vanwyhe G, Avitall B, McKinnie J, Tchou P, Akhtar M. Isoproterenol reversal of antiarrhythmic effects in patients with inducible sustained ventricular tachyarrhythmias. *J Am Coll Cardiol* 1989; 14: 705-11.
31. Calkins H, Sousa J, El-Atassi R, Schmaltz S, Kadish A, Morady F. Reversal of antiarrhythmic drug effects by epinephrine: quinidine versus amiodarone. *J Am Coll Cardiol* 1992; 19: 347-52.
32. Markel ML, Miles WM, Luck JC, Klein LS, Prystowsky EN. Differential effects of isoproterenol on sustained ventricular tachycardia before and during procainamide and quinidine antiarrhythmic drug therapy. *Circulation* 1993; 87: 783-792.

33. Sager PT, Behboodikhah M. Frequency-dependent electrophysiologic effects of d,l-sotalol and quinidine and modulation by beta-adrenergic stimulation. *J Cardiovasc Electrophysiol* 1996, 7: 102-112.
34. Waxman MB, Yao L, Cameron DA, Kirsh JA. Effects of posture, vasalva maneuver and respiration on atrial flutter rate: an effect mediated through cardiac volume. *J Am Coll Cardiol* 1991; 17: 1545-52.
35. Biffi M, Boriani G, Bronzetti G, Capucci A, Branzi A, Magnani B. Electrophysiological effects of flecainide and propafenone on atrial fibrillation cycle and relation with arrhythmia termination. *Heart* 1999; 82: 176-182.
36. Ingelmo C, Frame LH. Mechanism for site-dependent differences in the shape of the resetting response curve in fixed barrier reentry. *J Cardiovasc Electrophysiol* 2000; 11: 981-989.
37. Jalil E, Mensour B, Bouchard C, Vinet A, Kus T. Effects of propafenone on the spatio-temporal electrophysiological characteristics of the reentry circuit in a canine model of atrial flutter. (Submitted to *Cardiovasc Res*, 2001).

Figure legends:

Figure 1: Schematic representation of the atria in a left anterior oblique view, from the tricuspid (left) and mitral rings. A quadripolar electrode catheter was inserted via the right femoral vein under local anaesthesia, advanced to the right atrium through the inferior vena cava and the tip was positioned against the right atrial wall between the inferior vena cava and the tricuspid valve in the pathway of the reentry circuit.

Figure 2: Bipolar recording during atrial flutter. A premature stimulus was introduced after every 20th beat of atrial flutter by an adjacent endocardial stimulating electrode. TT, atrial flutter cycle length; TS, coupling interval of the premature stimulus, ST1, return cycle; and R, response to the premature stimulus. At the recording electrode shown, a coupling interval (TS) of 134 ms was observed. The subsequent return cycle (ST1) was prolonged to 319 ms. Because TT1 (453 ms) was shorter than twice TT (474 ms) by at least twice the standard deviation of the atrial flutter cycle length (235 ms), reset of the tachycardia was considered to have occurred.

Figure 3: Method to approximate the measure of the coupling interval and return cycle at the stimulation site. SR, conduction time between the stimulation site and the site at which the premature beat was recorded (see Figure 2). The flat portion of the curve indicates the presence of fully excitable tissue through which the propagation time is the same as in a free running flutter (without premature stimuli) between the stimulating and

recording electrodes. Extrapolating the value of the flat portion to the ordinate approximates τ , the time needed for the free running flutter to travel from the stimulating to the recording electrode. The value τ is then subtracted from the overestimated return cycle (ST1 of Figure 2) and added to an underestimated coupling interval (TS of Figure 2) to correct the data for the conduction delay from the stimulating to the recording electrode in order to construct the RRCs of Figure 4.

Figure 4: Effects of sotalol, propafenone and amiodarone on the reset-response curve.

The reset-response curve without drug consisted of a fully EG demonstrating partially and fully excitable tissue. The reset-response curve on all 3 drugs were shifted upward and to the right when compared with the drug free curve. Atrial flutter cycle length \pm SD: o Drug free (192 ± 4.0); * sotalol (279 ± 3.5); x propafenone (347 ± 2.3); + amiodarone (248 ± 2.7).

CHAPITRE VI

DISCUSSION ET CONCLUSION

DISCUSSION ET CONCLUSION

Propriétés électrophysiologiques du circuit de flutter avec la méthode du "reset-response"

Le flutter auriculaire chez l'humain est parmi les arythmies les plus difficiles à contrôler avec des thérapies pharmacologiques. La réentrée est le mécanisme de cette arythmie. Pour améliorer l'efficacité des médicaments antiarythmiques, il faut établir les caractéristiques du circuit de réentrée. Les propriétés électrophysiologiques du circuit du flutter auriculaire peuvent être caractérisées par la méthode de "resetting", qui consiste à introduire une ou plusieurs stimulations pour perturber la tachycardie. Le "resetting" a été utilisé dans les préparations in vitro de tachycardie ventriculaire soutenue (Bernstein et Frame, 1990), dans des modèles de flutter auriculaire chez des animaux (Frame et coll., 1986; Frame et coll., 1987; Derackchan et coll., 1994; Fei et coll., 1996; Jalil et coll., 1997) et aussi chez l'humain (Almendral et coll., 1986a; Almendral et coll., 1986b; Stamato et coll., 1989; Arenal et coll., 1992; Callans et coll., 1993; Callans et coll., 1996; Callans et coll., 1997; Jalil et coll., 1998).

Nos études ont démontré que de meilleures estimations de la période réfractaire effective, du créneau d'excitabilité et du tissu complètement excitable peuvent être obtenues en exprimant l'intervalle de couplage et le cycle de retour en référence au site de stimulation. Dans la méthode standard (Derackchan et coll., 1994; Jalil et coll., 1997; Jalil et coll., 1998), l'intervalle de couplage et le cycle de retour étaient exprimés en

référence à une électrode distale au site de stimulation (dans la direction de la propagation), de telle sorte que la période réfractaire effective était surestimée et le créneau d'excitabilité était sous-estimé. Un autre défaut de la méthode standard était que certains intervalles de couplage pouvaient être rejetés même s'ils provoquaient la formation de fronts antérogrades et rétrogrades parce qu'une compensation complète (i.e., $T-T1 \geq 2 CL$) s'y produisait. Notre analyse des courbes "reset-response a démontré que, dans certains cas, le "resetting" pouvait se faire à ces intervalles de couplage, mais être compensé dans d'autres portions du circuit.

Nous avons aussi démontré que le "resetting" n'était pas uniquement dû à l'effet de la prématurité (où le front de réentrée antérograde stimulé circule dans la queue du potentiel d'action du flutter) mais que l'effet de collision pouvait aussi contribuer au ralentissement de la propagation. Ce dernier effet résulte de la propagation du front de réentrée antérograde stimulé à travers du tissu encore partiellement réfractaire à cause du retard de repolarisation provoqué par la collision entre le front de réentrée rétrograde et le front du flutter original. L'analyse des temps de conduction entre les électrodes dans les différentes régions du circuit a révélé des ralentissements de la conduction qui pouvaient être provoqués par la prématurité, l'effet de collision ou l'hétérogénéité spatiale. Cette dernière peut provenir d'une inhomogénéité spatiale de la récupération d'excitabilité ou de variations de la courbure du front de réentrée dues à des limites anatomiques. Dans ce dernier cas, le front de réentrée, au lieu de suivre les bords de l'obstacle, peut se détacher près des bords adjacents et se propager autour d'un cercle, augmentant ainsi le temps de conduction local (Fast et Kleber, 1997). Nous avons attribué le délai de propagation dans

la région de la collision à l'effet de collision plutôt qu'à l'hétérogénéité intrinsèque du tissu.

Plusieurs observations ont appuyé cette hypothèse. Nous avons observé que la durée de la portion complètement excitable entre les sites de stimulation et de détection était prolongée par l'application d'un premier stimulus précédant le stimulus test, un effet généralement attribué au raccourcissement de la durée du potentiel d'action induit par le premier stimulus. Des études antérieures sur la tachycardie ventriculaire ont démontré une augmentation du créneau d'excitabilité avec des stimulations doubles et triples (Almendral et coll., 1986a; Almendral et coll., 1986b; Stamato et coll., 1987). Dans ces études, le premier stimulus était toujours fixe et ne faisait pas de "reset" sur la tachycardie. Le rôle de ce stimulus était de permettre l'introduction d'un stimulus prématuré qui pouvait entrer dans le circuit pour faire un "reset" sur la tachycardie pour une gamme plus large d'intervalles de couplage. Cependant, nous avons observé que le ralentissement de la conduction dû à l'effet de la collision était augmenté par l'application d'un nombre croissant de stimulations, ce qui est n'est pas compatible avec les effets décrits par les groupes d'Almendral et coll. (1986a et 1986b) et Stamato et coll. (1987). Ceci suggère que la courbe "reset-response" d'une séquence de stimulations rapides ne peut pas être complètement prédite par une courbe "reset-response" établie avec une stimulation unique à cause à la fois de raccourcissement des potentiels d'action et de l'accumulation des effets de collision. Par ailleurs, nous avons aussi observé plusieurs cas d'arrêt de flutter par stimulation où le front antérograde produit par la stimulation s'arrêtait précisément dans la zone de collision. Des travaux menés par

certains de nos collègues ont montré que l'annihilation par effet de collision existait dans des modèles mathématiques uni et bi-dimensionnels de réentrée autour d'un obstacle et qu'elle pouvait se produire sur des intervalles de couplage entre stimuli beaucoup plus larges que ceux permettant l'arrêt par bloc unidirectionnel causé par des stimulations appliquées dans la fenêtre de vulnérabilité. Ceci pourrait ouvrir des avenues intéressantes pour la conception de méthodes de stimulation permettant l'arrêt du flutter avec un nombre minimal de stimuli.

Les courbes "reset-response" ont été utilisées jusqu'à présent pour estimer les caractéristiques globales du circuit de réentrée en clinique (Almendral et coll., 1986; Della Bella et coll., 1991; Jalil et coll., 1998) et dans les modèles expérimentaux (Frame et coll., 1986; Kus et coll., 1991, Jalil et coll., 1997). Des études antérieures ont démontré des différences dans la courbe "reset-response" qui dépendaient du site de stimulation chez l'humain (Callans et coll., 1996; Callans et coll., 1997) et dans la tachycardie ventriculaire chez le lapin (Boersma et coll., 1994) et chez le chien (Hanna et coll., 2001). Ingelmo et Frame (2000) ont démontré que la forme de la courbe "reset-response" était différente quand les stimuli étaient introduits de façon distale plutôt qu'une localisation proximale au site de mesure dans des anneaux tricuspides in vitro de chien. Ces investigateurs ont démontré que la longueur de la portion complètement excitable de la courbe "reset-response" reflète avec précision la durée du créneau d'excitabilité pour les courbes obtenues à un site proximal, mais peut surestimer le créneau d'excitabilité des sites de stimulation distale.

Nous avons évalué la variation des temps de conduction en fonction de la prématurité dans chaque section du circuit. Le temps de conduction des battements antérogrades produits par chaque stimulus prématuré a été mesuré dans chaque portion du circuit. Dans les 6 chiens étudiés, la gamme de prématurité effective était large dans la première ou les deux premières sections adjacentes au site de stimulation dans la direction de la propagation. Les sections au-delà de ces portions avaient une gamme de prématurité de 10 ms ou moins et ne montraient que des changements minimes des temps de conduction (sauf pour les secteurs où la collision se produisait). Donc, nos études ont démontré que la courbe "reset-response" obtenue en stimulant à un site unique prédit très probablement le créneau d'excitabilité dans la région de la stimulation prématurée ou la section adjacente. Par contre, il peut ne pas prédire les caractéristiques globales du créneau d'excitabilité pour tout le circuit de réentrée, comme cela est implicitement assumé dans la plupart des études publiées (Frame et coll., 1986; Della Bella et coll., 1991; Jalil et al., 1998; Mensour et coll., 2000). Plusieurs études antérieures ont également montré que la fenêtre de "reset" ne mesure que le créneau d'excitabilité local et ne reflète pas le créneau d'excitabilité à n'importe quel point dans le circuit (Fei et coll., 1996; Peters et coll., 1998; Hanna et coll., 2001). Par contre, nos résultats suggèrent que, en divisant le circuit en 5-6 sections, des stimulations introduites à 3 ou 4 sites devraient être suffisantes pour fournir une représentation raisonnable des propriétés de "reset" autour du circuit.

Effets de la propafénone

La propafénone, qui est un antiarythmique de la classe IC, produit une diminution de la conductance au sodium mais inhibe également les canaux potassiques. Elle possède de légères propriétés bêta-bloquantes et calcium bloquantes (Dukes et Vaughan Williams, 1984). Nos études ont démontré que la propafénone prolonge significativement le cycle du flutter et sa période réfractaire effective. Il peut n'avoir que peu d'effets sur le créneau d'excitabilité (en enlevant les données qui correspondaient à une compensation complète (ex. $T-T1 = 2 CL$)) ou provoquer son augmentation. (en gardant les données qui correspondaient à une compensation complète, i.e., $T-T1 = 2 CL$). Par contre, ce médicament a un effet variable sur la portion complètement excitable en avant du front de réentrée, même après une infusion de 2 heures. Des études antérieures, dans le même modèle que le nôtre (Spinelli et Hoffman, 1989) et dans un modèle d'écrasement entre les deux veines caves (Inoue et coll., 1991), ont démontré une augmentation du créneau d'excitabilité avec la propafénone. Par contre, Derakhchan et coll. (1994), travaillant dans le même modèle que le nôtre, n'ont trouvé, aucun changement dans le créneau d'excitabilité sous propafénone.

La propafénone n'a pas d'effet sur le canal sodique dans l'état de repos mais se lie aux canaux sodiques dans l'état activé et inactivé (Honjo et coll., 1989). La propafénone a un effet tonique de bloc sur le canal sodique dû à sa dissociation lente du canal, qui se fait avec un demi-temps de récupération variant de 6.3 secondes (Koller et Franz, 1994) à 15.5 secondes (Kohlhardt et Seifert, 1980). Nos études démontrent que le cycle du flutter

et la période réfractaire effective augmentent de façon proportionnelle avec la propafénone, ce qui explique la persistance de tissu complètement excitable sous la propafénone. Cette augmentation de la période réfractaire effective pourrait être expliquée par un effet indirect de l'allongement du cycle qui tend à prolonger les potentiels d'action et donc résulter de l'action directe de classe I du médicament. L'augmentation de période réfractaire effective pourrait aussi être due à un effet direct de l'action tonique de la classe I du médicament qui réduit l'excitabilité. Une explication alternative serait que la propafénone inhibe le courant auriculaire transitoire sortant (I_{to}), le courant rectificateur interne (I_{K1}), le rectificateur externe (I_{Kr} et I_{Ks}) (Duan et coll., 1993; Delpon et coll., 1995), et aussi le rectificateur externe ultra-rapide (I_{kur}) (Gross et Castle, 1998). Toutes ces actions prolongent directement la durée du potentiel d'action et donc la période réfractaire effective. Pour obtenir une indication de l'effet direct classe I de la propafénone sur la période réfractaire (i.e. indépendante de la variation de cycle de la réentrée), nous avons analysé le "reset" maximum. Puisqu'un lien a été observé entre le "reset" maximum et la période réfractaire effective, le "reset" maximum a été corrigé pour la différence des périodes réfractaires effectives chez tous les chiens en utilisant une analyse de covariance. Une augmentation du "reset" maximum corrigé exprimé en pourcentage du cycle du flutter par la propafénone a été observée, indépendamment de ses effets sur les périodes réfractaires effectives. Nous avons interprété ce résultat comme étant un effet classe I du médicament sur le resetting, indépendamment de son effet sur le cycle du flutter et sur les variations de durée du potentiel d'action qui lui sont associés. Cet effet classe I contribue sûrement à la prolongation des périodes réfractaires effectives du tissu auriculaire.

Il a été démontré que la propafénone peut soit diminuer la conduction dans un circuit de tachycardie ventriculaire inchangé ou soit rallonger les barrières du circuit sans modifier le point de sortie du circuit (Callans et coll., 1991). Notre étude a examiné les caractéristiques spatiales des effets de la propafénone en analysant les temps de conduction entre les sites d'électrodes en absence de médicament, et après 60 min et 120 min d'infusion de la propafénone. La prolongation du cycle est en grande partie due à une augmentation des temps de conduction localisés surtout dans une ou deux sections du circuit de réentrée. Ceci démontre que l'effet tonique de la propafénone est inhomogène dans l'espace. Chez un chien, la section dans laquelle la conduction était ralentie par la propafénone est restée la même, peu importe la direction de rotation, suggérant que l'effet de la propafénone peut être caractéristique du substrat de réentrée. Cependant, les régions où il y avait un ralentissement de conduction ne correspondaient pas à un point de référence anatomique fixe. Ceci est intéressant parce que des études ont démontré que la vitesse de conduction autour d'un anneau tricuspide en utilisant le modèle de "Y" sur un cœur isolé de chien était relativement uniforme et qu'aucune région ne contribuait une fraction majeure des temps de conduction autour du circuit de réentrée (Frame et coll., 1987). Utilisant les schémas généraux d'activation obtenues par cartographie chez deux chiens, ces investigateurs ont démontré qu'il n'y avait pas de région localisée de conduction lente en absence de médicament, ni avec la lidocaïne, ni avec la métacholine (agoniste cholinergique). Ceci contredit l'hétérogénéité spatiale que nos études ont démontré avec la propafénone, et suggère que l'action homogénéité/hétérogénéité spatiale pourrait être spécifique à un médicament.

Gaspo et coll. (1997) ont démontré que l'activation auriculaire rapide cause une diminution dépendante du temps de la période réfractaire effective, de la vitesse de conduction, et de la longueur d'onde. Ceci, avec une augmentation régionale de l'hétérogénéité, fournit un substrat pour la fibrillation auriculaire. Des études antérieures ont démontré que la propafénone diminue la probabilité d'induire la fibrillation auriculaire (Connolly et Hoffert, 1989; Pritchett et coll., 1991), ce qui est compatible avec l'augmentation des périodes réfractaires effectives que ce médicament induit. Nous avons aussi observé dans nos préparations canines sous propafénone une baisse de la proportion des arrêts précédés par une période de fibrillations transitoires. Cependant, l'hétérogénéité spatiale de l'action de la propafénone devrait avoir l'effet opposé à moins que le médicament n'agisse spécifiquement pour contrebalancer l'hétérogénéité dans la récupération de l'excitation et/ou la repolarisation qui pourrait exister dans le substrat en condition contrôle. D'autres études seront nécessaires pour déterminer comment les sites d'actions préférentielles de la propafénone sont liés aux propriétés du substrat et sa susceptibilité à la fibrillation auriculaire en condition témoin.

Pour déterminer si les régions sensibles du circuit de réentrée à la propafénone peuvent être reliées à des caractéristiques du flutter auriculaire en absence de médicament, la variabilité dans les temps de conduction locaux dans la condition témoin a été analysée. Généralement, la variabilité des temps de conduction était inhomogène dans les différentes sections du circuit et n'était pas liée aux effets de la propafénone. Par contre, chez le chien qui avait le plus grand créneau d'excitabilité et aucune portion complètement excitable, le site avec la plus grande variation dans les temps de

conduction en condition de base était celui où il y avait le plus d'effet de la propafénone. Des grandes fluctuations du cycle du flutter local dans différentes parties du circuit avec la possibilité d'une instabilité locale intrinsèque peuvent expliquer les fluctuations dans les temps de conduction locaux. En effet, nos résultats ont démontré une corrélation entre le cycle local et les changements de battement en battement des temps de conduction locaux. Même si les fluctuations dans les temps de conduction avaient une plus grande corrélation avec l'effet de la propafénone quand la variabilité du cycle local était enlevée, la corrélation n'était pas significative avec l'exception du chien avec le plus grand créneau d'excitabilité et aucune portion plate. En général, il y avait une plus grande corrélation chez les chiens possédant un créneau d'excitabilité plus long et une portion horizontale plus courte. Ceci suggère que les sections démontrant une instabilité durant le flutter auriculaire sans stimulation pourraient prédire le site d'action du médicament seulement en absence de partie complètement excitable ou quand le créneau d'excitabilité est assez long. L'absence d'une portion horizontale indique que le potentiel d'action durant le flutter touche à la queue du potentiel d'action précédent, et donc que la propagation devient sensible à des petites fluctuations spontanées locales du cycle du flutter. Dans ce contexte, une région avec un peu de délai ou d'instabilité dans la récupération d'excitabilité peut être plus facilement détectée. En contraste, quand une portion horizontale est présente, les temps de conduction dans toutes les portions du circuit deviennent moins sensibles aux petites fluctuations spontanées du cycle. En principe, le délai ou l'instabilité de récupération pourrait être observé en analysant les propriétés de resetting de chaque portion du circuit, ce qui permettrait d'examiner s'ils peuvent prédire l'effet de la propafénone. En pratique, le resetting avec un seul site de

stimulation ne permet d'observer une plage importante de prématurité que dans les sections voisines au site de stimulation. Tel que nous l'avons énoncé plus tôt, un protocole employant de 3 à 5 sites de stimulation devrait permettre une évaluation de toutes les régions du circuit pour vérifier si nous pouvons prédire les sites d'action de la propafénone. La même observation peut-être faite pour l'ensemble de nos études.

Nous avons observé que l'arrêt du flutter suite à une ou plusieurs stimulations peut se produire 1) brusquement sans oscillation du cycle, 2) après une période de fluctuation du cycle, 3) après une période transitoire de fibrillation auriculaire, ou 4) à la suite d'un changement de direction. Dans les protocoles utilisant des séquences de stimulation rapide, la propafénone a diminué le risque de fibrillation auriculaire transitoire précédant un retour en rythme sinusal. La fréquence des arrêts du flutter auriculaire due à une dépression de conduction dans la région de la collision a été augmentée par la propafénone. Nous avons remarqué que la fibrillation transitoire avait tendance à se produire lorsque l'effet collision était petit et n'augmentait pas avec le cycle ou le nombre de stimulations. Cela suggère que l'évaluation de l'effet de la prématurité ainsi que l'effet de collision dans le flutter auriculaire pourraient être des indicateurs du risque d'induire une fibrillation auriculaire.

Le Système Nerveux Autonome

Bien que la durée et la composition du créneau d'excitabilité sont les facteurs majeurs permettant la réentrée, elles sont déterminées non seulement par la longueur du circuit et

ses caractéristiques électrophysiologiques mais aussi par des influences externes dont le système nerveux autonome. Dans nos études antérieures, nous avons examiné l'influence de la noradrénaline et de l'acétylcholine sur les caractéristiques électrophysiologiques du circuit de réentrée du flutter auriculaire chez le chien en absence de médicament antiarythmique. D'autres études ont démontré que la noradrénaline diminue significativement la période réfractaire effective dans les oreillettes (Govier et coll., 1966) et que la stimulation des nerfs sympathiques durant le flutter auriculaire diminue légèrement le cycle du flutter et la période réfractaire effective (Yano et coll., 1991). Rahme et coll. (2001) ont démontré que la noradrénaline diminue le cycle du flutter auriculaire et la période réfractaire effective, prolongeant ainsi le créneau d'excitabilité et le tissu complètement excitable en avant du front de réentrée. Ceci facilite la circulation continue du front de réentrée durant le flutter auriculaire.

Jusqu'à présent, peu d'études ont examiné l'interaction des systèmes parasympathiques et sympathiques avec les antiarythmiques dans la détermination des caractéristiques du créneau d'excitabilité dans le flutter auriculaire. Rahme et coll. (1997a,b) ont démontré que la noradrénaline et l'acétylcholine modifient la composition du créneau d'excitabilité dans le circuit de réentrée du flutter auriculaire et renversent les effets électrophysiologiques du d-sotalol sur le créneau d'excitabilité. Les interactions de la noradrénaline avec le dofétilide sur le créneau d'excitabilité ont également été étudiées dans le même modèle de flutter auriculaire chez le chien. Un autre antiarythmique de la classe III, le dofétilide, est un bloqueur spécifique des canaux potassiques I_{Kr} (Carmeliet, 1992). Le dofétilide seul a significativement prolongé le cycle du flutter, la période

réfractaire effective, la période réfractaire effective exprimé en pourcentage du cycle et a diminué le créneau d'excitabilité exprimé en pourcentage du cycle. Par contre, il y avait encore persistance du tissu complètement excitable en avant du front de réentrée. L'infusion de la noradrénaline a renversé les effets de la dofétilide en diminuant significativement le cycle du flutter et la période réfractaire effective, mais en augmentant le créneau d'excitabilité exprimé aussi bien en durée qu'en pourcentage du cycle. Comme pour le d-sotalol, la noradrénaline permettrait au flutter auriculaire de persister malgré une thérapie avec le dofétilide (résultats non publiés).

L'administration de la noradrénaline dans l'artère coronaire droite durant une infusion simultanée de la propafénone dans la présente étude a légèrement diminué le cycle du flutter et la période réfractaire effective, mais a eu un effet variable sur la portion complètement excitable. Puisque la diminution de la période réfractaire effective était le double de celle du cycle du flutter, la noradrénaline avait plus d'effet contre les actions de la classe III de la propafénone. Ceci a été confirmé par l'analyse du "reset" maximum (par covariance, pour avoir une indication de l'effet classe I direct) qui ne montrait qu'une légère augmentation non-significative du "reset" maximum exprimé en pourcentage du cycle pour la noradrénaline.

Les temps de conduction entre les sites d'électrodes avec la propafénone et avec une infusion subséquente de la noradrénaline ont été mesurés pour déterminer l'homogénéité spatiale. La diminution du cycle du flutter avec la noradrénaline en présence de la propafénone n'était pas due à une réduction homogène des temps de conduction dans

toutes les parties du circuit. En fait, les effets de la noradrénaline étaient localisés dans quelques portions du circuit. La propagation était même plus lente dans quelques sections du circuit. De plus, les sections où il y avait une action significative de la noradrénaline étaient différentes d'un chien à l'autre, et ne correspondaient pas aux sections où l'effet de la propafénone était le plus prononcé. Ces observations confirment les effets bêta-bloqueurs incomplets de la propafénone. En effet, il a été démontré que l'isoprotérénol chez les patients atteints du syndrome de pré-excitation peut renverser partiellement ou complètement les effets électrophysiologiques intraveineux (Goy et coll., 1991) et orale (Manolis et coll., 1992) de la propafénone en diminuant les périodes réfractaires effectives dans les faisceaux accessoires.

Quand l'influence sympathique a été enlevée par une infusion de salin, le cycle du flutter ainsi que la période réfractaire effective ont significativement augmenté pour atteindre des valeurs un peu plus élevées que sous la propafénone seule. Ceci est compatible avec la lente augmentation de la concentration plasmatique de la propafénone observée durant la deuxième heure d'infusion dans les études précédentes. Par contre, le renversement du cycle du flutter par le salin n'était pas associé à une augmentation homogène des temps de conduction dans toutes les sections du circuit de réentrée. Malgré le renversement incomplet des temps de conduction dans certaines sections, globalement, l'infusion de salin a renversé les effets de la noradrénaline sur le cycle du flutter auriculaire.

Dans nos expériences, la stimulation parasympathique a été produite en infusant l'acétylcholine dans l'artère coronaire droite. L'acétylcholine sans médicament

antiarythmique a significativement diminué le cycle du flutter auriculaire et la période réfractaire effective, prolongeant ainsi le créneau d'excitabilité et la portion du circuit caractérisée par du tissu complètement excitable. Les effets de l'acétylcholine ont excédé ceux de la noradrénaline, spécialement sur le tissu complètement excitable. Ceci tend à faciliter la circulation continue du front de réentrée durant le flutter auriculaire (Rahme et coll., 2001). Des études antérieures ont démontré, qu'en absence de médicament antiarythmique, l'acétylcholine réduit la longueur de l'onde dans l'oreillette de 30-40% et provoque donc une diminution des périodes réfractaires (Rensma et coll., 1988). Durant le flutter auriculaire, la stimulation vagale réduit considérablement le cycle du flutter de même que la période réfractaire effective (Yano et coll., 1991), et raccourcit le potentiel d'action monophasique dans l'oreillette de chien (Wu et coll., 1989). Par contre, dans nos expériences en présence de la propafénone, l'acétylcholine n'a pas affecté le cycle du flutter, la période réfractaire effective et le créneau d'excitabilité. Cependant, la région complètement excitable devant le front de réentrée a légèrement augmenté (même exprimé en pourcentage du créneau d'excitabilité). Ceci suggère un effet anticholinergique significatif de la propafénone.

L'addition d'acétylcholine avait un effet hétérogène sur les temps de conduction et n'a pas accéléré, ni ralenti les mêmes régions touchées par la propafénone. Ceci est intéressant parce que l'acétylcholine + propafénone n'a pas modifié le cycle du flutter en comparaison avec le salin + propafénone. Les temps de conduction dans les différentes sections n'étaient pas affectés de la même façon, pourtant le période globale restait la

même. Les régions de conduction ralentie ou accélérée étaient différentes d'un chien à l'autre et ne correspondaient pas à un point de référence anatomique fixe.

Plusieurs études ont rapporté des cas de flutter auriculaire où il y avait une conduction du nœud A-V 1 :1 (oreillette : ventricule) (Kauffman et coll., 1989; Botto et coll., 1994; El-Harari et Addams, 1998). Ceci est un effet proarythmique auriculaire reconnu de la thérapie sous propafénone, effet qui serait directement relié à une diminution de la fréquence de flutter produite par un bloqueur sodique de la classe IC en ralentissant la vitesse de front de réentrée. Les effets anticholinergiques de la propafénone sur le nœud AV et sur la facilitation de sa conduction n'ont pas été étudiés. Cependant, des études antérieures ont démontré que la propafénone a un effet vagolytique significatif sur l'automatisme du nœud sinusal chez les humains (Alboni et coll., 1985) et chez les chiens (Katoh et coll., 1987). Une activité vagolytique a aussi été sur la fréquence sinusale et le temps de récupération sinusale démontrée chez des chiens conscients (Li et coll., 1986a; Boucher et coll., 1996). Inomata et coll., (1993) ont confirmé un effet anti-cholinergique de la propafénone dans des myocytes auriculaires de cobayes. Ces investigateurs ont suggéré que le mécanisme sous-jacent à cet effet était un bloc des canaux potassiques activés par l'acétylcholine dans leur état ouvert plutôt qu'une interaction avec le récepteur muscarinique.

Implications cliniques

La propafénone n'élimine pas le créneau d'excitabilité et ne raccourci pas la région de tissu complètement excitable en avant du front de réentrée. Par conséquent, le front de

réentrée peut continuer de se propager, mais à une vitesse plus lente. La stimulation sympathique en présence de la propafénone a légèrement diminué le cycle du flutter et la période réfractaire effective. Elle a donc partiellement renversé les effets de la propafénone. Par contre, il y avait peu d'effet sur le créneau d'excitabilité et la portion complètement excitable avec la noradrénaline ce qui confirme un effet bêta-bloqueur significatif de la propafénone. L'acétylcholine n'a pas modifié le cycle du flutter, la période réfractaire effective, ni le créneau d'excitabilité. Ceci pourrait être bénéfique car sans médicament, le créneau d'excitabilité est significativement augmenté en présence d'acétylcholine, ce qui pourrait promouvoir la circulation continue du front de réentrée durant le flutter. Cette propriété vagolytique pourrait être utile pour la prévention de la fibrillation auriculaire paroxystique d'origine vagale (Coumel, 1994). Cependant, les effets anticholinergiques de la propafénone peuvent être aussi néfastes dans les arythmies auriculaires en augmentant la conduction du nœud A-V (Boucher et coll., 1996) accélérant ainsi la réponse ventriculaire à une conduction 1 :1 (Kauffman et coll., 1989; El-Harari et Adams, 1998). Le métabolite principal de la propafénone, 5-hydroxypropafénone, possède une puissance d'activité de bloqueur sodique similaire à la propafénone (Malfatto et coll., 1988). Par contre, la 5-hydroxy propafénone se dissocie plus lentement des canaux sodiques inactivés que la propafénone (Rouet et coll., 1989) et possède peu de propriétés bêta-bloquantes (Lee et coll., 1990). Les propriétés bêta-bloqueurs incomplètes de la propafénone ainsi que ses effets anticholinergiques significatifs ont une importance clinique qui peuvent être proarythmiques. Une thérapie concomitante pour bloquer le nœud A-V avec un bêta-bloqueur ou un bloqueur calcique est alors fortement recommandée. Des études antérieures ont démontré que les effets

proarythmiques dus à l'interaction du système nerveux autonome avec soit des antiarythmiques de la classe IA ou soit de la classe IC peuvent être diminués par une co-administration du propranolol (bêta-bloqueur) (Myerburg et coll., 1989; Friehling et coll., 1990; Stramba-Badiale et coll., 1994).

Étude Clinique

Le flutter auriculaire commun (type I) chez l'humain dépend d'un circuit de macroréentrée dans l'oreillette droite (Feld et coll., 1992; Cosio et coll., 1993; Cosio et coll., 1996) avec un front de réentrée circulant dans le sens anti-horaire (Feld et coll., 1992). Pour déterminer les raisons de l'inefficacité des médicaments antiarythmiques, nous avons étudié les paramètres électrophysiologiques du flutter auriculaire chez des patients ne prenant aucun médicament, prenant du sotalol, de l'amiodarone ou de la propafénone et qui se sont présentés au laboratoire d'électrophysiologie pour conversion en rythme sinusal par un entraînement rapide de l'oreillette droite par cathéter. Nous avons démontré que le cycle du flutter auriculaire et la période réfractaire effective sont significativement plus longs chez les patients prenant des médicaments. Par contre, la durée du créneau d'excitabilité n'était pas plus courte chez les patients sous médication, mais il couvrait une fraction significativement plus courte du cycle du flutter. Ceci est en accord avec des études cliniques sur des tachycardies ventriculaires qui ont démontré que l'amiodarone réduit légèrement le créneau d'excitabilité sans le modifier de façon significative (Naitoh et coll., 1998; Masotti et Pierangeli, 1999). Callans et coll., (1991) ont démontré que les patients traités avec la propafénone pour des tachycardies

ventriculaires possédaient un créneau d'excitabilité. Il a aussi été démontré que la propafénone convertit le flutter auriculaire de type II, qui ne possède pas ou peu de créneau d'excitabilité, en type I (commun). Il ralentit aussi la conduction, ce qui prolonge significativement le cycle du flutter. Cette conversion en flutter auriculaire commun facilite la capture et l'arrêt du flutter à cause de la présence du créneau d'excitabilité (Doni et coll., 1995; Doni et coll., 1996). Dans notre étude, chez tous nos patients le flutter auriculaire était du type I et possédait donc un créneau d'excitabilité.

Nous avons déjà démontré dans notre laboratoire (Jalil et coll., 1998) que la procainamide prolonge significativement le cycle du flutter, sa période réfractaire effective et son créneau d'excitabilité sans affecter la portion complètement excitable du circuit de réentrée. Dans cette étude, la fraction du créneau d'excitabilité couverte par la portion horizontale était significativement plus longue chez les patients sous médication. La persistance du créneau de même que la portion complètement excitable plus longue des patients sous médicament antiarythmique explique la persistance du circuit de réentrée et explique l'inefficacité des médicaments antiarythmiques dans ces cas.

Récemment, il a été démontré que l'ibutilide et le dofétilide (antiarythmiques de la classe III) sont efficaces pour effectuer la conversion du flutter auriculaire en rythme sinusal. Des études ont démontré qu'une infusion intraveineuse d'ibutilide était significativement plus efficace que le sotalol intraveineux pour convertir le flutter ou la fibrillation auriculaire en rythme sinusal (Vos et coll., 1998). Norgaard et coll. (1999) ont étudié l'efficacité du dofétilide pour la conversion de la fibrillation auriculaire et du flutter

auriculaire en rythme sinusal. La conversion pharmacologique a été observée dans 64% des patients en flutter et 24% des patients en fibrillation auriculaire traité avec le dofétilide par rapport à 0% et 4% dans le groupe placebo. Par contre, ces deux médicaments ont prolongé la repolarisation ventriculaire, et donc l'intervalle Q-T, et une légère incidence de torsades de pointes a été associée à l'usage de ces médicaments (Stambler et coll., 1996; Norgaard et coll., 1999).

À cause du succès partiel des antiarythmiques, d'autres thérapies ont été développées. Le progrès des techniques de cartographie électrophysiologique et d'ablation par cathéter à radiofréquence a amélioré l'efficacité de cette approche thérapeutique, pour atteindre un taux de guérison proche de 95% pour des patients en flutter auriculaire (Cosio et coll., 1996a; Cosio et coll., 1996b). L'ablation du flutter auriculaire par radiofréquence est sans danger et un taux de succès élevé est atteint si la lésion par radiofréquence est appliquée dans l'isthme entre l'orifice de la veine cave inférieure et la valve tricuspide (Fischer et coll., 1995; Schwartzman et coll., 1996). Par conséquent, l'usage de la thérapie préventive avec des médicaments antiarythmiques décroît en faveur des procédures d'ablation endocavitaires.

L'activation sympathique

Il a été démontré que la stimulation sympathique renverse les effets bénéfiques des médicaments antiarythmiques conventionnels, les rendant inefficaces et même proarythmiques (Ranger et coll., 1989; Cappato et coll., 1993). Des études cliniques ont

démontré que les effets des médicaments bloqueurs des canaux sodiques utilisés pour les tachycardies ventriculaires peuvent être renversés par l'activation des récepteurs bêta-adrénergiques (Morady et coll., 1988; Jazayeri et coll., 1989; Calkins et coll., 1992; Markel et coll., 1993; Sager and Behboodikhah, 1996). Des études antérieures ont démontré que le cycle du flutter auriculaire en absence de médicament antiarythmique (Waxman et coll., 1991) et le cycle de la fibrillation auriculaire en présence de la propafénone peuvent être raccourci par une position debout avec une table basculante. De plus, l'isoprotérénol peut raccourcir la moyenne de 100 intervalles consécutifs de fibrillation auriculaire chez des patients traités à la propafénone (Biffi et coll., 1999). Nous avons étudié chez trois patients les effets de l'activation sympathique et du retrait vagal par une position debout avec une table basculante. Un de ces patients ne prenait aucun médicament antiarythmique, un autre prenait de l'amiodarone et un dernier de la propafénone. En position debout, nous avons observé un raccourcissement du cycle du flutter chez les 3 patients, mais une diminution de la période réfractaire effective uniquement chez le patient ne prenant aucun médicament antiarythmique. Ceci suggère qu'il existe une interaction entre les médicaments et l'activation sympathique. L'activation sympathique avait un effet variable sur le créneau d'excitabilité et la portion complètement excitable en avant du front de réentrée. Donc, des changements dans les paramètres électrophysiologiques du flutter auriculaire peuvent se produire en position debout, et ceux-ci sont compatibles avec les effets observés dans nos préparations canines sous propafénone.

Les Limites des Études

Expérimentale

Notre première étude était limitée parce que, à cause du petit nombre des sites de détection et de leur distribution inégale autour du circuit, nous avons eu dans plusieurs cas des difficultés à distinguer l'effet de la prématurité et l'effet de la collision, ou à identifier le scénario se produisant lors d'arrêts du flutter. Pour diminuer cette ambiguïté, nous avons utilisé 16 sites d'enregistrement placés de façon uniforme autour du circuit. Dans certains cas, la mesure du créneau d'excitabilité et de la portion complètement excitable était difficile à cause de la variabilité du cycle du flutter et/ou des temps de conduction.

La lésion en forme de Y qui a été utilisée dans notre modèle de flutter auriculaire a dénervé significativement la région du circuit de réentrée (Pagé et coll., 1996). Par conséquent dans la troisième étude, les neurotransmetteurs ont été infusés dans l'artère coronaire droite qui alimente la région de la réentrée. Ceci a été vérifié en injectant du bleu méthylène qui s'est distribué dans l'oreillette droite incluant la région au-dessus de la valve tricuspide (Rahme et coll., 2001). Cependant, les infusions d'acétylcholine et de la noradrénaline n'ont pas nécessairement reproduit les concentrations apparaissant dans les synapses lors d'une stimulation du système nerveux autonome. Han et Moe (1964) ont décrit que la noradrénaline est plus uniforme durant une infusion intraveineuse qu'avec une stimulation nerveuse. Donc, les fibres autonomes peuvent être distribuées de façon non-homogène dans l'oreillette et les effets observés durant l'infusion de la

noradrénaline et l'acétylcholine ne reproduisent pas nécessairement les effets quantitatifs de l'activité autonome. L'inhomogénéité de l'effet de la propafénone sur les temps de conduction n'était pas due à l'écrasement de petites artères provoquant de l'ischémie dans la paroi auriculaire en faisant le "Y". En fait, le plus grand effet de la propafénone n'était pas dans la paroi antérieure mais plutôt dans les sections postérieures du circuit de la réentrée.

À des doses thérapeutiques, la puissance du bloc relatif fonctionnel de la propafénone par voie orale est environ 25% de celle du propranolol (Vaughan Williams, 1991). Pour la durée de nos expériences, la propafénone IV n'a pas été significativement métabolisée en son métabolite, 5-hydroxy propafénone, qui possède également les propriétés d'un bloqueur sodique mais non les caractéristiques bêta-bloquantes de la propafénone. Par conséquent, nos données démontrent sûrement des propriétés bêta-bloquantes plus prononcées qu'avec l'administration orale.

Clinique

Dans le quatrième article traitant de travaux menés chez des patients, la comparaison des caractéristiques du créneau d'excitabilité en absence et en présence de médicament antiarythmique ne pouvait pas être faite chez les mêmes patients. Par conséquent, nous ne démontrons pas l'effet des médicaments sur le créneau d'excitabilité mais nous démontrons plutôt la présence continue d'un créneau d'excitabilité et de tissu complètement excitable devant le front de réentrée quand les médicaments sont inefficaces pour la prévention du flutter. De plus, une généralisation des effets de la

position debout sur les caractéristiques du créneau d'excitabilité en présence ou absence de médicament antiarythmique est impossible à cause du petit nombre de patients étudiés.

Les mesures de la courbe "reset-response" ont été exécutées en utilisant un cathéter d'électrodes avec l'électrode distale de stimulation placé dans le chemin du circuit de réentrée, ce qui correspond au le site ciblé par les techniques courantes d'ablation par cathéter. Dans cette configuration, on admet généralement que les stimulations prématurées sont introduites directement dans le circuit de réentrée. Par conséquent, le délai de conduction ou un bloc dans le tissu à l'extérieur du circuit ne devraient pas affectés nos mesures. Dans le protocole, les stimulations et les enregistrements étaient mesurés seulement à un site et les données représentaient les propriétés globales du circuit. L'inhomogénéité spatiale du créneau d'excitabilité et des propriétés du "resetting" ne pouvait pas être évaluée (Ingelmo et Frame, 2000).

SOURCES
DOCUMENTAIRES

Références :

Alboni, P., Pirani, R., Paparella, N., Candini, G.C., Tomasi, A.M., Masoni, A., *A method for evaluating different modes of action of an antiarrhythmic drug in man. The effects of propafenone on sinus nodal functions.* Int J Cardiol 7: 255-265, 1985.

Al-Dashti, R., Sami, M., *Dofetilide : a new class III antiarrhythmic agent.* Can J Cardiol 17(1) : 63-67, 2001.

Allessie, M.A., Bonke, F.I.M., Schopman, F.J.G., *Circus movement in Rabbit Atrial Muscle as a mechanism of tachycardia: III. The leading circle concept: a new model of circus movement in cardiac tissue without the involvement of an anatomical obstacle.* Circ Res 1977; 41 (1): 9-18.

Allessie, M.A., Lammers, W.J.E.P., Bonke, F.I.M., Hollen, J., *Intraatrial reentry as a mechanism for atrial flutter induced by acetylcholine in rapid pacing in the dog.* Circulation 70 : 123-135, 1984.

Almendral J.M., Stamato N.J., Rosenthal M.E., Marchlinski F.E., Miller J.M., Josephson M.E., *Resetting Response patterns during sustained ventricular tachycardia: relationship to the excitable gap.* Circulation 74:722-730, 1986a.

Almendral J.M., Rosenthal M.E., Stamato N.J., Marchlinski F.E., Buxton, A.E., Frame, L.H., Miller J.M., Josephson M.E., *Analysis of the resetting phenomenon in sustained uniform ventricular tachycardia : Incidence and relation to termination.* J Am Coll Cardiol 8 : 294-300, 1986b.

Altschuld, R.A., Starling, R.C., Hamlin, R.L. Billman, G.E., Hensley, J., Castillo, L., Fertel, R.H., Hohl, C.M., Robitaille. P.M., Jones, L.R., et al., *Response of failing canine and human heart cells to β_2 -adrenergic stimulation.* Circulation 92 : 1612-1618, 1995.

Anderson, J.L., Prystowsky, E.N., *Sotalol: An important new antiarrhythmic.* Am Heart J 137(3): 388-409, 1999.

Antonaccio, M.J., Gomoll, A., *Pharmacology, pharmacodynamics and pharmacokinetics of sotalol.* Am J Cardiol 65: 12A-21A, 1990.

Antonaccio, M.J., Gomoll, A., *Pharmacologic basis of the antiarrhythmic and hemodynamic effects of sotalol.* Am J Cardiol 72: 27A-37A, 1993.

Ardell, J.L., *Structure and function of mammalian intrinsic cardiac neurones.* In: Armour, J.A., Ardell, J.L. (eds). Neurocardiology. New York, Oxford University Press, pp.95-114, 1994.

Ardell, J.L., Butler, C.K., Smith, F.M., Hopkins, D.A., Armour, J.A., *Activity of in vivo atrial and ventricular neurons in chronically decentralized canine hearts.* Am J Physiol 260: H713-H721, 1991.

Ardell, J.L., Randall, W.C., *Selective vagal innervation of sinoatrial and atrioventricular nodes in canine heart.* Am J Physiol 251: H764-H773, 1986.

Arenal, A., Almendral, J., San Roman, D., Delcan, J.L., Josephson, M.E., *Frequency and implications of resetting and entrainment with right atrial stimulation in atrial flutter.* Am J Cardiol 70: 1292-1298, 1992.

Armour, J.A., *Peripheral autonomic neuronal interactions in cardiac regulation.* In: Armour, J.A., Ardell, J.L. (Eds.), Neurocardiology. Oxford Univ. Press, New York, pp. 219-244, 1994.

Armour, J.A., Hopkins, D.A., *Activity of canine in situ left atrial ganglion neurons.* Am J Physiol 259: H1207-H1215, 1990.

Armour, J.A., Randall, W.C., *Functional anatomy of the canine cardiac nerves.* Acta Anat 91: 510-528, 1975.

Armour, J.A., Murphy, D.A., Yuan, B.-X., Macdonald, S., Hopkins, D.A., *Gross and microscopic anatomy of the human intrinsic cardiac nervous system.* Anat Rec 247: 247-298, 1997.

Bean, B.P., *Two kinds of calcium channels in canine atrial cells. Differences in kinetics, selectivity, and pharmacology.* J Gen Physiol 86(1): 1-30, 1985.

Bernstein R.C., Frame L.H., *Response to programmed stimulation in reentrant ventricular tachycardia around the canine mitral and aortic valves: an in vitro model (abstr).* JACC 9:127A, 1987.

Bernstein R.C., Frame L.H., *Ventricular reentry around a fixed barrier : Resetting with advancement in an in vitro model.* Circulation 81 : 267-280, 1990.

Bianconi, L., Boccadamo, R., Pappalardo, A., Gentili, C., Pistolese, M., *Effectiveness of intravenous propafenone for conversion of atrial fibrillation and flutter of recent onset.* Am J Cardiol 64(5):335-8, 1989.

Biffi, M., Boriani, G., Bronzetti, G., Capucci, A., Branzi, A., Magnani, B., *Electrophysiological effects of flecainide and propafenone on atrial fibrillation fibrillation cycle and relation with arrhythmia termination.* Heart 82: 176-182, 1999.

Boersma, L., Brugada, J., Kirchhof, C., Allessie, M., *Mapping of reset of anatomic and functional reentry in anisotropic rabbit ventricular myocardium.* Circulation 89(2): 852-862, 1994.

Boriani G, Strocchi E, Capucci A, Boschi S, Frabetti L, Ambrosioni E, Magnani B. *[Determination of oxidative phenotype in a sample population and correlation with the pharmacokinetics of propafenone].* *Cardiologia* 35(2):163-9, 1990.

Borthne., K., Haga, P., Langslet, A., Lindberg, H., Skomedal, T., Osnes, J.B. *Endogenous noradrenaline stimulates both α 1- and β - adrenoceptors in myocardium from children with congenital heart defects.* *J Mol Cell Cardiol* 27 : 693-699, 1995.

Botto, G.L., Bonini, W., Broffoni, T., Cappelletti, G., Falcone, C., Lombardi, R., Paulesu, A., Pedraglio, E., Ferrari, G., *Regular ventricular rhythms before conversion of recent onset atrial fibrillation to sinus rhythm.* *Pacing Clin Electrophysiol* 17(11 Pt 2):2114-7, 1994.

Boucher, M., Chassaing, C., Hamel, J.-D., Poirier, J.-M., *Cardiac electrophysiological effects of propafenone and its 5-hydroxylated metabolite in the conscious dog.* *Eur J Pharmacol* 315: 171-177, 1996.

Boyden P.A., Hoffman B.F., *The effects on atrial electrophysiology and structure of surgically induced right atrial enlargement in dogs.* *Circ Res* 49 : 1319-1331, 1981.

Boyden P.A., Frame L.H., Hoffman B.F., *Activation mapping of reentry around an anatomic barrier in the canine atrium - observations during entrainment and termination.* *Circulation* 79:406-416, 1989.

Boyden P.A., *Reentrant Excitation in the Atrium.* In: Dangman K.H., Miura D.S., eds. *Electrophysiology and Pharmacology of the Heart - A Clinical Guide.* Marcel Dekker Inc., New York, p. 239-250, 1991.

Brodde, O.-E. *β 1- and β 2- adrenoceptors in the human heart : Properties, function, and alterations in chronic heart failure.* *Pharmacol Rev* 43 : 203-242, 1991.

Brodde, O.-E., Michel, M.C., *Adrenergic and muscarinic receptors in the human heart.* *Am Soc Pharmacol Exp Ther* 51(4): 651-689, 1999.

Brooks, M.M., Gorkin, L., Schron, E.B., Wiklund, I., Champion, J., Ledingham, R.B., *Moricizine and quality of life in the Cardiac Arrhythmia Suppression Trial II (CAST II).* *Control Clin Trials* 15(6): 437-449, 1994.

Bryson, H.M., Palmer, K.J., Langtry, H.D., Fitton, A., *Propafenone: A reappraisal of its pharmacology, pharmacokinetics and therapeutic use in cardiac arrhythmias.* *Drugs* 45(1): 85-130, 1993.

Budde, T., Borggreffe, M., Podczec, A., Martinez-Rubio, A., Breithardt, G., *Acute and long-term efficacy of oral propafenone in patients with ventricular tachyarrhythmias.* *J Cardiovasc Pharmacol* 18(2):254-60, 1991.

Butler, C.K., Smith, F.M., Cardinal, R., Murphy, D.A., Hopkins, D.A., Armour, J.A., *Cardiac responses to electrical stimulation of discrete loci in canine atrial or ventricular ganglionated plexi.* *Am J Physiol* 259: H1365-H1373, 1990.

Calkins, H., Sousa, J., El-Atassi, R., Schmaltz, S., Kadish, A., Morady, F., *Reversal of antiarrhythmic drug effects by epinephrine: quinidine versus amiodarone.* *J Am Coll Cardiol* 19: 347-52, 1992.

Callans, D.J., Hook, B.G., Josephson, M.E., *The mechanism of propafenone-induced slowing of ventricular tachycardia in man as defined by analysis of resetting response patterns.* *PACE* 14(pt II): 2035-2041, 1991.

Callans D.J., Hook B.G., Josephson M.E., *Comparison of resetting and entrainment of uniform sustained ventricular tachycardia. Further insights into the characteristics of the excitable gap.* *Circulation*, 87(4):1229-1238, 1993.

Callans, D.J., Zardini, M., Gottlieb, C.D., Josephson, M.E., *The variable contribution of functional and anatomic barriers in human ventricular tachycardia: an analysis with resetting from two sites.* J Am Coll Cardiol 27(5): 1106-1111, 1996.

Callans, D.J., Schwartzman, D., Gottlieb, C.D., Dillon, S.M., Marchlinski, F.E., *Characterization of the excitable gap in human type I atrial flutter.* J Am Coll Cardiol 30: 1793-801, 1997.

Cappato, R., Alboni, P., Codeca, L., Guardigli, G., Toselli, T., Antonioli, G.E., *Direct and autonomically mediated effects of oral quinidine on RR-QT relation after an abrupt increase in heart rate.* J Am Coll Cardiol 22(1): 99-105, 1993.

Capucci, A., Gubelli, S., Carini, G., Frabetti, L., Magnani, B., *Pharmacologic cardioversion with propafenone of stable atrial fibrillation of recent onset.* G Ital Cardiol 17(11):975-82, 1987.

Capucci, A., Boriani, G., *Propafenone in the treatment of cardiac arrhythmias: a risk-benefit appraisal.* Drug Safety 12 (1): 55-72, 1995.

Capucci, A., Villani, G.Q., Aschieri, D., Piepoli, M., *Safety of oral propafenone in the conversion of recent onset atrial fibrillation to sinus rhythm: a prospective parallel placebo-controlled multicentre study.* Int J Cardiol 68(2):187-96, 1999.

Carerj, S., Cavalli, G., Magazu, A., Carerj, B., Cento, D., Arrigo, F., Oreto, G., Consolo, F., *Treatment of recent atrial fibrillation with intravenous propafenone.* Cardiologia 34(1):83-5, 1989.

Carmeliet, E., *Electrophysiologic and voltage clamp analysis of the effects of sotalol on isolated cardiac muscle and Purkinje fibers.* J Pharmacol Exp Ther 232: 817-825, 1985.

Carmeliet, E., J Pharmacol Exp Ther 262: 809-817, 1992. *Voltage- and time-dependent block of the delayed K⁺ current in cardiac myocytes by dofetilide.*

Carron, R., Perez-Vizcaino, F., Delpon, E., Tamargo, J., *Effects of propafenone on ^{45}Ca movements and contractile responses in vascular smooth muscle.* Br J Pharmacol 103(2): 1453-1457, 1991.

Charlier, R., *Cardiac actions in the dog of a new antagonist of adrenergic excitation which does not produce competitive blockade of adrenoceptors.* Br J Pharmacol 39: 668-674, 1970.

Colatsky, T.J., *The Sicilian Gambit and antiarrhythmic drug development.* Cardiovasc Res 26(6): 562-656, 1992.

Connolly, S.J., Kates, R.E., Lebsack, C.S., Echt, D.S., Mason, J.W., Winkle, R.A., *Clinical efficacy and electrophysiology of oral propafenone for ventricular tachycardia.* Am J Cardiol 52(10):1208-13, 1983.

Connolly, S.J., Mulji, A.S., Hoffert, D.L., Davis, C., Shragge, B.W., *Randomized placebo-controlled trial of propafenone for treatment of atrial tachyarrhythmias after cardiac surgery.* J Am Coll Cardiol 10(5):1145-8, 1987.

Connolly, S.J., Hoffert, D.L., *Usefulness of propafenone for recurrent paroxysmal atrial fibrillation.* Am J Cardiol 63: 114-116, 1989.

Connolly, S.J., Kates, R.E., Lebsack, C.S., Harrison, D.C., Winkle, R.A., *Clinical pharmacology of propafenone.* Circulation 68(3):589-96, 1993.

Cosio, F.G., Arribas, F., Lopez-Gil, M., Palacios, J., *Atrial flutter mapping and ablation, I: studying atrial flutter mechanisms by mapping and entrainment.* Pacing Clin Electrophysiol 19: 841-853, 1996a.

Cosio, F.G., Arribas, F., Lopez-Gil, M., Gonzalez, H.D., *Atrial flutter mapping and ablation II. Radiofrequency ablation of atrial flutter circuits.* Pacing Clin Electrophysiol 19(6): 965-975, 1996b.

Coumel, P., *Neurogenic and humoral influences of the autonomic nervous system in the determination of paroxysmal atrial fibrillation*. In: Attuel, P., Coumel, P., Janse, M.J. (eds), *The atrium in health and disease*, Futura publishing CO., Inc., Mount Kisco, NY. : 213-232, 1989.

Coumel, P., *Role of the autonomic nervous system in paroxysmal atrial fibrillation*. Clin Cardiol 13 : 209-212, 1990.

Coumel, P., *Neural aspects of paroxysmal atrial fibrillation*. In: Falk, R.H., Podrid, P.J. (eds), *Atrial fibrillation: Mechanisms and management*. Raven Press, Ltd., New York : 109-124, 1992.

Coumel, P., *Fibrillation auriculaire paroxystique; le rôle du système nerveux autonome*. Arch Mal Coeur 87 (III): 55-62, 1994.

Cragun, K.T., Johnson, S.B., Packer, D.L., *β -adrenergic augmentation of flecainide-induced conduction slowing in canine purkinje fibers*. Circulation 96:2701-2708, 1997.

Crijns H.J., de Langen C.D., Grandjean J.G., Bel K.J., Ebels T., Lie K.I., Wesseling H., *Sustained atrial flutter around the tricuspid valve in pigs: differentiation of procainamide (class IA) from flecainide (class IC) and their rate-dependent effects*. J Cardiovasc Pharmacol, 21(3):462-470, 1993.

Daoud, E.G., Morady, F.: *Pathophysiology of atrial flutter*. Annu Rev Med 49: 77-83, 1998.

Della Bella P., Marenzi G., Tondo C., Cardinale D., Giraldi F., Lauri G., Guazzi M., *Usefulness of excitable gap and pattern of resetting in atrial flutter for determining reentry circuit location*. Am J Cardiol, 68(5):492-497, 1991.

Delgado, C., Tamargo, J., Henzel, D., Lorente, P., *Effects of propafenone on calcium current in guinea-pig ventricular myocytes.* Br J Pharmacol 108(3): 721-727, 1993.

Delpon, E., Valenzuela, C., Pérez, O., Casis, O., Tamargo, J.: *Propafenone preferentially blocks the rapidly activating component of delayed rectifier K⁺ current in guinea pig ventricular myocytes.* Circ Res 76(2): 223-235, 1995.

Derakhchan K., Pagé P., Lambert C., Kus T., *Effects of procainamide and propafenone on the composition of the excitable gap in canine atrial reentry tachycardia.* J Pharmacol Exp Ther, 270:47-54, 1994.

D'Este, D., Bertaglia, E., Mantovan, R., Zanocco, A., Franceschi, M., Pascotto, P., *Efficacy of intravenous propafenone in termination of atrial flutter by overdrive transesophageal pacing previously ineffective.* Am J Cardiol 79(4):500-2, 1997.

DiCarlo, L.A. Jr., Morady, F., de Buitleur, M., Baerman, J.M., Schurig, L., Annesley, T., *Effects of chronic amiodarone therapy on ventricular tachycardia induced by programmed ventricular stimulation.* Am Heart J 113(1):57-64, 1987.

Dinh, H.A., Murphy, M.L., Baker, B.J., deSoyza, N., Franciosa, J.A., *Efficacy of propafenone compared with quinidine in chronic ventricular arrhythmias.* Am J Cardiol 55(13 Pt 1):1520-4, 1985.

Doni, F., Della Bella, P., Kheir, A., Manfredi, M., Piemonti, C., Staffiere, E., Rimondini, A., Fiorentini, C., *Atrial flutter termination by overdrive transesophageal pacing and the facilitating effect of oral propafenone.* Am J Cardiol 76(17):1243-6, 1995.

Doni, F., Staffiere, E., Manfredi, M., Piemonti, C., Todd, S., Rimondi, A., Fiorentini, C., *Type II Atrial flutter interruption with transesophageal pacing: Use of Propafenone and possible change of the substrate.* PACE 19(Pt II): 1958-1961, 1996.

Doni, F., Manfredi, M., Piemonti, C., Staffiere, E., Todd, S., Rimondini, A., Fiorentini, C., *New onset atrial flutter termination by overdrive transoesophageal pacing: effects of different protocols of stimulation.* Europace 2(4):292-6, 2000.

Dorian P., Myers M.G., *Antiarrhythmic Drugs.* In: Kalant H., Roschlau W.H.E. eds. Principles of Medical Pharmacology. 5th Ed. BC Decker Inc., Toronto, Philadelphia, p. 351-359, 1989.

Duan, D., Fermini, B., Nattel, S.: *Potassium channel blocking properties of propafenone in rabbit atrial myocytes.* J Pharmacol Exp Ther 264: 1113-1123, 1993.

Dubuc, M., Kus, T., Campa, M.A., Lambert, C., Rosengarten, M., Shenasa, M., *Electrophysiologic effects of intravenous propafenone in Wolff-Parkinson-White syndrome.* Am Heart J 117(2):370-6, 1989.

Dukes, I.D., Vaughan Williams, E.M.: *The multiple modes of action of propafenone.* Eur Heart J 5(2): 115-125, 1984.

Earm, Y.E., Shimoni, Y., Spindler, A.J., *A pace-maker-like current in the sheep atrium and its modulation by catecholamines.* J Physiol 342: 569-590, 1983.

El-Harari, M.B., Adams, P.C., *Atrial flutter with 1:1 atrioventricular conduction caused by propafenone.* Pacing Clin Electrophysiol 21(10):1999-2001, 1998.

Ellenbogen, K.A., Clemo, H.F., Stambler, B.S., Wood, M.A., VanderLugt, J.T., *Efficacy of Ibutilide for termination of atrial fibrillation and flutter.* Am J Cardiol 1996; 78 (Suppl 8A): 42-45.

Escande, D., Coulombe, A., Faivre, J.-F., Deroubaix, E., Coraboeuf E., *Two types of transient outward currents in adult human atrial cells.* Am J Physiol 252: H843-H850, 1987.

Fast, V.G., Kleber, A.G., *Role of wavefront curvature in propagation of cardiac impulse.* Cardiovasc Res 33(2): 258-271, 1997.

Fei, L., Statters, D.J., Hnatkova, K., Polonecki, J., Malik, M., Camm, A.J., *Change of autonomic influence on the heart immediately before the onset of spontaneous idiopathic ventricular tachycardia.* J Am Coll Cardiol 24: 1515-1522, 1994.

Fei, H., Frame, L.H., *d-Sotalol terminates reentry by two mechanisms with different dependance on the duration of the excitable gap.* J Pharmacol Exp Ther 277(1): 177-185, 1996.

Fei, H., Hanna, M.S., Frame, L.H., *Assessing the excitable gap in reentry by resetting.* Circulation 94: 2268-2277, 1996.

Feld G.K., Shahandeh-Rad F., *Activation patterns in experimental canine atrial flutter produced by right atrial crush-injury.* J Am Coll Cardiol 20:441-451, 1992.

Fermini, B., Wang, Z., Duan, D., et coll., *Differences in rate dependance of transient outward current in rabbit and human atrium.* Am J Physiol 263: H1747-H1754, 1992.

Fischer, B., Haissaguerre, M., Garrugues, S., Poquet, F., Gencel, L., Clementy, J., Marcus, F.I., *Radiofrequency catheter ablation of common atrial flutter in 80 patients.* J Am Coll Cardiol 25: 1365-72, 1995.

Fogoros, R.N., *Mechanisms of Cardiac Tachyarrhythmias.* In: Fogoros, N., (ed) *Antairrhythmic Drugs, A practical guide.* Malden, Massachussets, USA, Blackwell Science, Inc., p. 3-33, 1997.

Frame L.H., Page R.L., Hoffman B.F., *Atrial reentry around an anatomic barrier with a partially refractory excitable gap.* Circ. Res. 58:495-511, 1986.

Frame L.H., Page R.L., Boyden P.A., Fenoglio J.J. Jr., Hoffman B.F., *Circus movement in the canine atrium around the tricuspid ring during experimental atrial flutter and during reentry in vitro.* *Circulation* 76, No. 5, 1155-1175, 1987.

Franz M.R., Koller B., Woosley R.L., *Pharmacologic Therapy in Cardiac Arrhythmias.* In: Singh B., Dzau V., Vanhoutte P., Woosley R.L., *Cardiovascular Pharmacology and Therapeutics*, Churchill Livingstone, New York, p. 595-611, 1994.

Friehling, T.D., Lipshutz, H., Marinchak, R.A., Stohler, J.L., Kowey, P.R., *Effectiveness of propranolol added to a type I antiarrhythmic agent for sustained ventricular tachycardia secondary to coronary artery disease.* *Am J Cardiol* 65: 1328-1333, 1990.

Frohnwieser, B., Chen, L.Q., Schreiber, W., Kallen, R.G., *Modulation of the human cardiac sodium channel alpha-subunit by CAPM-dependant protein kinase and the responsible sequence domain.* *J Physiol* 498: 309-318, 1997.

Furukawa, Y.D., Wallick, D.W., Carlson, M.D., et al., *Cardiac electrical responses to vagal stimulation of fibers to discrete cardiac regions.* *Am J Physiol* 258: H1112-1118, 1990.

Gagliardi, M., Randall, W.C., Bieger, D., Wurster, R.D., Hopkins, D.A., Armour, J.A. *Activity of in vivo canine cardiac plexus neurons.* *Am J Physiol* 255: H789-H800, 1988.

Garrey W.E., *The nature of fibrillary contraction of the heart. Its relation to tissue mass and form.* *Am J Physiol*, 33:397-414, 1914.

Gaspo, R., Bosch, R.F., Talajic, M., Nattel, S., *Functional mechanisms underlying tachycardia-induced sustained atrial fibrillation in a chronic dog model.* *Circulation* 96: 4027-4035, 1997.

Geller, J.C., Geller, M., Carlson, M.D., Waldo, A.L., *Efficacy and safety of moricizine in the maintenance of sinus rhythm in patients with recurrent atrial fibrillation.* Am J Cardiol 87(2): 172-177, 2001.

Gentili, C., Giordano, F., Alois, A., Massa, E., Bianconi, L., *Efficacy of intravenous propafenone in acute atrial fibrillation complicating open-heart surgery.* Am Heart J 123(5):1225-8, 1992.

Gettes, L.S., Reuter, H., *Slow recovery from inactivation of inward currents in mammalian myocardial fibres.* J Physiol (Lond) 240: 703-724, 1974.

Giles, W.R., Imaizumi, Y., *Comparison of potassium currents in rabbit atrial and ventricular cells.* J Physiol (Lond) 405: 123-145, 1988.

Gintant, G.A., Liu, D.-W., *β -Adrenergic modulation of fast inward sodium current in canine myocardium. Syncytial preparations versus isolated myocytes.* Circ Res 70: 844-850, 1992.

Govier, W.C., Mosal, N.C., Whittington, P., Broom, A.H., *Myocardial alpha and beta adrenergic receptors as demonstrated by atrial functional refractory period changes.* J Pharmacol Exp Ther 154: 255-263, 1966.

Goy, J.-J., Metrailler, J.-C., Humair, L., de Torrente, A., *Restoration of sinus rhythm in atrial fibrillation of recent onset using intravenous propafenone.* Am Heart J 122(6):1788-90, 1991.

Granada, J., Uribe, W., Chyou, P.-H., Maassen, K., Vierkant, R., Smith, P.N., Hayes, H., Eaker, E., Vidaillet, H., *Incidence and predictors of atrial flutter in the general population.* J Am Coll Cardiol 36: 2242-2246, 2000.

Grant, A.O., *Propafenone: An effective agent for the management of supraventricular arrhythmias.* J cardiovasc Electrophysiol 7: 353-364, 1996.

Groschner, K., Lindner, W., Schnedl, H., Kukovetz, W.R., *The effects of the stereoisomers of propafenone and diprafenone in guinea-pig heart.* Brit J Pharmacol 102: 669-674, 1991.

Gross, G.J., Castle, N.A.: *Propafenone inhibition of human atrial myocyte repolarizing currents.* J Mol Cell Cardiol 30: 783-793, 1998.

Guyton A.C., *Textbook of medical physiology*, VIth edition. Philadelphia, PA, Saunders, p. 98, 114, 1991.

Haffajee, C.I., Love, J.C., Canada, A.T., Lesko, L.J., Asdourian, G., Alpert, J.S., *Clinical pharmacokinetics and efficacy of amiodarone for refractory tachyarrhythmias.* Circulation 67(6):1347-55, 1983.

Hammill, S.C., McLaran, C.J., Wood, D.L., Osborn, M.J., Gersh, B.J., Holmes, D.R. Jr. *Double-blind study of intravenous propafenone for paroxysmal supraventricular reentrant tachycardia.* J Am Coll Cardiol 9(6):1364-8, 1987.

Han, J., Moe, G.K., *Nonuniform recovery of excitability in ventricular muscle.* Circ Res 14: 44-60, 1964.

Hanna, M.S., Coromilas, J., Josephson, M.E., Wit, A.L., Peters, N.S., *Mechanisms of resetting reentrant circuits in canine ventricular tachycardia.* Circulation 103: 1148-1156, 2001.

Harrison D.C., *Current classification of antiarrhythmic drugs as a guide to their rational clinical use.* Drugs 31:93-95, 1986.

Hartzell, H.C., *Regulation of cardiac ion channels by catecholamines, acetylcholine and second messenger systems.* Prog Biophys Mol Biol 52(3): 165-247, 1988.

Harvey, R.D., Hume, J.R., *Autonomic regulation of delayed rectifier K⁺ current in mammalian heart involves G proteins.* Am J Physiol 257(3 Pt 2): H818-H823, 1989.

Harvey, R.D., Hume, J.R., *Autonomic regulation of a chloride current in heart.* Science 244(4907): 983-985, 1989.

Harvey, R.D., Clark, C.O., Hume, J.R., *A chloride current in mammalian cardiac myocytes: Novel mechanism for autonomic regulation of action potential duration and resting membrane potential.* J Gen Physiol 95: 1077-1102, 1990.

Hege, H.G., Hollmann, M., Kaumeier, S., Lietz, H., *The metabolic fate of 2H-labelled propafenone in man.* Eur J Drug Metab Pharmacokinet 9(1):41-55, 1984.

Hege, H.G., Lietz, H., Weymann, J., *Studies on the metabolism of propafenone. 3rd Comm.: Isolation of the conjugated metabolites in the dog and identification using fast atom bombardment mass spectrometry.* Arzneimittelforschung 36(3):467-74, 1986.

Heidbuchel, H., Vereecke, J., Carmeliet, E., *Three different potassium channels in human atrium.* Circ Res 66: 1277-1286, 1990.

Hélie F., *Effets pharmacologiques sur l'anisotropie de conduction et l'induction de tachycardies ventriculaires dans un modèle d'infarctus du myocarde chez le chien.* Mémoire de maîtrise, Université de Montréal, Montréal, 1993.

Higgins, C.B., Vatner, S.F., Braunwald, E., *Parasympathetic control of the heart.* Pharmacol Rev 25: 120-155, 1973.

Hille, B., *Ionic channels of excitable membranes*. Sinauer Assoc. Inc. 2nd ed., Sunderland, MA, 1992.

Honjo, H., Watanabe, T., Kamiya, K., Kodama, I., Toyama, J., *Effects of propafenone on electrical and mechanical activities of single ventricular myocytes isolated from guinea-pig hearts*. British J Pharmacol 97: 731-738, 1989.

Ingelmo, C., Frame, L.H.: *Mechanism for site-dependent differences in the shape of the resetting response curve in fixed barrier reentry*. J Cardiovasc Electrophysiol 11: 981-989, 2000.

Inomata, N., Ohno, T., Ishihara, T., Akaike, N.: *Antiarrhythmic agents act differently on the activation phase of the Ach-response in guinea-pig atrial myocytes*. Br J Pharmacol 108: 111-115, 1993.

Inoue, H., Yamashita, T., Nozaki, A., Sugimoto, T., *Effects of antiarrhythmic drugs on canine atrial flutter due to reentry: role of prolongation of refractory period and depression of conduction to excitable gap*. J Am Coll Cardiol 18: 1098-1104, 1991.

Jalife, J., Delmar, M., Davidenko, J.M., et coll., *Ion Channel Regulation*. In: Jalife, J., Delmar, M., Davidenko, J.M., et coll., *Basic Cardiac Electrophysiology for the Clinician*. Armonk, NY: Futura Publishing Co., Inc., 1999.

Jalil, E., Laflamme, M., Kus, T.: *Effects of procainamide on the excitable gap in canine model of atrial flutter*. Can J Physiol Pharmacol 75: 1-8, 1997.

Jalil, E., Kus T., Le Franc P., Lebeau R., Molin F., Costi P., *Effects of procainamide on the excitable gap composition in common human atrial flutter*. PACE 21: 528-535, 1998.

Janse M.M., *Mechanisms of Arrhythmias*. In: *Camm A.J. ed., Clinical Approaches to Tachyarrhythmias*. Vol.1, Futura Publishing Co. Inc., New York, 1993.

Jazayeri, M.R., Vanwyhe, G., Avitall, B., McKinnie, J., Tchou, P., Akhtar, M., *Isoproterenol reversal of antiarrhythmic effects in patients with inducible sustained ventricular tachyarrhythmias*. *J Am Coll Cardiol* 14: 705-11, 1989.

Jolly W.A., Ritchie W.T., *Auricular flutter and fibrillation*, *Heart* 2:177, 1910.

Josephson M.E., *Atrial Flutter and Fibrillation*. In: *Clinical Cardiac Electrophysiology*, 2nd Ed., Lea and Febiger, Pennsylvania, p. 275-310, 1993.

Kamiya, K., Nishiyama, A., Yasui, K., Hojo, M., Sanguinetti, M.C., Kodama, I., *Short-long-term effects of amiodarone on the two components of cardiac delayed rectifier K⁺ current*. *Circulation* 103: 1317-1324, 2001.

Kates, R.E., Yee, Y.G., Winkle, R.A., *Metabolite cumulation during chronic propafenone dosing in arrhythmia*. *Clin Pharmacol Ther* 37(6):610-4, 1985.

Kato, R., Ikeda, N., Yabek, S.M., Kannan, R., Singh, B.N., *Electrophysiologic effects of the levo- and dextro-totatory isomers of sotalol in isolated cardiac muscle and their in vivo pharmacokinetics*. *J Am Coll Cardiol* 7: 116-125, 1986.

Katoh, T., Karagueuzian, H.S., Sugi, K., Ohta, M., Mandel, W.J., Thomas, P., *Effects of propafenone on sinus nodal and ventricular automaticity: In vitro and in vivo correlation*. *Am Heart J* 113: 941-952, 1987.

Kauffmann, R., Goich, J., Parra, C., Ayala, A., Manzur, F., *Efficacy of propafenone in supraventricular arrhythmias*. *Rev Med Chil* 117(4):401-5, 1989.

Kaumann, A.J., Hall, J.A., Murray, K.J., Wells, F.C., Brown, M.J. *A comparison of the effects of adrenaline and noradrenaline on human heart; the role of β_1 and β_2 adrenoceptors in the stimulation of adenylate cyclase and contractile force.* Eur Heart J 10 (Suppl B) : 29-37, 1989.

Kaumann, A.J., Molenaar, P. *Modulation of human cardiac function through 4 β -adrenoceptor populations.* Naunym-Schmiedeberg's Arch Pharmacol 355 :667-681, 1997.

Khan, I.A., *Single oral loading dose of propafenone for pharmacological cardioversion of recent-onset atrial fibrillation.* J Am Coll Cardiol 37(2): 542-547, 2001.

Kimura, E., Kato, K., Murao, S., Ajisaka, H., Koyama, S., Omiya, Z., *Experimental studies on the mechanism of auricular flutter.* Tohoku J Exp Med 60: 197-207, 1954.

Kirstein, M., Eickhoren, R., Kochsiek, K., Langenfeld, H., *Dose-dependant alteration of rat cardiac sodium current by isoproterenol: results from direct measurements on multicellular preparations.* Eur J Physiol 431: 395-401, 1996.

Kohlhardt, M., Seifert, C., *Inhibition of V_{max} of the action potential by propafenone and its voltage-, time- and pH dependence in mammalian ventricular myocardium.* Naunym-Schmiedeberg's Archives of Pharmacology 315: 55-62, 1980.

Koller, B., Franz, M.R., *New classification of moricizine and propafenone based on electrophysiologic and electrocardiographic data from isolated rabbit heart.* J Cardiovasc pharmacol 24(5): 753-760, 1994.

Kongsgaard, E., Aass, H., *Management of atrial flutter.* Curr Cardiol Rep 2(4): 314-321, 2000.

Koumis, S., Wasserstrom, J.A., Ten Eick, R.E., *Beta-adrenergic and cholinergic modulation of inward rectifier K⁺ channel function and phosphorylation in guinea-pig ventricle.* J Physiol 486(Pt 3): 661-678, 1995.

Kroemer, H.K., Funck-Brentano, C., Silberstein, D.J., Wood, A.J.J., Eichelbaum, M., Woosley, R.L., Roden, D.M., *Stereoselectivity disposition and pharmacologic activity of propafenone enantiomers.* Circulation 79: 1068-1076, 1989.

Kurachi, Y., Nakajima, T., Sugimoto, T., *Acetylcholine activation of K⁺ channels in cell-free membrane of atrial cells.* Am J Physiol 251(3 Pt 2): H681-H684, 1986.

Kus, T., Derakhchan, K., Bouchard, C., Pagé, P., Effects of procainamide on refractoriness, conduction, and excitable gap in canine atrial reentrant tachycardia. PACE 14(Part II): 1707-1713, 1991.

Lanari, A., Lambertini, A., Ravin, A., *Mechanism of experimental atrial flutter.* Circ Res 4: 282-287, 1956.

Lathers C.M., O'Rourke D.K., *Antiarrhythmic Agents.* In: Smith C., Reynold A., eds. Textbook of Pharmacology. W.B. Saunders co. Harcourt Brace Jovanovich Inc. Philadelphie, p.506-540, 1992.

Lavallée, M., De Champlain, J., Nadeau, R.A., et al., *Muscarinic inhibition of endogenous myocardial catecholamine liberation in the dog.* Can J Physiol Pharmacol 56: 642-649, 1978.

Leather, R.A., Klein, G.J., Murdoch, C., Yee, R., Leitch, J.W., *The inefficacy of intravenous propafenone for rate control in atrial fibrillation.* Can J Cardiol 10: 433-438, 1994.

Leclercq, J.F., Attuel, P., Coumel P., *Role of the autonomic nervous system in atrial arrhythmogenesis.* In: Waldo, A.L., Touboul, P., (eds): *Atrial flutter: Advances in mechanisms and management.* Armonk, N.Y.: Futura Publishing Company, Inc., 293-302, 1996.

Ledda, F., Mantelli, L., Manzini, S., Amerini, S., Mugelli, A., *Electrophysiological and antiarrhythmic properties of propafenone in isolated cardiac preparations.* *J Cardiovasc Pharmacol* 3(6):1162-73, 1981.

Lee, J.T., Kroemer, H.K., Silberstein, D.J., Funck-Brentano, C., Lineberry, M.D., Wood, A.J., Roden, D.M., Woosley, R.L., *The role of genetically determined polymorphic drug metabolism in the beta-blockade produced by propafenone.* *N Engl J Med* 322(25): 1764-1768, 1990.

Lens, T.L., Hilleman, D.E., *Dofetilide, a new class III antiarrhythmic agent.* *Pharmacotherapy* 20(7): 776-786, 2000.

Levy, M.N., *Sympathetic-parasympathetic interactions in the heart.* *Circ res* 29: 437-445, 1971.

Levy, M.N., *Sympathetic-vagal interactions in the sinus and atrioventricular nodes.* In: Mazgalev, T., Dreifus, L.S., Michelson, E.L. (eds). *Electrophysiology of the sinoatrial and atrioventricular nodes.* New York: Liss; 187-197, 1988.

Lewis T., Feil H.S., Stroud W.D., *Observations upon flutter and fibrillation. Part II. The nature of auricular flutter.* *Heart*, 7:191-245, 1920.

Li, J.H., Boucher, M., Carpentier, A., Duchêne-Marullaz, P., *Propafenone in the conscious dog with chronic atrioventricular block: Mechanisms of chronotropic cardiac effects and plasma concentration-response relationships.* *J Cardiovasc Pharmacol* 8: 885-891, 1986.

Li, G.R., Feng, J., Wang, Z., Fermini, B., Nattel, S., *Adrenergic modulation of ultrarapid delayed rectifier K⁺ current in human atrial myocytes.* *Circ Res* 78: 903-915, 1996.

Loffelholz, K., Pappano, A.J., *The parasympathetic neuroeffector junction of the heart.* *Pharmacol Rev* 37: 1-24, 1985.

Lu, T., Lee, H.-C., Kabat, J.A., Shibata, E.F.: *Modulation of rat cardiac sodium channel by the stimulatory G protein α subunit.* *J Physiol* 518(2): 371-384, 1999.

Ludmer PL, McGowan NE, Antman EM, Friedman PL. *Efficacy of propafenone in Wolff-Parkinson-White syndrome: electrophysiologic findings and long-term follow-up.* *J Am Coll Cardiol* 9(6):1357-63, 1987.

Malfatto, G., Zaza, A., Forster, M., Sadowick, B., Danilo, Jr. P., Rosen, M.R.: *Electrophysiologic, inotropic and antiarrhythmic effects of propafenone, 5-hydroxypropafenone and N-depropylpropafenone.* *J Pharmacol Exp Ther* 1988; 246(2): 419-26.

Manolis, A.S., Katsaros, C., and Cokkinos, D.V., *Electrophysiological and electropharmacological studies in pre-excitation syndromes: results with propafenone therapy and isoproterenol infusion testing.* *Eur Heart J* 13: 1489-1495, 1992.

Markel, M.L., Miles, W.M., Luck, J.C., Klein, L.S., Prystowsky, E.N., *Differential effects of isoproterenol on sustained ventricular tachycardia before and during procainamide and quinidine antiarrhythmic drug therapy.* *Circulation* 87: 783-792, 1993.

Mason, J.W., Hondeghem, L.M., Katzung, B.G., *Amiodarone blocks inactivated cardiac sodium channels.* *Pflugers Arch* 396(1):79-81, 1983.

Masotti, C.S., Pierangeli, A., *Na⁺ channel blockers vs class III antiarrhythmic drugs in treating sustained ventricular tachycardia: reversing and preventing as different electrophysiological mechanisms.* *Panminerva Med* 41(4): 295-306, 1999.

Matsuda, J.J., Lee, H., Shibata, E.F.: *Enhancement of rabbit cardiac sodium channels by β -adrenergic stimulation.* *Circ Res* 70: 199-207, 1992.

Matsuda, Y., Levy, M.N., *Responses of the atrial myocardium to cardiac sympathetic nerve stimulation.* *Am J Physiol* 249: H207-H211, 1985.

McCleod, A.A., Stiles, G.L., Shand, D.G., *Demonstration of beta adrenoceptor blockade by propafenone hydrochloride. Clinical pharmacologic, radioligand binding and adenylate cyclase activation studies.* *J Pharmacol Exper Ther* 246: 461-466, 1984.

Mensour, B., Jalil, E., Vinet, A., Kus, T., *Influence of propafenone on resetting and termination of canine atrial flutter.* *PACE* 23(8): 1200-1219, 2000.

Mines G.R. *On dynamic equilibrium in the heart.* *J Physiol (Lond.)*, 46:349-383, 1913.

Mitchell, L.B., Wyse, D.G., Gillis, A.M., Duff, H.J., *Electropharmacology of amiodarone therapy initiation. Time courses of onset of electrophysiologic and antiarrhythmic effects.* *Circulation* 80(1):34-42, 1989.

Morady, F., Kou, W.H., Kadish, A.H., Nelson, S.D., Toivonen, L.K., Kushner, J.A., Schmaltz, S., De Buitelir, M., *Antagonism of quinidine's electrophysiologic effects by epinephrine in patients with ventricular tachycardia.* *J Am Coll Cardiol* 12: 388-94, 1988.

Myerburg, R.J., Kessler, K.M., Cox, M.M., Huikuri, H., Terracall, E., Interian, A. Jr., Fernandez, P., Castellanos, A., *Reversal of proarrhythmic effects of flecainide acetate and encainide hydrochloride by propranolol.* *Circulation* 80: 1571-1579, 1989.

Nabar, A., Rodriguez, L.M., Timmermans, C., van Mechelen, R., Wellens, H.J., *Class IC antiarrhythmic drug induced atrial flutter: electrocardiographic and electrophysiologic findings and their importance for long term outcome after right atrial isthmus ablation.* Heart 85(4): 424-429, 2001.

Nademanee, K., Feld, G., Hendrickson, J.A., Singh, P.N., Singh, B.N., *Electrophysiologic and antiarrhythmic effects of sotalol in patients with life-threatening ventricular tachyarrhythmias.* Circulation 72: 555-564, 1985.

Naitoh, N., Washizuka, T., Takahashi, K., Aizawa, Y., *Effects of class I and III antiarrhythmic drugs on ventricular tachycardia-interrupting critical paced cycle length with rapid pacing.* Jpn Circ J 62(4): 267-273, 1998.

Nakagawa, H., Lazzara, R., Khastgir, T., Beckman, K.J., McClelland, J.H., Imai, S., Pitha, J.V., Becker, A.E., Arruda, M., Gonzalez, M.D., Widman, L.E., Rome, M., Neuhauser, J., Wang, X., Calame, J.D., Goudeau, M.D., Jackman, W.M., *Role of the tricuspid annulus and the eustachian valve/ridge on atrial flutter: relevance to catheter ablation of the septal isthmus and a new technique for rapid identification of ablation success.* Circulation 94: 407-424, 1996.

Neuss, H., Schlepper, M., *Clinical pharmacology of propafenone.* In: Schlepper M., Olsson B. (eds) *Cardiac arrhythmias: diagnosis, prognosis, therapy.* Proceedings of the 1st International Rythmonorm Congress. New York: Springer-Verlag: 20-28, 1983.

Niwano, S., Ortiz, J., Abe, H., Gonzalez, X., Rudy, Y., Waldo, A.L., *Characterization of the excitable gap in a functionally determined reentrant circuit. Studies in the sterile pericarditis model of atrial flutter.* Circulation 90 (4): 1997-2014, 1994.

Norgaard, B.L., Wachtell, K., Christensen, P.D., Madsen, B., Johansen, J.B., Christiansen, E.H., Graff, O., Simonsen, E.H., *Efficacy and safety of intravenously administered dofetilide in acute termination of atrial fibrillation and flutter: a multicenter, randomized, double-blind, placebo-controlled trial.* Danish Dofetilide in Atrial Fibrillation and Flutter Study Group. *Am Heart J* 137(6):92-995, 1999.

Norris, J.E., Lippincott, D., Wurster, R.D., *Responses of canine endocardium to stimulation of upper thoracic roots.* *Am J Physiol* 233: H655-659, 1997.

Ono, K., Fozzard, H.A., Hanck, D.A.: *Mechanism of cAMP-dependant modulation of cardiac sodium channel current kinetics.* *Circ Res* 72: 807-815, 1993.

Opie, L.H., *Blood pressure and peripheral circulation.* In : Opie, L.H., *The heart : Physiology, from cell to circulation.* 3rd Edition. Lippincott-Raven Publishers, Philadelphia, p 421-446, 1998.

Otani, H., Otani, H., Das, D.K. *α 1-adrenoceptor-mediated phosphoinositide breakdown and inotropic response in rat left ventricular papillary muscles.* *Circ Res* 62 :8-17, 1988.

Oti-Amoako, K., Vozeh, S., Ha, H.-R., Follath, F., *The relative potency of major metabolites and enantiomers of propafenone in an experimental reperfusion arrhythmia model.* *J Cardiovasc Pharmacol* 1990; 15: 75-81.

Pagé P.L., Plumb V.J., Okumura K., Waldo A.L., *A new model of atrial flutter.* *J Am Coll Cardiol* 8:872-879, 1986.

Pagé, P., Dandan, N., Do, Q.B., Cardinal, R., *The right atrial Y-shaped incision model of atrial flutter affects atrial vagal innervation.* *Eur J of Cardiac Pacing and Electrophysiol* 6 (Suppl. 5): 31, 1996.

Pardini, B.J., Schmid, P.G., Lund, D.D., *Location, distribution, and projections of intracardiac ganglion cells in the rat.* J Auton Nerv Syst 20: 91-101, 1987.

Patlak, J.B., Ortiz, M., *Slow currents through single sodium channels of adult rat heart.* J Gen Physiol 86: 89-104, 1985.

Plecha, D.M., Randall, W.C., Geis, G.S., Wurster, R.D., *Localization of vagal preganglionic somata controlling sinoatrial and atrioventricular nodes.* Am J Physiol 255: R703-R708, 1988.

Podrid, P.J., *Amiodarone: reevaluation of an old drug.* Ann Int Med 122: 689-700, 1995.

Porciatti, F., Pelzmann, B., Cerbai, E., Schaffer, P., Pino, R., Bernhart, E., Koidl, B., Mugelli, A., *The pacemaker current $I(f)$ in single human atrial myocytes and the effect of beta-adrenoceptor and A1-adenosine receptor stimulation.* Br J Pharmacol 122(5): 963-969, 1997.

Potter, E.K., *Prolonged non-adrenergic inhibition of cardiac vagal action following sympathetic stimulation: neuromodulation by neuropeptide Y?* Neurosci Lett 54: 117-121, 1985.

Pritchett, E.L.C., McCarthy, E.A., Wilkinson, W.E., *Propafenone treatment of symptomatic paroxysmal supraventricular arrhythmias.* Ann Intern Med 114: 539-544, 1991.

Prystowsky E.N., Klein G.J., *Cardiac Arrhythmias - An integrated approach for the clinician.* McGraw-Hill Inc., New York, p. 99-177, 1994.

Rahme, M.M., Feracci, A., Kus, T., *Effects of D-Sotalol on excitable gap composition in canine atrial reentry tachycardia.* Pacing Clin Electrophys 18(Part II): 905, 1995.

Rahme, M. M., Laflamme, M., Kus, T., *Reversal of d-Sotalol effects on the excitable gap composition in canine atrial flutter by autonomic neurohormones.* J Am Col Cardiol, Vol. 29 (2), Suppl. A: 329A, 1997a.

Rahme, M. M., Kus, T., *Selective reversal of d,l-sotalol effects on excitable gap composition in canine atrial flutter by acetylcholine.* PACE, 20(part II): 1216, 1997b.

Ramirez, R.J., Nattel, S., Courtemanche, M., *Mathematical analysis of canine atrial action potentials: rate, regional factors, and electrical remodeling.* Am J Physiol 279: H1767-H1785, 2000.

Randall, W.C., *Selective autonomic innervation of the heart.* In: Randall, W.C.(ed): Nervous control of cardiovascular function. New York: Oxford University Press; 46-67, 1984.

Randall, W.C., Ardell, J.L: *Selective parasympathectomy of automatic and conductile tissue of the canine heart.* Am J Physiol 248 (17): H61-H68, 1985.

Ranger, S., Talajic, M., Lemery, R., Roy, D., Nattel, S., *Amplification of flecainide-induced ventricular conduction slowing by exercise.* Circulation 79: 1000-1006, 1989.

Redwood, D.R., Henry, W.L., Epstein, S.E. **Evaluation of the ability of echocardiography to measure acute alterations in left ventricular volume.** Circulation 50 : 901-904, 1974.

Reimold, S.C., Maisel, W.H., Antman, E.M., *Propafenone for the treatment of supraventricular tachycardia and atrial fibrillation: a meta-analysis.* Am J Cardiol 82(8A):66N-71N, 1998.

Reiter, M.J., Zetelaki, Z., Kirchhof, C.J., Boersma, L., Allessie, M.A., *Interaction of acute ventricular dilatation and d-sotalol during sustained reentrant ventricular tachycardia around a fixed obstacle.* Circulation 89(1): 423-431, 1994.

Renaudon, B., Bois, P., Bescond, J., Lenfant, J., *Acetylcholine modulates I(f) and IK(ACh) via different pathways in rabbit sino-atrial node cells.* J Moll Cell Cardiol 29(3): 969-975, 1997.

Rensma, P.L., Allesie, M.A., Lammers, W.J.E.P., Bonke, F.I.M., Schali, M.J., *Length of excitation wave and susceptibility to reentrant atrial arrhythmias in normal conscious dogs.* Circ Res 62: 395-410, 1988.

Roden, D.M., George Jr, A.L., *The cardiac ion channels: relevance to management of arrhythmias.* Annu Rev Med 47: 135-48, 1996.

Rosen M.R., *Cellular Mechanisms of Cardiac Arrhythmias.* In: Harrison D.C. ed., *Cardiac Arrhythmias - a decade of progress*, G.K. Hall Medical Publishers, Boston, p. 26, 1981.

Rosenblueth A., Garcia-Ramos J., *Studies on flutter and fibrillation. II. The influence of artificial obstacles on experimental auricular flutter.* Am Heart J 677-684, 1946.

Rouet, R., Libersa, C.C., Broly, F., Caron, J.F., Adamantidis, M.M., Honore, E., Wajman, A., Dupuis, B.A., *Comparative electrophysiological effects of propafenone, 5-hydroxy-propafenone, and N-depropylpropafenone on guinea pig ventricular muscle fibers.* J Cardiovasc Pharmacol 14(4):577-84, 1989.

Sager PT: *New advances in class III antiarrhythmic drug therapy.* Opin Cardiol 15: 41-53, 2000.

Sager, P.T., Behboodikhah, M., *Frequency-dependent electrophysiologic effects of d,l-sotalol and quinidine and modulation by beta-adrenergic stimulation.* J Cardiovasc Electrophysiol 7: 102-112, 1996.

Sanguinetti, M.C., Jurkiewicz, N.K., *Two components of cardiac delayed rectifier K⁺ current.* J Gen Physiol 96 : 195-215, 1990.

Sanguinetti, M.C., Jurkiewicz, N.K., Scott, A., Siegl, P.K., *Isoproterenol antagonizes prolongation of refractory period by the class III antiarrhythmic agent E-4031 in guinea pig myocytes. Mechanism of action.* Circ Res 68(1) : 77-84, 1991.

Schafers, R.F., Poller, U., Ponicke, K., Geissler, M., Daul, A.E., Michel, M.C., Brodde, O.-E. *Influence of adrenoceptor and muscarinic receptor blockade on the cardiovascular effects of exogenous noradrenaline and of endogenous noradrenaline released by infused tyramine.* Naunym-Schmiedeberg's Arch Pharmacol 355 : 239-249, 1997.

Schamroth, L., Myburgh, D.P., Schamroth, C.L., Scholtz, M.E., Pincus, D.R., Kawalsky, D.L., *Oral propafenone in the suppression of chronic stable ventricular arrhythmias.* Chest 87(4):448-51, 1985.

Schwartzman, D., Callans, D.J., Gottlieb, C.D., Dillon, S.M., Movsowitz, C., Marchlinski, F.E., *Conduction block in the inferior vena caval-tricuspid valve isthmus: Association with outcome of radiofrequency ablation of type I atrial flutter.* J Am Coll Cardiol 28: 1519-31, 1996.

Shen, E.N., Keung, E., Huycke, E., Dohrmann, M.L., Nguyen, N., Morady, F., Sung, R.J., *Intravenous propafenone for termination of reentrant supraventricular tachycardia. A placebo-controlled, randomized, double-blind, crossover study.* Ann Intern Med 105(5):655-61, 1986.

Siddoway, L.A., Thompson, K.A., McAllister, C.B., Wang, T., Wilkinson, G.R., Roden, D.M., Woosley, R.L., *Polymorphism of propafenone metabolism and disposition in man: clinical and pharmacokinetic consequences.* Circulation 75(4):785-91, 1987.

Singh, B.N., *Historical development of the concept of controlling cardiac arrhythmias by lengthening repolarisation : particular reference to sotalol.* Am J Cardiol 65 : 3A-11A, 1990.

Singh, B.N., *Electrophysiologic basis for the antiarrhythmic actions of sotalol and comparison with other agents.* Am J Cardiol 72 : 8A-18A, 1993.

Singh, B.N., Vaughan Williams, E.M., *The effect of amiodarone, a new anti-anginal drug, on cardiac muscle.* Br J Pharmacol. 39 : 657-667, 1970.

Skomedal, T., Borthne, K., Aass, H., Geiran O., Osnes, J.-B. *Comparison between alpha-1 adrenoceptor-mediated and beta adrenoceptor-mediated inotropic components elicited by noradrenaline in human atria.* J Pharmacol Exp Ther 233 :441-446, 1997.

Sorota, S., Rybina, I., Yamamoto, A., Du, X.Y., *Isoprenaline can activate the acetylcholine-induced K⁺ current in canine atrial myocytes via G_s-derived betagamma subunits.* J Physiol 514 (pt2) : 413-423, 1999.

Spinelli, W., Hoffman, B.F., *Mechanisms of termination of reentrant atrial arrhythmias by Class I and Class III antiarrhythmic agents.* Circ Res 65: 1565-1579, 1989.

Stamato, N.J., Rosenthal, M.E., Almendral, J.M., Josephson, M.E., *The resetting response of ventricular tachycardia to single and double extrastimuli: implications for an excitable gap.* Am J Cardiol 60(7):596-601, 1987.

Stamato N.J., Frame L.H., Rosenthal M.E., Almendral J.M., Gottlieb C.D., Josephson M.E., *Procainamide-Induced Slowing of Ventricular Tachycardia with Insights from Analysis of Resetting Response Patterns.* Am J Cardiol, 63:1455-1461, 1989.

Stambler, B.S., Wood, M.A., Ellenbogen, K.A., *Pharmacologic alterations in human type I atrial flutter cycle length and monophasic action potential duration. Evidence of a fully excitable gap reentrant circuit.* J Am Coll Cardiol 27 (2): 453-61, 1996.

Stambler, B.S., Wood, M.A., Ellenbogen, K.A., Perry, K.T., Wakefield, L.K., VanderLugt, J.T. *Efficacy and safety of repeated intravenous doses of ibutilide for rapid conversion of atrial flutter or fibrillation. Ibutilide Repeat Dose Study Investigators.* Circulation 94(7): 1613-1621, 1996.

Stanton, M.S., *Class I Antiarrhythmic drugs: Quinidine, Procainamide, Disopyramide, Lidocaine, Mexiletine, Tocainide, Phenytoin, Moricizine, Flecainide and Propafenone.* In: Zipes, D.P., Jalife J., *Cardiac Electrophysiology From Cell to Bedside*, 3rd Edition, W.B. Saunders Company, Philadelphia, USA, Chapter 98, pages 900-901, 2000.

Stramba-Badiale, M., Lazzarotti, M., Facchini, M., Schwartz, P.J., *Malignant arrhythmias and acute myocardial ischemia: Interaction between flecainide and the autonomic nervous system.* Am Heart J 28: 973-82, 1994.

Strauss H.C., Saroff A.L., Bigger J.T., Giardina E.G.V., *Premature atrial stimulation as a key to the understanding of sinoatrial conduction in man.* Circulation 47:86, 1973.

Suttorp, M.J., Kingma, J.H., Jessurun, E.R., Lie-A-Huen, L., van Hemel, N.M., Lie, K.I., *The value of class IC antiarrhythmic drugs for acute conversion of paroxysmal atrial fibrillation or flutter to sinus rhythm.* J Am Coll Cardiol 16 (7): 1722-7, 1990.

Takahashi, N., Zipes, D.P., *Vagal modulation of adrenergic effects on canine sinus and atrioventricular nodes.* Am J Physiol 244: H775-H781, 1983.

Ten Eick, R., Nawrath, H., McDonald, T.F., *On the mechanism of the negative inotropic effect of acetylcholine.* Plueger's Arch 361 : 297-213, 1976.

Thompson, K.A., Iansmith D.H.S., Siddoway, L.A., Woosley, R.L., Roden D.M., *Potent electrophysiologic effects of the major metabolites of propafenone in canine Purkinje fibers.* J Pharmacol Exp Ther 244: 950-955, 1988.

Touboul, P., Atallah, G., Kirkorian, G., Lavaud, P., Mathieu, M.P., Dellinger. A., *Effects of intravenous sotalol in patients with atrioventricular accessory pathways.* Am Heart J 114 : 545-550, 1987.

Trautwein, W., Hescheler, J., *Regulation of cardiac L-type calcium current by phosphorylation and G proteins.* Annu Rev Physiol 52 : 257-274, 1990.

Vaughan Williams E.M., *Classification of antiarrhythmic drugs.* Pharmacol Ther, 1:115-138, 1975.

Vaughan Williams, E.M., *A classification of antiarrhythmic actions reassessed after a decade of new drugs.* J Clin Pharmacology 24(4): 129-147, 1984.

Vaughan Williams, E.M., *Significance of classifying antiarrhythmic actions since the Cardiac Arrhythmia Suppression Trial.* J Clin Pharmacol 31: 123-135, 1991.

Vos, M.A., Golitsyn, S.R., Stangl, K., Ruda, M.Y., Van Wijk, L.V., Harry, J.D., Perry, K.T., Touboul, P., Steinbeck, G., Wellens, H.J., *Superiority of ibutilide (a new class III agent) over DL-sotalol in converting atrial flutter and atrial fibrillation. The Ibutilide/Sotalol Comparator Study Group.* Heart 79(6): 568-575, 1998.

Wagner, G.S., Waugh, R.A., Ramo B.W., (Eds) (Chapter 4), Churchill Livingstone. New York, N.Y. : 57-108, 1983.

Waldo A.L., MacLean W.A.H., *Diagnosis and treatment of arrhythmias following open heart surgery - emphasis on the use of epicardial wire electrodes.* New York: Futura, 1980.

Waldo A.L., Henthorn R.W., Plumb V.J., *Atrial Flutter - recent observations in man.* In: Josephson M.E., Wellens H.J.J., eds. *Tachycardias: mechanisms, diagnosis and treatment*, Philadelphia, Lea and Febiger, 1984.

Waldo A.L., *Atrial Flutter.* In: Podrid P.J., Kowey P.R. eds., *Cardiac Arrhythmia - Mechanisms, Diagnosis and Management.* Williams and Wilkins, Baltimore, p. 790-802, 1995.

Waldo A.L., *Electrophysiology. Treatment of atrial flutter.* *Heart* 84 : 227-232, 2000.

Wang, Z., Fermini, B., Nattel, S., *Sustained depolarization-induced outward current in human atrial myocytes. Evidence for a novel delayed rectifier K⁺ current similar to Kv1.5 cloned channel currents.* *Circ Res* 73: 1061-1076, 1993.

Wang, Z., Fermini, B., Nattel, S., *Rapid and slow components of delayed rectifier current in human atrial myocytes.* *Cardiovasc Res* 28 : 1540-1546, 1994.

Watson, J.M., Vogel, S.M., Cotterell, D.J., Dubocovich, M.L., *Cholinergic antagonism of beta-adrenergic stimulated action potentials and adenylate cyclase activity in rabbit ventricular cardiomyocytes.* *Eur J Pharmacol* 155(1-2) : 101-108, 1988.

Waxman, M.B., Sharma, A.D., Cameron, D.A., Huerta, F., Wald, R.W., *Reflex mechanisms responsible for early spontaneous termination of paroxysmal supraventricular tachycardia.* *Am J Cardiol* 49 : 259-272, 1982.

Waxman, M.B., Wald, R.W., Cameron, D.A., *Interactions between the autonomic nervous system and tachycardias in man.* *Cardiol Clin* 1(2):143-85, 1983.

Waxman, M.B., Yao, L., Cameron, D.A., Kirsh, J.A., *Effects of posture, vasalva maneuver and respiration on atrial flutter rate: an effect mediated through cardiac volume.* J Am Coll Cardiol 17: 1545-52, 1991.

Weidmann S., *The effect of the cardiac membrane on the rapid availability of the sodium carrying system.* J Physiol (Lond) 127 : 213-224, 1955.

Wells J.L., MacLean W.A.H., James T.N., Waldo A.L., *Characterization of atrial flutter. Studies in man after open heart surgery using fixed electrodes.* Circulation 60:665, 1979.

Wen, Z.-C., Chen, S.-A., Tai, C.-T., Huang, J.-L., Chang, M.-S., *Role of autonomic tone in facilitating spontaneous onset of typical atrial flutter.* J Am Coll Cardiol 31: 602-7, 1998.

Wijffels, M.C., Dorland, R., Mast, F., Allessie, M.A., *Widening of the excitable gap during pharmacological cardioversion of atrial fibrillation in the goat: effects of cibenzoline, hydroquinidine, flecainide, and d-sotalol.* Circulation 102(2) : 260-267, 2000.

Wit A.L., Cranefield P.F., *Reentrant excitation as a cause of cardiac arrhythmias.* Am. J. Physiol., 235:H1-H17, 1978.

Wu, K.-M., Hoffman, B.F., *Effect of procainamide and N-acetylprocainamide on atrial flutter: studies in vivo and in vitro.* Circulation 76(6): 1397-1408, 1987.

Wu, K.-M., Ross, S., Hoffman, B.F., *Monophasic action potentials during reentrant atrial flutter in the dog: Effects of clofilium and acetylcholine.* J Cardiovasc Pharm 13: 908-914, 1989.

Yano, K., Hirata, T., Hirata, M., Hano, O., Matsumoto, Y., Mitsuoka, T., and Abe, K., *Effects of sympathetic and parasympathetic stimulation on the induction of atrial flutter in dogs with aseptic pericarditis.* Jap Heart J 32 : 811-825, 1991.

Yuan, B.X., Ardell, J.L., Hopkins, D.A., Armour, J.A., *Differential cardiac responses induced by nicotinic sensitive canine atrial and ventricular neurons.* Cardiovasc Res 27 : 760-769, 1993.

Yuan, B.X., Ardell, J.L., Hopkins, D.A., Losier A.M., Armour J.A., *Gross and Microscopic anatomy of the canine intrinsic cardiac nervous system.* Anat Rec 239 : 75-87, 1994.

Yue, L., Feng, J., Wang, Z., Nattel, S., *Adrenergic control of the ultrarapid delayed rectifier current in canine atrial myocytes.* J Physiol 516.2 : 385-398, 1999.

Zygmunt, A.C., Gibbons, W.R., *Calcium-activated chloride current in rabbit ventricular myocytes.* Circ Res 68 : 424-437, 1991.